

**SOME ASPECTS OF SPATIAL AND TEMPORAL
DISTRIBUTION AND DEVELOPMENT OF PREDICTION
MODELS OF WATERSHED SEDIMENT YIELD**

Thesis

Submitted to the
G. B. Pant University of Agriculture and Technology
Pantnagar 263 145, Uttarakhand, India



By

Seyed Hamidreza Sadeghi

IN PARTIAL FULFILLMENT OF THE REQUIREMENTS
FOR THE DEGREE OF

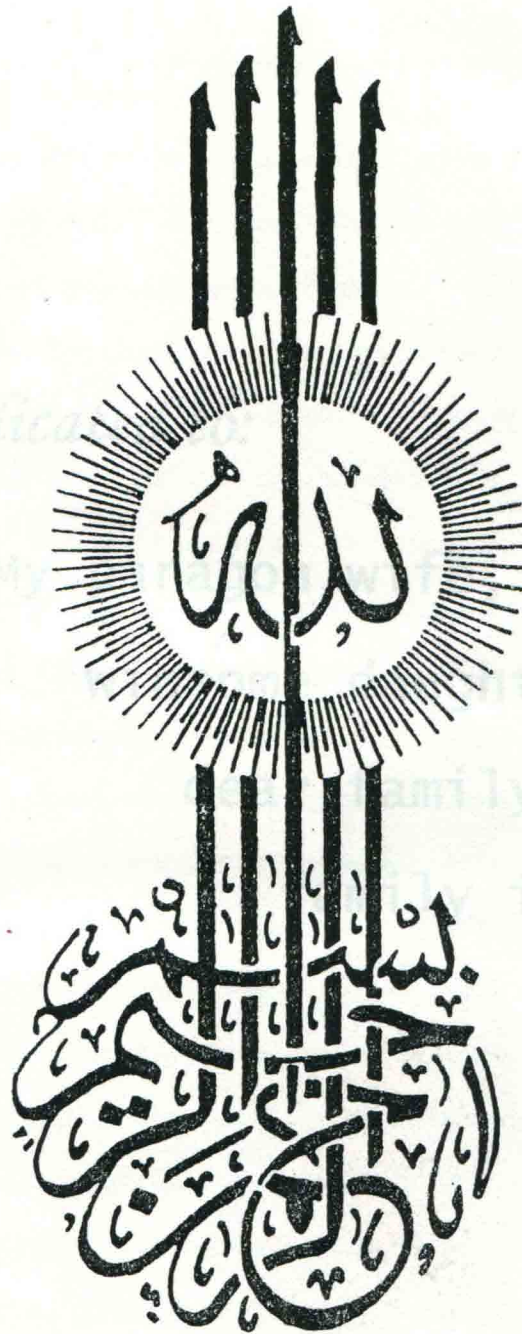
Doctor of Philosophy

In

SOIL AND WATER CONSERVATION ENGINEERING

December, 2000

Om



Praise be to Allah, the Lord of the worlds

Dedicated to:

My paragon wife,

winsome daughter,

dear family and

family in law

ACKNOWLEDGMENT

The one who does not praise creatures, he is not praising The Creator.

(Prophet Mohammad)

The author bows his head with great reverence to Him who is omnipresent, omnipotent and omniscient and is the cause behind every effort. The author feels extremely privileged to express his deep sense of reverence and indebtedness to his advisor and Chairman of his Advisory Committee, Dr. J.K. Singh, Professor, Department of Soil and Water Conservation Engineering, College of Technology, G.B. Pant University of Agriculture and Technology, Pantnagar, Uttaranchal, India and Dean Student Welfare of the university not only for his invaluable suggestions and revisions in the present thesis, but also for his incessant encouragement, sympathy, unceasing interest and ungrudging help and the rare kindness that he has bestowed during the course of investigation in India. It is his sincere, tireless, meticulous guidance that finally materialized in present research.

The author is extremely thankful to Dr. Ghanshyam Das, Emeritus fellow (AICTE), Department of Soil and Water Conservation Engineering, and a member of Advisory Committee for his constructive and valuable efforts during the study period. The author is also so grateful to Dr. K.N. Shukla, Professor, Department of Irrigation and Drainage Engineering and Dr. Manoj Kumar, Assistant Professor, Department of Mathematics, Statistics and Computer Science, members of Advisory Committee for reviewing the manuscript and providing appropriate suggestions during the research duration.

The author's thanks are due to Dr. Sant Ram, Dean, Post Graduate Studies and Dr. C. S. Jaiswal, Dean College of Technology for providing essential facilities during the program.

The author is so grateful to Dr. V. Kumar, Professor and Head and the other faculty members of the Department of Soil and Water Conservation Engineering for providing the necessary facilities and their obliging assistance to him. He wishes to thank Dr. A. Kumar, specially, for his constructive suggestions in finalizing the manuscript time to time.

The Ministry of Culture and Higher Education of Iran for awarding the Ph.D. scholarship, Dr. Ibrahim Hajizadeh, First Secretary and Director, Science and Education

Section, Embassy of Iran, New Delhi and his esteemed colleagues for facilitating the official processes of the study in India are also thanked by the author.

The author is also much obliged to the Informatic and library sections of Watershed Management Division, Ministry of Jihad-e-Sazandegi and Water Resources Research Organization, Ministry of Energy, Iran, for providing hydrological data used in this study.

The author wishes to place on record his great and deep sense of gratitude to his wife and daughter for their continuous cooperation, patience and understanding without which this study could never been completed. The everlasting inspiration and constant encouragement of the members of the author's family and his in-laws are humbly appreciated. He is so grateful to the family members of his advisor who treated him as a member of their own family during his stay in Pantnagar.

The special thanks of the author are due to his Yemeni friend Mr. Omar Ahmad Bamaga, Ph.D. scholar in Farm Machinery and Power Engineering and his family owing to their constant company and encouragement during the different aspects of the study period. The author acknowledges his countrymates Mr. I. Mahdavi, Ph.D. scholar in Production Engineering, Mrs. Z. Amiri, Ph.D. scholar in Food Science and Technology, Mr. S.S. Pourdad and Mr. G. Najafian, Ph.D. scholars in Plant Breeding and Genetics at the same university and R. Toroghi, Ph.D. scholar in Veterinary Sciences in IVRI, Barielly and their families for their company and providing the perpetual enjoyable Iranian atmosphere. The author would like to remember the kind of the Sudanese friends, Mr. A. Abdoallah, Ph.D. scholar in Plant Breeding and Genetics, Mr. M. Benjamin, Ph.D. scholar in Farm Machinery and Power Engineering, the Syrian friend, Mr. M. Meselmani, Master scholar in plant physiology and their families and the Chinese friend Mr. Li, Ph.D. scholar in Plant Breeding and Genetics as good friends in abroad.

Last, but not the least, the author is thankful to Mr. Bhatt, Mr. Bhandari and Mr. Joshi in the Department of Soil and Water Conservation Engineering and every one else who helped him directly and indirectly in facilitating his pleasant sojourn at Pantnagar campus.

December 2000

(SEYED HAMIDREZA SADEGHI)




**DEPARTMENT OF SOIL AND WATER CONSERVATION ENGINEERING
COLLEGE OF TECHNOLOGY
G. B. PANT UNIVERSITY OF AGRICULTURE AND TECHNOLOGY
PANTNAGAR 263 145, UTRANCHAL, INDIA**

Dr. J. K. Singh
Professor

CERTIFICATE

This is to certify that the thesis entitled "*SOME ASPECTS OF SPATIAL AND TEMPORAL DISTRIBUTION AND DEVELOPMENT OF PREDICTION MODELS OF WATERSHED SEDIMENT YIELD*", submitted in partial fulfillment of the requirements for the degree of **DOCTOR OF PHILOSOPHY** with major in **Soil and Water Conservation Engineering** and minor in **Irrigation and Drainage Engineering** of the College of Post Graduate Studies, G. B. Pant University of Agriculture and Technology, Pantnagar, is a record of *bona fide* research carried out by **Mr. Seyed Hamidreza Sadeghi**, Id. No. **24812** under my supervision, and no part of the thesis has been submitted for any other degree or diploma.

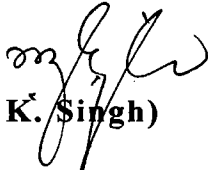
The assistance and help received during the course of this investigation have been acknowledged.


(J. K. Singh)

Chairman
Advisory Committee

CERTIFICATE

We, the undersigned, members of the Advisory Committee of **Mr. Seyed Hamidreza Sadeghi**, Id. No. **24812**, a candidate for the degree of **DOCTOR OF PHILOSOPHY** with major in **Soil and Water Conservation Engineering** agree that the thesis entitled **"SOME ASPECTS OF SPATIAL AND TEMPORAL DISTRIBUTION AND DEVELOPMENT OF PREDICTION MODELS OF WATERSHED SEDIMENT YIELD"** may be submitted in partial fulfillment of the requirements for the degree.



(J. K. Singh)

Advisor and Chairman



(Ghanshyam Das)

Member



(M. Kumar)

Member



(K. N. Shukla)

Member



(V. Kumar)

Ex-Officio Member

LIST OF CONTENTS

<i>Content</i>	<i>Page</i>
1. INTRODUCTION	1
2. REVIEW OF LITERATURE	7
2.1 Statistical Regression Models	8
2.2 Deterministic Models	16
2.3 Stochastic Models	20
2.4 Parametric Models	22
2.5 Dynamic Models	23
2.6 Physically Based Models	24
2.7 Sediment Routing, Rating and Delivery Ratio Models	26
2.8 Sediment Graph Models	33
2.9 Computer Models	42
3. STUDY AREA AND HYDROLOGICAL DATA	45
3.1 Description of Study Area	45
3.1.1 Physiographical characteristics	45
3.1.1.1 General feature	47
3.1.1.2 Shape	47
3.1.1.3 Longitudinal profile of the main river	49
3.1.1.4 Slope	49
3.1.1.5 Elevation	50
3.1.1.6 Drainage pattern and Gorge factor	51
3.1.1.7 Drainage density	52
3.1.2 Geology and geomorphology	54
3.1.3 Soil	55
3.1.4 Land use pattern	57
3.1.5 Soil erosion process	57
3.1.6 Climatological characteristics	58
3.1.7 Hydrological characteristics	62
3.2 Instrumentation and Collection of Hydrological Data	62
3.2.1 Precipitation	64
3.2.2 Runoff	66
3.2.3 Sediment	68
4. DEVELOPMENT OF SEDIMENT GRAPH MODEL	72
4.1 Development of Sediment Graph Model Based on Hydrological Data	74
4.1.1 Development of sediment mobilized sub-model	74
4.1.1.1 Estimation of excess runoff	75
a. Analysis of available flow discharge data	75
a-1 Development of discharge rating curves	75
a-2 Derivation of direct runoff hydrograph	77
a-3 Derivation of unit hydrograph	78
a-4 Derivation of average unit hydrograph	78
b. Precipitation-runoff models	79
b-1 Statistical regression model	80

<i>Content</i>	<i>Page</i>
b-1-1 Bivariable model	80
b-1-2 Multivariable model	81
b-2 SCS curve number technique	82
b-3 Selection of best applicable precipitation-runoff model	
4.1.1.2 Estimation of excess sediment	89
a. Analysis of available sediment data	89
a-1 Development of sediment rating curves	89
a-2 Derivation of continuous sediment graph	92
a-3 Derivation of direct sediment graph	95
b. Sediment models	96
b-1 Sediment yield sub-model	97
b-1-1 Annual erosion sub-model	97
b-1-1-1 Universal soil loss equation	97
b-1-1-2 Hudson's method	104
b-1-1-3 EUSLE	105
b-1-1-4 AOF	105
b-1-1-5 Time area method	105
b-1-2 Storm-wise sediment yield sub-models	111
b-1-2-1 MUSLE for sediment yield	113
b-1-2-2 MUSLE for soil erosion	113
b-1-2-3 MUSLT	114
b-2 Sediment routing sub-model	118
b-2-1 Estimation of model system parameters	120
b-2-2 Estimation of runoff parameters	121
b-2-2-1 Area-CN role factor technique	123
b-2-2-2 First order decay function technique	125
b-2-2-3 Reverse flood routing technique	126
b-2-3 Determination of sediment routing coefficient	
b-3 Selection of best applicable sediment yield sub-model	
4.1.1.3 Sediment mobilized sub-model	140
4.1.2 Development of unit sediment graph	141
4.1.3 Development of average unit sediment graph	141
4.1.4 Design sediment graph	144
4.2 Development of Sediment Graph Model Based on Watershed Characteristics	
4.2.1 Development of instantaneous unit hydrograph	145
4.2.1.1 Time area histogram	146
4.2.1.2 Flow routing	148
4.2.2 Determination of sediment concentration	150
4.2.2.1 Determination of sediment routing parameter	151
a. Using Williams' method	151
b. Using Banasik's method	152
c. Using modified method	152
4.2.2.2 Dimensionless sediment concentration distribution	153
4.2.3 Development of instantaneous unit sediment graph	154
4.2.4 Development of unit sediment graph	155
4.2.5 Design sediment graph	156

<i>Content</i>	<i>Page</i>
4.3 Evaluation of models	157
4.3.1 Qualitative evaluation	157
4.3.2 Quantitative evaluation	158
4.3.2.1 Absolute relative error (ARE)	158
4.3.2.2 Coefficient of efficiency (CE)	159
4.3.2.3 Integral square error (ISE)	159
4.3.2.4 Relative square error (RSE)	160
4.3.2.5 Root mean square error (RMSE)	160
4.3.2.6 Ratio of error (REO)	160
4.3.2.7 Bias (B_s)	161
4.3.2.8 Coefficient of determination (R^2)	162
5. RESULTS AND DISCUSSION	163
5.1 Spatial Distribution of Total Runoff and Sediment Yield	164
5.2 Temporal Distribution of Sediment Yield (Sediment Graph)	169
5.2.1 SGs derived based on hydrological data (Model A)	169
5.2.2 SGs derived based watershed characteristics (Model B)	173
5.3 Performance Evaluation of Developed Models	190
5.3.1 Qualitative evaluation	190
5.3.2 Quantitative evaluation	191
5.3.2.1 Absolute relative error (ARE)	200
5.3.2.2 Coefficient of efficiency (CE)	202
5.3.2.3 Integral square error (ISE)	203
5.3.2.4 Relative square error (RSE)	204
5.3.2.5 Root mean square error (RMSE)	204
5.3.2.6 Ratio of error (REO)	205
5.3.2.7 Bias in sediment yield (B_s)	205
5.4 Comparison of Models' Performance	206
5.5 Sensitivity Analysis	211
6. SUMMARY AND CONCLUSION	213
LITERATURE CITED	226
APPENDICES	242

LIST OF TABLES

<i>Table</i>	<i>Page</i>
2.1 Some of the computer models in the field of erosion processes	43
3.1 Elevation profile of the Amameh main river	49
3.2 Elevation wise area distribution in Amameh watershed	50
3.3 Geometric factors of Amameh watershed	54
3.4 Soil characteristics of Amameh watershed	57
3.5 Land use distribution in Amameh watershed	57
3.6 Specifications of selected storms in Amameh watershed	69
4.1 Regression summery of bivariable Precipitation-Runoff relationship	81
4.2 Correlation matrix between precipitation and runoff parameters for Amameh watershed	81
4.3 Correlation matrix between precipitation, runoff and SCS parameters in Amameh watershed	86
4.4 Results of ANOVA for SRC for the period, 1970-1998	92
4.5 Sediment yield and peak sediment for selected storms in Amameh watershed	96
4.6 Comparison of different methods for slope length factor (LS) determination	100
4.7 Seasonal values of crop management factor in Amameh watershed	104
4.8 The characteristics of time-area segments in Amameh watershed	106
4.9 Correlation matrix between observed and estimated sediment yield values by various models	108
4.10 Storm-wise comparison of different soil erosion models in Amameh watershed	109
4.11 Storm-wise observed and computed sediment yield (tonnes) by various Models	114
4.12 Statistical analysis of multiple regression for calculation of exponent m	118
4.13 Characteristics of sub-study areas of Amameh watershed	122
4.14 Curve Number values for study sub-areas in Amameh watershed for selected storms	131
4.15 Hydrograph analysis by Reverse Routing Technique for storm event of April 23,70	133
4.16 Determination of sediment routing parameter for Amameh watershed	139
4.17 Ordinates of USGs for selected storms in Amameh watershed	142
4.18 Time area histogram characteristics of Amameh watershed	147
4.19 Derivation of IUH by using the concept of TAH and channel routing	149
4.20 Sediment routing parameter by various methods for selected storms in Amameh watershed	153
5.1 Average partial contributions of individual sub-watershed in total runoff from Amameh watershed	164
5.2 Average partial contributions of individual sub-watershed in sediment yield from Amameh watershed	166
5.3 Partial contribution of individual sub-watershed in total outputs from Amameh watershed	167

<i>Table</i>	<i>Page</i>
5.4 Observed sediment graphs (SGs) for selected storms in Amameh watershed	170
5.5 Predicted sediment graph for Amameh watershed using Model 'A'	172
5.6 IUSGs and associated 0.5h-USGs for Amameh watershed for different values of x and Z	176
5.7 Predicted sediment graph for Amameh watershed using Model 'B-1'	178
5.8 Predicted sediment graph for Amameh watershed using Model 'B-2'	180
5.9 Predicted sediment graph for Amameh watershed using Model 'B-3'	182
5.10 Predicted sediment graph for Amameh watershed using Model 'B-4'	184
5.11 Predicted sediment graph for Amameh watershed using Model 'B-5'	186
5.12 Predicted sediment graph for Amameh watershed using Model 'B-6'	187
5.13 Predicted sediment graph for Amameh watershed using Model 'B-7'	188
5.14 Predicted sediment graph for Amameh watershed using Model 'B-8'	189
5.15 Storm-wise estimated values of Absolute Relative Error for developed models	201
5.16 Coefficient of Efficiency (CE) values for different sediment graph models	203
5.17 Integral Square Error (ISE) values for different sediment graph models	203
5.18 Relative Square Error (RSE) values for different sediment graph models	204
5.19 Root Mean Square Error (RMSE) values for different sediment graph models	204
5.20 Ratio of Error (REO) values for different sediment graph models	205
5.21 Bias (B_s) values for different sediment graph models	206
5.22 Summary of prediction performance of sediment graph models using factorial scoring for Amameh watershed	208
5.23 a. Coefficient of determination (R^2) values between observed and predicted total sediment yield using various regression equations b. Coefficient of determination (R^2) values between observed and predicted sediment peak using various regression equations	209

LIST OF FIGURES

<i>Figure</i>	<i>Page</i>
2.1 Line diagram of physically based models	24
3.1 General view and location of Amameh watershed in Iran	46
3.2 Contour map of Amameh watershed	48
3.3 Longitudinal profile of Amameh River	49
3.4 Altimetric curve of Amameh watershed	51
3.5 Hypsometric curve of Amameh watershed	51
3.6 Drainage pattern of Amameh watershed	53
3.7 Severely folded and alternative geological formations in Amameh watershed	55
3.8 Geological formations of Amameh watershed	56
3.9 A view of intensive termoclastic weathering in Amameh watershed	58
3.10 A general view of soil erosion in Amameh watershed	58
3.11 Soil erosion map of Amameh watershed	60
3.12 Monthly distribution of precipitation in Amameh watershed	61
3.13 Sub-classification of climate in Amameh watershed	63
3.14 Hydro-climatic network of Amameh watershed	65
3.15 a. Baghtangeh hydrometry station in Amameh watershed b. Kamarkhani hydrometry station in Amameh watershed	67
3.16 Analysis of observed hyetograph, hydrograph and sediment graph for the storm event of April 23,70	70
3.17 Analysis of observed hyetograph, hydrograph and sediment graph for the storm event of Oct. 28,90	71
4.1 Flow chart of sediment graph model development for Amameh watershed	73
4.2 Discharge rating curve for Kamarkhani station in Amameh watershed	76
4.3 Derivation of an average 0.5-h unit hydrograph for Amameh watershed	79
4.4 Precipitation-Runoff relationship for selected storms in Amameh Watershed	81
4.5 Quadratic surface nomograph for estimation of runoff depth	82
4.6 Map showing Curve Numbers in Amameh watershed	84
4.7 Relationship between peak and volume of runoff in Amameh Watershed	88
4.8 a. Sediment rating curve for the period of 1980-1998 for Amameh watershed b. Sediment rating curve for the period of 1970-1998 for Amameh watershed	91
4.9 Confidence Area Ellipse for Amameh watershed	94
4.10 Nomograph for determination of soil erodibility factor (K) for USLE	99
4.11 Contour base and extreme point of Amameh watershed	101
4.12 Time-Area segments for Amameh watershed	107
4.13 Observed and computed sediment yield by various soil erosion models	110
4.14 Comparison of storm-wise soil loss estimation by using Hudson, EUSLE and AOF with USLE	112
4.15 Comparison of observed and computed sediment yield by using various models	116

<i>Figure</i>	<i>Page</i>
4.16 Sub-divided study units in Amameh watershed	130
4.17 Outflow hydrographs from individual sub-watershed obtained by reverse routing technique for storm event of April 23, 70	135
4.18 Log transformed ES-ER relationship	140
4.19 Derived 0.5-h and 0.25-h unit sediment graph for Amameh watershed	143
4.20 Magnitude of Isochrones in Amameh watershed	146
4.21 Time Area Histogram for Amameh watershed	147
4.22 Comparison of 0.5-h UHs obtained by using different IUH with average 0.5-h UH	150
4.23 Dimensionless Sediment Concentration Distribution curve by different methods for Amameh watershed	154
5.1 a. Average partial contribution of different sub-watersheds in generation of total runoff from Amameh watershed	
b. Average partial contribution of different sub-watersheds in total sediment yield from Amameh watershed	168
5.2 Derived IUSGs using different alternatives for Amameh watershed	177
5.3 Derived USGs using different alternatives for Amameh watershed	177
5.4 Observed and predicted sediment graphs for the storm event of April 14, 1971	192
5.5 Observed and predicted sediment graphs for the storm event of Nov 3, 1972	193
5.6 Observed and predicted sediment graphs for the storm event of July 18, 1974	194
5.7 Observed and predicted sediment graphs for the storm event of April 23, 1975	195
5.8 Observed and predicted sediment graphs for the storm event of July 22, 1976	196
5.9 Observed and predicted sediment graphs for the storm event of April 29, 1980	197
5.10 Observed and predicted sediment graphs for the storm event of April 23, 1983	198
5.11 Observed and predicted sediment graphs for the storm event of April 6, 1997	199
5.12 Relationship between observed and predicted total sediment yield values	211
5.13 Relationship between observed and predicted sediment peak values	211

LIST OF ABBREVIATIONS

%	Percent
β	Sediment routing coefficient
Δt	Time interval
Av.	Average
Aug.	August
AMC	Antecedent moisture condition
ANOVA	Analysis of variance
APE	Absolute prediction error
ASAE	American Society of Agricultural Engineers
ASCE	American Society of Civil Engineers
B _s	Bias
C	Crop management factor
CE	Coefficient of efficiency
cm	Centimeter
CN	Curve number
Dec.	December
DSCD	Dimensionless sediment concentration distribution
ER	Excess runoff (rainfall excess)
ES	Excess sediment (sediment mobilized)
Eq.	Equation
Eqs.	Equations
<i>et al.</i>	And others
Feb.	February
Fig.	Figure
Figs.	Figures
°C	Degree Celsius
g	Gram
h	Hour
ha	Hectare
i.e.	That is
ISE	Integral square error
IUH	Instantaneous unit hydrograph
IUSG	Instantaneous unit sediment graph
Jan.	January
k	Storage coefficient
K	Soil erodibility factor
km	Kilometer
L	Length slope factor
Mar.	March
Max	Maximum
mm	Millimeter
MSIC	Maximum storage index coefficient
MUSLE	Modified universal soil loss equation
MUSLT	Theoretical modified universal soil loss equation
NSMD	Not considering sediment mobilized distribution

No.	Number
Nov.	November
Oct.	October
P	Land management factor
Preci.	Precipitation
r	Correlation coefficient
R ²	Coefficient of determination
RE	Relative error
REO	Ratio of error
RMSE	Root mean square error
RRT	Reverse routing technique
RSE	Relative square error
RUSLE	Revised universal soil loss equation
S	Slope steepness factor
s	Second
S.E.	Standard error of estimation
SCS	Soil Conservation Service
Sed.	Sediment
Sep.	September
SG	Sediment graph
SMD	Considering sediment mobilized distribution
SRC	Sediment rating curve
t	Tonne
TAH	Time area histogram
TAM	Time area method
UH	Unit hydrograph
USG	Unit sediment graph
USLE	Universal soil loss equation
Viz.	Namely
x	Weighting factor
Z	Sediment routing parameter

Chapter One

INTRODUCTION

1. INTRODUCTION

Soil erosion caused by water and/or wind, also called as *creeping death*, is a continuing process which threatens the capacity of the earth to produce food, fiber, fuel and renewable sources of energy for an ever-increasing population of human and animal. It is therefore a serious cause of concern for soil conservationist, hydraulic engineers and environmentalists, world-wide. The reduction in agricultural production, increase in frequency and magnitude of floods and droughts, sedimentation in water reservoirs and conveyance systems, land degradation and ecological imbalance are some of the major tangible and intangible ill effects of soil erosion. Additionally, eroded sediment is a major air and water pollutant, causing many detrimental in-site and off-site impacts.

Conservation of soil and water and reduction of sediment outflow in watershed systems is increasingly becoming a challenge for soil and water conservationists and hydraulic engineers owing to vibrant and location specific nature of the problem. Further, soil erosion and sediment outflow are the results of very complex processes involving a large number of variables relating to rainfall, soil, topography, vegetation and also management practices. A careful measurement and analysis of such data is a basic pre-requisite for a successful planning and design of any soil and water conservation program. Sediment outflow rate is a function of runoff magnitude, which is said to be the response of a watershed system. The basic purpose of a hydrologic data analyst is to separate the response of the watershed processes from the inherent noise. This sorting can be viewed in the perspective of extracting information from recorded data because rarely are hydrologic data recorded in the forms needed for verifying hypotheses, planning and design. Since the measurement of inputs and outputs of a watershed is difficult to make with absolute

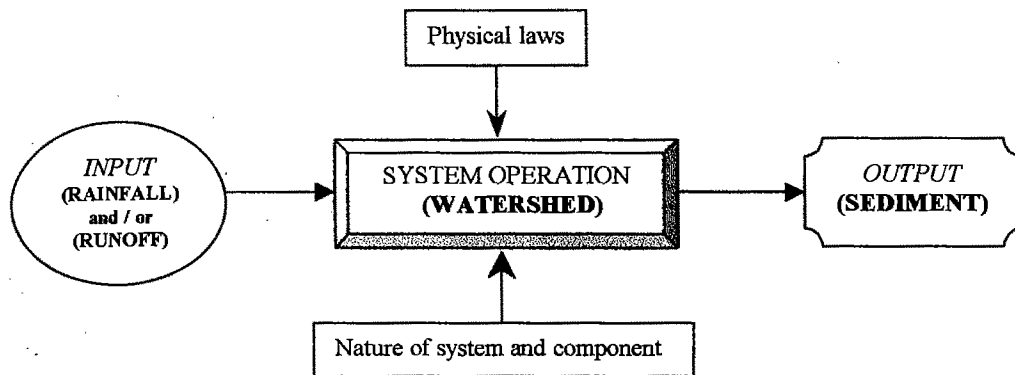
accuracy, the mathematical relationships between these variables or parameters can be established with reasonable accuracy.

A mathematical model is defined as a simplified representation of a complex process/system in which the behavior of the system is represented by a set of equations, perhaps together with logical statements, expressing relations between variable and parameters. While the consistency, type, accessibility of data, and the amount of investment influence the modeling process, the use of explainable, definable and understandable data makes it more practical.

The use of models in hydrology can be categorized into two classes. First is the *assessment* of the existing state of the water resources for the prevailing hydrological response of the watershed, based on historical, meteorological and hydrological records. The second is the *prediction* of future conditions of hydrological response, which may develop due to such influences as urbanization, intensification in agricultural and forestry land-uses, climate changes, or any physical alteration to the land surfaces due to natural and man induced causes (FAO, 1979). Models are then applied to predict the elements of information, which are required for the reconnaissance, planning, design, operation, and maintenance of the many facets of the human interaction with the natural environment. The model used for such types of predictions should be relatively simpler, and possibly the most economical one besides serving the purpose stated above.

Although, most of the modern sediment transport models are developed by linking erosion-sedimentation models with hydrologic models, but the experience of sediment modeling is not as mature as pure hydrologic modeling. Therefore, sediment modeling needs to be considered in a wider perspective and depth. Once, any one of the stages of erosion process i.e. detachment, transportation and sedimentation is modeled, various hydrologic aspects also get incorporated. Different approaches related to sediment

modeling have been suggested by several scientists working in this area of research. From the point of view of systematic approach, the watershed fluvial system can schematically be illustrated as below.



A model of basin sediment yield should, therefore, be capable of representing the increasing availability of sediment as the inter-storm period lengthens, and also should reflect the power of the storm to transport the available sediment. The *single-event modeling* process wherein the time frame of simulation is shortened, has a greater flexibility for the use of distributed parameter and shorter time increment. In such types of modeling, the rainfall excess and the sub-area hydrograph are generally obtained for a given set of initial conditions, and then the sub-area hydrographs are routed through streams, valleys, and reservoirs to the watershed outlet. Thus, event based modeling has been reported to have some merits as compared to the *long-term (sequential) modeling*. Some of the remarkable advantages of single-event models are, increase in prediction accuracy on complex watersheds, determination of sub-watershed contribution in total output, realistic modeling of sediment particle-size distribution and more appropriate computation of hydrographs and sediment graphs.

The studies in the field of sediment modeling were first reported during the 1930's, while the modeling of sediment graphs was started in the 1970's. Sediment transport models or sediment graphs, which relate sediment flow rate as a function of time, are used

for soil erosion control, hydraulic structure design, water resources planning, river morphology and water quality assessment. Besides being important for water quality modeling, sediment graphs are also useful for designing efficient sediment control structures for maximum trap efficiency and are required for the simulation of influences due to changes in land-uses on the sediment yield and its distribution.

Most of the recent works reported during the last decade in the area of sediment graphs are based on the models of **Johnson (1943)**, **Rendon-Herrero (1974 and 1978)** and **Williams (1978)**. The Johnson's study, widely applied as a general behavioral model of suspended sediment response to heavy rainfall showed that there was generally a rapid initial rise of sediment concentration with increase in discharge and that the suspended sediment concentration reached a peak before the discharge peak. The commonly used technique for the development of the *unit sediment graph* (USG) suggested by **Rendon-Herrero (1978)** is applicable only to gauged basins and the units used by him for the ordinates of the USGs are complicated and are not in general use. During the same period, **Williams (1978)** developed a model based on the *instantaneous unit sediment graph* (IUSG) applicable to un-gauged watersheds, that is based on watershed characteristics. However **Gracia (1996)** has observed that Williams' assumption of IUSG varying linearly with source runoff volume is questionable. At the same time, **Banasik (1996)** for the same model stated that the assumption of source sediment production being proportional to the square of effective rainfall can also be questioned. **Chen and Kuo (1986)** proposed a procedure to generate synthetic USG by using the *correlation analysis* but the model is able to synthesize sediment graph from one unit of effective sediment yield of a storm of one-hour duration only. Recently, **Gracia (1996)** and **Banasik (1996)** have suggested some techniques for which measured sediment graphs and hydrographs, as well as, many other inputs such as rainfall erosivity factor and intensity for a specific storm and time

parameters of hydrographs are required. A few more models, particularly computer ones, have been developed for specified areas or particular agro-climatic zones by which temporal distribution of sediment can be estimated, but their applicability appears to be limited to only well-controlled watersheds or laboratory studies, because of the requirement of a high number and specified inputs, which may not be obtained easily under field conditions.

Under the circumstances, there appears to be a need for a sediment graph model having wide applicability under natural field conditions and requiring only a few and easily accessible input data. The physical characteristics of a watershed and precipitation data are the most widely available data. If a fairly accurate and acceptable sediment prediction model, based on only these data, is developed, it may become a viable and convenient tool for researchers working in this area under actual field conditions.

The availability of reliable and accurate hydrologic data is a real problem in the Islamic Republic of Iran like many other Asian countries, which encounter different problems regarding soil erosion and flooding. Iran comprises 1648145 km² area, distributed almost evenly under the mountainous and the plain areas with an average precipitation of 365 and 95mm per annum, respectively (Mahdavi, 1992). The total runoff generated in the country is about 105 billion m³, out of which about 30 percent can be stored by dams and the rest cannot be utilized efficiently due to unsuitable temporal and spatial distribution of precipitation. Out of the total area, almost half of it is governed by arid and semi-arid climate, facing wind and water erosions, while the rest is threatened mainly by water erosion. The average annual rate of soil erosion in Iran, based on FAO's report in 1985, is above 12 tonne.ha⁻¹. The capacity of some of the important dams such as Dez, Sefidroud and Latian has significantly decreased owing to the high rate of sedimentation over the years.

Soil erosion control activities in Iran were started almost 35 years back in a very limited scale under the Ministry of Agriculture. Later, soil and water conservation measures, particularly water erosion control, were extended throughout the country in the year 1990 by establishing the Watershed Management Division under the Ministry of Jihad-e-Sazandegi. In spite of youthfulness of these treatments applied during the later periods, their effects on protection of natural resources are well visible. However, a proper assessment of the effects of these programs on watershed basis specially in respect of runoff and sediment yield has not been conducted, which could have been helpful to managers and designers to evolve a better and a more effective plan on mitigation of soil erosion and flood incidents.

In the present study, an endeavor has been made to develop a conceptual model of sediment graph, which requires only precipitation data and the information on the watershed characteristics as input. For development and application of the models, the Amameh watershed, located in the northeast direction and about 40km from the capital of Iran, Tehran, has been selected. The Amameh watershed is one of such watersheds, which has been well equipped for the collection of hydro-climatological data since about last 30 years. The study has been undertaken with the following as its broad objectives:

- i. Verification and calibration of a few hydrologic and sediment yield models, selected on the basis of available data, for their applicability on the study area**
- ii. Development of spatial distribution models to quantify partial contribution of sub-watersheds in the generation of total runoff and sediment yield from a watershed**
- iii. Development of temporal distribution models (sediment graphs) for the study area based on (i) hydrological data and (ii) watershed characteristics**
- iv. Performance based selection of best suited sediment graph model for the study watershed**

Chapter Two

REVIEW OF LITERATURE

2. REVIEW OF LITERATURE

Information relating to procedure for deriving the sediment graphs is limited and frequently only qualitative (Gracia, 1996), while their necessities were realized by the people who are working in the concerned fields. Since most of the models developed in the field of erosion process are closely related to the hydrologic models, it will be therefore difficult to categorize them in a well-separated manner. However, in the present study, an attempt is being made to review and present the available literature, which are directly related to sediment yield processes with rainfall and runoff as the inputs.

Various available models related to sediment yield and erosion processes on annual and storm basis are being classified in to nine classes as below and accordingly the review of literature is presented in this chapter.

- Statistical regression Models,
- Deterministic Models,
- Stochastic Models,
- Parametric Models,
- Dynamic Models,
- Physically based Models,
- Sediment rating, routing and delivery ratio Models,
- Sediment graph Models and
- Computer models.

The first six groups of models may basically be used to get ideas regarding sediment yield modeling for the prediction of total sediment yield delivered to the main

outlet of the watershed. While the sediment routing models considered under group seven may further be applied to model the spatial distribution of sediment yield within a watershed for which no work could be found in the literature. The references in connection with temporal distribution of sediment yield are reported under sediment graph models. Finally, the computer models under group nine are listed for general information of the readers, a perusal of which will give an idea of the genesis of development of computer models throughout the world in the field of hydrology in general and sediment yield modeling in particular.

2.1 Statistical Regression Models

In such type of models the relationship between independent (predictor) variables and dependent (criterion) variables are established. Different types of regression models consisting of linear, power, exponential and logarithmic have been used to estimate sediment yield by means of either computing gross erosion and sediment delivery ratio or directly determining sediment yield. Most of the models in this class are applicable only for the areas for which these equations were developed.

Rubey (1933) showed that the average suspended sediment concentration is proportional to $R^{1/2}S^{2/3}$, since flow discharge is proportional to $R^{3/2}S^{1/2}$ from the Chezy equation where R is hydraulic radius and S is energy line gradient.

Cook (1936) identified the three major factors viz. susceptibility of soil to erosion, potential erosivity of rainfall and runoff, and soil protection afforded by plant cover, which affect the soil erosion by water.

Gussak (1937) developed the following relationship as reported by **Warner et al. (1982)** between slope inclination (S) and soil erosion (E) for a resistant soil on the basis of data collected from experimental plots of $1.0 \times 0.4 \text{ m}^2$ in size with surface inclination of 5, 10, 20 and 30% as,

$$E = f(S^{0.4}) \quad \dots(2.1)$$

Neal (1938) found a relationship between slope (S) and soil erosion (E) and reported by **Renard (1997)** as follows:

$$E = f(S^{0.8}) \quad \dots(2.2)$$

Zingg (1940) suggested the *slope practice method* as a set of relationships between soil loss rate (A_1) and slope length (L), and degree of slope (S_g):

$$A_1 \propto L^{0.6} \quad \text{and} \quad A_1 \propto S_g^{1.49} \quad \dots(2.3)$$

Smith (1941) further modified the slope practice method (**Zingg, 1940**) by introducing crop and conservation practice factor (C') in Eq. (2.3) and suggested the following equation:

$$A = C' S_g^{7/5} L^{3/5} \quad \dots(2.4)$$

where C' is a constant depending on soil crop rotation, storm characteristics and soil treatments.

The National Committee of USA (1946) further introduced the concept of rainfall factor in the land slope practice method and suggested the following equation, which is also known as the *Musgrave* equation.

$$A = F.C. \frac{S_g^{1.35}}{10} \frac{L^{0.35}}{72.6} \frac{P_{30}}{1.375} \quad \dots(2.5)$$

where A is the sheet erosion in t.acre^{-1} , F is a factor for basic soil erosion in $\text{t.acre}^{-1}.\text{year}^{-1}$, C is cover factor and P_{30} is the maximum 30 minute rainfall depth for two years frequency in inch.

Browning *et al.* (1947) added soil erodibility and management factors to the Eq. (2.4) and prepared more extensive tables of relative factor values for different soils, crop rotations, and slope lengths.

Musgrave (1947) modified the above model (Eq. 2.5) for estimating gross erosion from watersheds in flood abatement programs. The proposed equation was,

$$A = KCR \frac{S_g^{1.35}}{10} \frac{L^{0.35}}{72.6} \quad \dots(2.6)$$

where R is the rainfall factor (rainfall erosion index) and K is the soil factor in $\text{t.acre}^{-1}.\text{Year}^{-1}.\text{unit rainfall index}^{-1}$.

Smith and Whitt (1948) presented a *rational* equation for the estimation of soil erosion (A) in Missouri as follows,

$$A = C.S.L.K.P \quad \dots(2.7)$$

where C factor is the average annual soil loss from clay pan soils for a specific rotation, slope length, slope steepness, and row direction. The other factors for slope steepness (S), slope length (L), soil erodibility (K), and support practice (P) are dimensionless multipliers used to adjust the value of C to other conditions.

Wischmeir and Smith (1958) proposed a functional relationship in the form of multiple regression, to compute kinetic energy of a rainstorm as a function of rainfall intensity, and its interaction with soil loss for cropland east of Rocky mountains, U.S.A.

They suggested the following empirical equation for the calculation of rainfall energy as a function of rainfall intensity and amount.

$$E = \sum_{k=1}^r 210.3 + 89 \log_{10} I_k P_k \quad \dots(2.8)$$

where E is the total kinetic energy of a storm in t.m.cm^{-1} , I_k is the rainfall intensity for any time interval k of rain storm, P_k is the rainfall amount in time interval k and r is the number of discrete time intervals in which the total duration is divided.

Fournier (1960) presented a simple regression models between average annual sediment yield as dependent variable and a number of climatic and topographic parameters as independent parameters by using the collected data from 78 watersheds as reported by **Morgan (1986)**. In this model the effects of rainfall erosivity and variation of vegetation cover during the year have not been taken into account.

Smith and Wischmeir (1962) developed the following relationship between soil loss (A) in $\text{m}^3.\text{ha}^{-1}$ and land inclination (S) in percent:

$$A = 0.43 + 0.30 S + 0.043 S^2 \quad \dots(2.9)$$

Dragoun and Miller (1964) found that a runoff factor was the best single predictor for the prediction of sediment yield on two small watersheds in Nebraska, USA.

The Committee of Sedimentation of Hydraulic Division, ASCE (1969) based on the previous study (**Dragoun and Miller, 1964**) stated that runoff is the best single indicator for sediment yield estimation and also pointed out that the use of runoff rate for determining sediment yield is feasible throughout the USA.

Renard (1969) has used multiple-linear-regression technique to answer some of the problems of a sediment-rating curve for semi arid ephemeral streams. He took eight

independent variables consisting of lapse time from beginning of flow, type of sampling (coding), rate of change of stage (positive for rising limb), antecedent moisture conditions of channel alluvium (exponential decay equation), distance along the channel from the moving center of the runoff producing thunder storm, peak discharge of the runoff event being sampled, storm position on the watershed in relation to vegetation cover (coding) and water discharge as measured at the flume of sampling and five dependent variables comprising of concentration of sand, silt, clay, sand+clay+silt and silt+clay have been considered.

Williams *et al.* (1971) presented a method of predicting sediment yields based on individual storms. He also found that the most often used dependent variable, the volume of sediment, is highly correlated with the volume of runoff. Williams categorized independent variables as climatic factors, watershed characteristics and land use and treatment by using the *method of factor analysis* (**Cooley and Lohnes, 1962**) for condensing the number of correlated variables to the lesser number of relatively independent factors.

Jansen and Painter (1974) presented four logarithmic regression equations for different climatic regions between sediment yield as dependent variable and area, altitude, relief, precipitation, temperature, vegetation condition and rock proneness to erosion as the independent variables. They also estimated the global denudation rate of $26.7 \times 10^9 \text{ t.year}^{-1}$ which is satisfactorily comparable with existing figures quoted by **Kuenen (1950)**, **Lopatin (1952)**, **Gilluly (1955)**, **Pechinov (1959)**, **Fournier (1960)**, **Schumm (1963)** and **Holman (1968)** as 32.5×10^9 , 12.7×10^9 , 31.7×10^9 , 24.2×10^9 , 58.1×10^9 , 20.1×10^9 and $18.3 \times 10^9 \text{ t.year}^{-1}$, respectively.

Jansen and Painter (1974) further reported the finding of **Fornier (1960)** that found the effect of the climate on soil erosion is inverted i.e. erosion being greatest in the seasonally humid tropics and declining progressively through the equatorial regions to the temperate and cold regions. They also reported the work of **Corbel (1964)** that examined erosion in four temperature zones, using three rainfall and two relief classes, and found that erosion rates vary inversely with temperature, being lowest in the tropics.

McPherson (1975) chose 36 basins in southern Alberta to investigate sediment duration curve and developed some regional equations for suspended, dissolved and total sediment yield estimation.

Stehlik (1975) devised an equation for predicting the annual rate of soil loss in Czechoslovakia by considering climatic, petrological, erodibility, slope steepness, slope length and vegetation factor.

Dendy and Bolton (1976) as reported by **Singh (1992)** proposed a relationship between annual sediment yield as dependent variable, and area and annual runoff as independent variables by using data from over 500 reservoirs throughout the USA.

Foster and Neilbing (1977) made some modification in the USLE to consider the sedimentation of eroded materials. As reported by **Warner *et al.* (1982)**, they supposed that the transportation capacity is a linear function of runoff volume and peak flow while it is related to the slope steepness with a nonlinear function.

Elwell (1978) developed a Soil Loss Estimation Model for the Southern Africa (formerly Rhodesia), called as *SLEMSA*. The model is considered to be suitable particularly for those countries, which are unable to support expensive research programs

on soil loss, but require a decision-making aid to combat soil erosion. The major constraint of this model is that it assigns a constant value for the land management factor (P).

Dunne (1979) developed a regional relationship between annual sediment yield as the criterion variable and mean annual runoff and relief as predictor variables for different land-uses for 91 watersheds in Kenya as reported by **Renard (1997)**.

FAO (1979) recommended an erosion prediction equation, which states that

$$D = f(C.S.T.K) \quad \dots (2.10)$$

where D is soil degradation $\text{t.ha}^{-1}.\text{yr}^{-1}$, C is climatic factor; rainfall in terms of yearly total, S is soil factor, T is topographic factor and K is a constant which represents the standard condition for natural vegetation and land use management factor.

Foster et al. (1980) claimed that inter-rill detachment rate (d_i), which is considered to be largely caused by rainfall impact can be expressed as:

$$D_i = a(\sin\alpha + b)RKCP \quad \dots (2.11)$$

where a and b are empirical coefficient, R , K , C , P are the USLE factors, already explained earlier, and α is slope angle.

Meyer (1981) related soil erosion to rainfall intensity as proposed a power equation between these two for a wide range of soils and cropping conditions for USA.

Murphree and Mutchter (1981) derived relationships of sediment yield and runoff with rainfall using data from two adjacent flatland watersheds in the Mississippi delta. Because of the varying conditions of antecedent soil moisture and tillage, they stratified the data into monthly periods and corresponding equations were developed.

Singh *et al.* (1981) presented a relationship between annual average erosion index and average seasonal erosion index (June-Sep.) as well as average annual rainfall and average seasonal rainfall for Naula watershed in the Ramganga river catchment, India.

Jaiswal (1982) presented a logarithmic equation for Naula watershed in the Ramganga river catchment, India, to calculate erosivity index by using the amount of rainfall.

Renard and Foster (1983) presented the factors affecting soil erosion in an equation form as,

$$E=f(C, S, T, SS, M) \quad \dots(2.12)$$

That is erosion E is a function of climate, C , soil properties, S , topography, T , soil surface conditions, SS , and human activities, M .

Tiwari (1986) developed a sediment model by considering rainfall erosivity parameter as the predictor of soil loss for different sub-watersheds of the Ramganga river catchment, India. He found that the topography, cropping practices and energy are the main control components for estimation of storm-wise sediment yield.

Kusre (1995) developed seven weekly sediment yield models with different combination of weekly rainfall erosion index, runoff volume and peak runoff rate as input for the Naula watershed of the Ramganga river catchment in India.

McConkey *et al.* (1997) investigated the seasonal variation of sediment yield and soil erodibility for three rectangular field for semi-arid cropland nearby Saskatchewan in western Canada and found that the soil erodibility varies from season to season.

2.2 Deterministic Models

A method which treats the processes as if they formed part of a determinate system, with no attempt made to represent the random processes which may or may not be present in the system is termed as *deterministic model* (FAO, 1979). In other words when probability and chance occurrence of the phenomena are ignored, the model is called as deterministic model.

Wischmeir and Smith (1965) developed a soil erosion model widely known as Universal Soil Loss Equation (USLE) by using the data assembled at the Data Center and based on the Masgrave's work. The USLE quantifies soil erosion (A) as the product of six factors representing rainfall and runoff erosiveness (R), soil erodibility (K), slope length (L), slope steepness (S), cover-management practices (C), and support conservation practices (P).

$$A = R.K.L.S.C.P \quad \dots (2.13)$$

Williams (1972) developed Modified Universal Soil Loss Equation as **MUSLE**, which is one of the modified versions of the USLE. The rainfall energy factor was replaced with a runoff factor. The runoff factor includes both the total storm runoff volume and the peak runoff rate. Compared with the USLE, this model is applicable to individual storms, and eliminates the need for sediment delivery ratios, because the runoff factor represents energy used in detaching and transporting the sediment. The following equation was fitted for 778 individual storms in 18 watersheds with 92 percent regression coefficient:

$$Y = 95(Q.q_p)^{0.56} K.L.S.C.P \quad \dots (2.14)$$

where Y is sediment yield in tones, Q is volume of runoff in acre-ft, q_p is peak flow rate in $\text{ft}^3 \text{s}^{-1}$ and other variables are similar to USLE.

Wischmeier and Foster (1974) modified the USLE for the application on the heterogeneous slopes by sub-dividing them into homogeneous sections (**Warner *et al.*, 1982**) to estimate the soil detachment at each given section.

Onstad and Foster (1975) developed an event based soil loss model as follows, in which soil detachment and transport are related to an energy factor (XI), which contains the storm rainfall term EI of the USLE in addition to storm runoff volume (Q) and peak runoff rate (q_p).

$$XI = 0.646EI + 0.45(Q \cdot q_p)^{0.33} \quad \dots (2.15)$$

Kuh *et al.* (1976) as reported by **Warner *et al.* (1982)** developed a two-dimensional model in USA for estimation of sediment load in small watersheds. To apply this model, the watershed is divided in grids and erosion rate and transportation capacity by rainfall and runoff is estimated for each grid.

Williams and Berndt (1977) expressed the Williams' sediment yield model in SI units for a slope range of 1 to 30% for agricultural watershed under American conditions as,

$$Y = 11.8(Qq_p)^{0.56}KLSCP \quad \dots (2.16)$$

where Y is sediment yield for an individual storm in metric tonnes, Q is runoff volume in m^3 , q_p is peak flow rate in m^3s^{-1} and other variables are similar to the USLE factors.

Foster *et al.* (1980) developed a model for field sized areas in USA to evaluate sediment yield under various management practices.

Das (1982) calibrated the Williams equation (MUSLE) for Naula watershed in the Ramganga river catchment, India, by introducing the exponent of 0.257 in place of 0.56.

Foster *et al.* (1982) suggested adjustments to the MUSLE to express Q and q_p respectively in mm and mmh^{-1} , and erosivity and erosion on a unit area basis.

Walling and Webb (1982) introduced the concept of *exhaustion effects* and the sediment availability for sediment yield modeling in the watersheds by analyzing the detailed records of suspended sediment concentration in several basins in Devon, UK.

Hensel and Bork (1987) introduced the MUSLE87, which is a more catchment oriented version of the USLE. It has been developed by using the parameters of upstream catchment area for each raster cell for which the soil loss is calculated, instead of the slope length factor L .

Renard *et al.* (1987) suggested a Revised form of Universal Soil Loss Equation as *RUSLE* that was designed to predict the longtime average annual soil loss carried by runoff from specific field slopes in specified cropping and management systems as well as from rangeland.

Madeyski and Banasik (1989) based on his study on small Carpathian watersheds reported that the MUSLE tends to overestimate the predicted sediment yield.

Flacko *et al.* (1990) presented the Differentiated Universal Soil Loss Equation (**DUSLE**) which is another version of the USLE modified for the Mid-European conditions, combined with a digital elevation model having the structure of a triangulated irregular network (TIN). The topography factor LS is differentiated for application on complex slope geometry.

Finney *et al.* (1993) based on their studies in Belgium mentioned that the MUSLE is a method easy to transfer to other regions although it overestimates the sediment yield.

Nicks *et al.* (1994) proposed the Theoretical Modified Universal Soil Loss Equation (MUSLT) which is another form of the MUSLE with a different coefficient and exponent in the runoff energy factor (RI) as follows:

$$RI = 2.5(Q.q_p)^{0.5} \quad \dots(2.17)$$

Nicks *et al.* (1994) further used a version of the MUSLE for prediction of soil erosion by substituting the following equation for the calculation of runoff energy (RI) in which the drainage area factor (DA) is also used besides runoff parameters:

$$RI = 1.586(Q.q_p)^{0.56} DA^{0.12} \quad \dots(2.18)$$

Nicks *et al.* (1994) introduced the EUSLE that is essentially the USLE in which the annual erosivity is replaced by an estimated storm erosivity index (EI) value derived by the following equation:

$$EI = R[12.1 + 8.9(\log r_p - 0.434)] r_{0.5}/1000 \quad \dots(2.19)$$

where R is rainfall amount, r_p is peak rainfall rate and $r_{0.5}$ is the maximum 0.5-hour intensity.

Nicks *et al.* (1994) also designated EI model for estimation of soil erosion on storm basis by replacing the erosivity factor in the USLE with a value calculated from the storm parameters by using the following equation:

$$EI = R_{0.5} \Sigma(210 + 89 \log_{10} I) \quad \dots(2.20)$$

where I is incremental rainfall intensity and $R_{0.5}$ is maximum storm 30 minutes rainfall.

2.3 Stochastic Models

When probability and chance of occurrences are considered the model is known as *Stochastic model*. All stochastic flow processes have some degree of non-stationarity in them. Sediment flow rate, analogous to runoff rate, can also be described as stochastic process having deterministic and stochastic components. Several of these models were developed by linking MUSLE with various stochastic runoff models for simulating sediment yield from channel (Smith *et al.* 1977 and Renard *et al.* 1975).

Rodriguez-Iturbe and Nordin (1968) are pioneers in the stochastic modeling of sediment hydrology. They performed time series analysis of the monthly runoff and sediment yield for the Rio Grande, New Mexico.

Woolhiser *et al.* (1971-1975) developed stochastic models of sediment yield on an event basis by considering the probabilistic relationship among sediment yield, rainfall and runoff processes.

Williams (1974) determined sediment frequency by using runoff frequency curve, obtained by using the MUSLE in two small basins at Iowa for five different frequencies.

Renard and Lane (1975) linked a stochastic runoff model to the MUSLE model for simulating sediment yield from the channels.

Vansickle (1982) found that in Pacific North Western USA nearly all sediment transported during the brief distinct runoff event that can be described stochastically by Poisson distribution.

Chaurasia (1985) developed a stochastic model of sediment flow for the Naula watershed of the Ramganga reservoir catchment, India, to generate long term likely future sequences of sediment flow and forecast short term future events by proposing a second order auto-regressive model for the watershed.

Singh and Krstanovic (1987) applied the principle of maximum entropy to derive a probability distribution of sediment yield conditioned on the probability distribution of direct runoff volume. The model was tested for three watersheds in USA.

Agarwal *et al.* (1989) used a second order auto-regressive seasonal model to develop a stochastic model of wash load for a watershed of the Ramganga river catchment in India.

Mall (1990) simulated monthly sediment yield for future events by using the forecasted rainfall values obtained by a stochastic model for the Naula watershed, India.

Pathak (1990) successfully applied the *Walsh Auto Regressive* (WAR) model, developed by **Singh (1979)**, for one-year future prediction of weekly rainfall for Bino watershed of the Ramganga river catchment in India to predict weekly sediment yield values for one-year in advance.

Singh (1990) developed a new technique of data characterization through Fourier Spectrum analysis in conjunction with Box-Jenkins type auto regressive model to predict weekly rainfall values which were used to develop a sediment yield prediction model for Bino watershed in the Ramganga river catchment, India.

2.4 Parametric Models

Parametric models are based on the watershed parameters and lies between deterministic and stochastic modeling. The parametric approach strives for the definition of functional relation between hydrology, geometry and land use characteristics of the catchment. This modeling approach involves the *model formulation, data collection, data processing, model evaluation, visualization of model parameters* and *prediction for ungauged watersheds*.

Negev (1967) developed a basin sediment yield model as an extension to the Stanford watershed model by incorporating some of the basic hydrological principle.

Gunawardena (1989) modified and tested the Stanford sediment model for four small catchments in Sri Lanka and found it reasonably accurate estimator of sediment yield from upland areas for different vegetative and topographic condition.

Sharma *et al.* (1989) estimated silt production rate for Machkund basin in Orissa, India by using rainfall and some of the catchment characteristics such as drainage density, stream frequency, stream grade, shape index as independent variables.

Ojasvi *et al.* (1994) developed a model by considering the rotundity, circularity and compactness factors for estimating sediment production rate on yearly basis for Khowai river catchment in TriPura.

Bundela *et al.* (1995) developed a dimensionally homogenous and statistically optimal model for the prediction of sediment yield from small watersheds in Barakar river valley Bihar, India.

2.5 Dynamic Models

Dynamic models are *input-output models* in which the present response is affected by past values of excitation and the response, which are present on the memory of the system. In other words the dynamic models represent processes that involve changes over time.

Sharma *et al.* (1979-1980) considered log-transformed values of runoff and sediment sequences on a monthly or daily basis as input and output respectively for a watershed fluvial system in Thames river catchment in Southern Ontario, Canada. They found the first order dynamic model to be adequate to model the monthly runoff-sediment yield process and second order dynamic model for daily runoff-sediment yield process.

Srivastava *et al.* (1984) developed a linear time-invariant dynamic model for a small watershed of Nainital in India using system approach.

Tabrizi *et al.* (1990) developed a dynamic prediction model using identification techniques to predict water table fluctuation in terms of rainfall, potential evaporation and ditch elevation. They also observed that such an approach can be adopted to model runoff or sediment yield processes.

Sharma *et al.* (1993) developed a linear time invariant dynamic model for predicting the sediment transport in the arid zone drainage basin of Luni river in India. They considered the sediment transport as a function of present runoff rate and recent past runoff rates and sediment transport values.

Pyasi (1997) found that only past three successive events with the weights of 44.84, 32.13 and 23.03% respectively have had influences on the present outputs of the

rainfall-runoff-sediment processes models for Naula watershed in the Ramganga river catchment, India. He also found that the dynamic non-linear sediment yield models developed for the runoff- sediment and the rainfall- runoff-sediment processes on daily and weekly basis are applicable for the study area.

Kumar and Das (2000) found that the rainfall-runoff-sediment yield processes is a better approach than the models based on runoff-sediment processes to model sediment yield prediction on the Naula watershed of the Ramganga river catchment, India.

2.6 Physically Based Models

The general algorithm for models in this category is shown in Fig. 2.1, in which the dynamics of each phase may be described by fundamental hydraulic, hydrologic, meteorological and other physical relationships plus parameters describing the soil properties that influence erosion. In the figure, D and T represent detachment and transportation, and suffices R and F stand for rainfall and flow, respectively.

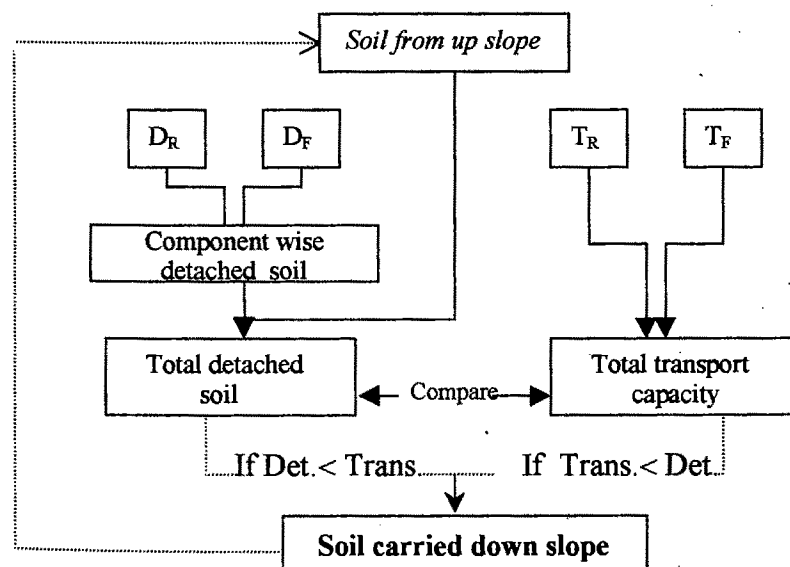


Fig. 2.1 Line diagram of physically based models

Yalin (1963) proposed an equation for the determination of sediment transport capacity based on flow hydraulics, sediment diameter and density (**Warner, *et al.* 1982**).

Meyer and Wischmeier (1969) suggested an approach for erosion simulation that considered soil detachment and transport by rainfall, and soil detachment and transport by runoff and appropriate equations were presented by them for each segment.

Foster and Meyer (1972) developed a relatively simpler method for soil erosion estimation by using the *mass conservation law* and the relationship between sediment detachment and transportation capacity as quoted by **Warner *et al.* (1982)**.

Foster *et al.* (1977) as reported by **Wilson *et al.* (1981)** developed a soil erosion model for prediction of rill and inter-rill erosion, called as *FMO*, based on continuity equation for sediment transport.

Warner *et al.* (1982) reviewed the work of **Crosby and Overton (1979)** on sediment parametric models as presented by **Foster and Meyer (1972)**

Moore and Clarke (1983) modeled processes of sediment accumulation and detachment within a river basin and sediment transport to the basin outlet.

Julein and Simon (1985) identified that slope, unit discharge rate, rainfall intensity and shear stress are acting to detach soil, as the dominant geometric and flow variables and determining the sediment transport capacity.

Hartley (1987) developed Simplified Process (*SP*) model, which predicts sheet and rill erosion due to single storms from sloping surfaces, subjected to a constant rainfall intensity.

Borah (1989) presented the sediment discharge component of a watershed simulation model called as *RUNOFF* to simulate space and time distributed soil erosion, sediment transport and sediment deposition for prediction of sediment discharges in a small watershed resulting from a single rainfall event. The model is based on discretization of a watershed into a number of representative overland and channel flow elements and simulation of sediment processes in each of these elements.

Guy et al. (1992) have evaluated the ability of six fluvial transport equations for estimation of sediment generated by shallow over land flow affected by rainfall.

Kothyari et al. (1997) mentioned that the flow of sediment laden runoff is treated as one dimensional and unsteady phenomenon in which imbalance between sediment supply and transport capacity cause erosion or deposition in the watersheds. They further suggested that these processes are inter-related and must satisfy locally the conservation principles of sediment mass, expressed by the sediment continuity equation.

Nema (1998) developed a laboratory setup in Pantnagar, India, to study the effects of rainfall and land slope variability on the soil erosion process. He found that the multiple regression power models, relating interrill soil erosion rate and sediment transport capacity with rainfall intensity and land slope have a very high level of dependency.

2.7 Sediment Rating, Routing and Delivery Ratio Models

These types of model have been probed in recent decades for their effective application in sediment yield modeling. In sediment rating models the relationship between sediment concentration and water discharge are considered, through which by knowing the specific flow rate, the amount of sediment is determined. It should be noted

that the dissolved sediment rating-curves indicate that there is a decrease in sediment concentration with increasing discharge, whereas the suspended sediment rating curves indicate the reverse trend. A Sediment routing model increases sediment yield prediction accuracy, allows determination of sub-watersheds' contribution to the total sediment yield and predicts the location and amounts of flood plain scour and deposition. The ratio between the sediment at the watershed outlet and the gross erosion is termed as *sediment delivery ratio*.

Wolman and Miller (1960) stated that the amount of sediment transport by flows of a given magnitude depend on the form of the relationship between discharge and sediment load and on the frequency distribution of the discharge events. The product of transport rate and frequency gives the cumulative sediment load transported by a given discharge as reported by **Barfield *et al.* (1981)**.

Maner (1958-1962) developed the relationships between sediment delivery ratio and relief-length ratio as well as watershed area and found that the power equation working well for Oklahoma and Texas, USA.

Roehl (1962) also considered area as a dominant factor on delivery ratio and developed a curve between area and delivery ratio.

Beer *et al.* (1966) as reported by **Barfield *et al.* (1981)** reviewed and evaluated the various techniques currently to predict values for the three components of the erosion process, viz. erosion, transport and deposition in Western Iowa.

Williams(1975) developed a sediment routing technique to route sediment yield from small watershed ($\leq 65 \text{ km}^2$) through stream and valley to the outlet of large

watersheds ($\leq 2600 \text{ km}^2$). The procedure was based on the assumption that sediment deposition depends on settling velocity of the sediment particle, length of travel time and amount of sediment in suspension. These assumptions are expressed by the following sediment routing equation:

$$Y = \sum_{i=1}^n Y_i e^{-\beta T_i \sqrt{d_i}} \quad \dots(2.21)$$

where Y is sediment yield from an individual storm for the entire watershed, Y_i is the sediment yield from the i^{th} sub-watershed predicted by MUSLE, β is the routing coefficient, T_i is the travel time from sub-watershed i to the watershed outlet and d_i is the median particle diameter of sediment.

Betson (1976) introduced a relationship between sediment concentration as the dependent variable, and flow discharge and watershed area as the independent variables based on the data collected from 19 watersheds in USA (**Warner, et al., 1982**).

Gong and Jiang (1977) defined a relationship between runoff discharge and sediment discharge by using log-log paper and provided six logarithmic equations with correlation coefficient of 0.983 to 0.991 for six watersheds in china with area within 0.18 to 187.0 km^2 .

Li et al. (1977) developed a single event sediment routing model for application on small watershed and channel processes were not considered. The model considers suspended and bed load, separately (**Warner et al., 1982**).

Onstad and Bowic (1977) simplified the Williams routing model for use in routing average annual sediment yields, in this model they neglected particle size and did not include a degradation component.

Williams (1977) computed sediment delivery ratio on 15 watersheds in Texas using sediment and runoff models. These ratios were related to area, watershed relief, maximum valley length and long term average of curve number (*CN*).

Alonso *et al.* (1978) modified the infiltration, water and sediment routing schemes of the Li's model. Both the models require calibration with measured sediment data.

Williams and Hann (1978) refined William's routing model by replacing the median particle size with entire particle size distributions i.e. the sediment load is separately estimated for each class of particle size.

Barfield *et al.* (1979) as reported by **Wilson *et al.* (1984)** estimated the value of sediment delivery ratio by considering the particle size distribution as fine and large particle size.

Novotny (1980) found that the Williams' equation is applicable only to cases for shallow flow and impoundment.

Williams (1980) recommended the following equation as quoted by **Wilson *et al.* (1984)** to calculate the delivery ratio for the MUSLE to the sub-watershed outlet.

$$D_R = \left(\frac{q_p}{I_{ep}} \right)^{0.56} \quad \dots(2.22)$$

where D_R is delivery ratio, q_p is the peak discharge for the sub-watershed and I_{ep} is the peak rainfall excess rate.

Barfield *et al.* (1981) presented an equation for the determination of sediment delivery ratio for a mined watershed by incorporating the effects of surface conditions, vegetation cover, channel system and disposal materials.

Phien (1981) presented a procedure to estimate sediment volume accumulated in a reservoir for a given time span. He used the basic relationship between the sediment flow rate and river discharges on annual basis, and proposed the following equation

$$G = aQ^b \quad \dots(2.23)$$

where G is the suspended sediment load in t.day^{-1} , Q is river discharge in m^3s^{-1} and a , b are constants.

Das (1982) developed a sediment routing model for Naula watershed of the Ramganga reservoir catchment in India by using runoff as input. The model developed was:

$$S_y = \sum_{i=1}^n Y_i e^{-T_i / K_s} \quad \dots(2.24)$$

where S_y is the total sediment yield in metric tonnes, Y_i is the sediment yield in metric tonnes from sub-watershed i obtained from MUSLE and T_i is the travel time in hours between sub-watershed i to watershed outlet, taken to be equal to time of concentration between two points, K_s is the storage coefficient and n is number of sub-watershed.

Deva *et al.* (1982) developed a one-dimensional numerical model for simulating the movement of well-graded sediments through a stream network. The model is based on the physical process governing the mechanics of sediment movement in alluvial channel.

Walling (1983) while analyzing the Williams' routing equation expressed doubts on the consideration of sediment particle diameter and the settling velocity of sediment particle in the equation.

Hadley *et al.* (1985) subdivided the watershed into square grids and then defined sediment delivery ratio as the proportion of average land slope of the given (draining) cell to that of the adjacent (receiving) cell.

Loughran (1986) developed a relationship between suspended sediment concentration and flow discharge separately for winter and summer seasons in New South Wales, Australia.

Probst (1986) used *partial balance method* to calculate monthly suspended sediment load. In this technique, sediment estimation was done by using a suspended sediment concentration-discharge relationship.

Tiwari (1986) attempted to develop a routing model for sediment yield estimation with rainfall energy as the input, and to apply a previously developed routing model with runoff as input on the Marchula watershed of the Ramganga reservoir catchment, India.

Ashmore and Day (1988) developed histograms to show relationships between discharge and sediment (and also frequency). These histograms were classified into five group's viz. single mode, erratic, effective discharge within the normal duration, effective discharge at the upper end of the range and broad peaks.

Williams (1989) introduced different shapes of discharge versus sediment concentration plots viz. single valued (straight or curve), clockwise loop, counterclockwise loop, single valued plus a loop and figure eight.

Chakrapani and Subramanian (1990) considered annual, seasonal, monthly and daily variation of water and sediment in Mahandi river basin, India. They showed that 95 percent of sediment load in this river is carried during monsoon.

Das and Chauhan (1990) developed a routing model, using the *first order decay function*, to predict sediment yield by applying the calibrated MUSLE on each sub-watershed of Naula watershed in the Ramganga river catchment, India.

Ebisemiju (1990) found that a man-induced change from vegetated to bare soil results in a 400-fold increase in the volume of eroded soil, while it causes only 3-fold increase in soil loss magnitude. He also found that the slope gradient and length are the dominant factors in south-western Nigeria controlling sediment delivery to stream channels from bare and vegetated slopes, respectively by applying stepwise multiple regression models.

Crawford (1991) introduced the method of *flow-duration, rating-curve (FDRC)* which is commonly and for long been used to estimate mean suspended-sediment loads. The model is based on power relationship between suspended sediment and stream flow.

Singh (1992) found that the sediment discharged to large river is usually less than one-fourth of that eroded from the land surface.

Kothyari et al. (1994) developed the time area technique based on Kling's method (**Hadley et al., 1985**) of delivery ratio for the prediction of sediment yield in comparison with some of the conventional techniques for the estimation of soil loss.

Sharma et al. (1996) used the upland sediment delivery model and tested it for 10 arid upland basin of Luni river in India. To account the basin complexity, each basin was segmented into upper, middle and lower zones based on the degree of steepness and stream order.

Ferro *et al.* (2000) proposed a sediment distribution (SEDD) model applicable on morphological unit scale, into which a basin is divided. The model is based on the USLE coupled with a relationship for evaluating the sediment delivery ratio of each morphological unit.

2.8 Sediment graph Models

Sediment graph is graph of suspended load associated with hydrograph caused by rainfall (**Banasik, 1995**). In another definition sediment graph is defined as graph of suspended sediment flux versus time. The available literature in this field is reviewed as follows:

Johnson (1943) presented one of the first studies on the relationships between the ordinates of the stream flow hydrograph and the sediment graph for a small catchment. He developed a distribution graph of suspended sediment concentration, which is analogous to hydrograph. He showed that there was commonly a rapid initial rise of sediment concentration with increasing discharge and the suspended sediment concentration reached a peak before the discharge peak.

Einstein (1950) found that Johnson's method for analysis of sediment distribution has a practical application with a minimum of cost for small and uniform watersheds.

Heidel (1956) pointed out that depending on the location of the gauging point in a stream, the sediment graph peak will either *precede*, *coincide* with or *lag* behind the peak of the watershed hydrograph.

Rendon-Herrero (1974) developed an approach called as *series graphs* for small watersheds in Bixler Run. The series graph method is analogous to Sherman's unit hydrograph procedure of a direct discharge hydrograph. The series graph method is used where the quantitative analysis of wash load is necessary for estimation of total sediment discharge from a storm or its variation with time or both.

Bruce *et al.* (1975) introduced a mathematical model describing the rate of quantity of runoff, sediment and pesticides transported from a watershed in the piedmont plain in Georgia on storm basis. They found that sediment contribution from inter-rill erosion is a function of rainfall intensity and soil susceptibility to erosion, whereas the rill erosion is a function of surface water runoff and the rate of change of water runoff.

Piest *et al.* (1975) found a relationship between sediment graph and hydrograph for the gully erosion in Kentucky, USA.

Renard and Laursen (1975) computed a sediment graph by multiplying the storm hydrograph flow rates with the concentration predicted by Laursen's sediment transport model (1958). This approach was found to be adequate for areas where the sediment transport model is applicable.

Rendon-Herrero (1978) proposed that in watersheds where the loci of the hydrograph and sediment graph are *parallel* to each other, the assumptions made in unit hydrograph analysis are also applicable for the analysis of the unit sediment graph. That is, the surface runoff that produces a hydrograph is in many situations also the cause of and agent for transporting upslope sediment to the streams in the basin.

Williams (1978) developed a technique for estimating the sediment graph, based on the *instantaneous unit sediment graph (IUSG)* and the modified universal soil loss equation (MUSLE). He proposed that the IUSG is similar to the IUH in that it is the distribution of sediment from an instantaneous burst of rainfall producing one unit of runoff.

Overton and Crosby (1979) developed a sediment graph for a mined watershed in USA based on the determination of watershed *load modules* i.e. mass of sediment to volume of runoff (**Warner, 1982**).

Ward et al. (1979) used hydrograph for the development of sediment graph for a certain amount of sediment yield and proposed a power equation between sediment concentration and flow discharge.

Asokan (1981) derived series graphs, based on the methodology proposed by Rendon-Herrero (1974), for Bino sub-watershed of the Ramganga catchment, India.

Singh and Chen (1981) demonstrated that a linear relationship between log-transformed values of sediment yield and effective rainfall existed for 21 watersheds in USA ranging in area from 45 to 2200 km².

Singh et al. (1981) used a modified version of the IUSG, as proposed by Williams (1978). To estimate the suspended *sediment concentration distribution (SCD)* they replaced the sediment routing parameter and the square root of particle diameter by a single parameter *B*. They found that the IUSG is essentially identical to the IUH for a specified event and in turn suggested that the *B* is close to zero (0.08h⁻¹) by using rainfall-runoff-sediment yield data for 13 events on a small watershed (4km²) in Mississippi.

Linsley *et al.* (1982) as reported by Chen and Kuo (1986) suggested the technique of *dimensionless unit sediment graph*, similar to dimensionless unit hydrograph for transposing unit sediment graph in case of absence of sufficient recorded data of discharge and sediment rate.

Das (1982) developed a synthetic unit Sediment graph model for application on the Himalayan watersheds of the Ramganga river catchments in India. He developed the design sediment graph by using mobilized sediment as the input.

Walling and Webb (1982) mentioned that the suspended sediment concentration - discharge relationship or rating curve for a drainage basin is essentially *deductive* and reflects the overall pattern of erosion and sediment delivery operation isolating and interpreting salient features of basin sediment response. This relationship can be presented in the form of sediment concentration-discharge relationship (plotting on logarithmic coordinates) and storm flow sediment concentration-storm flow discharge relationship (in the form of hydrograph and sediment graph).

Prasad (1983) derived a unit sediment graph and dimensionless USG for Bino watershed of the Ramganga reservoir catchment in India by modifying Snyder's method (1938) and Williams model (1978). He used synthetic and dimensionless USG to generate sediment flow graphs.

Srivastava *et al.* (1984) derived USGs for two small agricultural watersheds of the Ramganga river in India to predict sediment flow graph. He also developed linear-time invariant dynamic model for generating sediment graph.

Kumbhare and Rastogi (1985) developed a unit sediment graph for Gagas watershed of the Ramganga reservoir catchment and found that the generated sediment flow graphs were in good agreement with observed graphs.

Bajpai (1986) developed an IUSG model applicable to Naula watershed in the Ramganga catchment in India by combining the IUSG model developed by **Williams (1978)** and the sediment routing model for Naula watershed proposed by **Das (1982)**.

Chen and Kuo (1986) presented a model based on a one-hour unit sediment graph, which is defined as the direct sediment graph resulting from one unit of effective sediment yield of a storm of one-hour duration generated uniformly over the basin at a uniform rate. Authors supposed the *linearity* and *time invariance* concept to derive sediment graph for small un-gauged watersheds.

Raghuvansi (1986) developed series graphs for the prediction of temporal distribution of sediment wash load from Chaukhatia watershed of the Ramganga river in India.

Dube (1987) applied **HYMO** model that is a problem-oriented language, for modeling the design sediment graphs for large watersheds on per storm basis. Curve number, routing model and two parameters of Nash conceptual model were used to get necessary factors for sediment graph development.

Kumar and Rastogi (1987) determined the parameters of the Nash model from storm sediment graphs instead of storm runoff hydrographs, which express the shape of the IUSG. The hydrological parameters of Nash model have been substituted by parameters, which are related to sediments. The trend in crest segments and peak ordinates

of IUSGs for different years were used to find out the effects of soil conservation measures on sediment flow.

Jha (1988) developed an IUSG for Chaukhatia watershed of the Ramganga river in India by routing the mobilized sediment graph through a series of linear reservoirs and a series of linear channels.

Kumar (1988) developed sediment graph models for mountainous areas in the Ramganga river catchment in India by using the concept of IUSG proposed by **Williams (1978)**.

Banasik (1989) used the direct hydrograph data of some storm events in Devon, UK, and presented an equation for calculating direct sediment yield by using the volume of direct hydrograph and peak discharge of direct hydrograph. He also calculated sediment concentration as dimensionless parameter for obtaining IUSG ordinates.

Banasik (1990) suggested an idea for the estimation of sediment graph based on the concept of IUSG. He considered two hydrologic and sedimentologic sub-models. The SCS method and Nash model were used to evaluate excess runoff and IUH in hydrologic sub-model while MUSLE was applied in sedimentologic sub-model for the analysis of sediment yield and unit sediment graph.

Das and Agarwal (1990) utilized the concepts of Clark model (1945) for IUH to predict sediment graphs by using rainfall data as input. The time area histogram (TAH) by applying a time area diagram of sediment mobilized (as equivalent to rainfall excess in runoff analysis) and sediment storage constant were used for the development of model.

Kumar *et al.* (1990) routed mobilized sediment through a series of linear reservoir, for Gunawardena for the prediction of sediment graph. The storm sediment graphs were generated by convoluting IUSG with corresponding values of mobilized sediment of storms.

Jeje *et al.* (1991) as quoted by **Gracia (1996)** offered detailed information about sediment graph measurement and the respective phenomenon was well described but no computation criteria were proposed.

Wang *et al.* (1991) developed discrete linear models for estimating runoff hydrographs and sediment discharge graphs from the Losses plateau in China. They proposed the linear discrete transfer function model is superior to regression equation, which can not account for the time-series nature of rainfall, runoff and sediment discharge processes.

Banasik and Woodward (1992) studied the influence of partial deforestation upon sediment yield and shape of sediment graph. They developed a sediment graph model by incorporating hydrologic and sedimentologic sub models. The IUSG (**Williams, 1978**), which is the product of IUH flow rates and the sediment concentration distribution was then used for the development of sediment graph.

Basu (1993) developed three unequal linear reservoir cascade model, two unequal linear reservoir cascade model and Muskingum model for Mynaly and Ebbanad sub-watershed of lower Bhanvani catchment, Tamil Nadu, India. He determined the parameter of model by using optimization techniques, namely, *down hill simplex method*, *quadratic programming* and *Langrange multipliers method*. The models were used to compute temporal distribution of suspended sediment yield on storm basis.

Raghuwanshi *et al.* (1993) developed a conceptual model of the IUSG based on routing time area histograms to generate the temporal distribution of wash load on storm basis and applied the model on Chaukhutia watershed of the Ramganga river catchment, India. The IUSG was converted into a USG and was convoluted with the mobilized sediment for generation of sediment graph.

Kumar (1994) developed discrete linear models of sediment mobilized-sediment discharge, direct runoff-sediment discharge and rainfall excess-sediment discharge for Chaukhutia watershed of the Ramganga river basin in India. The results of developed model were then compared with actual sediment graphs satisfactorily.

Sharma and Murthy (1994) derived a sediment graph model at the outlet of the channel in Luni basin in North-West India by using the *standard sediment rating curve technique* and a lumped model based on the IUSG concept. They found that IUSG gives a better estimate of sediment transport rather than sediment rating curve because it considers the availability of erodible material in the channel bed. They used the concept of Nash conceptual model for developing IUSG. Then IUSG convoluted with the mobilized sediment, estimated by an empirical multiple regression, generates the sediment graph at the channel outlet.

Banasik (1995) developed the following equation associated with the ordinates of IUSG:

$$S(t) = \frac{U(t).C(t)}{\int_0^{\infty} U(t).C(t)dt} \quad \dots(2.25)$$

in which $S(t)$ is the ordinates of IUSG, $U(t)$ is the ordinates of IUH obtained by applying conceptual model (Nash), and $C(t)$ is the ordinates of dimensionless sediment

concentration distribution. Some of the characteristics of IUSG i.e. time to peak and peak rate of sediment flow of the IUSG were calculated by some empirical equations.

Banasik and Walling (1996) studied the relationship between the lag time of the direct runoff hydrograph and the lag time of the sediment graph. The relationship then was used in derivation of IUSG and its applicability was examined for prediction of sediment graph for the River Dart, a west-bank tributary of the River Exe, in South-West England.

Gracia (1996) developed a method for generation of *synthetic sediment graph* based on the IUH theory for flood prediction and on the convolution integral theory (McCuen, 1989). The method is applicable in areas where physical information of the watershed i.e. areas, slopes, length of channels and soil type are available. He classified the sediment graphs of suspended sediment concentration into *advanced, delayed, in phase* and *multiple peaks*. Gracia applied Horton method for concentration time, Manning's formula for travel time and USLE for soil erosion computations.

Kothyari et al. (1996) combined the notion of time-area curve with the concept of sediment delivery to develop a method for prediction of the variation of sediment yield with time. Surface erosion within any time-area segment was computed using USLE. The delivery ratio for two adjacent segments was taken equal to the ratio of their land slope. The sediment yield curve was drawn for each segment with the base time of double travel time considered for isochrone and peak value was such that the area under the curve is equal to the sediment yield from the respective segment. Superposition of individual curves resulted the temporal variation of sediment yield.

Kothyari et al. (1997) applied the *kinematics wave equation* for simulation of over land flow whereas continuity equation for sediment flow and expressions for sediment

detachment and transport were used to compute the temporal variation of sediment yield for single storm-events in small watersheds. The technique was solved numerically, and applied on 12 experimental watersheds with varying climates, and ranging in size from 0.002 km² to 92.5 km².

2.9 Computer Models

Computer models are used to represent complex processes, such as erosion and sediment yield and also to save time and investment. Although all the mentioned models and techniques presented under other categories (Articles 2.1 to 2.8) can be computerized, but for simplicity and to have a general idea about the trend of development of computer models a brief review is offered in a tabular form as follows:

Table 2.1 Some of the computer models in the field of erosion processes

No.	ACRONYM	MODEL FULL NAME	YEAR REFERENCE	TYPE	Process
1	ACTMO	Agricultural Chemical Transport Model	Frere <i>et al.</i> 1974,1975	L	ERPN
2	AGNPS	Agricultural Non-point Source	Young <i>et al.</i> 1987	DPCV	ERN
3	AGRUN	Agricultural Runoff model	Doniglan <i>et al.</i>	Y	ER
4	ANSWERS	Areal Non-point Source Watershed Environmental Response Simulation	Beasley and Luggins 1980	PCV fd	ERN
5	APEX		Williams <i>et al.</i> 1998	DE	ER
6	ARM	Agricultural Runoff Model	Donigian and Crawford 1977	LECT	ERPN
7	CELMOD5		Karnieli <i>et al.</i> 1994	DEC	ER
8	CHISCI	Author	Chisci <i>et al.</i> 1983	V	ER
9	CREAMS	Chemical Runoff and Erosion from Agricultural Management Systems	Kinsel 1980	LOCT V	ERNP
10	CSU	Colorado State University model	Li 1976-1980	DPCV fd	ER
11	CURJIS	Author	Curlts 1976	D	ER
12	DUSLE	Differentiated USLE	Flacke <i>et al.</i> 1990	DECT	E
13	EPIC	Erosion Productivity Impact Calculator	Willimas <i>et al.</i> 1984	LOFT	ERNC
14	ERARRB	Environmental Pollution Assessment Erosion Sediment and Rural Runoff	True 1976		E
15	EROSION2D	2-D rainfall erosion model	Schmidt 1991	DPSV fe	ER
16	EUROSEM	European Soil Erosion Model	Morgan <i>et al.</i> 1991	DPCV fe	ER
17	GAMES	Guelph model for evaluating the effects of Agricultural Management Systems on Erosion and Sedimentation	Dickinson <i>et al.</i> 1986	DECT fe	E
18	GAMESP	Agricultural Management Systems on Erosion, Sedimentation, Phosphorus	Rousseau <i>et al.</i> 1985		EP
19	GLEAMS	Groundwater Loading Effects of Agricultural Management Systems	Leonard <i>et al.</i> 1987	LOCTV	ERNP
20	GUST	Griffith University Erosion System Template	Misra and Rose 1989	DOCV	ER
21	HILLS	HILLSlope imulation model	Smith and Hebbert, 1983	L	R
22	HSPF	Hydrological Simulation Prog. Frotra	Barnwell and Johanson 1981	LECT	ERNP
23	KINEROS	KINematic EROsion Simulation	Alonso and Decoursey 1985	DPCV fe	ERN
24	KYERMO	Kentucky Erosion Model	Hirschi and Barfield 1988	DPCV fd	ER
25	LAMDRYM	Land use effect on water quality	Novotny 1976		ER
26	LISEM	Limburg Soil Erosion Model	In preparation 1994	DPCV fd	ER
27	LUMOD	Land Uso MOdel	Leaf chales, Glen.E, Brink		E
28	MEDALUS	Mediterranean Desertification And Land Use	Kirkby <i>et al.</i> 1992	DPST fe	ERC
29	MODANSW	MODified ANSWers model	Park <i>et al.</i> 1982	DPCV fd	ER
30	NEGEV	Author	Negev M.A. 1976		E
31	NPS	Non-point Pollutant source	Donigian and Crawford 1976-1977		ERNP
32	NTRM	Nitrogen Tillage residue management	Shaffer <i>et al.</i> 1983		EC

Continued Table 2.1

33	OPUS	Field scale water quality model	Smith and Kinsel 1985	DPFTV fd	ERNC
34	PERFECT	Productivity, erosion, Runoff Functions to Evaluate conservation Techniques	Littleboy <i>et al.</i> 1989		ERC
35	ROSE	(author)	Rose <i>et al.</i> 1983	DOSV	ER
36	ROTO	Routing Outputs To the Outlet	Arnold, 1995	DCE	ER
37	RUSLE	Revised USLE	Renard <i>et al.</i> 1987	LEFT	E
38	RUNOFF	Renamed SEDLAB, 1981	Borch, 1989	DCE	ER
39	SEDEL	SEdiment DELivery ratio	Borce R. C 1975	LEM	E
40	SEDIMOT	SEmentology Distributed MOdel Treatment	Wilson <i>et al.</i> 1986	DCE	ER
41	SEM/SHE	Soil Erosion Model/SHE	Storm <i>et al.</i> 1987	DPCV fd	ER
42	SHESED-UK	Soil Erosion Model/SHE-UK	Wicks <i>et al.</i> 1988	DPCV fd	ER
43	SIMSED	SIMplified SEDiment yield model	Cotton, Li 1983		E
44	SOLOSS	Modified USLE for N.S.W Australia	Rosewell and Edwards 1988		E
45	SP	Simplified Process model	Hartly 1987	DOFV	ER
46	SPNM	Sediment, Phosphorus, Nitrogen Model	Williams 1980		EN
47	SPUR	Simulation of Production and Utilization of Range lands	Lane 1982, Wight 1983		ER
48	SSAM	Stream flow Simulation and Analysis Model	Beston, Roger and Harold 1977	EC	ER
49	SWAM	Small Watershed Model	Alonso and Decoursey 1985	DPCV fe	ERN
50	SWAT	Roto and SWWRB interface	Arnold <i>et al.</i> 1990	DCT	ER
51	SWMM	Storm Watershed Management Model	Metcalf and Eddy 1971; Huber <i>et al.</i> 1981	E	ERP
52	SWRRB	Simulator for Water Resources in Rural Basins	Williams <i>et al.</i> 1985	DC	ER
53	TOPOG		Vertessy <i>et al.</i> 1990		ER
54	WEPP	Water Erosion Prediction Project	Nearing <i>et al.</i> 1989	DSPTV fd	ER
55	WEPS	Wind Erosion Prediction System	Hagen <i>et al.</i> , 1995	PT	E
56	WEST	Watershed Erosion, Sediment Transport	Leytham, Johanson 1979; foster 1987; Lane 1988	P	ER
57	Wright/Webster	(Authors)	Wright and Webster 1991	DPSV	ER

Legend:

Type:

D/L = Distributed/Lumped
P/O/E = Physically-based/Conceptual/Empirical
C/T/F = Catchment/Hillslope/Field
V/T = Event/Continuous
fe/fd = Finite element/Finite difference

Process:

E = Erosion
R = Runoff
N = Nutrient
P = Pesticide
C = Crop growth

Chapter Three

STUDY AREA AND HYDROLOGICAL DATA

3. THE STUDY AREA AND HYDROLOGICAL DATA

To verify the applicability of models during their stages of development and calibration a reasonably reliable data set are required. At times, the nature and complexity of models are controlled by the type and the extent of available data. For the present study, the *Amameh watershed* in the *Islamic Republic of Iran* was selected, for which reliable physical and hydrometeorological data are available (Fig. 3.1).

3.1 Description of Study Area

The Amameh is one of the most important seven tributaries of upper Jajroud River originates in the Kuh Siah and joins to the Jajroud River, which leads to the Latian Dam. Latian Dam having 90 million m³ capacity of water storage is also one of the main sources of drinking water of 12 million populated capital of Iran. Due to easy accessibility of the watershed, it has been very well equipped by the governmental agencies for efficient collection of the hydrometeorological data. The physiographic, geologic, climatologic, hydrologic characteristics and other related properties of the Amameh watershed are described under following heads.

3.1.1 Physiographical characteristics

The Amameh watershed has been introduced as a representative area for the southern skirt of the Albourz mountain range of Iran since about 30 years. The watershed is located at about 40 km at the northeast direction from the capital of Iran, Tehran. Some of the important physical specifications of the watershed are detailed under this head. The

contour map of the watershed on a 1:50000 scale with contours of 100m main interval has been used for the study.

3.1.1.1 General feature

The Amameh watershed lies between 35°-51'-00" to 35°-75'-00" N latitude and 51°-32'-30" to 51°-38'-30" E longitude. The entire watershed falls in the Tehran province, located in the southern foothills of the Albourz mountain range. The main watershed covers about 37.12 km² in area. It drains into the Jajroud River over which the Latian dam has been constructed, and finally ends to the Houz-e-Soltan Lake in the main central watershed of Iran. The Amameh River is 13.5 km in length and located in the NE-SW direction and has a rainfall-snowfall combination regime. The watershed lies mainly in the mountainous region with its complex characteristics. The topographical map of the watershed with intermediate contour of 20m is shown in Fig. 3.2.

3.1.1.2 Shape

The shape, or the outline form, of the watershed was obtained by projecting it on the horizontal datum plane of a map. The following dimensionless ratio of the *Form Factor* (Horton, 1932) was used to evaluate the shape of the watershed:

$$R_f = \frac{A_u}{L_b^2} \quad \dots(3.1)$$

where R_f is form factor, A_u is area and L_b is the length of the watershed. The area and the length of the watershed were found to be equal to 37.12 km² and 13.5 km, respectively. The form factor comes out to be 0.204. Since the value of the form factor is much smaller than one, it implies that watershed is of an elongated shape.

3.1.1.3 Longitudinal profile of the main river

The length and the slope of the main river of the watershed are the most important parameters that affect the time of concentration. The length of each uniform segment of the main waterway, measured from the contour map by using a curvimeter, along with its elevation is shown in Table 3.1. The longitudinal profile of the main river was then obtained as shown in Fig. 3.3.

Table 3.1 *Elevation profile of the Amameh main river*

Distance (km)	0	1.5	3	4.5	6	7.5	9	10.5	12	13.5
Elevation (m)	1800	1910	1970	2060	2100	2270	2670	3050	3200	3800

The gross slope of the main river was calculated by dividing the elevation difference between the top most point and the outlet by the total length of the river, and it was found to be 13.33 percent. The weighted and the smoothed slopes of the river were calculated to be equal to 14.70 and 7.10 percent, respectively.

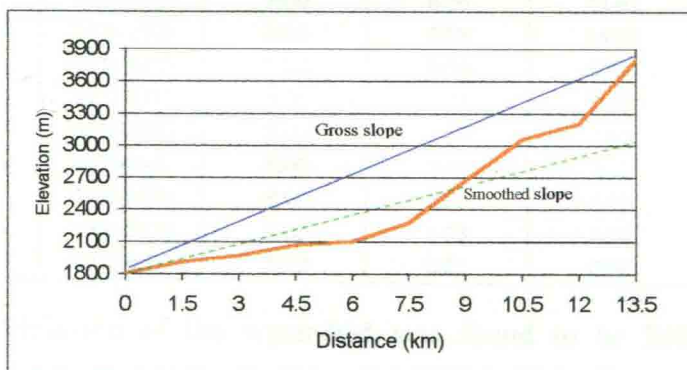


Fig. 3.3 *Longitudinal profile of Amameh River*

3.1.1.4 Slope

The slope at each direction was calculated by using the *grid method* with 1cm distance in the geographical direction i.e. north-south and east-west. The grid method states that:

$$s = \frac{N\Delta H}{L} \quad \dots (3.2)$$

where s is slope in given direction, N is the total number of intersections between grid line and contour line, ΔH is the elevation interval between two consecutive contour lines and L is the total length of the grid line in entire area under consideration. The slopes in two directions were then averaged to get the mean slope for the entire watershed. Thus, the average slope of the Amameh watershed was found to be 28.5 percent.

3.1.1.5 Elevation

The elevation of the Amameh watershed has a large variation and it varies from 1800m, at the outlet, to 3868m, at the top most point on the boundary. The variations in elevation with respect to the area of the watershed are shown in Table 3.2 and Fig. 3.4.

Table 3.2 *Elevation wise area distribution in Amameh watershed*

Classes	Elevation (m)	Mean Elevation(m)	Partial area (km ²)	Partial area (%)	Commulative area(%)
1	1800-2000	1900	1.71	4.61	4.61
2	2000-2200	2100	4.74	12.77	17.38
3	2200-2400	2300	8.76	23.60	40.98
4	2400-2600	2500	5.55	14.95	55.93
5	2600-2800	2700	3.54	9.54	65.47
6	2800-3000	2900	2.46	6.63	72.09
7	3000-3200	3100	2.83	7.62	79.72
8	3200-3400	3300	3.44	9.27	88.99
9	3400-3600	3500	2.55	6.87	95.85
10	3600-3800	3700	1.33	3.58	99.44
11	3800-4000	3900	0.21	0.57	100.00

The mean elevation of the watershed was found to be 2620m by using the hypsometric curve, shown in Fig. 3.5. Based on the available information, *maximum basin relief* (elevation difference between basin outlet and highest point located on the perimeter of the watershed), *relief ratio* (ratio of relief to the horizontal distance) and *relative relief* (maximum basin relief to basin perimeter in hundred) were found to be equal to 2068m, 0.153 and 7.01, respectively.

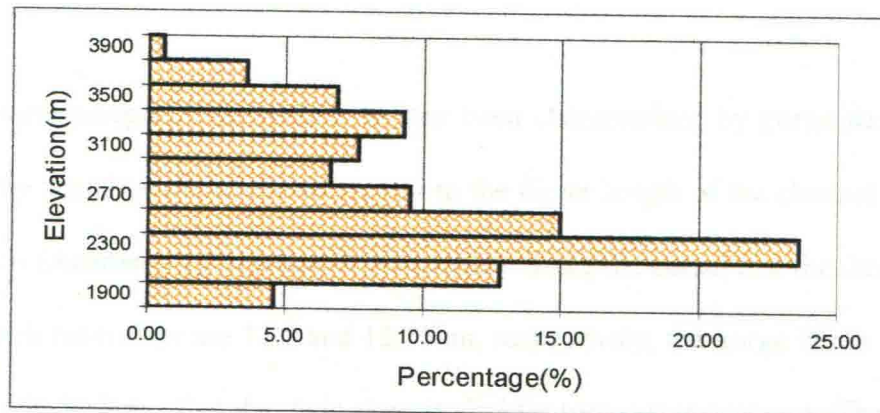


Fig. 3.4 Altimetric curve of Amameh watershed

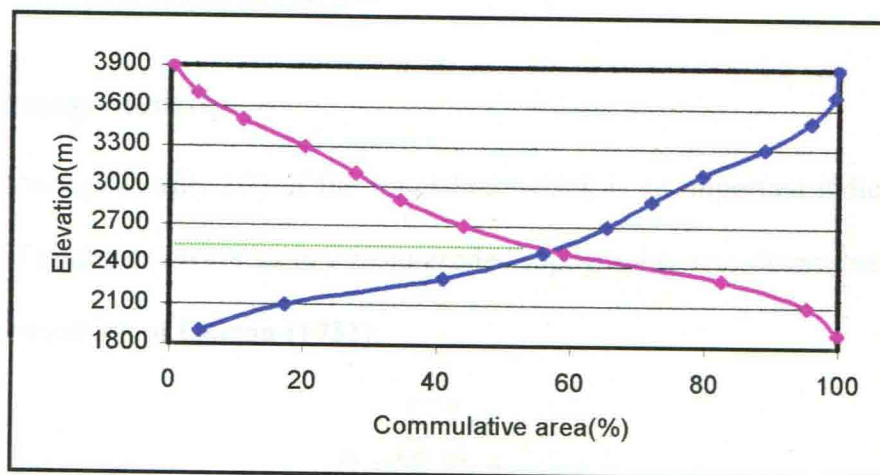


Fig. 3.5 Hypsometric curve of Amameh watershed

3.1.1.6 Drainage pattern and gorge factor

The drainage pattern of the area, which refers to the pattern of watercourses and their tributaries, was found to be *dendritic* with medium texture. The *bifurcation ratio* of the watershed i.e. the ratio of number of stream segments of a given order to the number of stream segments of next higher order, was calculated to be equal to 6.38 by using the concept of law of stream number (**Horton, 1932**). The number of river segments in different orders from the first to the fourth (*trunk order*), were found to be 192, 44, 8 and 1, respectively. The high value of bifurcation ratio verifies the presence of steeply dipping rock strata in the watershed. Also, the *stream* or the *channel frequency* (**Horton, 1932**) of



the watershed, defined as the number of stream segments per unit area was found to be 6.6 per km².

The tortuousness of the main river has been characterized by *gorge factor* that is the ratio of the actual length of the waterway to the direct length of the channel regardless of small bends (**Academy of Science, SSSR, 1961**). Since the actual and the direct lengths of the Amameh main river are 13.5 and 12.25km, respectively, the gorge factor was found to be 1.102, which shows that the main river is slightly tortuous to tortuous. The pattern of drainage distribution is shown in Fig. 3.6.

3.1.1.7 Drainage density

The drainage density (D) of the watershed, which is an important indicator of the linear scale of landform elements in stream-eroded topography, was determined by using the following equation of **Horton (1932)**:

$$D = \frac{\sum_{u=1}^k \sum_{i=1}^N L_u}{A_u} \quad \dots(3.3)$$

The drainage density (D) is the ratio of total channel-segments length (N) of order u , i.e. from the first order to the trunk (k), to the watershed area (A_u). The total length of the stream segments, measured on the topographic map was found to be 125.84km. Therefore, the drainage density of the watershed comes out to be equal 3.39km.km⁻², which implies a medium density. Also, the *constant of channel maintenance*, which is watershed surface area (km²) required to sustain one linear km of channel (**Schumm, 1969**), was found to be 0.295 km².km⁻¹ and is an inverse of the drainage density.

The important physiographical specifications of the study area are summarized in Table 3.3 as follows:

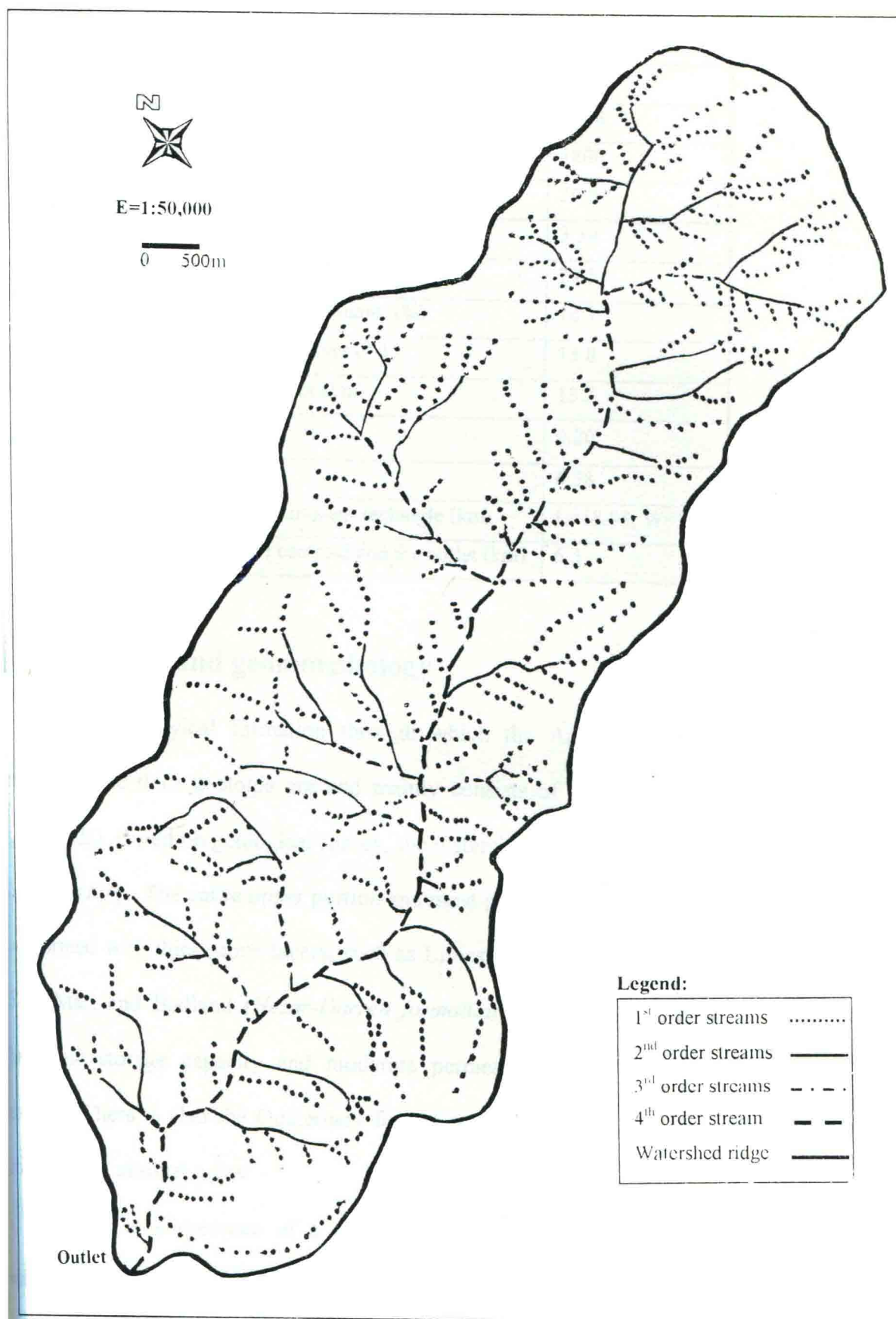


Fig. 3.6 Drainage pattern of Amameh watershed

Table 3.3 Geometric factors of Amameh watershed

Mean elevation (m)	2620
The highest elevation (m)	3868
Outlet elevation above sea level (m)	1800
Watershed perimeter (km)	29.5
Drainage density (km.km ⁻²)	3.39
Average slope (%)	28.5
Weighed average slope of main (%)	14.7
Average slope of main river (%)	13.8
Length of the main river (km)	13.5
Form factor	0.20
Bifurcation ratio	6.38
Length & width of equivalent rectangle (km)	L=18.98, W=3.57
Length between the centroid and the outlet (km)	6.5

3.1.2 Geology and geomorphology

The geological formation through which the Amameh River passes, belongs mainly to the third geologic era and mainly consists of the Karaj formation (Albourzs green beds). Based on geological survey, the watershed is situated in an area known as the *South Tertiary*. The entire upper portion and most parts of the lower area of the watershed are formed with thick stone layers, such as Limestone, Tuff, Shale, Conglomerate, Marl, Shale-Marl and Badland (*Hezar-Darreh formation*). Most of the mentioned formations have low storage capacity and moderate permeability. The Marl formation is very erodible. There is also the Quaternary formation but it is only to a limited extent in the collovial and alluvial areas.

There is a presence of a variety of geomorphological facies in the Amameh watershed, such as various forms of Karstic, outcrops, faults, joints and rock cracks that can trap water, most of which is due to snowmelt. In some portions of the area

Conglomerate, Marls and Schist layers are found alternatively in a severely folded form. A brief geology and lithology of the Amameh watershed is presented in Figs. 3.7 and 3.8.



Fig. 3.7 Severely folded and alternative geological formations in Amameh watershed.

3.1.3 Soil

Based on the land capability survey and soil classification conducted for the Amameh watershed, the land types in the watershed mainly consist of mountain, hill, flat plain and piedmont plain. The soil is grouped as *Regosol*, *Lithosol* and *Rego-Calceric* types on different land-uses with various values of clay, silt and sand contents, which shows immaturity of soil spread over the entire watershed. Some of the important

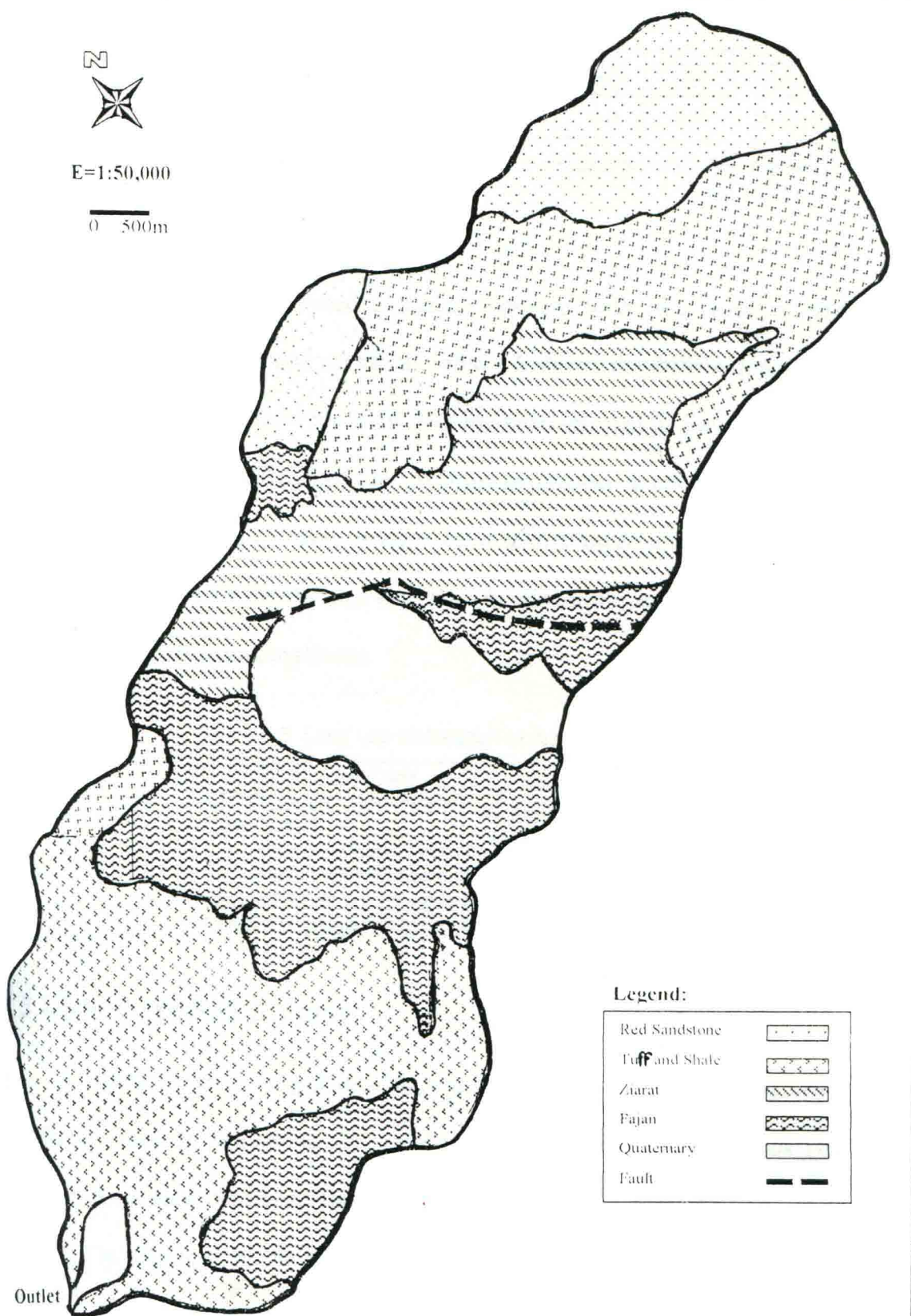


Fig. 3.8 Geological formations of Amameh watershed (Adopted from Ghloami, 2000)

properties of soil and their range of variations, based on the recent studies (Gholami, 2000), are summarized in the following table.

Table 3.4 Soil characteristics in Amameh watershed

Parameter	Depth (m)	MRD (m)	BD (gr/cm ³)	OC (%)	Clay (%)	Silt (%)	Sand (%)	RF (%)
Range	0.50-1.35	0.10-0.45	1.4-1.6	0.00-2.44	0-55	0-45	25-100	0-35

Indices: MRD= Maximum rooting depth, BD= Bulk density, OC= Organic carbon, RF= Rock fragment.

3.1.4 Land use pattern

The Amameh watershed is mainly covered with two types of land-uses viz. mountainous rangelands and orchards. Table 3.5 shows the distribution of different land uses in the watershed. Since the study area has been selected by the government of Iran as a representative watershed for the hydrometeorological studies in the area from the beginning, no major man-made changes have been allowed to be done in the watershed. Mostly, the inhabitants in the area earn their livelihood through animal husbandry, which is mainly dependent on rangelands.

Table 3.5 Land use distribution in Amameh watershed

Land uses	Area (ha)	Percentage
Orchards (Agricultural land)	242	6.5
Rangelands		
-Fair (<30% cover density)	1603	43.2
-Good (30-75% cover density)	1139	30.7
-Excellent (>75% cover density)	292	7.9
Others (Bare land, Rural area, ...)	436	11.7

3.1.5 Soil erosion process

Based on the physiographical and climatical conditions of the Amameh watershed, different types of weathering viz. mechanical and chemical and various types of soil erosion have been observed. The *Termocalsty* type of mechanical weathering, shown in Fig. 3.9 is dominant in the watershed, particularly on its upper regions. A presence of chemical weathering has been observed in the central portions of the watershed and in

places where limestone parent materials are abundantly available. Besides rainfall splash and running water, snowmelt and avalanche are the other factors, which have been found to be responsible for soil erosion. Sheet erosion in the watershed has been mostly found to occur in parts, which are covered with good and excellent rangeland. Rill erosion has been specially recognized in the area under furrowing treatment, done many years ago, and adjacent to the accessible road of the watershed as shown in Fig. 3.10. Gully erosion was found in a limited area located at the center of the watershed. The erosion due to avalanche has been occurred on steep slope areas, exposing to termoclasty. The type and distribution of different features of erosion, based on recent studies (Gholami, 2000) and satellite image interpretation, are shown in Fig. 3.11. It may be seen from the Fig. that badland and landslides erosion, and sheet erosion have occupied the least and the most area of the watershed, respectively.

3.1.6 Climatological characteristics

The type of the precipitation in the study area is of *leeward side* or *rain-shadow type*, which originally occurs due to lifting of moisture laden air masses along the orographic plane of northern Albourz slope, moving up and cooling of the same adiabatically. There are four distinct seasons viz. spring (March-May), summer (June-August), autumn (September-November) and winter (December-February) in the area. The area has a snow-rainfall precipitation regime. The mean annual precipitation in the area is 848.8 mm. The distribution of average monthly precipitation is shown in Fig. 3.12. Most of the precipitation (almost 73 percent) falls during the winter and spring seasons from December to May. Generally, the snowfall line is experienced in the Amameh watershed at the elevations of 2450m and beyond at the onset of snowfall during November (Gholami, 2000).



Fig. 3.9 A view of intensive thermoclastic weathering in Amameh watershed.



Fig. 3.10 A general view of soil erosion in Amameh watershed.

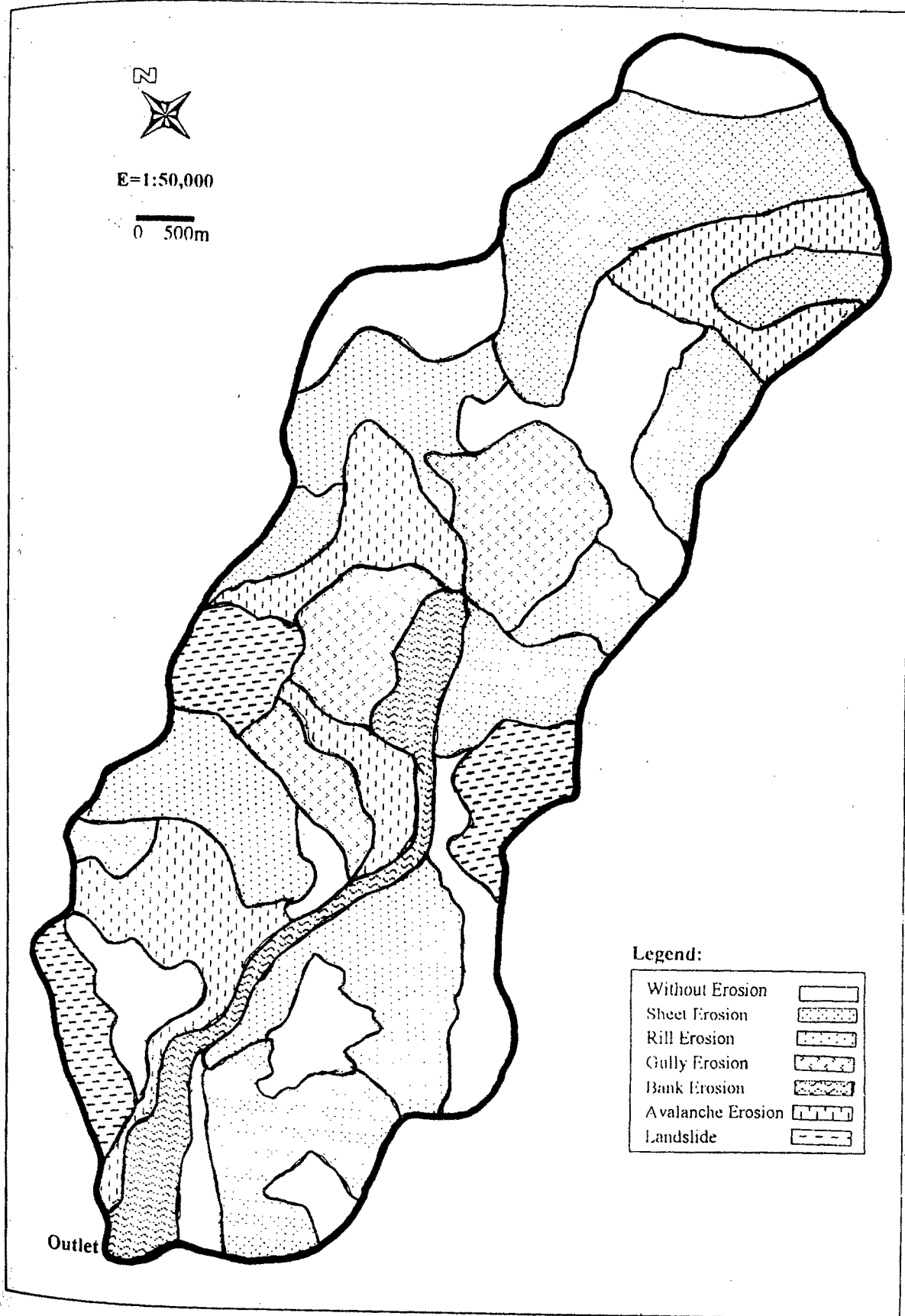


Fig. 3.11 Soil erosion map of Amameh watershed

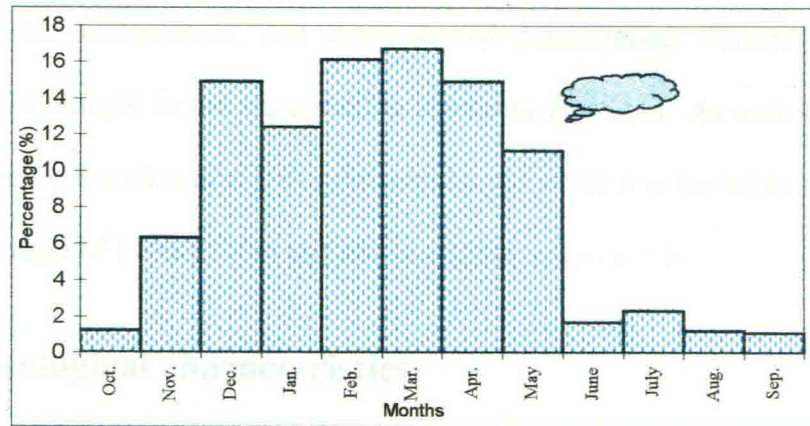


Fig. 3.12 Monthly distribution of precipitation in Amameh watershed

The annual mean temperature in the area is 8.6°C, whereas, the absolute maximum and minimum temperatures are 35 and -24°C, respectively. The annual average of evaporation is about 130 mm. The least and the highest values of evaporation occur during the months of February and July, respectively.

The climate of the study area is influenced by the Albourze mountain range. In general, precipitation regime of this area is a result of the *Mediterranean regime* and in addition, it is influenced by the moist air in contact with the northern Siberian air masses, in the form of fronts and seldom is there a influence of monsoon from Indian Ocean (Gholami, 2000).

A very humid climate is dominant over most of the parts of the watershed, but humid and semi humid climates are found in the lower portions of the area based on De Martonne's method that introduced the term of *dry ratio* I , as a relationship between annual mean precipitation P in mm and annual mean temperature T in °C (Abbasi, 1991).

$$I = P/(T+10) \quad \dots(3.4)$$

By using this equation climate can be classified as dry, semi dry, Mediterranean, semi humid, humid and very humid for the values of I as less than 10, 10-20, 20-24, 24-28, 28-35 and more than 35, respectively. The threshold elevation of each climate was then determined based on the given criteria and developed relationships between elevation

and mean annual temperature, and mean annual precipitation. Accordingly, the sub-classification of climate in the watershed is shown in Fig. 3.13. As seen in the Fig., the area located below the elevation 1900m is semi humid while it is humid and very humid in the elevation range of 1900-2300m and above 2300m, respectively.

3.1.7 Hydrological characteristics

The maximum and the minimum of observed instantaneous discharges at Kamarkhani station during 1969-1986 were 21.20 and $0.01 \text{ m}^3\text{s}^{-1}$, respectively, while the long-term average of annual discharge was $0.58 \text{ m}^3\text{s}^{-1}$. The maximum and the minimum of observed instantaneous discharges at Baghtangeh station for the same period were 5.40 and $0.05 \text{ m}^3\text{s}^{-1}$, respectively, whereas the long-term average of annual discharge was $0.29 \text{ m}^3\text{s}^{-1}$. The months of April and September are respectively the wettest and the driest months during the year. The average annual runoff has been found to be 503.6 mm , which is almost 59 percent of the yearly precipitation.

The average long-term discharge of the suspended load from the watershed is normally around $5.47 \text{ tonne.day}^{-1}$ or $0.537 \text{ tonne.ha}^{-1}\text{.year}^{-1}$. Most of the eroded material is produced due to sheet and avalanche erosions. Based on conducted granulometric study, the range of distribution of sediment particles size was wide and the mean diameter size of the collected samples from the river bed was found to be 7.5 mm (Sadeghi, 1993).

3.2 Instrumentation and Collection of Hydrological Data

Hydrological parameters of the study area, consisting of precipitation, runoff and sediment outflow rate are required for modeling of a watershed system. At this section, a brief report is provided regarding climatological and hydrometry stations and collected data for the Amameh watershed.

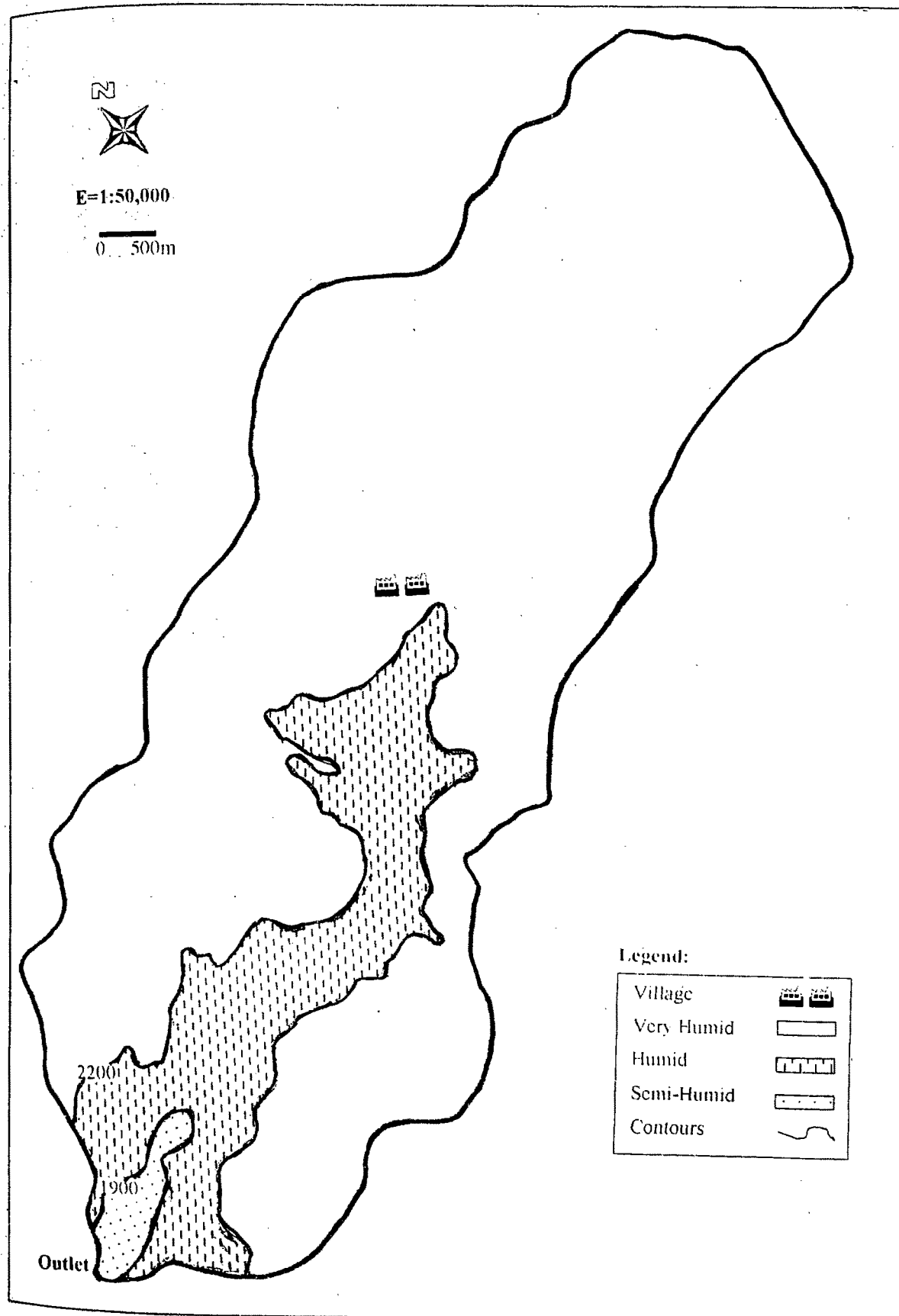


Fig. 3.13 Sub-classification of climate in Amameh watershed

Hydroclimatological data measured during the activity period i.e. 1970-1997 of the stations in the watershed were collected from different authorized sources in Iran. The daily data of precipitation, flow discharge and sediment concentration were scrutinized carefully and their synchronization was considered for the subsequent calculation. The storm-wise data were collected from the published reports. An attempt was made to select isolated, intense, short duration, uniformly distributed and single peaked storms. The locations of various hydro-climatological stations, and the selected storms and other necessary information are, respectively, shown in Fig. 3.14 and Table 3.6. The details in connection with each parameter are explained in following sections.

3.2.1 Precipitation

There are three climatological stations containing recording type raingauges and ten storage type raingauges in the area. Two of the recording raingauges are located in the watershed i.e. at the outlet and the center of the watershed called as Glookan and Amameh, respectively. Another recording raingauge is located just outside the watershed at Rahat Abad, which has also been considered for the analysis. All the three *arithmetic*, *isohyetal* and *Thiessen* methods were used to determine the mean annual precipitation in the area. The mean depth of precipitation estimated by the Thiessen method was found to be 848.8 mm, which lied between the values obtained by the two other methods and thus, this value was considered as the mean annual precipitation for the watershed.

Variation in precipitation with respect to time is shown graphically by a *hyetograph* and a *mass curve*. To get the hyetograph for the selected storms, the raingauges charts of Glookan and Amameh stations, located in the watershed, were collected. Based on the intensity variation of precipitation and its duration, a time interval of half an hour or quarter an hour were considered to be appropriate. The amount of

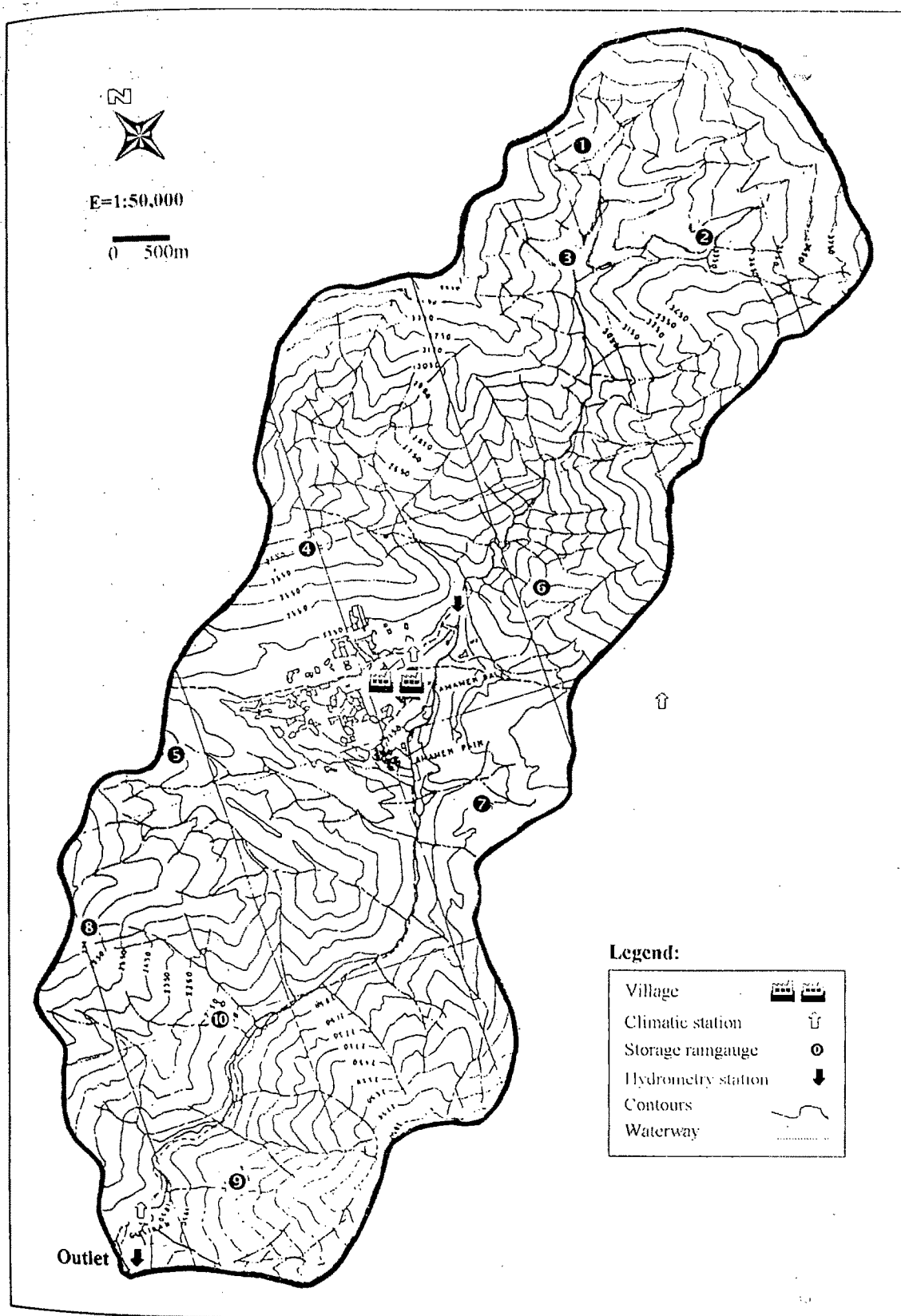


Fig. 3.14 Hydro-climatic network of Amameh watershed

precipitation at each time increment was then determined. The intensity of precipitation in mm.h^{-1} was plotted against local time, as a bar graph, which gave the hyetograph of a particular storm. The mass curve of precipitation was shown as a plot of cumulative depth of precipitation in mm against local time. The hyetograph and the mass curves were utilized for the determination of maximum intensity and total depth of precipitation, respectively. A comparison of the graphs of these two stations, located in the watershed, did not show much difference between the type and the amount of precipitation excepting the effect of elevation on depth. Therefore, the graphs provided for the Amameh station located at the center of the watershed was used for further computations. The graphical presentations showing hyetographs and mass curves of only two selected storms have been shown in the text (Figs. 3.16a and 3.17a) and for the rest, these are shown in Appendix B (B-1a through B-18a).

3.2.2 Runoff

There are two runoff recording (hydrometry) stations, located at the outlet and at the middle of the watershed viz. Kamarkhani and Baghtangeh, respectively. The locations of these stations have been shown in Fig. 3.14. The stream discharge is measured by broad crested weirs at both the aforesaid stations on the main river. Both stations are equipped with a scale, a limnograph (recorder) and a bridge, which were established about 30 years ago. The Baghtangeh station measures the output of 1610 ha of the upper portion of the watershed and is located at an altitude of 2220m. The photographic views of these stations are shown in Figs. 3.15a and 3.15b. The coefficient of variation for flow discharge has been reported to be 26 and 32 percent at Baghtangeh and Kamarkhani stations, respectively. Due to better accessibility, the frequency and accuracy of data collection at the Kamarkhani station is more than the Baghtangeh station. Therefore, the recorded daily



Fig. 3.15a *Baghtangeh hydrometry station in Amameh watershed.*



Fig. 3.15b *Kamarkhani hydrometry station in Amameh watershed.*

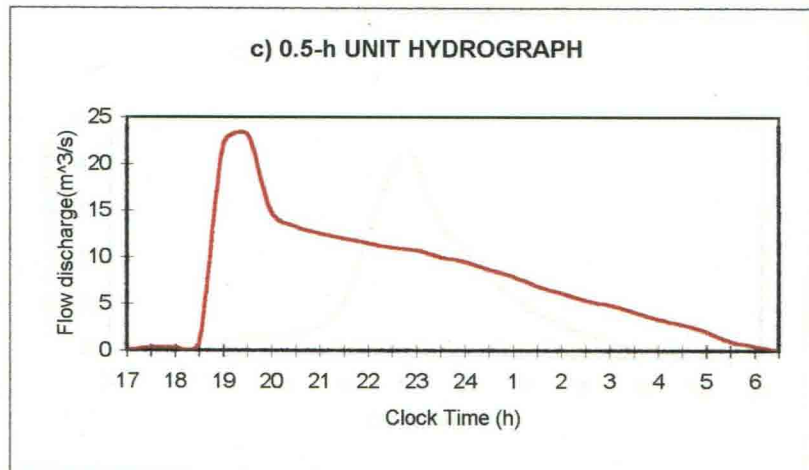
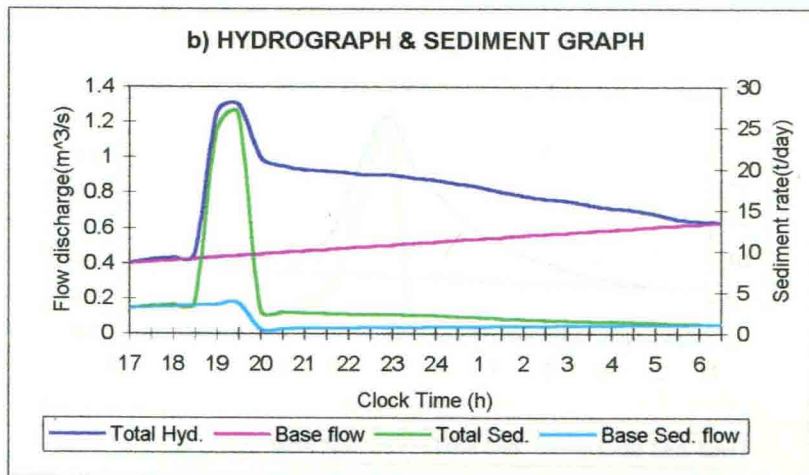
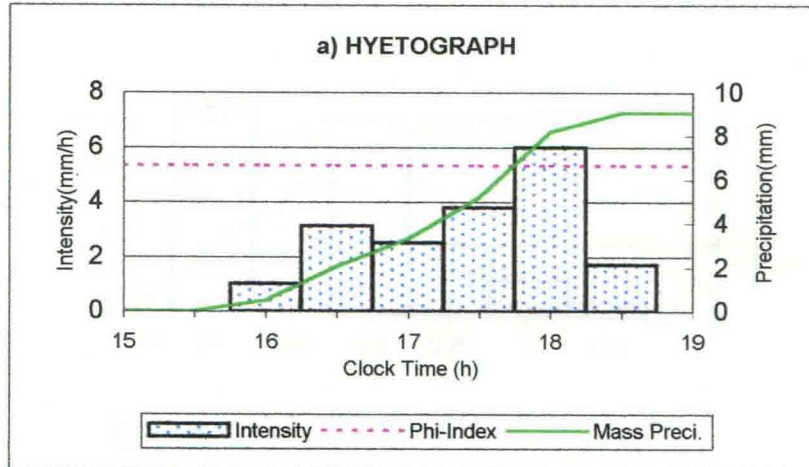
outputs at the Kamarkhani post were considered to be more appropriate for analysis of runoff and sediment data for the study. The details of runoff data for the selected storms and the time parameters of associated hydrographs are shown in Table 3.6. The concerned hydrographs of selected storms along with other information have also been presented in Figs. 3.16b and 3.17b and in B-1b through B-18b in Appendix B.

3.2.3 Sediment

At the site, the presence of sediment in runoff water is sampled by one-litre bottle samplers using the *depth integration method*. The sediment concentration is determined by using the filter paper in milligram per litre and reported in tonnes per day. It may be mentioned here that collection of sediment samples in most of the watersheds in Iran is not very satisfactory, and the same is true with the study watershed also. Therefore, the finding of synchronized precipitation, runoff and sediment data was very difficult task and due to that the number of selected storms is limited for precipitation-runoff-sediment study. It was observed that for some of the storms no recording of sediment was made. To overcome these inconsistencies in the collected sediment data, an attempt has been made to develop a reliable relationship between the sediment yield rate and the flow discharge discussed in the next chapter and therefore corresponding sediment data will be given in the concerned section. The data of flow discharge and the corresponding discrete sediment are given in Table 1 in Appendix A.

Table 3.6 Specifications of selected storms in Amameh watershed

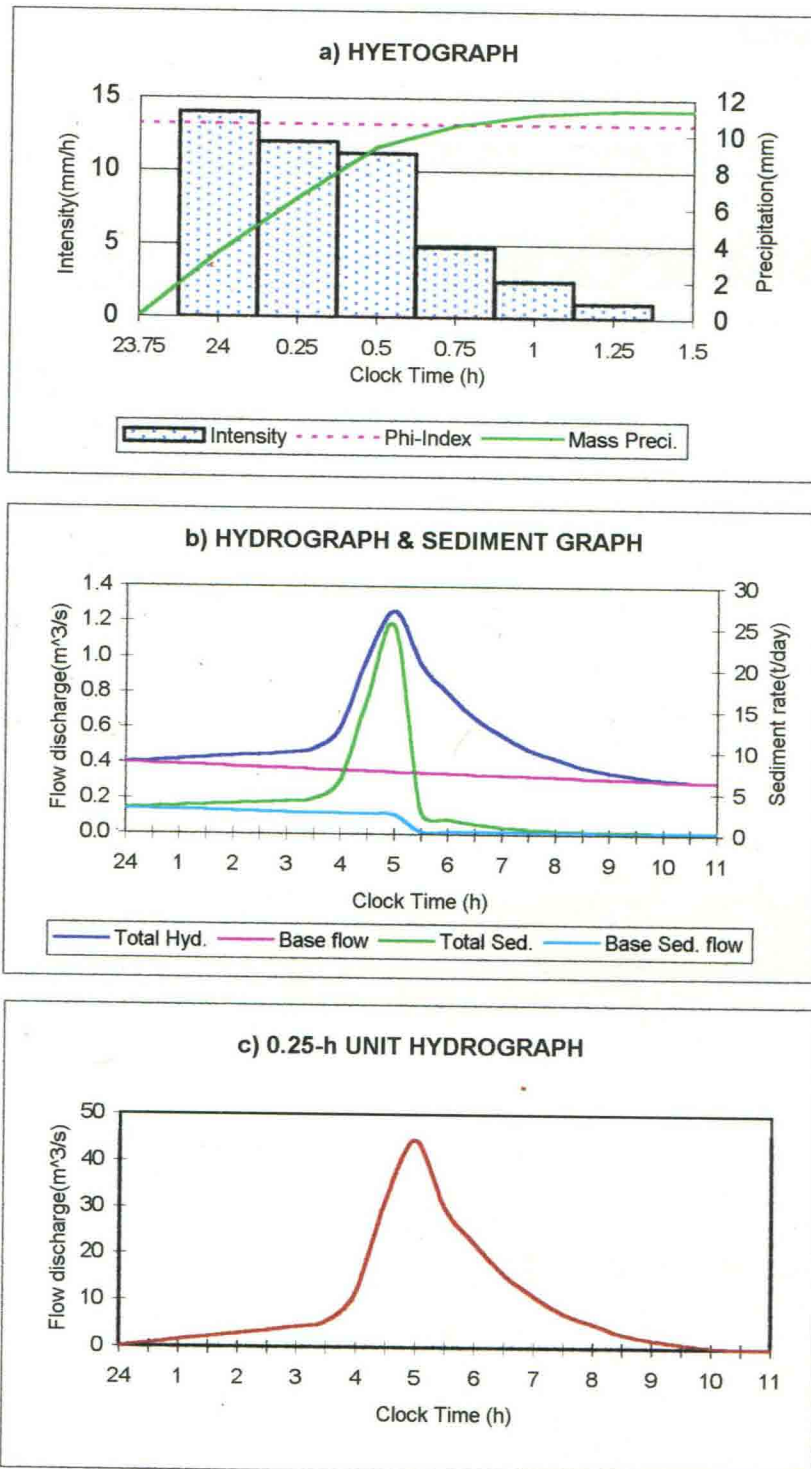
Serial Number	Storm (Date)	Precipitation		Max. I_{50}	Discharge		Time parameters of Hydrograph(h)				
		Depth(mm)	Duration(h)		Volume(m^3)	Peak($m^3 s^{-1}$)	Time to peak	Base time	Lag time	Lag to peak	Effective duration
1	April 23,70	9.05	3.00	12.00	13680	0.857	2.50	13.5	2.48	2.32	0.50
2	April 14,71	19.05	6.50	18.60	95580	8.552	4.50	14.0	1.35	1.59	0.50
3	Aug. 2,72	7.50	2.00	11.60	11466	0.886	1.50	14.0	2.98	2.75	0.50
4	Nov. 3,72	9.55	2.25	29.60	64350	3.400	5.00	15.0	2.26	3.02	1.00
5	July 18,74	13.15	1.75	51.00	27540	3.600	2.00	14.0	1.36	1.85	0.25
6	Sep. 22,74	14.10	3.00	10.92							
7	April 23,75	14.00	5.00	9.60	66600	6.800	3.00	10.0	1.74	2.86	1.50
8	July 22,76	21.25	5.00	29.00	64440	10.440	1.75	7.5	0.17	0.01	0.50
9	April 17,80	26.80	6.00	16.51		6.800					
10	April 29,80	11.00	4.00	13.70	97065	4.148	8.00	32.0	4.98	7.05	1.00
11	Oct. 5,82	25.50	1.50	29.20							
12	April 25,83	20.35	6.50	30.00	68634	3.432	5.00	13.5	1.83	2.64	1.25
13	May 5,84	6.86	2.50	8.12	8712	1.381	1.50	3.5	0.43	1.03	1.00
14	Aug. 5,87	8.00			260190	10.350	1.50	16.0			
15	July 25,88	4.00	2.00	10.40	32040	2.149	3.00	13.0	2.46	3.49	1.25
16	Nov. 18,88	9.50	4.00	35.00	16353	0.816	6.00	14.0	3.85	5.63	0.25
17	May 14,89	12.50	3.00	7.11							
18	Mar. 13,89	16.36	2.50	80.00	80064	1.800	10.00	40.0	4.28	3.88	0.25
19	Oct. 28,90	11.38	1.50	52.00	7578	0.908	5.00	11.0	2.41	4.77	0.25
20	Feb. 24,91	37.00			34920	10.250	1.00	2.5			
21	April 22,92	34.50	8.50	8.89							
22	April 27,92	20.00			299880	13.800	7.00	34.0			
23	May 1,92	13.30	7.00	6.86							
24	May 13,93	9.00			24822	1.882	3.00	17.0			
25	April 30,94	9.00			126306	5.259	15.00	34.0			
26	April 6,97	9.20	7.25	9.60	35656	2.005	8.00	23.5	4.03	5.88	1.00



Depth of the direct runoff=0.037cm
 Effective rainfall duration=0.5h
 Phi index=5.30mm/h

Runoff volume=13680m³
 Peak discharge=0.857m³/s
 Sediment yield=1.419tonnes

Fig. 3.16 Analysis of observed hyetograph, hydrograph and sediment graph for the storm event of April 23,70



Depth of the direct runoff=0.020cm
 Effective rainfall duration=0.25h
 Phi index=13.20mm/h

Runoff volume=7578m³
 Peak discharge=0.908m³/s
 Sediment yield=1.098tonnes

Fig. 3.17 Analysis of observed hyetograph, hydrograph and sediment graph for the storm event of Oct. 28,90

Chapter Four

DEVELOPMENT OF SEDIMENT GRAPH MODEL

4. DEVELOPMENT OF SEDIMENT GRAPH MODEL

The basic objective to carry out the present study is to develop a sediment graph model, which can be applied on an un-gauged watershed with reasonable accuracy for prediction of sediment yield. Based on the availability of the data a model has been conceived with sediment mobilized as input, which was obtained from a relationship between sediment mobilized and excess runoff. The excess runoff (rainfall excess) was estimated by using a most appropriate precipitation-runoff relationship developed for the watershed. Then the design sediment graph was obtained by developing a unit sediment graph for which two concepts viz. *average unit sediment graph* and *instantaneous unit sediment graph* were tried in the study. The average unit sediment graph was obtained by using the available hydrological data while the instantaneous unit sediment graph was derived conceptually mainly based on the watershed characteristics. The thus developed unit sediment graph for T-hour mobilization period, analogous to T-hour unit hydrograph, was then converted to sediment graph by convoluting its ordinates with the unit amount of sediment mobilized. The flow chart shown in Fig. 4.1 details the step-wise procedure for the development of design sediment graph model for the Amameh watershed in Iran. The characteristics of the study watershed and the hydrological data, required for the modeling process of sediment graph, have already been explained in chapter 3. The details of hydrological analysis, the required sub-modeling and the processes leading to the development of sub-models are described in the current chapter.

Different computer packages viz. *Excel*, *Eureka*, *MATLAB*, *Curve Expert*, *STATISTICA* and *StatView*, and some computer programs developed in *Fortran Language* (Appendix C) have been used expediently in the present study.

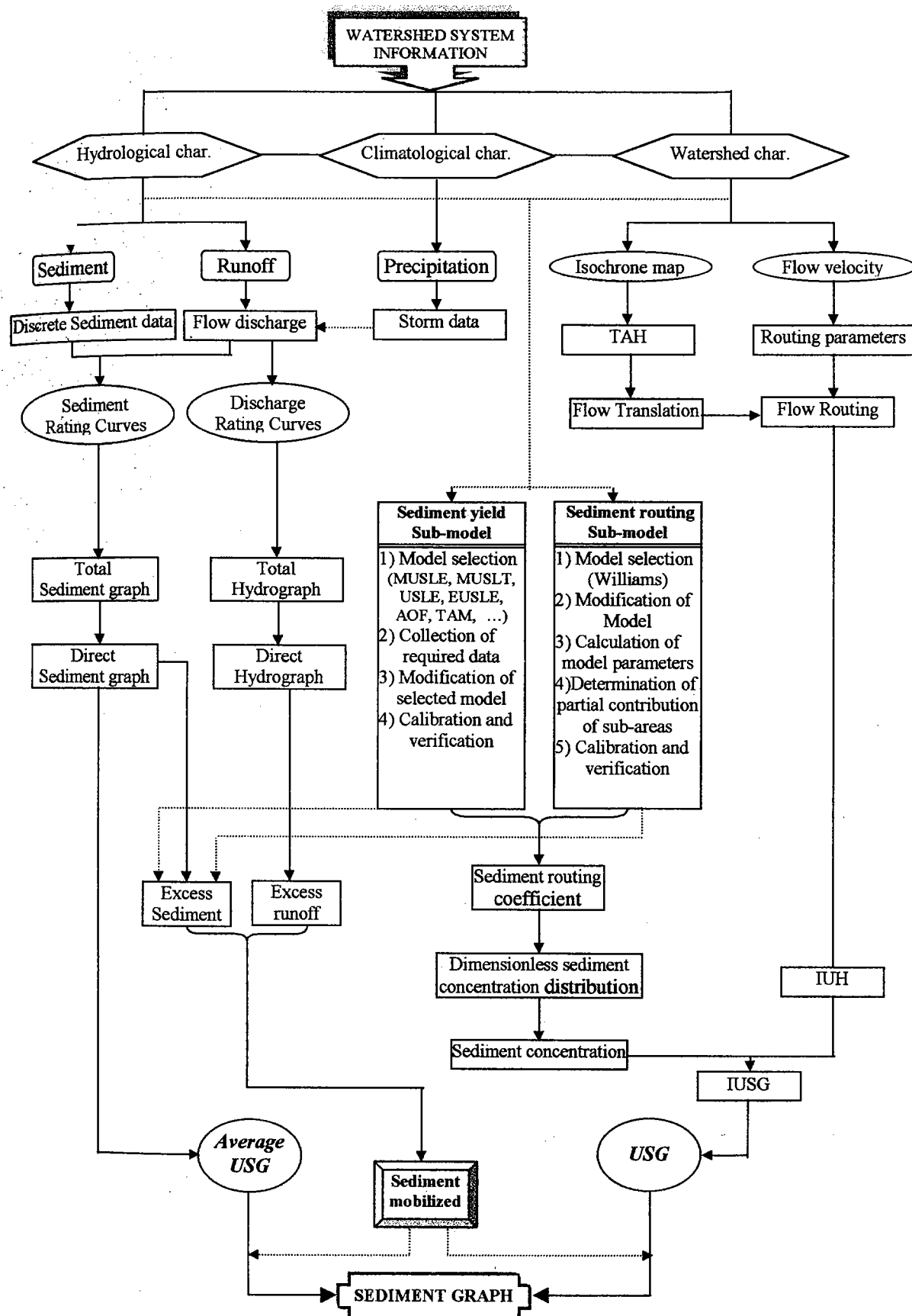


Fig. 4.1 Flow chart of sediment graph model development for the Amameh watershed

Thus in the present study, two sediment graphs (SG) models have been developed by following two concepts independently; one based on available hydrological data and other one based on watershed characteristics, as discussed in the following sections.

4.1 Development of SG Model Based on Hydrological Data

For the development of sediment graph model based on hydrological data, an appropriate sediment mobilized model and Unit Sediment Graph (USG) for the watershed are required. The step-wise procedure adopted in developing the sediment mobilized sub-model and the USG derived from hydrological data for the watershed is described in the following sub-heads. All the calibrated/developed models used for the development of SG model in the Amameh watershed have been named as *sub-model* in the present study.

4.1.1 Development of sediment mobilized sub-model

Since the sediment mobilized is used to develop the synthetic SGs from USGs for simulation of un-recorded sediment data related to storm events, the relationship between the pertinent hydrological data and sediment mobilized (excess sediment) is required. However, the relationship between the historical data of sediment mobilized and excess runoff (rainfall excess) is a commonly adopted method for prediction of sediment mobilized (excess sediment). Additionally, the sediment mobilized model may also be used for determination of the distribution of sediment yield during storm by knowing the amount of rainfall excess or excess runoff for any particular time segment. Thus, the estimation of excess runoff and excess sediment are two necessary components for the development of the sediment mobilized sub-model that is the excess sediment-excess runoff relationship.

4.1.1.1 Estimation of excess runoff

The value of excess runoff or rainfall excess, also called as *supra rainfall* is being estimated either by determining the area under the curve of direct runoff i.e. available data or by using the established relationships between excess runoff (*ER*) and some of the other hydrological and physical characteristics of the watershed.

a. Analysis of available flow discharge data

As explained earlier, the collected data at the Kamarkhani station were used for the runoff analysis. It was observed that the shape of hydrographs, in general, was sharp owing to the small size of watershed, with steep slopes and a dense drainage system. Since some of the recorded stages were not having the associated discharge while they were needed for other hydrological analysis, an attempt has been made to develop *Discharge Rating Curves* (DRC) for the considered station. A relationship between the surface flow and the effective precipitation i.e. precipitation minus losses was also established for the modeling process by separating the quick response flow including interflow from the slow response runoff. For further analysis, the unit hydrographs of the selected storms and the average unit hydrograph of the watershed study have also been derived as discussed below.

a-1 Development of discharge rating curves

Stage-discharge relationships or *discharge rating curves* (DRC) were developed by using the available stage readings and the measured flow discharge. About 126 measured values of flow discharge were plotted against the corresponding stages, which represented an integrated effect of channel and flow parameters in the following logarithmic form for a steady flow.

... (4.1)

where q is discharge in $\text{m}^3 \cdot \text{s}^{-1}$, G is stage on scale in cm, a is a constant represents the gauge reading corresponding to zero discharge, and c and b are the rating curve constants. The value of constant a was found to be -0.0099 , which can be taken as equal to zero, by using the *analytical technique* (Subramanya, 2000). The rating curve constants c and b calculated by the least square error method, were found to be 0.0043 and 1.4276 , respectively. The single valued stage-discharge relationship for the average situation i.e. for a steady flow can be expressed in the following form:

$$q = 0.0043(G + 0.0099)^{1.4276} \quad \dots (4.2)$$

Since the type of flow during the passing of floods is unsteady, more discharge passes through the river during rising stages than in falling ones at the same stage. In the retreating phase of the flood wave the converse occurs with reduced approach velocities giving lower discharges than in an equivalent steady flow case. Thus the DRC for an unsteady flow will not be a single-value relationship as in steady flow and it will be a looped curve as shown in Fig. 4.2.

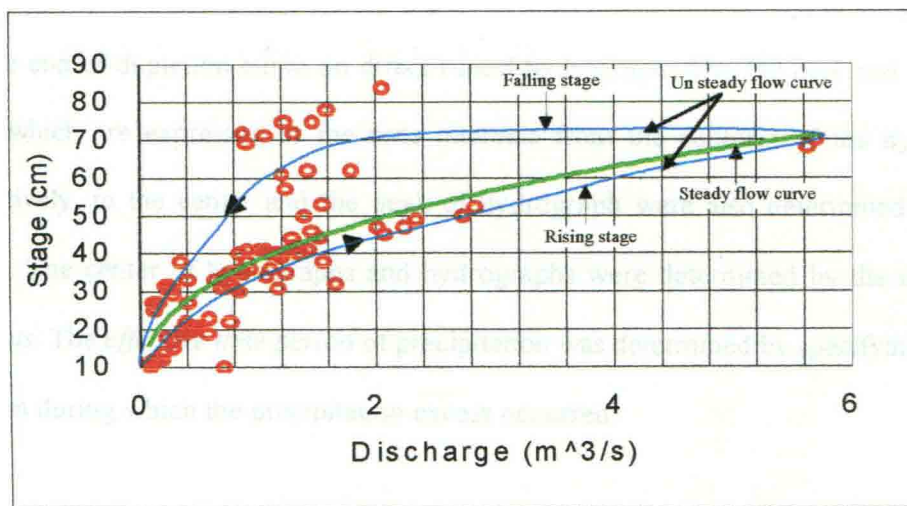


Fig. 4.2 Discharge rating curve for Kamarkhani station in Amameh watershed

a-2 Derivation of direct runoff hydrograph

The storm flow components of individual storm runoff events were separated from the base flow by the *method of straight line* (Hibbert and Cunningham, 1967, and Walling and Webb, 1982). The selected method among the available techniques for base flow separation was found to be simple and readily automated by computer. The procedure of base flow separation and direct hydrograph are depicted in Figs. 3.16b and 3.17b in the last chapter and B-1b through B-18b in Appendix B.

The volume of excess runoff or rainfall excess (*supra rainfall*) was then estimated by determining the area under the curve of direct runoff by using the method of *numerical integration (Trapezoidal Rule)*.

The ϕ -index of infiltration that is the average precipitation, above which the precipitation volume is equal to the runoff volume, was also calculated. The ϕ -index was derived from the particular storm hyetograph in such a way that the remaining volume to be equal to the excess runoff volume, calculated from the direct runoff hydrograph of corresponding storm, as shown in Figs. 3.16a and 3.17a, and B-1a to B-18a in Appendix B. The *time to peak* and the *base time* were determined as the time interval from the starting point of concentration (rising) limb of hydrograph, respectively, to the peak point and the end of depletion curve on direct runoff hydrograph. The *lag time* and the *lag to peak*, which are expressed as the time intervals from the centroid of the hyetograph, respectively, to the center and the peak of hydrograph were also determined for these storms. The center of hyetographs and hydrographs were determined by the method of *moments*. The *effective time period* of precipitation was determined by specifying the time duration during which the precipitation excess occurred.

a-3 Derivation of unit hydrograph

Once, the direct hydrograph of a selected storm and its effective time period were known, the *T-h Unit hydrograph* (T-UH) of the considered storm events were determined individually by dividing the ordinates of the direct hydrograph by the depth of excess runoff. The corresponding unit hydrographs are shown in Figs. 3.16c and 3.17c in chapter 3, and B-1c through B-18c in Appendix B.

a-4 Derivation of average unit hydrograph

Because of spatial and temporal variations in the rainfall due to storm departure from the assumption of unit hydrograph theory, the unit hydrographs thus developed were not likely to be identical. A number of unit hydrographs of a given duration were derived by the above method and then plotted on a pair of common axes to obtain the *average unit hydrograph* for the watershed. The time of concentration for the study watershed as reported in earlier study (Sadeghi, 1993) is 2 hours, 55 minutes and 55 seconds. The average value of reported basin lag time in Table 3.7 is about 2 hours and 25 minutes which is about 0.8 of concentration time of the watershed and is very close to the suggested ratio of 0.7 by SCS (1975). Since the effective duration of precipitation/unit hydrograph should fall in the range of 1/5 to 1/3 of the basin lag (Subramanya, 2000), the duration of 0.5 h has been considered to derive average unit hydrograph. In the present study, four storm events with their original effective rainfall duration of 0.5h and five other storm events with different duration, after their conversion to 0.5-h unit hydrograph, were considered. The base time and the time to peak of the unit hydrographs were averaged and the master curve, judged by eye, was drawn through the averaged peak to close on an averaged base length. The departure from unity owing to eye judgment in drawing was corrected by adjusting the value of averaged peak flow until it got a unit

depth of volume of runoff. The average (master) 0.5-h unit hydrograph for the Amameh watershed is shown in Fig. 4.3;

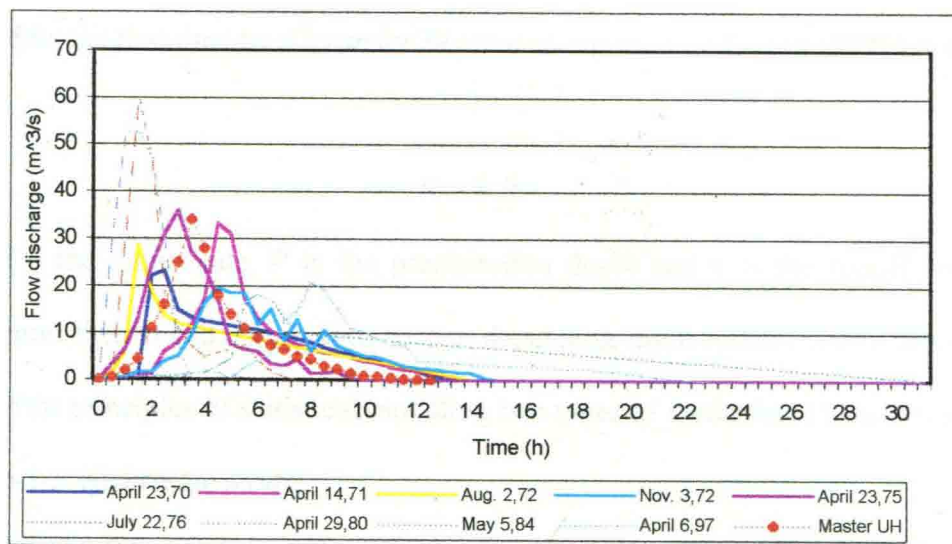


Fig. 4.3 Derivation of an average 0.5-h unit hydrograph for Amameh watershed

b. Precipitation-runoff models

Development of reasonably applicable relationships between excess runoff and precipitation and/or some of the physical characteristics of the watershed is very essential in the hydrologic study, since the hydrological data in connection with precipitation and watershed specifications are more frequently available than runoff data. Importantly, the applications of such a relationships help analyst to save time.

To develop a relationship between precipitation and runoff for the watershed, the available hydrographs and hyetographs of the last many years, having the same time coincidence, were collected and analyzed. Twenty one numbers of storms with known storm characteristics viz. duration, intensity, amount, volume and peak of runoff and time of incident were selected for the analysis (Table 3.7), out of which fifteen storms were used for calibration and the other six were considered for verification of the model.

b-1 Statistical regression model

A precipitation-runoff model is conceptualized based on a simple relationship by considering runoff to be a proportionate part of precipitation. The concept was probably proposed for the first time by *Alexander Binonie* as reported by **Gupta (1991)** is expressed as:

$$R = k.P \quad \dots(4.3)$$

where R is the runoff rate, P is the precipitation depth and k is the runoff coefficient, which varies theoretically from zero to one depending upon factors which affect runoff. Based on the principles of statistical modeling two types of model have been worked out.

b-1-1 Bivariable model

Based on the characteristics of the watershed, a minimum amount of precipitation is required to generate runoff. Assuming that the minimum value of precipitation P_0 is required for generating runoff, the Eq. (4.3) can be written as:

$$R = k(P-P_0) \quad \dots(4.4)$$

or,

$$R = kP - kP_0 \quad \dots(4.5)$$

where $-kP_0$ and k are respectively intercept and slope coefficients of the bivariable model. Different types of fitting techniques viz. linear, logarithmic, power and exponential were attempted, based on least square method, to get an equation giving the highest degree of agreement between the depths of runoff and precipitation. The following linear equation, having the highest value of correlation coefficient, i.e. 63 %, was found to be a better predictor of precipitation for the watershed.

$$R = 0.1065P - 0.0554 \quad (r=0.63) \quad \dots(4.6)$$

The Eq. (4.6) can be represented in the form of Eq. (4.4) by assigning values to K and P_0 as:

$$R = 0.1065(P-0.5202) \quad (r=0.63) \quad \dots(4.7)$$

Table 4.1 *Regression summary of bivariable Precipitation-Runoff relationship*

Dependent variable: Runoff depth (mm) Independent variable: Precipitation depth (mm)						
Determination coefficient, $R^2 = 0.39995793$ Adjusted $R^2 = 0.35380085$						
$F(1,13) = 8.6651$ $P < 0.01141$ Standard Error of Estimate = 0.69610						
Standard deviation of Runoff = 0.8660(mm), Standard deviation of Precipitation = 5.1399(mm)						
N=15	Standard regression coefficient (BETA)	St. Err. of BETA	Non-standard regression coefficient (B)	St. Err. of B	t-value (13)	P-Level
Intercept			-0.055372	0.474963	-0.116583	0.908973
P (mm)	0.632422	0.214842	0.106548	0.036196	2.943662	0.011410

The aforesaid relationship (Eq. 4.7) between runoff and precipitation has been demonstrated in Fig. 4.4 as shown below:

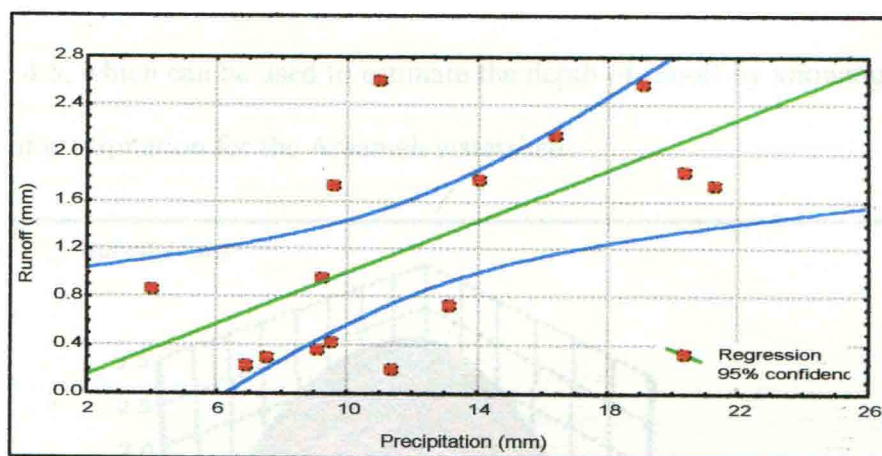


Fig. 4.4 *Precipitation-Runoff relationship for selected storms in Amameh watershed*

b-1-2 *Multivariable model*

In order to develop another model with a better agreement than that of developed bivariable model, a multivariable modeling approach was attempted. A correlation matrix was developed between parameters of precipitation and runoff from the watershed as given below:

Table 4.2 *Correlation matrix between precipitation and runoff parameters for Amameh watershed*

Variable	Runoff (mm)	Precipitation (mm)	Duration (h)	Max I_{30} (mm/h)
Runoff	1.00	0.63*	0.49	0.11
Precipitation		1.00	0.53*	0.38
Duration			1.00	-0.32
Max I_{30}				1.00

*Marked correlation coefficients are significant at $P < 0.05$ level.

As shown in Table 4.2, it can be observed that only the runoff has the acceptable correlation coefficient with precipitation depth. It can be seen that the duration and the depth of precipitation are also related to each other with a significant correlation. Therefore an attempt was made to develop the following multiple regression equation considering the depth of precipitation (P) in mm and its duration (D) in h :

$$R = -0.182 + 0.087P + 0.098D \quad (r=0.658) \quad \dots(4.8)$$

The developed multivariable model having a higher correlation coefficient is preferred to the bivariable model. A *quadratic surface nomograph* based on Eq. (4.8) is shown in Fig. 4.5, which can be used to estimate the depth of runoff by knowing the depth and duration of precipitation for the Amameh watershed.

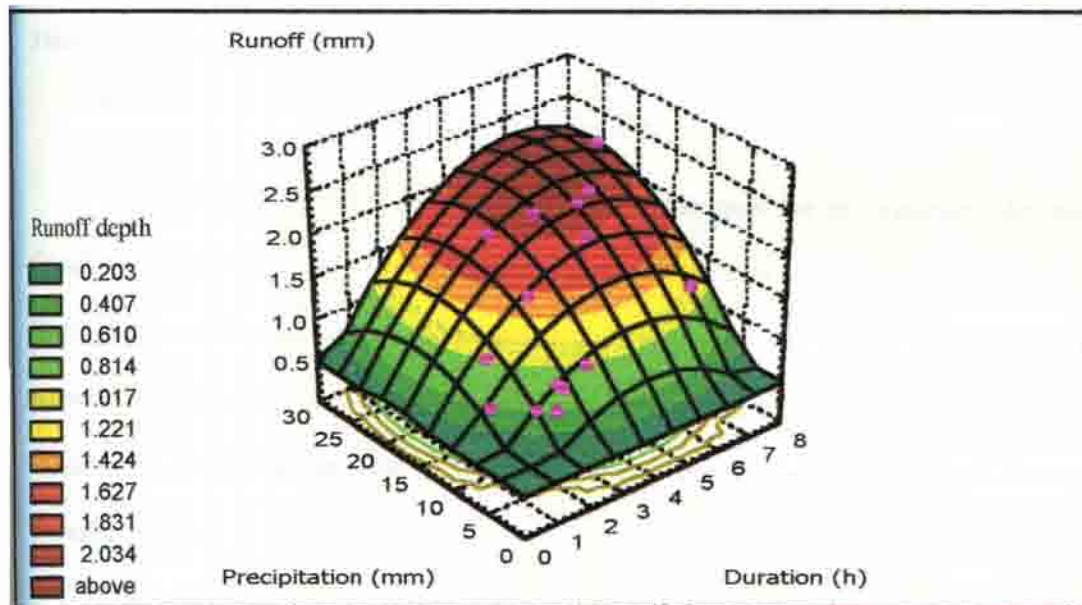


Fig. 4.5 Quadratic surface nomograph for estimation of runoff depth

b-2 SCS curve number technique

The *Curve Number (CN)* method (USDA, 1964) is a conceptual lumped model, which is also called as *infiltration loss model* because of its lumping nature. The popularity of the Curve Number (CN) method as a runoff prediction tool lies in the fact that it is simple to use, does not require calibration and is purported to give reliable results.

If I_a , Q , P and S are respectively initial abstraction, direct runoff, rainfall depth and maximum storage coefficient of the soil, then the precipitation-runoff relationship for the American agroclimatic conditions, where I_a is $0.2S$ that means the *Maximum Storage Index Coefficient (MSIC)* has been taken as 0.2, is expressed as below:

$$R = \frac{(P-0.2S)^2}{(P+0.8S)} \quad \text{subject to } P \geq 0.2S \quad \dots(4.9)$$

The potential maximum retention (S) is predicted by using a dimensionless number, called as Curve Number (CN). CN varies from 0 to 100 based on antecedent moisture condition (AMC), hydrological group of soil (A, B, C and D), hydrological surface conditions (Poor, fair and good) and three major types of land-uses (Agriculture, Rangeland and Forest). The USDA presented the following equation to determine the value of S in mm:

$$S = \frac{25400}{CN} - 254 \quad \dots(4.10)$$

The capability of soil to generate runoff depends upon the *Antecedence Moisture Condition (AMC)* is classified into three groups viz. AMC I, II and III (Dry, Average and Wet), based on the summation of previous 5 days precipitation and vegetative cover (Growth and Dormant seasons). It has been reported that the model is very sensitive to variations in CN (Hawkins, 1975; Bondelid, 1982; Wood and Blackburn, 1984 and Sadeghi, 1993).

The distribution of CN values for the Amameh watershed under average conditions is shown in Fig. 4.6. The CN values for the watershed and the associated runoff were estimated on per storm basis and the calculated runoff values were compared with the measured ones. The error of estimation was found to be very high. At this stage an attempt was therefore made to modify the CN method. First of all, the SCS model was calibrated for the watershed in respect of two important model parameters namely the Curve Number

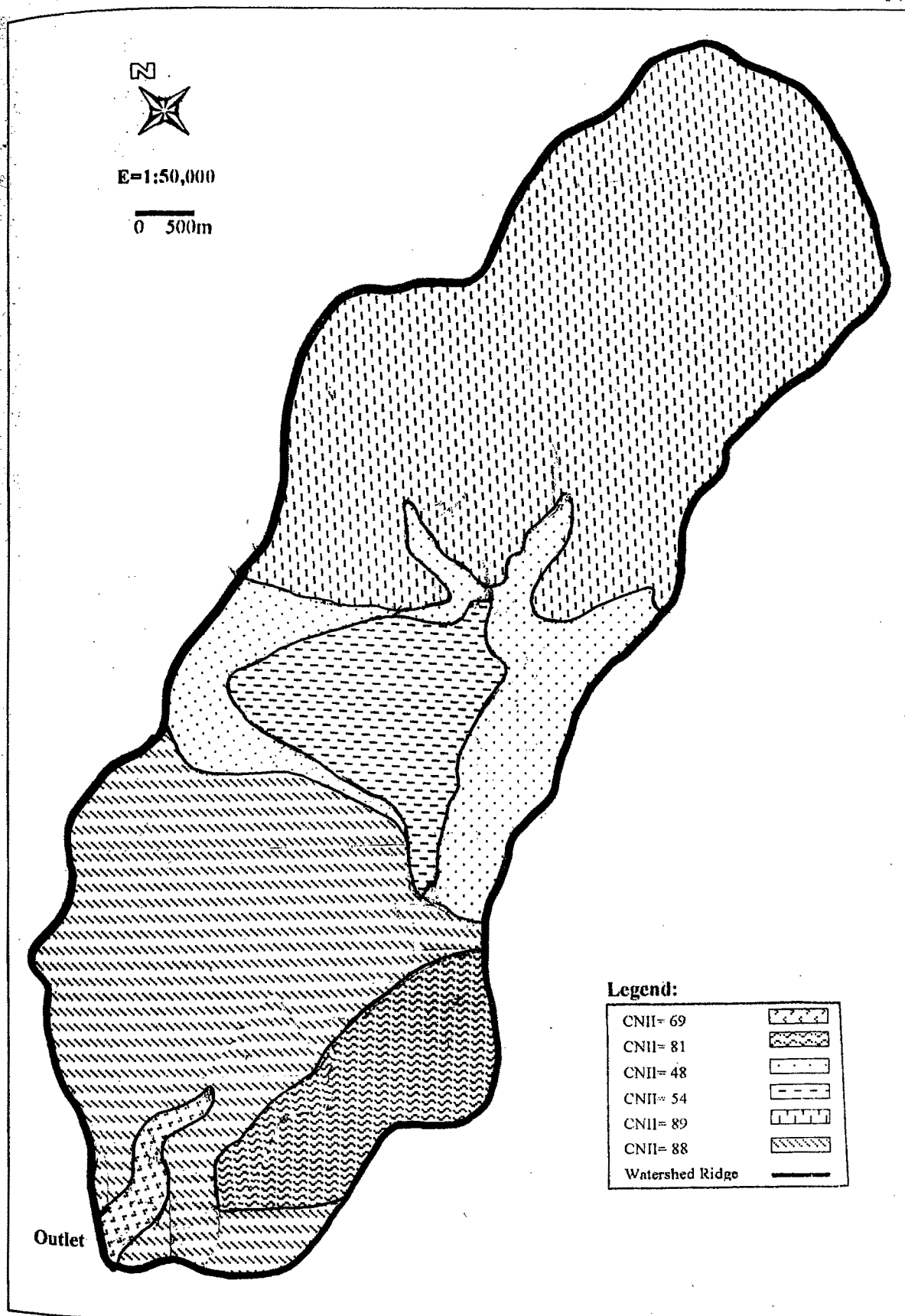


Fig. 4.6 Map showing Curve Numbers in Amameh watershed

(*CN*) and the Maximum Storage Index Coefficient (*MSIC*). To determine the suitable value of *MSIC*, the following equation was derived by substituting Eq. (4.10) in Eq. (4.9).

$$MSIC = \frac{(2P-R) + \sqrt{(R-2P)^2 - 4\{P^2 - R[P + (\frac{25400}{CN} - 254)]\}}}{2(\frac{25400}{CN} - 254)} \quad \dots(4.11)$$

Values for *CN* were selected from the standard *CN* tables based on the soil hydrological groups, *AMC*, vegetation cover and their hydrological situation obtainable from the available manuals and the values of *MSIC* were estimated for each of the 15 pairs of precipitation and runoff by Eq. (4.11). It was found that the *MSIC* values ranged from 0.09 to 0.28 for various storms with an average value of 0.185. The applicability of the model was then tested by substituting the average value of *MSIC* in Eq. (4.9). However, it was observed that the estimated values did not match the measured values well and therefore an attempt was made to determine more appropriate values of *CN* based on the actual conditions of soil moisture. Since the *AMC* is closely related to the summation of previous 5 days precipitation and vegetation conditions, it was thought to apply the concepts of interpolation to determine more accurate values of *CN*. It was observed that, in all the cases, these values of *AMC* fell within the dry condition (*AMC I*), though the values of the summation of past 5 days precipitation were changing widely in a range of 0 to 13 mm. Therefore, the values of *CN* were interpolated based on the actual values of 5 days antecedent precipitation. The thus calculated values of *MSIC* were found to vary from 0.10 to 0.57 for different storm events with an average value of 0.24. On substituting these values in Eq. (4.9) it was observed that the estimated runoff values were satisfying the measured values in a few cases only. Therefore, another attempt was then made to develop a set of recessive equations considering various characteristics of precipitation and runoff.

To develop the *Recessive series equations*, a correlation matrix was developed to identify the interrelationship between each pair of parameters as shown in Table 4.3.

Table 4.3 Correlation matrix between precipitation, runoff and SCS parameters in Amameh watershed

Variable	Volume (m ³)	Peak (m ³ /s)	CN	Precipitation (mm)	Duration (h)	Max I ₃₀ (mm/h)	MSIC
Volume	1.00	0.65*	0.47	0.63*	0.49	0.11	0.77*
Peak		1.00	0.00	0.71*	0.49	-0.11	0.45
CN			1.00	0.48	0.19	0.38	0.82*
Precipitation				1.00	0.53*	0.38	0.82*
Duration					1.00	-0.32	0.54*
Max I ₃₀						1.00	0.30
MSIC							1.00

*Marked correlation coefficients are significant at P<0.05 level.

From the Table 4.3, a close relationship can be observed between *MSIC* and *CN* as well as *MSIC* and depth of precipitation with correlation coefficient of 82 % in each case. Accordingly the following regression equations were obtained between/among these parameters.

$$MSIC = -1.154 + 0.019CN \quad (r=0.819) \quad \dots(4.12)$$

$$MSIC = -0.027 + 0.022P \quad (r=0.820) \quad \dots(4.13)$$

$$MSIC = -0.881 + 0.013CN + 0.015P \quad (r=0.952) \quad \dots(4.14)$$

The volume of runoff was then related to the *MSIC* by using different types of relationship viz. *linear*, *polynomial*, *power*, *exponential* and *logarithmic*, out of which the following models were found to be the most workable for the watershed.

$$Q = 3096.042 + 179390.400MSIC \quad (r=0.767) \quad \dots(4.15)$$

$$Q = 123988 + 49746.194\ln(MSIC) \quad (r=0.821) \quad \dots(4.16)$$

$$Q = 245932(MSIC)^{1.271} \quad (r=0.749) \quad \dots(4.17)$$

where *Q* is the volume of runoff in m³. Since *MSIC* is directly related to the depth of precipitation, no relationship was required to be developed between the volume of runoff and the depth of precipitation. Eq. (4.16) with highest value of correlation coefficient was accepted as the most appropriate equation for the study area. Thus, Eqs. (4.14) and (4.16) with better *r* values are statistically and logically more preferable than other equations for determination of *MSIC* and volume of runoff, respectively. Critical inspection of Eq. (4.16) shows that no runoff is generated if the value of *MSIC* is less than 0.083. Now

considering this value of $MSIC$ as the critical value, the values of CN and precipitation depth estimated by using Eqs. (4.12) and (4.13) are obtained as equal to 65.11 and 5.00mm, respectively. Thus, it implies that for generation of runoff from the watershed the minimum values of CN and precipitation depth have to be more than 65.11 and 5.00mm, respectively. Also, on substituting this critical value of $MSIC$ in Eq. (4.14), which has been found most suitable equation for determination of $MSIC$, the following inequality can be derived.

$$0.014CN + 0.016P > 1 \quad \dots (4.18)$$

It clearly shows that the combination of CN and precipitation values should be such that the product of left-hand side of the Eq. (4.18) is more than one for generation of runoff. Since precipitation is a major factor responsible for generating runoff, the precipitation value of 5.00mm obtained above is considered as the minimum amount (threshold) of precipitation for generating runoff from the watershed under study.

Since the peak runoff is also a very important parameter in hydrological study, different types of relationship were also developed between peak runoff, q_p in $m^3.s^{-1}$ versus runoff volume in m^3 and, q_p versus precipitation in mm as shown below:

$$q_p = 0.6564 + 0.000061Q \quad (r=0.654) \quad \dots (4.19)$$

$$q_p = -19.3582 + 1888 \ln(Q) \quad (r=0.661) \quad \dots (4.20)$$

$$q_p = 0.0009V^{0.7627} \quad (r=0.803) \quad \dots (4.21)$$

$$q_p = 0.9593e^{0.000002V} \quad (r=0.768) \quad \dots (4.22)$$

$$q_p = 7.930 + 1.2262P \quad (r=0.711) \quad \dots (4.23)$$

$$q_p = 8.5924 + 3.9562 \ln(P) \quad (r=0.659) \quad \dots (4.24)$$

Eq. (4.21) appears to be the most logical relationship to estimate the peak of runoff by virtue of having the highest correlation coefficient. A graphical presentation of Eq. (4.21) is shown in the Fig. 4.7.

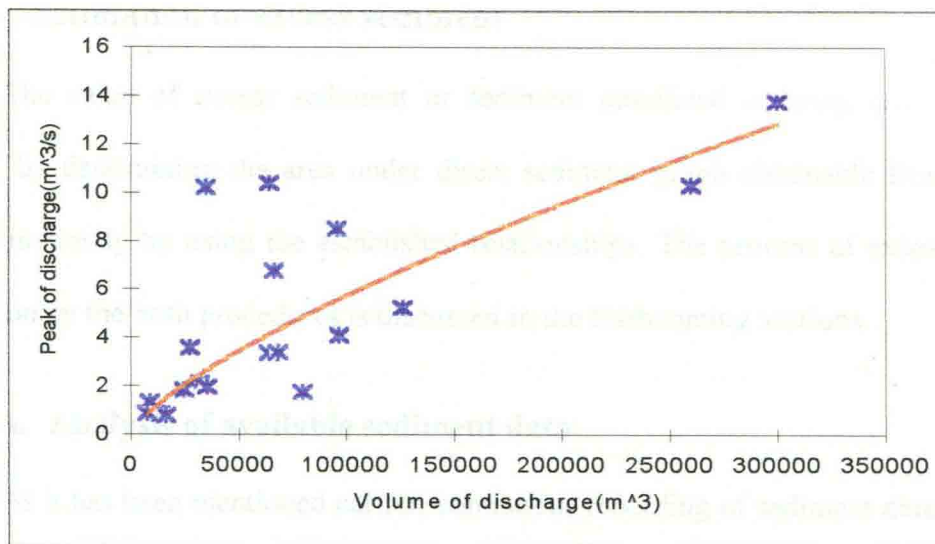


Fig. 4.7 Relationship between peak and volume of runoff in Amameh watershed

b-3 Selection of best applicable precipitation-runoff Model

As already stated earlier, six numbers of storms, other than those used for development of model, were considered for the verification and evaluation of the developed models for estimation of *MSIC* (Eq. 4.14), runoff volume (Eq. 4.16) and peak runoff (Eq. 4.21). The error of estimation for all the predicted variables i.e. *MSIC*, volume and peak of runoff were found to be small and well within the acceptable range of below 30 %.

It was further observed that the developed technique was not performing satisfactorily in cases of low discharge storms, which may be probably due to snowmelt or interflow feeding. The direction of layer bending of the geological formations may also be one of the reasons for poor applicability of the developed models in case of low discharge storms, as it is likely that a greater part of the initiated runoff may be interring into the ground surface and joining to the sublayer flows. The verification of various precipitation-runoff models strongly showed that the modified SCS curve number method developed by introducing the concept of recessive equations, is more reliable and efficient for estimation of runoff in the Amameh watershed.

4.1.1.2 Estimation of excess sediment

The value of excess sediment or sediment mobilized is being estimated either directly by determining the area under direct sediment graph obtainable from available data or indirectly by using the established relationships. The process of excess sediment estimation by the both procedures is discussed in the forthcoming sections.

a. Analysis of available sediment data

As it has been mentioned earlier, continuous recording of sediment data during the storm period are not available in Iran in general. The sediment data in the Amameh watershed are mostly available in discrete form as shown in Table 1 in Appendix A, whereas the continuous recorded data are required for the development of the direct sediment graphs to determine excess sediment. A sharp line of demarcation could not also be drawn between the material carried as bed load and suspended load in the watershed study. It has been, however, reported that about 85 % of the total sediment load is being produced as the suspended load in the watershed (Heydarian, 1994). Many researchers viz. Chow (1964); Graf (1971); Shen (1971) and Rendon-Herrero (1974) in other parts of the world have also indicated almost similar conditions. Therefore, the scope of this study was solely limited to suspended load. Keeping these in mind, an attempt has been made to develop a reliable relationship between the sediment discharge and the flow discharge, hereafter is called as *Sediment Rating Curve*, to overcome aforesaid inconsistency.

a-1 Development of sediment rating curves

Sediment Rating Curve (SRC), which is the relationship between sediment discharge and flow discharge, has been developed for the Amameh watershed by using

291 pairs of data as reported in Table 1 in Appendix A. The following form of the power equation has been found fitting well for this curve.

$$S_d = mq^n \quad \dots(4.25)$$

where S_d represents suspended sediment discharge in tonne.day⁻¹, q is flow discharge in m³s⁻¹ and m and n are equation constants.

In order to get the most accurate equation with the highest correlation coefficient, the available data then were classified based on a particular flow discharge, monthly, seasonal and annual wise and the corresponding equations were obtained. The correlation coefficient for the developed relationships between flow discharge and sediment discharge was less than 65 % in all the considered limits of flow discharge. The classification of data into different sub-periods viz. monthly, seasonal and annual did not make much improvement in correlation coefficients and those were below 72 %. Therefore, the data belonging to two periods of 1980-1998 and 1970-1998 were considered separately and associated SRCs were developed for which the correlation coefficients were increased to 85 %. The developed SRCs and corresponding equations are depicted in Figs. 4.8a and 4.8b. The acceptability of correlation coefficients at level of 5 % was verified by using the table given by **Snedecor and Cochran (1989)**.

Period 1980-1998	$S_d = 7.166q^{1.9931}$	$(r=0.857)$...(4.26)
------------------	-------------------------	-------------	-----------

Period 1970-1998	$S_d = 7.184q^{1.8781}$	$(r=0.854)$...(4.27)
------------------	-------------------------	-------------	-----------

The sediment data estimated by Eq. (4.26) has a standard deviation of 0.99 and a standard error of estimation of 0.51; whereas, the estimated sediment data by Eq. (4.27) belonging to the entire period i.e. from 1970 to 1998 has been found to have a standard deviation of 0.96 and a standard error of estimation of 0.49. The similarity of estimated data in standard deviation and standard error of estimation and even the correlation coefficient verifies that there is no much variation in the trend of sediment

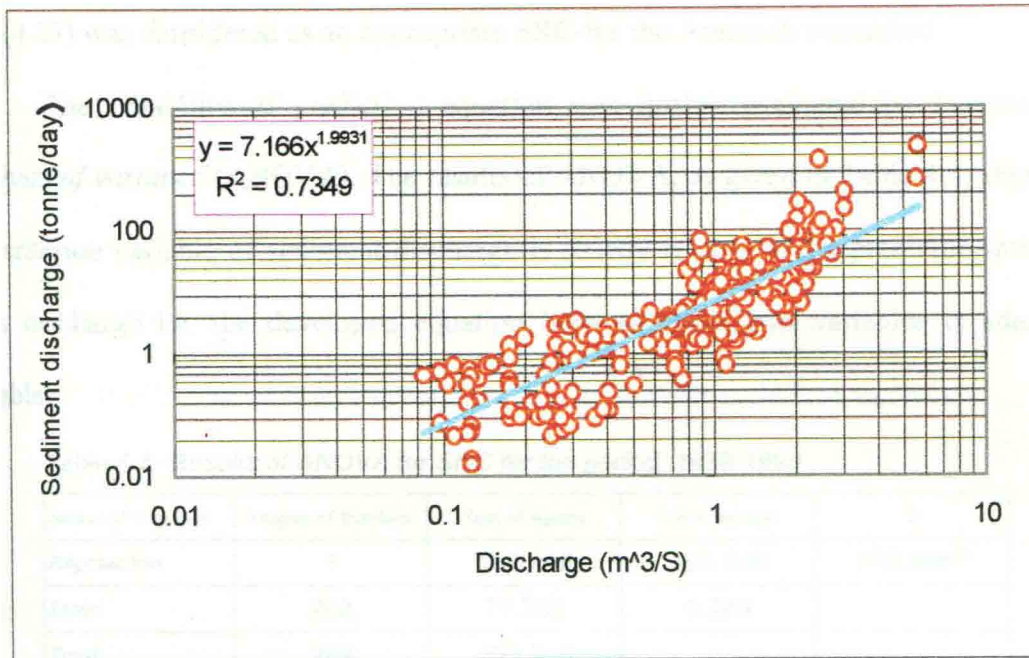


Fig. 4.8a Sediment rating curve for the period of 1980-1998 for Amameh watershed

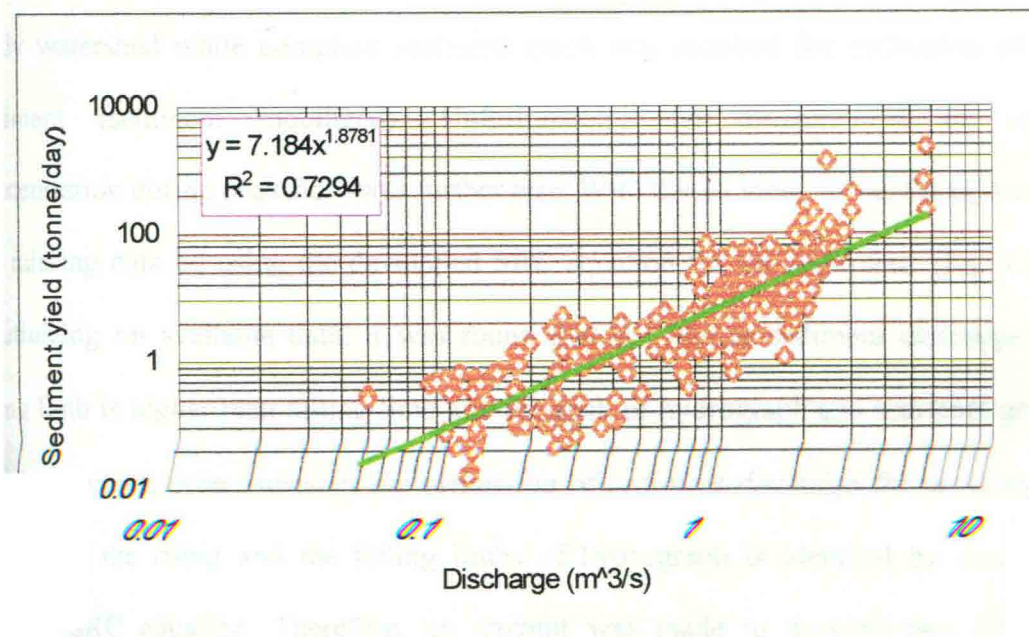


Fig. 4.8b Sediment rating curve for the period of 1970-1998 for Amameh watershed

discharge of the watershed with respect to flow discharge in mentioned periods. The thus Eq. (4.27) was considered as an appropriate SRC for the Amameh watershed.

The reliability of prediction equation was further evaluated by *F-statistic for analysis of variance* (ANOVA). The results of ANOVA, as given in Table 4.4, shows that the criterion variable of sediment discharge is strictly related to the predictor variable of flow discharge i.e. the developed equation between these two variables is adequately reliable.

Table 4.4 Results of ANOVA for SRC for the period, 1970-1998

Source of Variance	Degree of freedom	Sum of square	Mean Squares	F
Regression	1	193.448	193.448	778.989**
Error	288	71.768	0.249	
Total	289	265.216		

F table in 1 % level is less than F calculated so null hypothesis is rejected i.e. there is a significant relationship between flow discharge and sediment discharge.

a-2 Derivation of continuous sediment graph

As mentioned earlier, some times only a few sediment samplings have been made during each storm i.e. storm wise continuous sediment graph were not available for the study watershed while complete sediment graph was required for estimation of excess sediment (sediment mobilized). Unfortunately, the measurement of sediment concentration during peak flow was further rare. With this in view, it was thought to fill up the missing data by using the developed SRC equation for the watershed (Eq. 4.27). By scrutinizing on available data, it was found that the rate of sediment discharge on the rising limb is higher than falling limb and the peak of hydrograph and sediment graph are matched on each other, whereas the estimation of sediment discharge for the same flow discharge on the rising and the falling limbs of hydrograph is identical by using the developed SRC equation. Therefore, an attempt was made to develop two different equations for these two limbs, separately. Two different approaches viz. *confidence area*

ellipse and separation of data using regression line were introduced to achieve the purpose.

Accordingly, the concept of Confidence Area Ellipse, which is based on the assumption that the two variables follow the bivariate normal distribution was considered. The orientation of this ellipse is determined by the sign of the linear correlation between two variables i.e. the longer axis of the ellipse is superimposed on the regression line. The probability that the values will fall within the area marked by the ellipse is determined by the value of confidence level.

The normality of distribution of log values of sediment discharge data with an average of $0.547 \text{ tonne.day}^{-1}$ and a standard deviation of $0.956 \text{ tonne.day}^{-1}$ was checked by using *Kolminorv-Smirnov* (K-S) and χ^2 test at 5% level of significance. Both the methods yielded lesser values of test statistic (0.0362 and 9.521) than their critical values (0.080 and 12.596) for K-S and χ^2 , respectively, which verified that the sediment discharge data are distributed normally. The same procedure was used to check the distribution of the log value of flow discharge, with an average of $-0.165 \text{ m}^3\text{s}^{-1}$ and standard deviation of $0.435 \text{ m}^3\text{s}^{-1}$. The calculations showed that the flow discharge data have the higher values of test statistic than their critical values ($0.12 > 0.080$ and $98.35 > 25$ for K-S and χ^2 , respectively) confirming that the log values of flow discharge are not distributed normally. If the distribution of two variables were normal, then only the equations of lines drawn (red line) in equidistant from the regression line (blue line) and the perimeter of ellipse at 95 % confidence limit (green line), would apply for completing the gaps of sediment measurement. The details of procedure have been shown in Fig. 4.9.

Since the approach of Confidence Area Ellipse could not be used for the case study area owing to not satisfying the defined condition of normally distribution of data for its application, another technique was introduced. The second technique is based on the

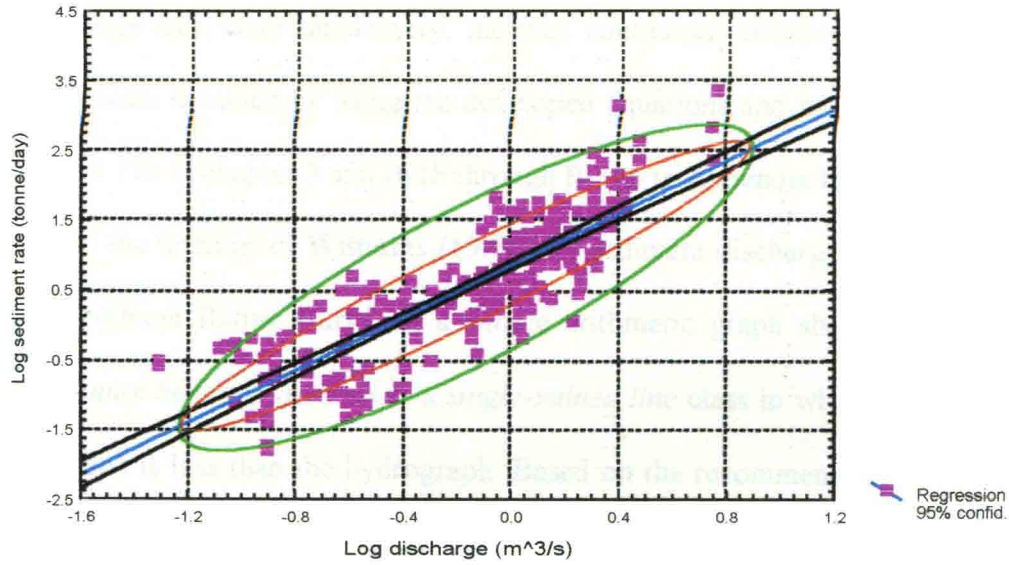


Fig. 4.9 Confidence Area Ellipse for Amameh watershed

separation of data by using the developed regression line as shown in Fig. 4.8. Since the regression line is the average estimation line for the data set, it was proposed that the points which are located below regression line belonging to the falling limb while the points which are situated above the regression line assigned to the rising limb. For the purpose, the values of sediment discharge were estimated by using the developed SRC (Eq. 4.27) for each particular flow discharge and the estimated values were compared with the reported values. Therefore if the estimated value of sediment discharge were smaller than measured one it would indicate a point on rising limb, whereas if the estimated value of sediment discharge were more than measured one it would consider for falling limb of the hydrograph. In other words, the entire data (1970-1998) were grouped into two categories consisting of data belonging to pre and post peak value. Ultimately, the following fitting equations were separately developed for each group of data for the estimation of sediment discharge corresponding rising and falling limbs of hydrographs in the Amameh watershed.

$$\text{Rising limb:} \quad S_d = 16.41q^{1.8424} \quad (R^2=0.892) \quad \dots(4.28)$$

$$\text{Falling limb:} \quad S_d = 2.84q^{2.0519} \quad (R^2=0.880) \quad \dots(4.29)$$

Since the results of application of this approach in comparison with the available sediment discharge data were satisfactory, the thus continuous sediment graphs for the selected storms were obtained by using the developed equations and have been shown in Figs. 3.16b and 3.17b in chapter 3 and B-1b through B-18b in Appendix B.

Based on the findings of **Williams (1989)**, the sediment discharge-water discharge plot (i.e. the Sediment Rating Curve on a simple arithmetic graph sheet) of the study watershed is a *curve bending upwards* in a *single-valued line* class in which the spread of the sediment graph is less than the hydrograph. Based on the recommendation of **Gracia (1996)**, the type of sediment graph in the Amameh watershed can be classified as *in-phased* sediment graph, which implies that sediment discharge is increased until it reaches a maximum at the same time as the hydrograph peak.

a-3 Derivation of direct sediment graph

As has been mentioned, most of the available sediment graphs in the study area are based on discrete data due to unavailability of recording type sediment concentration measurers. The *Direct Sediment Graph* (DSG) was obtained by separating of base flow of sediment load from each of the storm-wise continuous sediment graph. The base flow sediment graph were drawn by estimating sediment discharge for the respective base flow discharge with the help of Eqs. (4.28) and (4.29), respectively for falling and rising limbs. Thus, the ordinates of DSGs were obtained by the following simple equation (**Rendon-Herrero, 1974; Walling, 1982 and Chen et al., 1986**):

$$S_{Di} = S_{Ti} - S_{Bi} \quad \dots(4.30)$$

in which S_{Di} is direct sediment discharge, S_{Ti} is the total sediment discharge and S_{Bi} is the base sediment discharge rate, in t.day^{-1} , and suffix i refers to a particular ordinate of the sediment graph. Then, total sediment yield during each storm in tonne, was calculated by

using the trapezoidal rule along with the appropriate unit conversions. The base flow of sediment discharge for various storms is also depicted in Figs. 3.16b and 3.17b, and B-1b to B-18b in Appendix B.

The values of sediment yield and peak rate of the resulted sediment graphs belonging to selected storms are summarized and given in Table 4.5.

Table 4.5 Sediment yield and peak sediment for selected storms in Amameh watershed

Storm	April 23,70	April 14,71	Aug. 2, 72	Nov. 3,72	July 18,74	April 23,75	July 22,76	April 29, 80	April 25, 83	May 5, 84
Sediment yield (tonne)	1.419	51.407	0.555	12.360	7.421	31.742	39.512	36.742	28.718	1.575
Peak sediment (tonne.day ⁻¹)	22.954	1058.120	16.107	164.770	207.906	677.646	1248.866	342.022	273.430	34.689

Continued Table 4.5

Storm	Aug. 5, 87	July 25, 88	Nov. 18, 88	March 13, 89	Oct. 28, 90	Feb. 24, 91	April 27, 92	March 13, 93	April 30, 94	April 6, 97
Sediment yield (tonne)	115.104	5.133	1.110	18.805	1.093	36.964	349.583	7.130	53.410	7.598
Peak sediment (tonne.day ⁻¹)	1301.261	81.056	16.821	95.116	22.719	1351.067	3274.942	112.614	491.769	103.315

b. Sediment models

Due to very less availability and reliability of the collected sediment data, particularly during the entire period of storms, the applicability of continuous sediment graph for obtaining excess sediment gets very limited. Therefore, the development of an acceptably accurate and applicable sediment model by the help of easily accessible data is required for the estimation of excess sediment (sediment mobilized), which facilitates researchers to have a faster and an acceptable analysis. In addition to the application of sediment models for providing a sediment mobilized sub-model for convolution of USGs into SGs, they are also supposed as a tool to give a general idea about the quality and quantity of the soil erosion process components (Erosion, Transportation and Sedimentation) on the watershed. The details of sediment model development in the Amameh watershed are presented under two broad categories of sediment yield and sediment routing sub-models as follows:

b-1 Sediment yield sub-model

There are many different techniques available for the estimation of soil erosion process components (Erosion, Transportation and Sedimentation). Soil erosion process models are mainly divided into *annual* and *storm wise basis*. In the present study, some of the most important and commonly used models were chosen for evaluation under each category for which the input requirements were accessible for the Amameh watershed and suitable modifications, if necessary, were incorporated to suit the conditions of the study area.

b-1-1 Annual erosion sub-model

In the present study an attempt was made to test some of the commonly used models based on the prediction of annual soil loss models for their applicability for storm-wise prediction of sediment yield on the study watershed. The estimates of storm-wise erosion by *USLE*, *Hudson*, *EUSLE*, *AOF* and *Time Area Method* (TAM) were converted into sediment yield through *delivery ratio*. The simulated storm-wise sediment yield from the above mentioned models were compared with the measured sediment yield.

The coincidence data of the measured precipitation, discharge and sediment yield for only 15 storm events were available. The characteristics of these storms are shown in Table 3.7. A brief description of the soil erosion models and their implementation procedures, adopted in the case study area, are as follows:

b-1-1-1 Universal soil loss equation

The Universal Soil Loss Equation, as proposed by **Wischmeier and Smith (1965)**, is the product of a series of factors stated as:

$$A = R.K.L.S.C.P \quad \dots(4.31)$$

where

A = computed spatial average soil loss and temporal average soil loss per unit of area, expressed in the units selected for K and for the period selected for R .

R = rainfall-runoff erosivity factor,

K = soil erodibility factor,

L = slope length factor,

S = slope steepness factor,

C = cover-management factor and

P = support practice factor.

i. Erosivity factor (R)

The factor, in the original form of USLE, is calculated by the following equation:

$$R = EI_{30}/100 \quad \dots (4.32)$$

where R is in t.m.cm.ha^{-1} , I_{30} is the maximum 30 minutes intensity in cm.h^{-1} , E is the kinetic energy per unit depth of rainfall in t.m.ha^{-1} and is calculated using following equation:

$$E = 210.3 + 89 \log_{10} I \quad \dots (4.33)$$

in which I is intensity in cm.h^{-1} . Eq. (4.33) is applicable only for intensities less than or equal to 7.6 cm.h^{-1} (Renard *et al.*, 1997). The erosivity factor for the selected storms were calculated by using Eq. (4.32) and are summarized in Table 4.9.

Since the application of Eq. (4.32) is very lengthy and cumbersome, the following linear regression equation was found as the best fitted equation between erosivity factor (R) and maximum 30 minutes precipitation intensity (Max.I_{30}), which is simple and does not have any limitation for its applicability for the watershed.

$$R = 1.747(\text{Max.I}_{30}) - 16.312 \quad (r=0.971) \quad \dots (4.34)$$

This empirical equation eliminates the requirement for the factor E in Eq. (4.33), and can be used for the determination of the erosivity factor without the computation of the rainfall energy for each segment of hyetograph with a high level of acceptability.

ii. Soil erodibility parameter (K)

The soil erodibility parameter is determined by using a nomograph (Wischmeier, 1965) based on the results of lab analysis of soil samples of the area. The nomograph used for the determination of soil erodibility factor in USLE is shown in Fig. 4.10. Eleven soil samples were collected from different points of the watershed (sub-watershed wise), and the necessary parameters, viz. percentage of silt and very fine sand, sand, organic matter, soil structure and permeability were determined. The weighted average value of K for the entire watershed was found to be equal to $0.24 \text{ t.ha.m}^{-1}\text{t}^{-1}\text{cm}^{-1}$ with respect to the area occupied by each soil sample, considering that there was no significant variation in the soil erodibility factor during the study period.

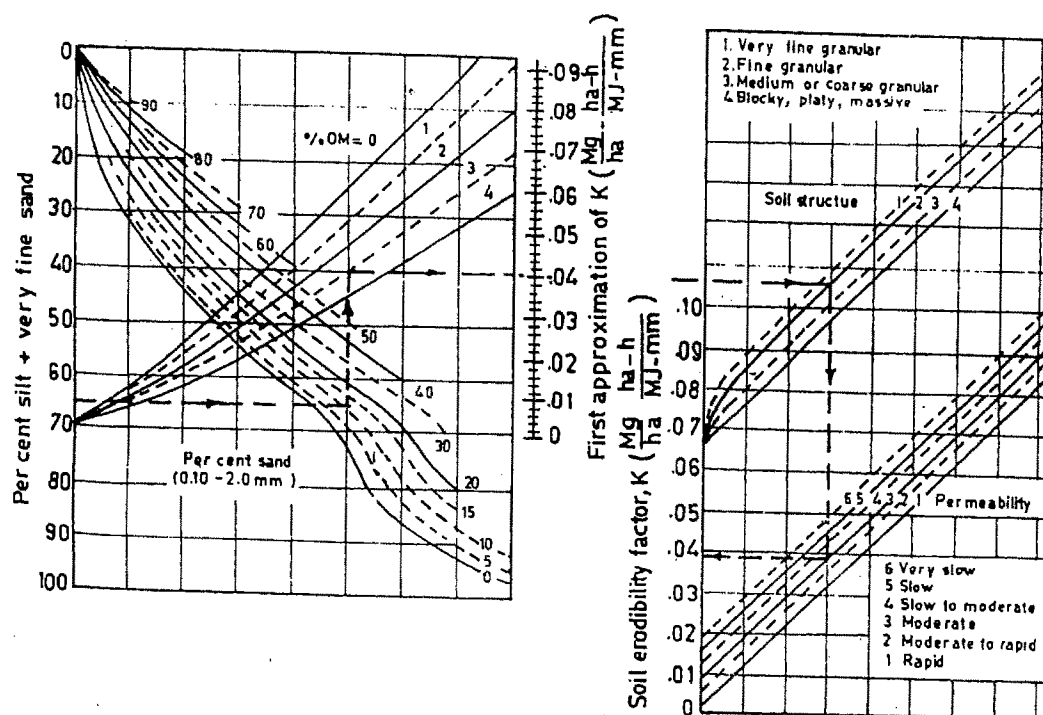


Fig. 4.10 Nomograph for determination of soil erodibility factor (K) for USLE
(Adopted from Das, 2000)

iii. Topography factor (LS)

The slope steepness (S) and slope length (λ) are required for the determination of topography factor. The S factor was determined to be 28.5 % by using grid method as described in section 3.1.1.4. The other three methods viz. *weighted, thumb* and *Williams' contour methods* (Williams and Berndt, 1976) were applied and checked for the determination of slope of watershed. The results of the first two methods (weighted and thumb) were found to be almost the same as that of the grid method, but the last method (Williams' contour) appeared to be overestimating. Therefore, the value of 28.5 % was taken as the slope of the watershed.

Four different techniques were used to determine the slope length factor (λ), the results of which are summarized in Table 4.6. The total length of contours (L_C and L_B) was obtained by summing up the length of contours located at 25, 50 and 75 % of total watershed relief, H , (3868-1800= 2068m). The contour base and the extreme points used for the contour-extreme point method are shown in Fig. 4.11 and the following information were obtained from the contour map:

$L_{C25} = 23500$ m	$L_{C50} = 8250$ m	$L_{C75} = 10400$ m
$L_{B25} = 20500$ m	$L_{B50} = 7400$ m	$L_{B75} = 9650$ m

Table 4.6 Comparison of different methods for slope length factor (LS) determination

Method	Equation	Length (m)
Contour-extreme point (Williams and Berndt, 1976)	$\lambda = \frac{L_C \times L_B}{2EP \sqrt{L_C^2 - L_B^2}} \dots(4.35)$	275.536
Drainage density (Williams and Berndt, 1972)	$\lambda = 1/(2D) \dots(4.36)$	147.493
Modified contour-extreme point (Williams and Berndt, 1976)	$\lambda = \frac{L_B}{2EP} \sqrt{1 + \left(\frac{S_c}{S_g}\right)^2} \dots(4.37)$	140.836
Modified drainage density (Horton, 1945)	$\lambda = 1 / (2D \sqrt{1 - \frac{S_g}{S_c}}) \dots(4.38)$	211.960
Measured	—	166

Legend: L_C = Total length of contour, L_B = Total length of base contour, EP= No. of extreme points, D= Drainage density and S_c/S_g = Ratio of the channel slope to the land slope.

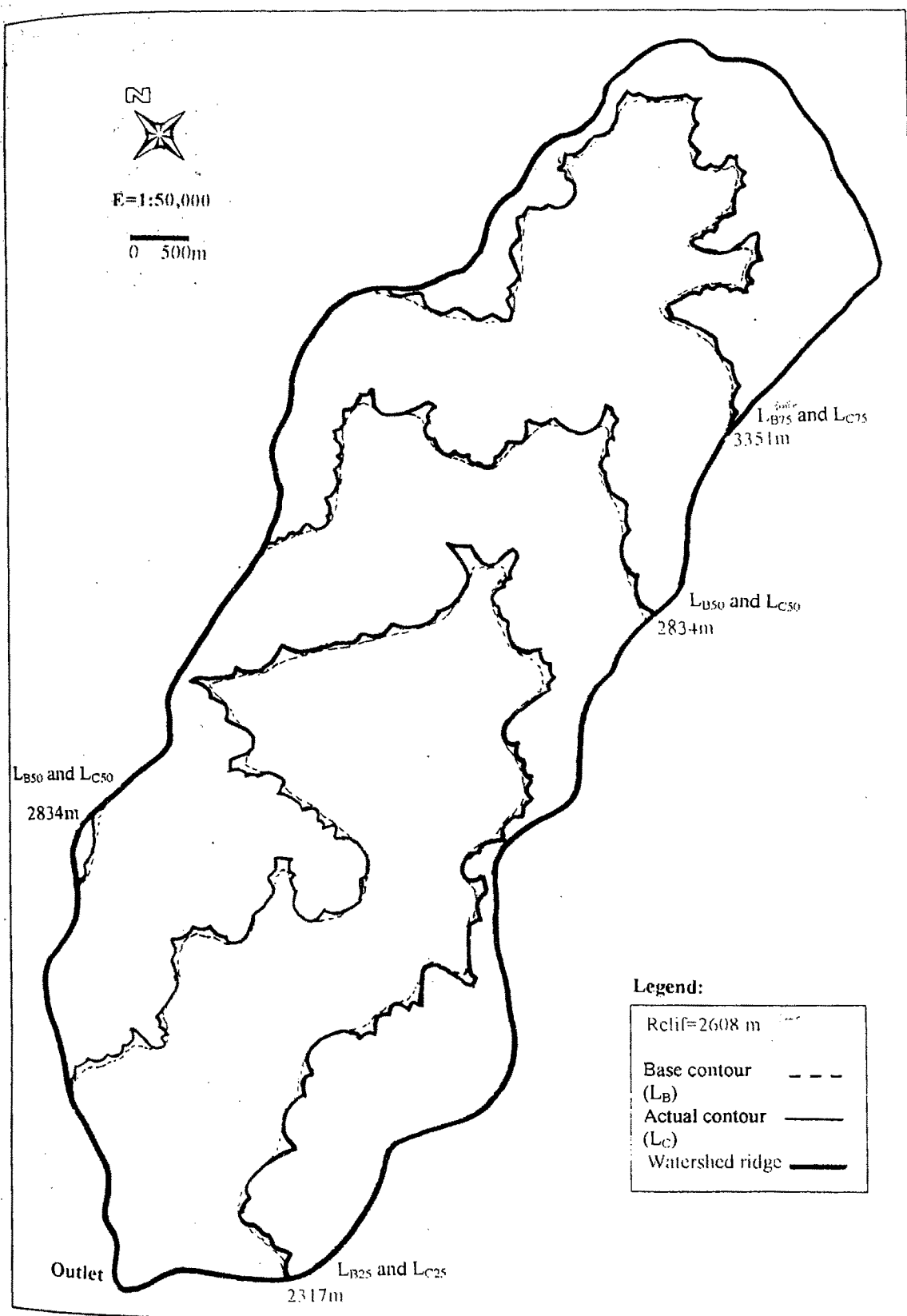


Fig. 4.11 Contour base and extreme point of Amameh watershed

The number of extreme points were found to be 77, 35 and 38, respectively for the elevations of $0.25H$ (2317.0m), $0.50H$ (2834.0m) and $0.75H$ (3351.0m). The drainage density, the channel slope and the weighted slope of the watershed, determined by conducting the physiographical study, were found to be equal to 3.39 km.km^{-2} , 14.7 % and 28.5 %, respectively.

The slope-length factor, λ , was calculated by using the equations listed in Table 4.6. It may be seen from the table that among the applied methods, two of them are overestimating and the two others are underestimating the length of the slope in comparison with the measured value. The measured value of slope-length factor (λ) was, therefore, considered to be the average slope length of the watershed for the study.

The following method was applied for the measurement of the actual slope length by using the contour maps. The entire watershed was subdivided based on the required accuracy and the area under consideration. Generally, the water would flow along the shortest route between two points located at the divide and the waterway. The line connecting these points and passing through the contour lines falling in between at the right angle would give the shortest line i.e. the shortest route. The contour lines can be considered to be almost parallel for a finite element, therefore the lines, which were found to be nearly perpendicular to the contours between the ridge and the channel, were considered as the shortest routes or slope lengths. The design slope length for each of the sub-division was determined by taking an average of the scale measurements of about 40 to 50 lengths. After obtaining the design slope-length for respective sub-divisions, the weighted average of slope-length for the watershed was then determined and found to be equal 166m.

After determining the values of average slope length, the value of LS factor was obtained by using the following equation (**Wischmeier and Smith, 1965**), and was found to be equal to 18.18.

$$LS = \left(\frac{\lambda}{22.13}\right)^M (0.065 + 0.0454S + 0.0065S^2) \quad \dots(4.39)$$

where λ is the length of slope in m, S is the slope steepness in percentage and M is a constant that varies from 0.3 for slopes $\leq 3\%$, 0.4 for slopes $=4\%$ to 0.5 for slopes $\geq 5\%$.

iv. Crop management factor (C)

As with most other factors in USLE, the C factor is based on the ratio of soil loss under actual conditions to losses experienced under the reference situation i.e. clean tilled continuous fallow (**Renards, 1997**). In almost all cropland scenarios and in many cases where rangeland or pastures are being managed, the crop and soil parameters change with time due to either specific management practices or natural cyclic effects such as winter knockdown and spring growth. This demands that the soil erosion ratio (C) values be calculated frequently enough over the course of a year or a crop rotation to provide an adequate measure of how they change (**Renards, 1997**). It has also been indicated by **Wischmeier (1975)**, **Muphree and Mutchler (1982)** and **Meyer and Harmon (1992)** that the general impact of cropping and management on soil losses can be divided into series of sub-factors. With this in view, it seems that the C factor may vary from period to period. Since the periodical variations of this factor has not usually been considered in available guides, it was tried to suggest the appropriate values for the C factor in the Amameh watershed based on the situation of available land uses in different seasons to improve the accuracy. The suggestion was made with respect to the comparative capability of land-uses to protect the surface soil against erosion in different seasons. Therefore, the seasonal values for the C factor were determined based on the available manuals and experience for

different land uses and are shown in Table 4.7. The value of 0.45 was considered for other land-uses consisting of bare lands, outcrops, residential areas, which are not contributing to soil erosion generation as much as reference condition.

Table 4.7 Seasonal values of crop management factor in Amameh watershed

Season Land use	Spring (20 th March-20 th June)	Summer (20 th June-20 th Sep.)	Autumn (20 th Sep.-20 th Dec.)	Winter (20 th Dec.-20 th March)
Orchards	0.15	0.04	0.09	0.20
Rangelands				
-Fair	0.20	0.15	0.20	0.33
-Good	0.15	0.09	0.15	0.25
-Excellent	0.09	0.04	0.09	0.20
Others	0.45	0.45	0.45	0.45
Average	0.202	0.151	0.198	0.301

v. Land management factor (P)

Since no specific values of P factor were determined for the Amameh watershed, the values proposed by Wischmeier and Smith (1965) were taken for the study area. Two prevalent land treatments consisting of terracing and bunding are available for which the values of 0.14 and 0.70 were considered, respectively. The weighted average value of P factor with respect to occupied area by each land treatment was obtained as 0.66.

The determined values for the USLE factors viz. R , K , LS , C and P were then substituted in Eq. (4.31) and the results of its storm-wise application are summarized in Table 4.10.

b-1-1-2 Hudson's method

Hudson (1981) has applied the same equation with that of the USLE, excepting that the erosivity factor (R) is considered only for the rainfall segments of hyetograph having rainfall intensities greater than 2.5 cm.h^{-1} . The rest of the parameters are determined with the same manner with that of the USLE. The results of application of this method for the estimation of soil erosion per storm basis are presented in Table 4.10.

b-1-1-3 EUSLE

The EUSLE (Nicks *et al.*, 1994) is essentially the USLE model, in which the Rainfall-Runoff erosivity factor, R , is replaced by a new term EI , and is estimated by the following equation:

$$EI = DR[12.1 + 8.9(\log r_p - 0.434)](r_{0.5})/1000 \quad \dots(4.40)$$

where DR is the daily rainfall depth in cm, r_p is the peak rainfall rate in cm.h^{-1} and $r_{0.5}$ is the maximum 30 minutes intensity in cm.h^{-1} . The results of application of this model are also presented in Table 4.10.

b-1-1-4 AOF method

The method suggested by Onstad and Foster in 1975, designated as AOF, uses the same general equation as that of the USLE, except for the erosivity factor, which is estimated by using the following equation. In contrast to previous methods, the runoff erosivity is also considered in this equation.

$$R = 0.646E + 0.45(Q.q_p)^{0.33} \quad \dots(4.41)$$

where E is kinetic energy per unit depth of rainfall in t.m.ha^{-1} , Q is the volume of runoff in m^3 and q_p is the peak of flow in $\text{m}^3.\text{s}^{-1}$. The outputs of the AOF model for the Amameh watershed are shown in Table 4.10.

b-1-1-5 Time-area method

Hadely *et al.* (1985) reported a method suggested by Kling for routing the eroded soil in a watershed by arbitrarily dividing the watershed into cells. In this approach the sediment delivery ratio (SDR) was obtained by determining the ratio of the average slope of draining (giving) cell to that of the adjacent (receiving) cell. Kothyari *et al.* (1994) however, observed that the method of subdivision of a watershed into selected cells has no basis and is absolutely arbitrary. Therefore, they tried to modify this method by

simplifying the process of cell division. The major lacuna in Kling's method was observed while determining the fraction of soil erosion from an individual cell that drained into more than one adjacent cell. To overcome this difficulty, they proposed an alternative method by introducing the concept of time area histogram for subdividing of the watershed called as time area method (TAM). However, the method proposed by **Hadley et al. (1985)** was adopted for the determination of *SDR*. When the slope of the receiving segment was milder than the slope of the giving segment, the *SDR* was taken as unity. The eroded material was routed from one segment to the next and the procedure was continued up to the last subdivision. That is, if Y_i and $(SDR)_i$ ($i = 1, 2, 3, \dots, n$) are the amounts of soil erosion and sediment delivery ratio of the i^{th} segment, respectively. The sediment yield (Y) resulting from the entire watershed at the outlet is calculated by the following equation.

$$Y = (SDR)_1 Y_1 + (SDR)_1 (SDR)_2 Y_2 + \dots + (SDR)_1 (SDR)_2 \dots (SDR)_{n-1} (SDR)_n Y_n \dots (4.42)$$

In the present study, the time of concentration for the watershed as detailed under article 4.1.1.1 is equal to approximately 3 h. The entire area was divided into 6 segments i.e. the time interval between each two isochrone was taken as half an hour as shown in Fig. 4.12. The specifications of each segment are shown in Table 4.8. As can be seen from the table that since the segments III and IV are having milder slope in comparison to respectively segments IV and V, the *SDR* values are taken as unity that means the entire eroded material are translated to the next segment.

Table 4.8 *The characteristics of time-area segments in Amameh watershed*

Segment	Elevation range (m)	Inter-Area (ha)	Percentage (%)	Erodibility, K (tonnes/ha.El)	Slope Length (m)	Slope (%)	LS factor	CP factor	SDR
I	1800-1930	66.26	1.79	0.1985	184.0	31.71	23.185	0.1395	-----
II	1930-2060	151.28	4.08	0.2414	195.6	28.17	19.330	0.1464	0.888
III	2060-2170	237.55	6.40	0.2404	189.6	23.24	13.554	0.1288	0.825
IV	2170-2670	1767.86	47.63	0.2404	176.8	26.28	16.245	0.1248	1.000
V	2670-3100	575.12	15.49	0.247	147.3	34.74	24.476	0.1413	1.000
VI	3100-3800	913.93	24.62	0.228	138.0	29.84	17.998	0.2000	0.859

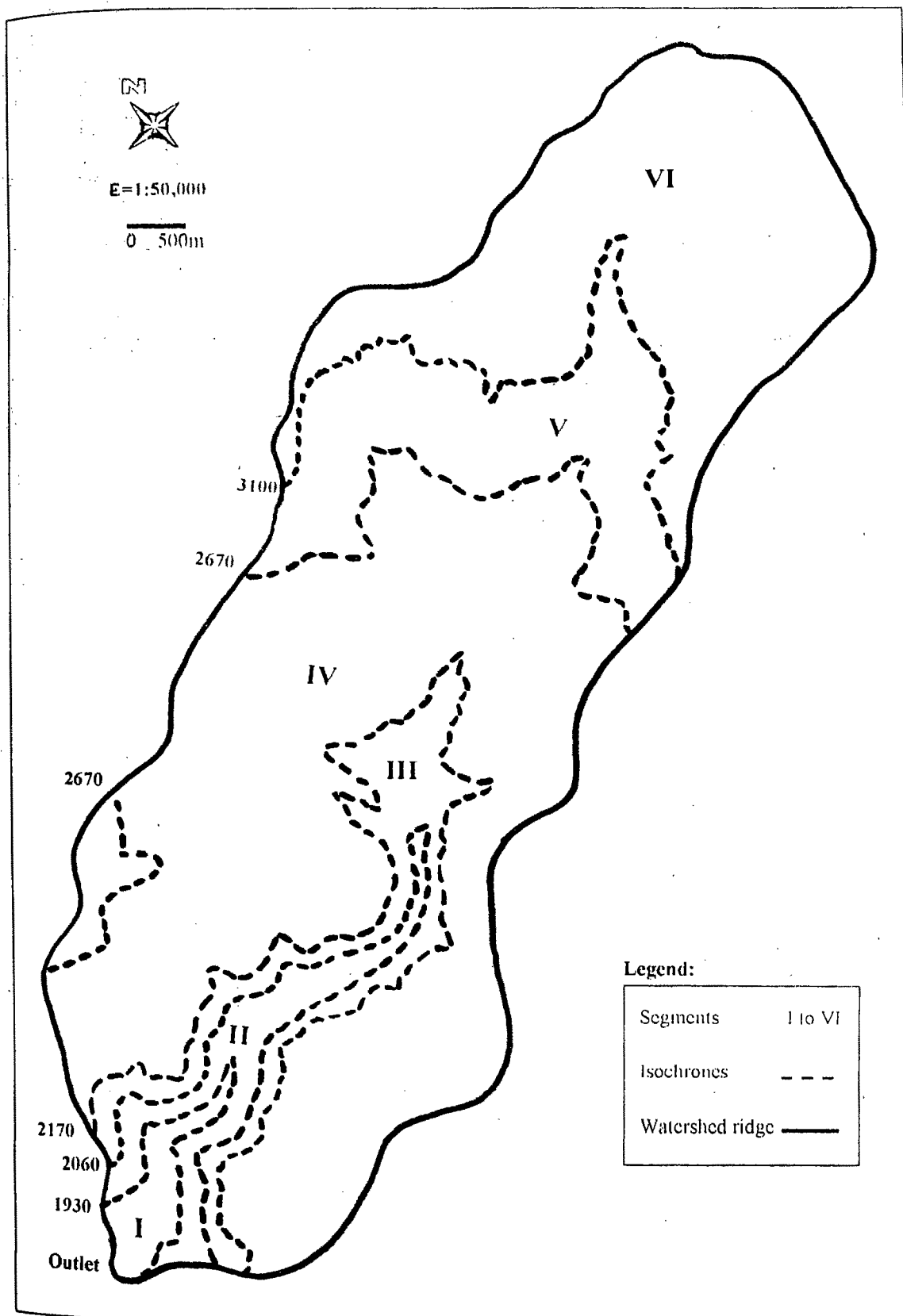


Fig. 4.12 Time-Area segments for Amameh watershed

It may be mentioned here for caution that the models USLE, Hudson, EUSLE, AOF and TAM (owing to application of the USLE as a base) have originally been recommended for application on an annual basis and their application on a storm basis is not expected to give reasonable results as per the efforts made in this study. The amount of soil erosion was converted into sediment yield by applying sediment delivery ratio (SDR), which was determined by using the inverse relationship between the SDR and the basin area (Roehl, 1962). The value of sediment delivery ratio was then adjusted by taking into account the factors such as soil texture, type of erosion, transport system and depositional area. The thus adjusted value of SDR was obtained as 0.18 for the study area. The procedure suggested by Williams (1972), based on a step-wise multiple regression equation between SDR and the slope of the main stem channel, was also checked for the determination of SDR and almost the same value was obtained.

It may also be seen from Table 4.10 that all the models not only tend to overestimate, but also have no acceptable relationship between estimated and measured data. Thus, from this analysis it appears that the applied models are probably considering those indices for soil loss estimation, which are not applicable for the case study area. The predicted values for all models were then also compared with the measured sediment yield and the associated correlation matrix is shown in Table 4.9. A high degree of correlation coefficient between each pair of models may be seen from the table but none of the models could yield better correlation with the measured data.

Table 4.9 *Correlation matrix between observed and estimated sediment yield values by various models*

Models	USLE	Hudson	EUSLE	AOF	TAM	Observed
USLE	1.000					
Hudson	0.975	1.000				
EUSLE	0.988	0.965	1.000			
AOF	0.959	0.919	0.793	1.000		
TAM	0.965	0.931	0.940	0.910	1.000	
Observed	-0.020	-0.060	0.059	0.227	-0.070	1.000

Table 4.10 Storm-wise comparison of different soil erosion models in Amameh watershed

Models	USLE				Hudson			EUSLE			AOF			TAM	Measured
	Crop factor, C	Erosivity	Soil erosion	Sediment	Erosivity	Soil erosion	Sediment	Erosivity	Soil erosion	Sediment	Erosivity	Soil erosion	Sediment	Sediment	Sediment
Storms															
April 23,70	0.202	4.261	9201.2	1656.2	0.000	0.0	0.0	1.647	3555.7	640.0	12.661	27339.0	4921.0	7118.0	1.452
April 14,71	0.202	14.007	30245.2	5444.1	0.000	0.0	0.0	5.973	12897.2	2321.5	49.257	106359.0	19144.7	23398.8	67.825
Aug. 2,72	0.151	3.567	5756.7	1036.2	0.000	0.0	0.0	1.308	2110.9	380.0	11.755	18973.6	3415.3	5958.7	0.606
Nov. 3,72	0.198	26.760	56637.0	10194.7	7.632	16153.3	2907.6	4.822	10206.5	1837.2	43.313	91673.8	16501.3	44702.7	6.946
July 18,74	0.151	69.249	111776.0	20119.6	53.476	86316.3	15536.9	12.544	20247.8	3644.6	64.779	104560.0	18820.8	115680.9	2.967
April 23,75	0.202	5.173	11169.5	2010.5	0.000	0.0	0.0	1.922	4150.1	747.1	36.431	78664.4	14159.6	8641.5	38.415
July 22,76	0.151	27.819	44903.7	8082.7	10.574	17067.6	3072.2	11.446	18475.1	3325.5	55.677	89868.7	16176.4	46471.8	11.287
April 29,80	0.202	6.019	12996.9	2339.4	0.000	0.0	0.0	2.362	5100.7	918.1	35.718	77124.7	13882.5	10054.8	24.603
April 25,83	0.202	55.021	118805	21384.9	11.374	24559.6	4420.7	9.781	21125.4	3802.6	62.212	134333.0	24180.0	91912.9	19.655
May 5,84	0.202	2.119	4574.9	823.5	0.000	0.0	0.0	0.761	1642.2	295.6	11.362	24534.0	4416.1	3539.8	0.616
July 25,86	0.151	3.420	5519.5	993.5	0.000	0.0	0.0	0.508	820.3	147.7	19.981	32251.1	5805.2	5713.1	3.330
Nov. 18,88	0.198	30.767	65117.9	11721.2	0.000	0.0	0.0	6.302	13338.8	2401.0	30.216	63652.8	11511.5	51396.5	1.153
Mar. 13,89	0.301	137.254	441620.0	79491.6	106.578	342919.0	61725.4	28.314	91100.0	16398.0	111.343	358251.0	64485.1	229283.7	16.142
Oct. 28,90	0.198	62.209	131667.0	23700.0	52.687	111513.0	20072.3	10.906	23082.8	4154.9	48.498	102646.0	18476.3	103920.5	0.577
April 6,97	0.202	68.46	14781.3	2660.6	0.000	0.0	0.0	1.165	2515.1	452.7	22.416	48401.6	8712.3	11436.3	6.038

*The values of soil erosion and sediment yield have been presented in tonne.

The estimated values of storm-wise sediment yield have also been plotted against observed values in Fig. 4.13. The relationship between the USLE and the other models (Hudson, EUSLE and AOF) are also shown in Fig. 4.14.

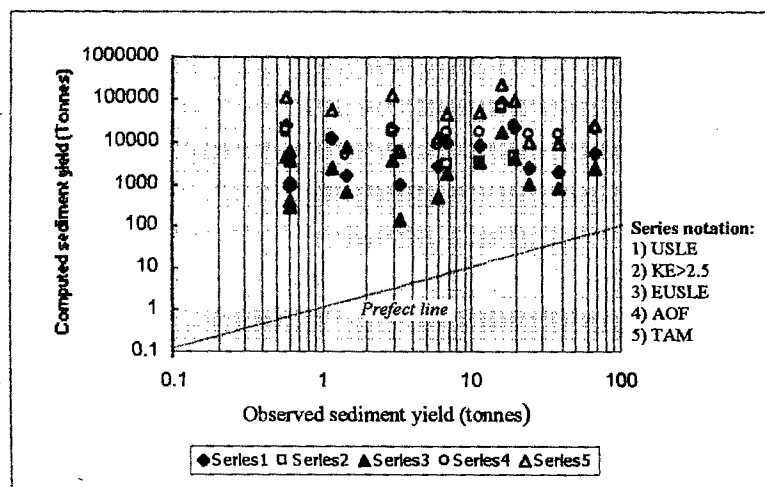


Fig. 4.13 Observed and computed sediment yield by various soil erosion models

Therefore, it appears that the soil erosion models developed basically on annual basis are not applicable on the study area for sediment prediction when applied on storm basis. The type of precipitation i.e. snowfall in some of the selected storm events may possibly be the another reason for the disagreement between the observed and the predicted values. Though both of these forms of precipitation viz. rainfall and snowfall, may have the same duration and depth, their effects to create runoff are very different. It may be more pertinent to analyze separately both of these two types of precipitation. Nicks *et al.* (1994) have also expressed similar views.

Since the runoff has been considered to be the best single indicator for sediment yield prediction (ASCE, 1969 and Williams, 1975), an attempt was made to modify the AOF model by eliminating the rainfall erosivity term from Eq. (4.41) and considering only runoff erosivity as the input for estimating erosivity factor R . Thus the Eq. (4.41) reduces to:

$$R = 0.45(Q.q_p)^{0.33} \quad \dots(4.43)$$

Where Q and q_p are respectively the volume of runoff in m^3 and peak runoff rate in $m^3 s^{-1}$ and R is erosivity factor in $t.m.cm.ha^{-1}$. On substituting Eq. (4.43) in place of erosivity factor (R) in the USLE model (Eq. 4.31) and by knowing the other parameters of K , LS , C and P , the soil erosion was estimated for selected storms. The estimated values were then regressed with the observed values of sediment yield by using different fit equations. The following power equation was found well fitted to the set of measured sediment yield and estimated soil erosion data for the Amameh watershed:

$$Y = 5.3775 \cdot 10^{-11} (Q \cdot q_p)^{0.33} K \cdot LS \cdot C \cdot P \quad (r=0.961) \quad \dots(4.44)$$

where Y is storm-wise sediment yield in tonne and other parameters have already been defined. Therefore, it appears here also that the runoff factor is a better index for sediment yield prediction in this watershed with a high level of acceptability as compared to the rainfall factor.

b-1-2 Storm-wise sediment yield sub-models

Since the performance of annual erosion models was not satisfactory for the estimation of sediment yield on storm basis, efforts were made to evaluate the workability of some of the available storm-wise prediction models in literature. With this in view, the MUSLE (Williams, 1975) and two of its newly modified versions viz. the MUSLE for soil erosion (Nicks *et al.*, 1994), and the MUSLT (Nicks *et al.*, 1994), were selected and their efficiency for sediment yield prediction in the Amameh watershed were assessed. The same storm events used in evaluation of erosion models were also considered for these models. A brief description of the models and their applicability is given in the following sections.

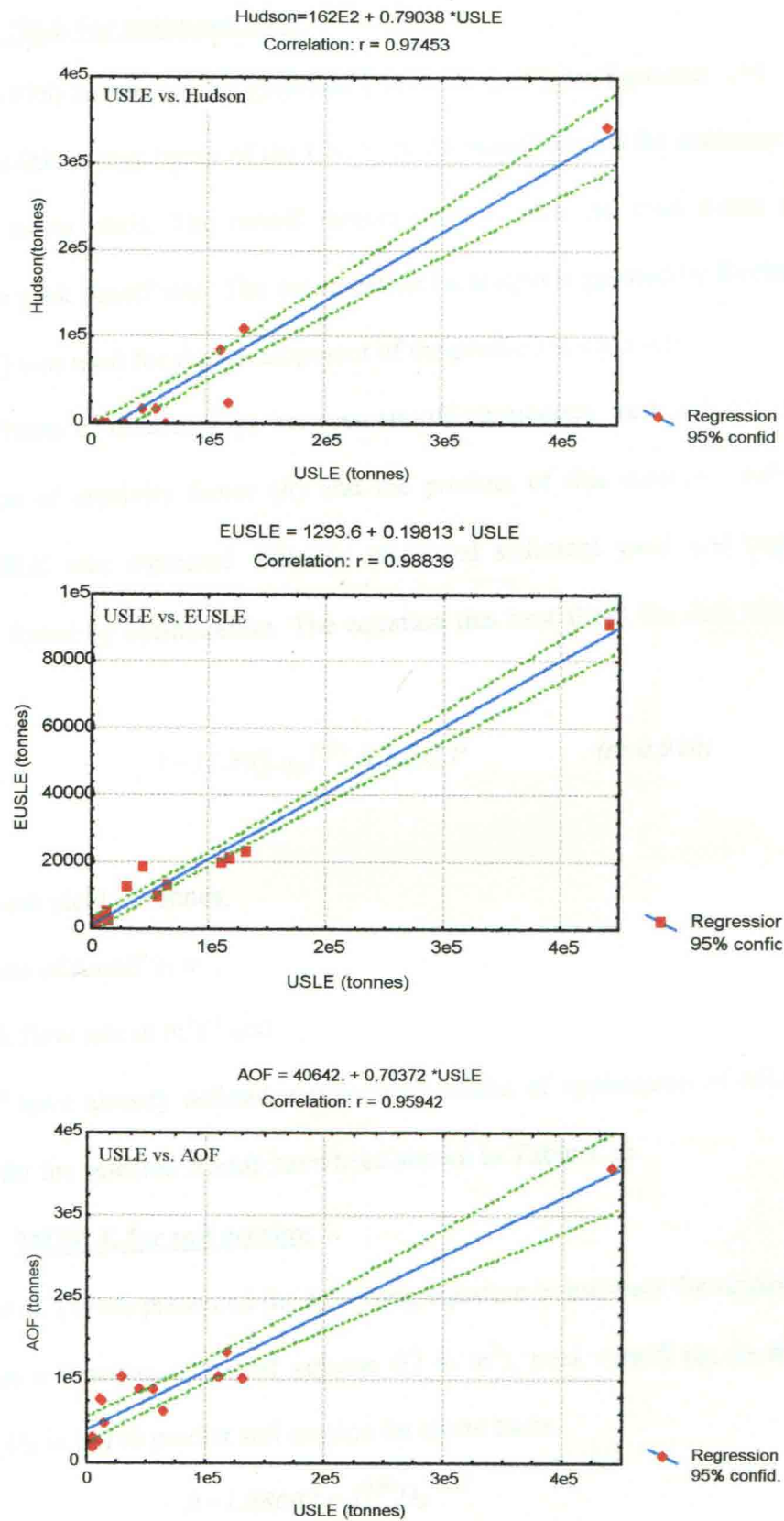


Fig. 4.14 Comparison of storm-wise soil loss estimation by using Hudson, EUSLE and AOF with USLE

b-1-2-1 MUSLE for sediment yield

Williams (1975) developed the Modified Universal Soil Loss Equation. (MUSLE) by replacing the rainfall energy factor of the USLE by the runoff factors for sediment yield prediction on per storm basis. The runoff factors include both the total storm runoff volume and it's the peak runoff rate. The optimization technique suggested by **Decloursey and Snyder (1969)** was used for the development of the prediction equation.

Different forms of relationships between runoff parameters were substituted into the USLE in place of erosivity factor (R) and the product of this erosivity with other factors of the USLE was regressed with the measured sediment yield and regression coefficients were found by optimization. The equation that best fitted the data was of the following form:

$$Y = 11.8(Q.q_p)^{0.56} K.LS.C.P \quad (r=0.920) \quad \dots(4.45)$$

where

Y = sediment yield in tonnes,

Q = volume of runoff in m^3 ,

q_p = peak flow rate in $m^3 s^{-1}$ and

K , LS , C and P have already defined earlier. The results of application of MUSLE for sediment yield for the selected storms have been shown in Table 4.11.

b-1-2-2 MUSLE for soil erosion

Nicks *et al.* (1994) presented the following equation to estimate the erosivity factor of the USLE as a function of runoff volume (Q in m^3), peak runoff (q_p in $m^3.s^{-1}$) and drainage area (D_A in ha) to predict soil erosion on storm basis.

$$R = 1.586(Q.q_p)^{0.56} D_A^{0.12} \quad \dots(4.46)$$

The values of R were calculated for selected storm events by using Eq. (4.46) and used to predict soil erosion on storm basis by Eq. (4.31). The results of the model after

conversion into sediment yield with the SDR of 0.18 are shown in Table 4.11.

b-1-2-3 MUSLT

Nicks *et al.* (1994) proposed another model named as Theoretical Modified Universal Soil Loss Equation with different coefficient and exponent of the runoff energy factor for estimation of soil erosion as below:

$$R = 2.5(Q.q_p)^{0.5} \quad \dots(4.47)$$

The calculated values of R were used to estimate soil erosion rate in the same manner as with the USLE and the estimates were then converted to the sediment yield with the same SDR of 0.18. The storm-wise estimates of sediment yield are also presented in Table 4.11.

It has to be mentioned here that the same values were considered for the system parameters of the USLE model (K , C and P) in all of the aforesaid models, since no significant changes had been made in the inherent characteristics of the watershed and the prevalent land-uses. The claim of uniformity of system parameters during the collection period of data (1973-1998) was checked by analysis of sediment rating curves (SR_C) and interpretation of the satellite images.

Table 4.11 Storm-wise observed and computed sediment yield (tonnes) by various models

Method Storm	Measured Sediment	MUSLE for sediment yield	MUSLE for soil erosion	MUSLT
April 23,70	1.419	1303.947	84.588	28.343
April 14,71	51.407	14045.780	911.156	236.663
Aug. 2,72	0.555	899.584	58.356	19.722
Nov. 3,72	12.380	6581.299	426.932	120.016
July 18,74	7.421	3221.938	209.009	61.613
April 23,75	31.742	10090.970	654.606	176.159
July 22,76	39.512	9414.720	610.737	160.497
April 29,80	36.742	9447.725	612.878	166.098
April 25,83	28.718	6997.629	453.939	127.045
May 5,84	1.575	1322.991	85.823	28.712
July 25,88	5.133	2626.928	170.410	51.346
Nov. 18,88	1.110	1374.223	89.146	29.639
Mar. 13,89	18.805	7919.086	513.714	148.075
Oct. 28,90	1.098	948.364	61.521	21.284
April 6,97	7.598	3588.906	232.814	69.990

The comparison of the measured and estimated values of sediment yield using different versions of the MUSLE are also shown in Fig. 4.15. The power regressions expressing the relations between observed and estimated sediment yield by respective models have been reported in the concerned figures. It can be observed from the Table 4.11 as well as Fig. 4.15 that all the models overestimated the sediment yield even though a high degree of harmony (more than 97 %) was found between the measured and the estimated values. These results lead to the conclusion that a suitable calibration should be made to get an accurate simulation for sediment yield for the study area.

Since the MUSLE (Williams, 1975) eliminates the need for a sediment delivery ratio to convert soil erosion to sediment yield and has an edge in correlation coefficient between measured and estimated data over all models of soil erosion (Article b-1-1) and sediment yield (Article b-1-2) estimation applied in this study, it was thought to calibrate the MUSLE for the Amameh watershed by determining the appropriate power quotient (m) for the runoff erosivity parameters. Thus the Eq. (4.45) will appear as,

$$Y=11.8(Q.q_p)^m K.LS.C.P \quad \dots (4.48)$$

All the 15 storms used for models evaluation and having known values of sediment yield, were considered for the determination of power quotient. Thus, 15 different values of m have been obtained. The magnitudes of power quotient m for all the storms were found to be very low as compared to 0.56 given by Williams (1975). It may possibly be due to a very low quantity of sediment yield from the watershed. The value of power quotient m was found to be varying in between -0.241 to 0.152 with a mean value of -0.0104 and a standard deviation of 0.142 . The average positive and the negative values of m were found to be 0.081 and -0.192 , respectively. If the constant value of 11.8 (unit conversion factor) were ignored in Eq. (4.45) for simplification, the value of m was found to range from 0.070 to 0.336 for different storms with an average value of 0.213 .

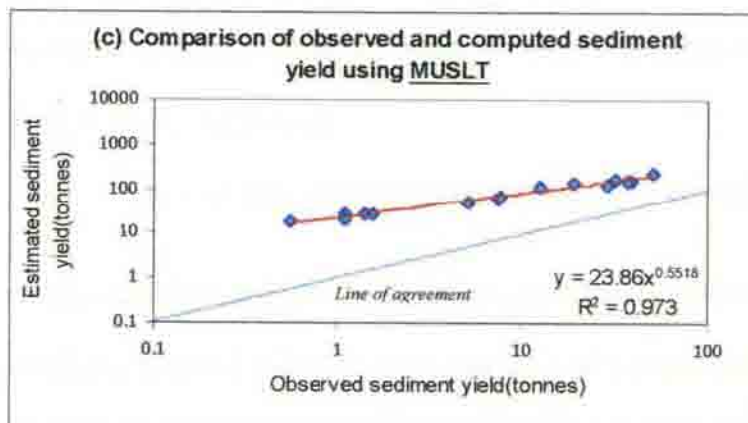
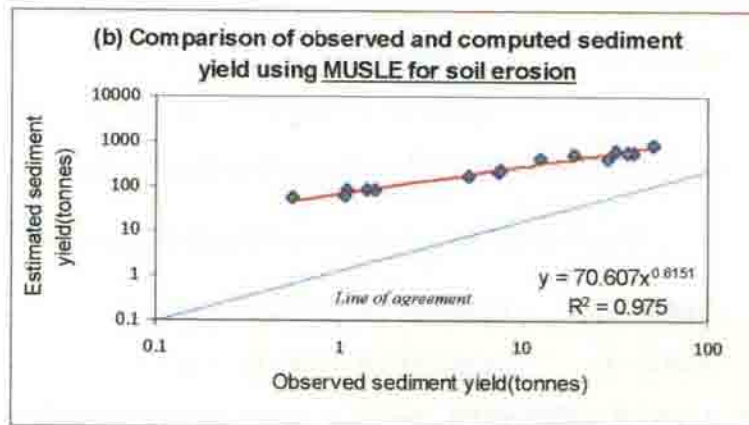
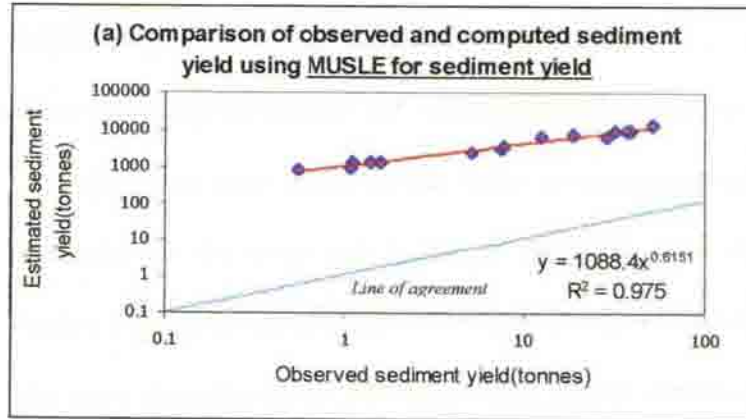


Fig. 4.15 Comparison of observed and computed sediment yield by using various models

Williams (1975) allocated that the MUSLE model for sediment yield prediction is more suitable for large storms but no criteria has been suggested by him to classify storms in large or small. An effort has been made in this study to categorize the storms under small and large categories for the study area based on the quotient m value of the Eq. (4.48) in such a way that the vegetative values represent the small size storm.

The m values were determined by relating it with runoff volume (Q in m^3), i.e. $m=b_0+b_1Q$, and with peak runoff rate (q_p in m^3s^{-1}), i.e. $m=b_0+b_1q_p$, where b_0 and b_1 are the regression coefficients and the following regression equations were obtained:

$$m = -0.1912 + 0.00004Q \quad (r=0.890) \quad \dots(4.49)$$

$$m = -0.1368 + 0.037064q_p \quad (r=0.776) \quad \dots(4.50)$$

The logarithmic regression relationships between m and Q as well as m and q_p were also tried and the equations of the following forms were developed:

$$m = -1.5990 + 0.1486\ln(Q) \quad (r=0.942) \quad \dots(4.51)$$

$$m = -0.1477 + 0.1542\ln(q_p) \quad (r=0.924) \quad \dots(4.52)$$

From the above four equations a closer relationship between m versus runoff volume than m versus peak flow rate can be observed but both the variables (Q and q_p) have a statistically significant correlation with the values of m . with this into consideration, an attempt was made to develop a multivariable regression relationship of the following form (i.e. $m=b_0+b_1Q+b_2q_p$):

$$m = -0.298 + 0.00003Q + 0.02193q_p \quad (r=0.918) \quad \dots(4.53)$$

The following multiple regression equation was also obtained by using the natural logarithm of the volume (Q) and the peak discharge (q_p) at a time, which gives better correlation coefficient, to determine the appropriate value of m for the application of MUSLE (for sediment yield) in the study area:

$$m = -1.005 + 0.089\ln(Q) + 0.078\ln(q_p) \quad (r=0.982) \quad \dots(4.54)$$

The statistical parameters of Eq. (4.54) are shown in Table 4.12:

Table 4.12 Statistical analysis of multiple regression for calculation of exponent m

N=15	Standard regression coefficient (BETA)	St. Err. Of BETA	Non-standard regression coefficient (B)	St. Err. of B	t-value (12)	P-Level
Intercept			-1.00539	0.142411	-7.05978	0.000013
Ln (Volume)	0.563027	0.093203	0.08881	0.014702	6.04084	0.000058
Ln (Peak)	0.468919	0.093203	0.07821	0.015545	5.03114	0.000294
Determination coefficient, $R^2=0.963946$ and Adjusted $R^2=0.957937$						
F-test value (2,12)=160.42, $p<0.000001$ and Standard Error of estimate: 0.02915						

Based on the correlation coefficient, the Eq. (4.54) has been used in this study to quantify the magnitude of storms (large and small). That is, the storm is respectively large for positive and small for negative values of m . Therefore, the Eq. (4.55) can be obtained by substituting the average of positive values for m , as already explained, in the Eq. (4.48) for sediment yield (Y) prediction in the Amameh watershed.

$$Y = 11.8(Q.q_p)^{0.081} K.LS.C.P \quad \dots (4.55)$$

subject to

$$0.089 \ln(Q) + 0.078 \ln(q_p) \geq 1$$

The performance of the developed model (Eq. 4.55) for the estimation of sediment yield was found to be satisfactory. The average error of estimation was found to be 19.40 %, and the mean ratio of the observed sediment values to the estimated ones was obtained as 1.29.

b-2 Sediment routing sub-model

Since the eroded sediments are produced from different sources throughout the watershed, it is often advantageous to model sediment delivery process at watershed scale using a spatially distributed approach (Ferro and Porto, 2000). Sediment routing sub-model investigates the routing process in a watershed and assists in the determination of sediment concentration as well. Besides that, the factors which influence the sediment yield of the watershed vary considerably and are not usually uniformly distributed

throughout the watershed. Therefore, a sediment routing sub-model is required for the purpose of increasing the accuracy in sediment yield estimation and for determination of contribution from individual sub-watersheds to the total sediment yield in the Amameh watershed.

The procedure is based on the *Williams' routing model* (1975), in which it is assumed that sediment deposition depends upon settling velocities of the sediment particles, the length of travel time, and the amount of sediment in suspension. For turbulent flow, the settling velocity is proportional to the square root of the particle diameter (**Einstein, 1964**). These assumptions can be expressed by the following equation:

$$\frac{dY}{dt} = -\beta Y \sqrt{d} \quad \dots(4.56)$$

where

dY = variation in sediment yield (Y) at a particular channel section,

dt = time interval,

β = decay constant, also called *sediment routing coefficient*, and

d = particle diameter.

Integrating Eq. (4.56) and solving it within integral limits of travel time (0,T) of the watershed yields the following equation:

$$Y_T = Y = Y_0 e^{-\beta T \sqrt{d}} \quad \dots(4.57)$$

where

$Y_T = Y$ = total sediment yield of the entire watershed,

Y_0 = sediment yield at an upstream section, i.e. upstream sub-watersheds, and

T = travel time between the two sections.

The information regarding particle size distribution of the sediment needs accurate granulometric study. Since the range of variation of particle size and also its effect on the sediment yield due to the type of proportion (root), is less in comparison to the other

parameters in the sediment routing model (Eq. 4.57), the sediment routing parameter (β) and the square root of particle diameter (d) is represented by a single parameter Z (Williams, 1978; Singh *et al.*, 1981 and Banasik, 1996). That is,

$$B = \beta \sqrt{d} \quad \dots(4.58)$$

Accordingly, the total sediment yield delivered to the watershed outlet is estimated by summing up the sub-watersheds' contributions as shown in the following equation:

$$Y = \sum_{i=1}^n Y_i e^{-BT_i} \quad \dots(4.59)$$

where, Y is sediment yield from the entire watershed, Y_i is sediment yield from the i^{th} sub-watershed and n is the number of sub-watersheds. Other parameters have already been defined. Following the Eq. (4.55) the sediment yield from i^{th} sub-watershed may be expressed as,

$$Y_i = 11.8(Q_i q_p)^{0.081} K_i LS_i C_i P_i \quad \dots(4.60)$$

Substituting Eq. (4.60) in Eq. (4.59) and equating it with the Williams' model modified for the study area, i.e. Eq. (4.55), results into the following equation:

$$11.8(Q q_p)^{0.081} K LS C P = 11.8 \sum_{i=1}^n (Q_i q_{p_i})^{0.081} K_i LS_i C_i P_i e^{-B_i T_i} \quad \dots(4.61)$$

The suffix i refers to the parameters of the i^{th} sub-watershed. In the original Williams' routing model (1975), the system parameters of K , LS , C and P were considered to be the same throughout the watershed. However, in the present study, the actual values of these system parameters along with travel time (T) and runoff parameters (Q and q_p) have been determined individually for each sub-area as described in the following sections.

b-2-1 Estimation of model system parameters

The system parameters of sediment routing model viz. K , LS , C , P and travel time T in Eq. (4.61), were found out by the procedure as explained in the following.

The Amameh watershed was divided into twelve sub-areas based on drainage pattern and land use conditions, as discussed under articles 3.1.1.6 and 3.1.4 in chapter 3 and the sub-divisions are shown in Fig. 4.16. The soil erodibility factor (K), topography factor (LS), crop management factor (C) and land management factor (P) were determined for each sub-watershed as per the procedure explained earlier under the article b-1-1-1 (USLE). The area was determined by *strip method* at one-centimeter interval. The *method of SCS upland curve* (1972) was found to be the most acceptable method for estimation of time of concentration in the Amameh watershed with almost 5 % underestimation among many other compared methods with measured data (Abbasi, 1993). Therefore, the SCS upland curve method has been used in the present study for the determination of time of concentration and the travel time, defined as elapsed time between the outlet of the sub-watershed and the main outlet, of each sub-watershed with respect to the slope and the waterway conditions. The characteristics of sub-watersheds consisting of area, time of concentration, travel time, erodibility, slope length, slope steepness, topography crop management and land management factors are shown in Table 4.13.

b-2-2 Estimation of runoff parameters

The runoff parameters viz. Q and q_p for each sub-watershed can be estimated by determination of their contribution in total output. Evaluation of partial contribution of each sub-watershed in the generation of total runoff from the watershed is difficult and poses a real value problem in designing a comprehensive watershed management programs specially when there is no provision for recording outputs from each sub-watershed. Among the available references in the field of hydrology no definite procedure for the estimation of runoff generated at each un-gauged sub-watershed has been presented. Therefore, an attempt was made to develop an applicable procedure to estimate

Table 4.13 Characteristics of sub-study areas of Amameh watershed

No. of sub-area	Area (ha)	Time of concentration (h)	Travel time (h)	Erodibility factor ($t \cdot ha \cdot m^{-3} \cdot s^{-1} \cdot cm^{-1}$)	Slope length (m)	Slope steepness (%)	Topography factor	Crop and land management factor
1	216.1	0.188	1.444	0.22	150	26.4	15.08	0.20
2	333.5	0.209	1.444	0.22	133	29.0	16.79	0.23
3	35.0	0.083	1.444	0.22	125	33.4	20.99	0.23
4	517.1	0.291	1.153	0.26	146	33.4	22.69	0.15
5	400.9	0.288	1.153	0.25	125	35.2	23.09	0.14
6	78.7	0.305	0.990	0.18	155	24.6	13.54	0.10
7	309.8	1.363	0.990	0.10	215	25.5	16.40	0.06
8	332.3	1.009	0.990	0.28	187	17.7	8.44	0.08
9	529.6	0.895	0.495	0.29	160	18.5	8.41	0.14
10	186.2	0.487	0.495	0.23	129	29.0	16.543	0.16
11	715.7	0.415	0.080	0.23	213	34.3	28.76	0.15
12	37.5	0.080	0.000	0.14	130	22.0	10.20	0.12
Watershed	3712.0	3.000	1.543	0.24	166	24.5	18.18	0.14

partial contribution of runoff from un-gauged sub-watersheds. Three different approaches, viz. *Area-CN role factor*, *first order decay function* and *Reverse Routing Technique (RRT)* were developed to estimate runoff from such types of un-gauged sub-watersheds or sub-areas.

b-2-2-1 Area-CN role factor technique

In a hypothetical watershed, where the physical and hydrological variables except the area are considered to be constant, it can be assumed that the ratio between the area of the sub-watershed to the entire area is equal to the ratio of their respective runoff characteristics i.e. the value of runoff per unit area is supposed to be the same for the entire watershed. That is,

$$\frac{R_i}{R_T} = \frac{A_i}{A_T} \quad \dots (4.62)$$

where R_i and R_T are the runoff properties (i.e. volume and peak runoff) of i^{th} sub-watershed ($i=1,2,\dots,n$) and total watershed respectively, A_i is the area of i^{th} sub-watershed and A_T is the total area of the watershed. This relationship then gives the partial contribution of the sub-watershed as equal to the multiplication of the ratio of the area and the total output from the main watershed.

However in general most of the watersheds are heterogeneous in nature resulting varying hydrogeological conditions. In the study area also this can be noticed respectively from Fig. 4.7 and the results of precipitation-runoff modeling that the *CN* has different values through the watershed and has a high degree of agreement (82 %) with runoff. Therefore, It can be assumed that in the study area other factors affecting runoff generation do not have significant effect. Owing to this heterogeneity of the Amameh watershed, the ratio of runoff parameters (Q and q_p) from sub-watersheds to the entire watershed has also been considered to be varying proportionally to the ratio of respective

CN values. Since CN factor is based on most of the physical and hydrological characteristics of the watershed, the above concept can be expressed as follows:

$$R_T = f(CN_T) = f\left(\frac{\sum_{i=1}^n CN_i A_i}{\sum_{i=1}^n A_i}\right) \quad \dots(4.63)$$

where CN_i and CN_T are the values of curve number for the i^{th} sub-watershed and the total watershed, respectively. The relationship for each sub-watershed having m number of land-uses ($m=1,2,\dots,M$) can be represented as below:

$$R_i = f(CN_i) = f\left(\frac{\sum_{m=1}^M CN_{im} A_{im}}{\sum_{m=1}^M A_{im}}\right) \quad \dots(4.64)$$

Since $\sum A_{im} = A_i$ and $\sum A_i = A_T$, the ratio between R_i and R_T is obtained by dividing Eq. (4.64) by Eq. (4.63) as,

$$\frac{R_i}{R_T} = f\left(\frac{\sum_{m=1}^M CN_{im} A_{im}}{A_i} / \frac{\sum_{i=1}^n CN_i A_i}{A_T}\right) = f\left(\frac{\sum_{m=1}^M CN_{im} A_{im}}{A_i} \cdot \frac{A_T}{\sum_{i=1}^n CN_i A_i}\right) = f\left(\frac{CN_i}{1} \cdot \frac{1}{CN_T}\right) = f\left(\frac{CN_i}{CN_T}\right) \quad \dots(4.65)$$

The above functional equation can be solved by introducing a watershed constant. When the area of sub-watersheds varies, then the ratio of a particular sub-watershed area to the total area of the entire watershed can be assumed to be equal to the sub-watershed constant in total runoff generation. With this in view, the Eq. (4.65) can be reformed to the following form for the i^{th} sub-watershed:

$$\frac{R_i}{R_T} = \frac{A_i}{A_T} \frac{CN_i}{CN_T} \quad \dots(4.66)$$

$$\text{or} \quad R_i = R_T \frac{A_i}{A_T} \frac{CN_i}{CN_T} \quad \text{and} \quad R_T = R_i \frac{A_T}{A_i} \frac{CN_T}{CN_i} \quad \dots(4.67)$$

The concept presented above can also be expressed in another manner for better understanding. Eq. (4.62) is being used for the determination of contribution of each sub-watershed in generation of total runoff when the areas of sub-watersheds are different. The

summation of partial contributions of n number of sub-watersheds is also equal to the total output of the main watershed. That is,

$$R_T = R_1 + R_2 + \dots + R_n \quad \dots (4.68)$$

If W_i is the result of multiplication (based on the concepts of system efficiency) of changing variable ratios, i.e. a proportion of total runoff, the following equation can be written by using the Eq. (4.68):

$$R_T = R_T \sum_{i=1}^n W_i \quad \dots (4.69)$$

Eq. (4.69) shows that the summation of W_i should be equal to one, which is also logically correct. By considering Eqs. (4.62) and (4.69), the following equation can be expressed for the conditions when the sub-watersheds are different from each other only in point of view of area, i.e. hydrologically homogeneous:

$$R_T = \frac{A_1}{A_T} R_T + \frac{A_2}{A_T} R_T + \dots + \frac{A_n}{A_T} R_T \quad \dots (4.70)$$

If the sub-watersheds have different values of CN besides the area, then the following equation can be written by combining Eqs. (4.66) and (4.69) for the heterogeneous watershed:

$$R_T = \frac{A_1}{A_T} \frac{CN_1}{CN_T} R_T + \frac{A_2}{A_T} \frac{CN_2}{CN_T} R_T + \dots + \frac{A_n}{A_T} \frac{CN_n}{CN_T} R_T \quad \dots (4.71)$$

Since the parameter of time required for runoff from each sub-watershed to reach to the main outlet has not been considered in this procedure, the application of this model may be limited to the small size watershed only. With this in mind, the following two approaches have been tried in this study to overcome this limitation.

b-2-2-2 First order decay function technique

The flow, which reaches the main outlet, can be considered that it has already been routed in the channel. This concept may be presented by the help of *first order decay function* used by **Chow (1964)** for the analysis of recession limb of hydrographs. If the

flow rates at the beginning (just at the outlet of the i^{th} sub-watershed) and after time t (at the main outlet) are R_i and R_T , respectively, then the flow recession can be shown in the form of a first decay order function as given below:

$$R_T = R_i e^{-\frac{t}{k}} \quad \dots(4.72)$$

The power of function can be defined as the ratio of times of concentration of the sub-watershed, TC_i and the total watershed TC_T . The storage coefficient k has the dimension of time and is governed by the time during which water lasts in the reach. Accordingly, the Eq. (4.72) can be expressed in terms of R_i as,

$$R_i = \frac{R_T}{\exp(-\frac{TC_i}{TC_T})} \quad \dots(4.73)$$

Since the calculation has to proceed backwards from the downstream end to the upstream, the decay power is to be applied in the reverse form and the final equation after considering the defined relationship for the determination of partial contribution in Eq. (4.67) can be expressed as:

$$R_i = R_T \frac{A_i}{A_T} \frac{CN_i}{CN_T} \frac{1}{e^{-k_i}} \quad \text{where } k_i = \frac{TC_i}{TC_T} \quad \dots(4.74)$$

The technique was tentatively verified for its applicability for the Amameh watershed with the results obtained by the computer model *SEDIMOT-II* in case of the volume of runoff and was found yielding reasonable results. Since a detailed information of runoff properties, i.e. volume and peak, are required for each sub-watershed to solve Eq. (4.61) for routing parameter Z , a method called as *reverse flood routing* was developed as given below.

b-2-2-3 Reverse flood routing technique

In flood routing, a flow hydrograph is routed from upstream to downstream end of a given reach. However, if the same procedure is performed in the opposite direction, i.e. downstream to upstream, it can appropriately be called as *reverse flood routing*. Since the

outlet hydrograph at the main outlet is available, a reverse flood routing technique (RRT) as detailed below has been used to determine the outflow hydrographs or partial contribution of sub-watersheds. In case of linear reservoir routing, the value of storage is a function of only the output, whereas in case of channel routing, it is a function of the input as well as the output. If S is the storage, k is the storage coefficient, x is the weighing factor, I is the inflow rate and Q is the outflow rate, then the general form of routing equation as proposed by McCarthy in 1934 (Chow, 1964) is,

$$S = k[xI + (1-x)Q] \quad \dots(4.75)$$

and the outflow rate for the n^{th} time step is calculated by using the following equation:

$$Q_n = C_0 I_n + C_1 I_{n-1} + C_2 Q_{n-1} \quad \dots(4.76)$$

where the coefficients C_0 , C_1 and C_2 are obtained by using the following relations (Chow, 1964), where Δt is the routing period, or discretized time interval that varies between $2kx$ and k .

$$C_0 = \frac{-kx + 0.5\Delta t}{k - kx + 0.5\Delta t} \quad C_1 = \frac{kx + 0.5\Delta t}{k - kx + 0.5\Delta t} \quad C_2 = \frac{k - kx - 0.5\Delta t}{k - kx + 0.5\Delta t} \quad \dots(4.77)$$

In general, the smaller the value of Δt , the more accurate is the result (Singh, 1993). In case of a linear reservoir, as suggested by Clark (1945) for development of conceptual hydrograph, the effect of inflow on storage is neglected, i.e. $x=0.0$ and thus the Eq. (4.75) get reduced to the following form:

$$S = kQ \quad \dots(4.78)$$

Also for $x=0.0$, the coefficient C_0 is equal to C_1 . Since the inflows are derived from excess runoff histogram, the $I_1 = I_2$ for each time interval (Δt). Owing to the above explanation, the Eq. (4.76) reduces to,

$$Q_n = 2C_0 I_n + C_2 Q_{n-1} \quad \dots(4.79)$$

$$\text{and} \quad I_n = (Q_n - C_2 Q_{n-1}) / 2C_0 \quad \dots(4.80)$$

The Eq. (4.79) having only one unknown, I_n , and can be solved easily to determine the output hydrograph of an un-gauged sub-watershed, located at the upstream of the reach under consideration and its partial contribution in total runoff generation can be evaluated. However, no effect of input on storage has been considered in this equation that appears to be little illogical. To overcome this deficiency the effects of the both input and output on storage are considered in the present study. Thus when $x \neq 0.0$, the Eq. (4.76) may be written,

$$I_{n-1} = \frac{Q_n - C_2 Q_{n-1} - C_0 I_n}{C_1} \quad \dots(4.81)$$

Since the Eq. (4.81) is having two unknowns, I_n and I_{n-1} , the solution is difficult to obtain. Therefore, the concepts of a direct hydrograph, in which the first and the last ordinates are equal to zero, were applied. That is in the first step, I_n is considered to be equal to Q_n and then the subsequent calculations are followed easily to obtain the total input hydrograph to the reach i.e. output hydrograph of upstream area.

Any of the above two Eqs. (4.80) and (4.81) can be applied to rout the output hydrograph reversibly. The value of k is assumed to be equal to the total travel time in the reach, whereas the value of x is estimated by using the following equation (**Wilson et al., 1981 and Subramanya, 2000**):

$$x = (0.5V_m)/(1.7 + V_m) \quad \dots(4.82)$$

where V_m is the average velocity of the flow in m.s^{-1} , determined by applying SCS Upland Curves. The Eqs. (4.80) and (4.81) were applied for evaluation of their performance on some solved problems. The error of estimation in case of Eq. (4.80) was found to be very less (below 10 %) at the beginning, which gradually increased in estimated ordinate values towards the end of the process, that is, commencement of hydrograph but as an average it was below 32 %. Whereas in case of Eq. (4.81) the error reduced considerably for all the

ordinates of the hydrograph and thus it was found preferable over the Eq. (4.80) to apply in the present study. The results obtained through Eq. (4.81) for a few storm events were also compared with the available respective hydrographs at the station Baghtangeh, located at the center of the Amameh watershed (*junction** 2 in Fig. 4.16) and a very high degree of agreement between observed and estimated values was observed. This also confirms the applicability of the *RRT* (Eq. 4.81) for the Amameh watershed.

The principle of area-CN role factor explained earlier is used for determination of partial contribution of each sub-watershed in generation of the total runoff, which passes from the point located at its downstream end. To apply reverse routing technique (*RRT*) in the study area for the determination of partial contribution, the detailed information regarding variation of *CN* in the sub-watersheds were obtained and are shown in Table 4.14. The average values of *CN* above each junction and entire watershed are also shown in the last six rows of the table.

This technique was used to determine the output hydrograph at the end of each sub-watershed during each storm event. The ordinates of outflow hydrographs of different sub-watersheds have been shown in columns represented by runoff 1 to runoff 12 referring to sub-watersheds from number 1 to 12. The *net hydrograph* at each junction is obtained by subtracting the ordinate values of hydrograph(s) of sub-watershed(s) from the outflow hydrograph at that particular outlet point or junction. The net hydrograph obtained at each outlet point/junction are then routed reversibly by *RRT* (Eq. 4.81) to obtain the outflow hydrograph from the preceding sub-watersheds. An example of the application of this method for the storm of April 23, 70 has been given in Table 4.15. The outflow hydrographs of each sub-watershed along with junctions hydrographs generated due to

* Junction in this study refers to the outlet points on the main stream where the output of one or more sub-watersheds drain to the next reach.

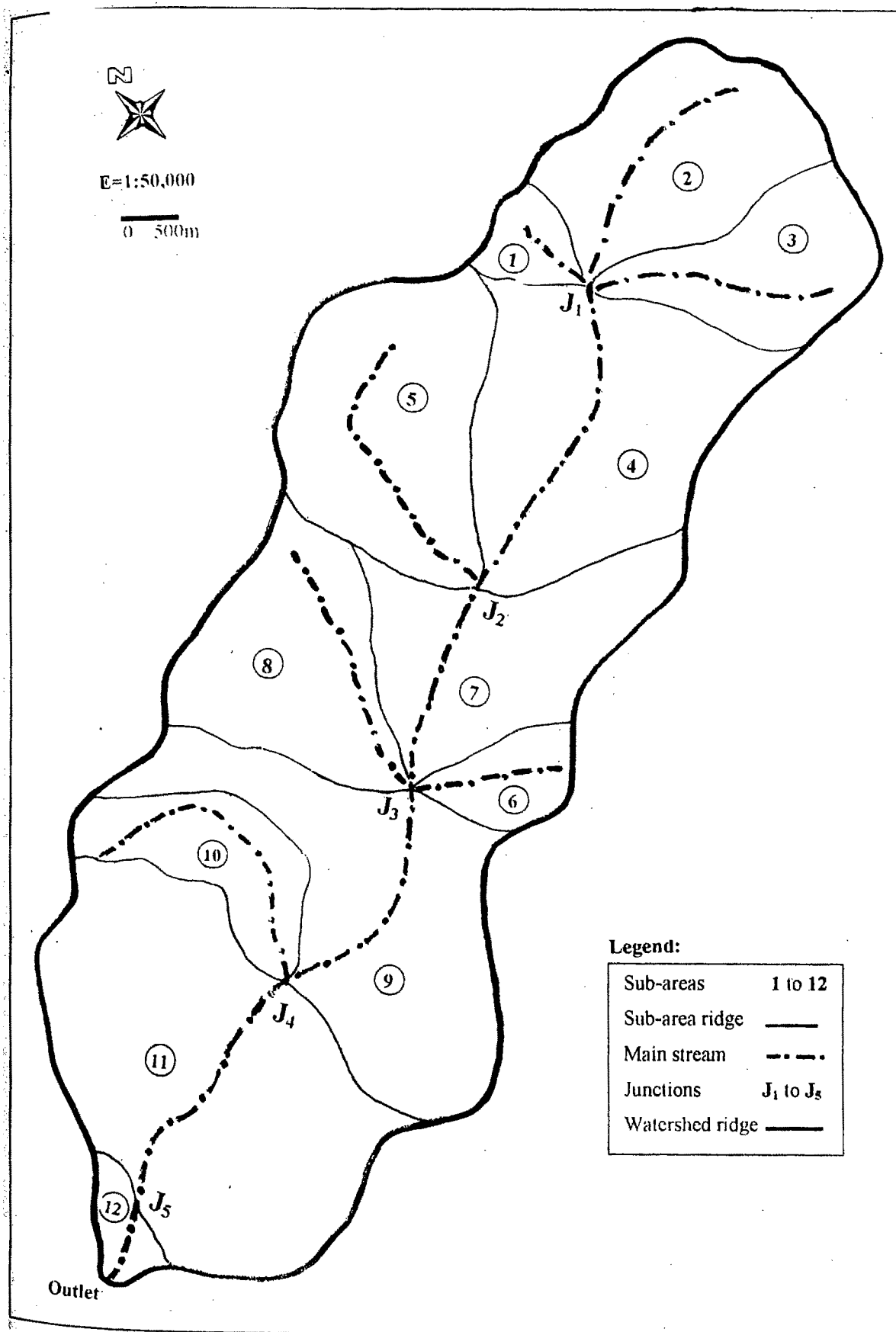


Fig. 4.16 Sub-divided study units in Amameh watershed

Table 4.14 Curve Number values for study sub-areas in Amameh watershed for selected storms

Sub-area	Area (ha)	April 23,70	April 14,71	Aug. 2,72	Nov. 3,72	July 18,74	April 23,75	July 22,76	April 29,80	April 25,83	May 5,84	Aug. 5,87	July 25,88	Nov. 18,88	Mar. 13,89	Oct. 28,90	April 6,97
1	216.08	77.47	86.67	79.44	78.50	78.84	76.00	76.00	86.88	90.07	77.38	77.38	76.00	80.38	84.76	85.44	76.00
2	333.46	78.45	87.19	80.31	79.41	79.74	77.00	77.00	87.39	90.41	78.34	78.34	77.00	81.20	85.37	86.01	77.00
3	54.99	78.45	87.19	80.31	79.41	79.74	77.00	77.00	87.39	90.41	78.34	78.34	77.00	81.20	85.37	86.01	77.00
4	517.04	76.47	85.67	78.44	77.50	77.84	75.00	75.00	85.88	89.06	76.38	76.38	75.00	79.38	83.76	84.44	75.00
5	400.86	77.47	86.67	79.44	78.50	78.84	76.00	76.00	86.88	90.07	77.38	77.38	76.00	80.38	84.76	85.44	76.00
6	78.69	30.60	48.68	35.15	33.39	34.02	30.00	30.00	49.10	56.36	30.61	30.61	30.00	36.91	44.93	46.40	30.00
7	309.77	39.11	56.70	43.38	41.65	42.27	38.00	38.00	57.11	63.20	39.58	39.58	38.00	45.11	53.05	54.45	38.00
8	332.26	39.11	56.70	43.38	41.65	42.27	38.00	38.00	57.11	63.20	39.58	39.58	38.00	45.11	53.05	54.45	38.00
9	529.54	64.62	77.54	67.52	66.22	66.69	63.00	63.00	77.83	82.30	64.66	64.66	63.00	68.82	74.85	75.84	63.00
10	186.18	76.47	85.67	78.44	77.50	77.84	75.00	75.00	85.88	89.06	76.38	76.38	75.00	79.38	83.76	84.44	75.00
11	715.62	76.47	85.67	78.44	77.50	77.84	75.00	75.00	85.88	89.06	76.38	76.38	75.00	79.38	83.76	84.44	75.00
12	37.50	57.53	72.30	60.94	59.46	60.00	56.00	56.00	72.64	77.76	57.70	57.70	56.00	62.41	69.23	70.38	56.00
Entire area	3712.0	67.53	78.91	70.09	68.94	69.35	66.12	66.12	79.17	83.12	67.56	67.56	66.12	71.23	76.54	77.41	66.12
Junction 5	3674.5	67.63	78.97	70.18	69.04	69.45	66.22	66.22	79.23	83.18	67.66	67.66	66.22	71.32	76.62	77.48	66.22
Junction 4	2958.8	65.49	77.35	68.18	66.99	67.42	64.10	64.10	77.63	81.76	65.55	65.55	64.10	69.37	74.89	75.80	64.10
Junction 3	2243.1	64.79	76.62	67.49	66.30	66.73	63.45	63.45	76.89	81.02	64.86	64.86	63.45	68.67	74.16	75.07	63.45
Junction 2	1522.4	77.38	86.46	79.32	78.39	78.73	75.92	75.92	86.67	89.81	77.29	77.29	75.92	80.25	84.58	85.25	75.92
Junction 1	604.5	78.10	87.00	80.00	79.08	79.42	76.64	76.64	87.21	90.29	78.00	78.00	76.64	80.91	85.15	85.81	76.64

Note: The figures in bold font represent the average CN values.

storm event of April 23, 70 are shown in Figs. 4.17a to 4.17f. The outflow hydrographs of all the sub-watersheds/sub-areas are also depicted on the same coordinates in Fig. 4.17g. The generated volume and peak of runoff for each sub-area during a particular storm event were determined from the hydrographs obtained with the same procedure explained above and are shown in Table 4.16. Here, the details of procedure are explained in the following steps for better understanding of the reader.

- Determination of direct outflow hydrograph from the entire watershed at main outlet.
- Determination of contribution ratio of sub-watershed 12 (Fig. 4.16) in generation of total output by the area-CN factor method (Eq. 4.66),
Determination of ordinates of outflow hydrograph of sub-watershed 12 by multiplying its contribution ratio into the ordinates of total outflow hydrograph (Eq. 4.67),
- Determination of ordinates of net out flow hydrograph at main outlet by deduction of hydrograph ordinates of sub-watershed 12 from the corresponding ordinates of the total hydrograph,
- Routing of net out flow hydrograph reversibly towards junction 5 by *RRT* (Eq. 4.81),
- Continuing the same steps till reach to the junction 1 and
- Completion of procedure by determination of partial contribution of sub-watersheds 1 to 3 at junction 1.

b-2-3 Determination of sediment routing coefficient

Since all the system and runoff parameters in Eq. (4.61) are known storm wise as well as sub-watershed wise, the sediment routing coefficient Z can be estimated by trial and error. In view of the fact that the trial and error method is cumbersome and time consumer specially in case of large number of sub-watersheds and system events. A more powerful and less time consuming method called as *Newton classical method* for solving

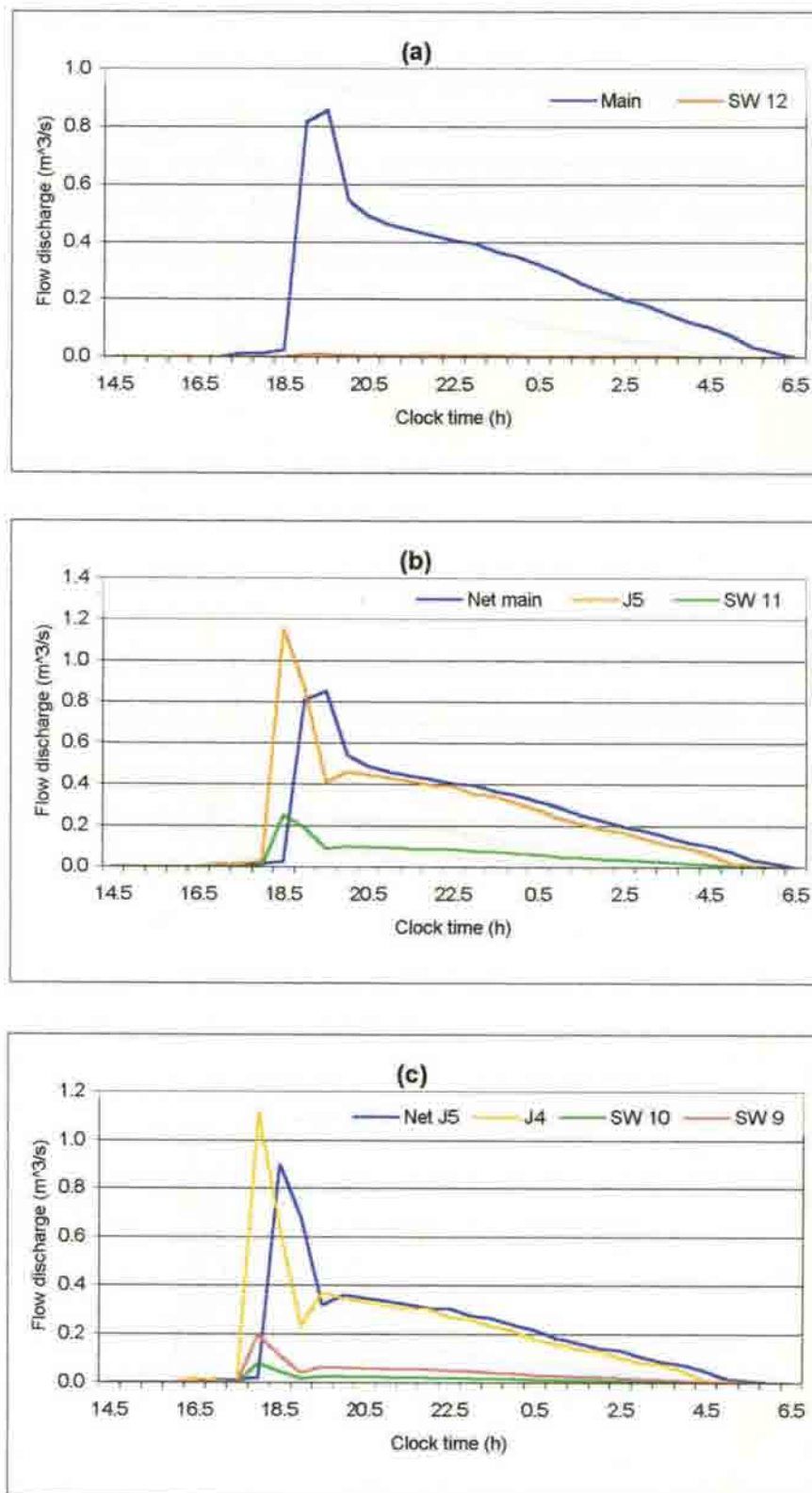
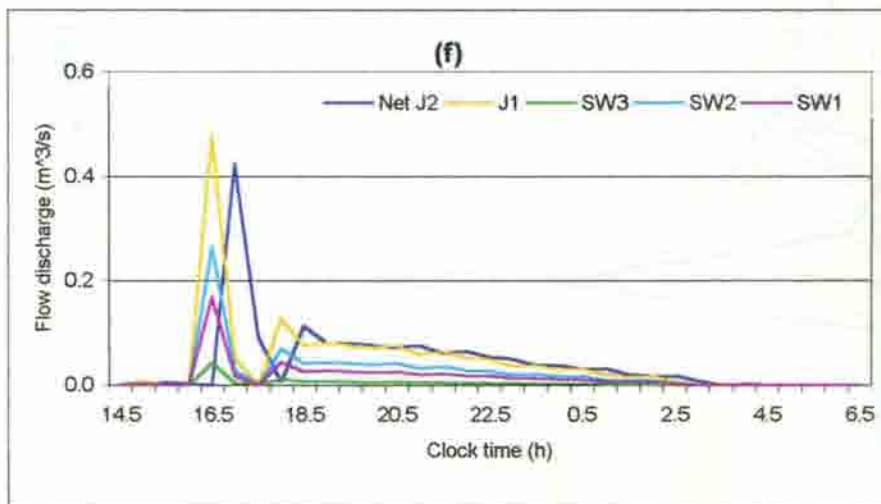
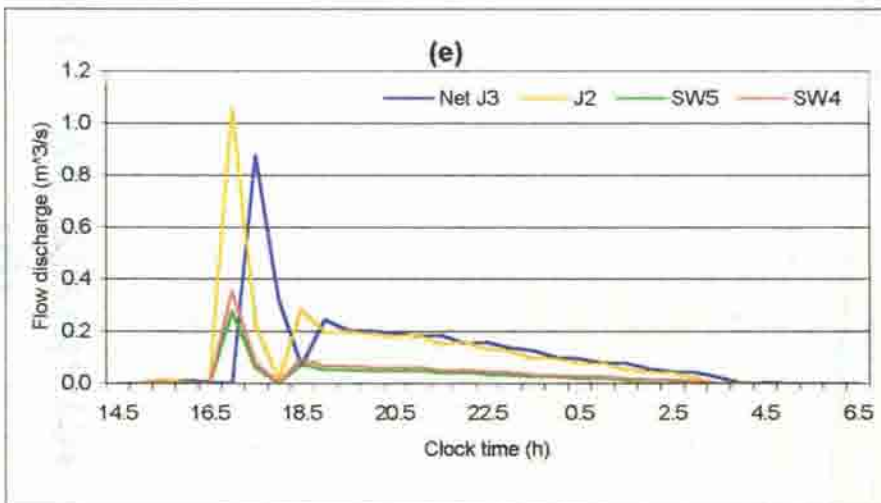
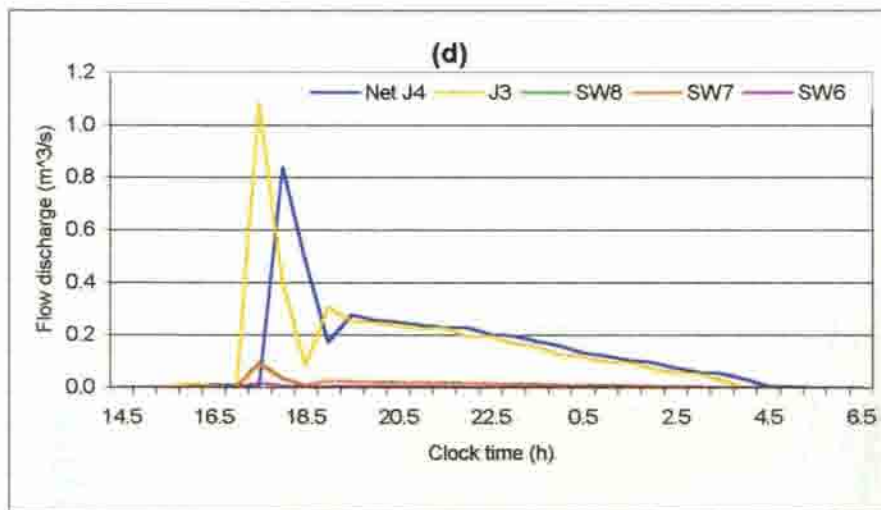
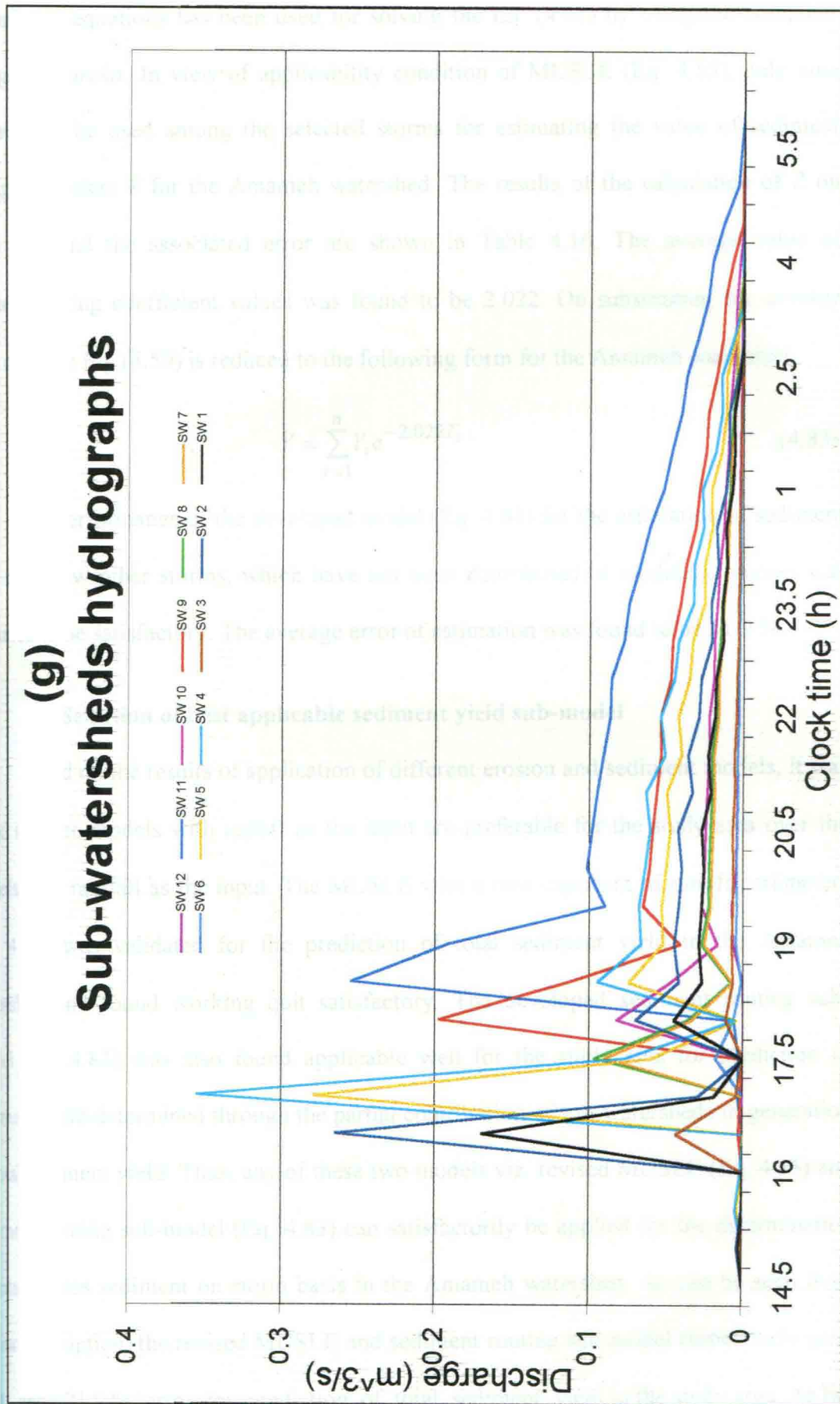


Fig. 4.17 Outflow hydrographs from individual sub-watershed obtained by reverse routing technique for storm event April 23, 70



Continued Fig. 4.17



Continued Fig. 4.17

The nonlinear equations has been used for solving the Eq. (4.61) by using the computer package of *Eureka*. In view of applicability condition of MUSLE (Eq. 4.55), only nine storms could be used among the selected storms for estimating the value of sediment routing coefficient Z for the Amameh watershed. The results of the calculation of Z on storm wise and the associated error are shown in Table 4.16. The average value of sediment routing coefficient values was found to be 2.022. On substituting the average value of Z , the Eq. (4.59) is reduced to the following form for the Amameh watershed.

$$Y = \sum_{i=1}^n Y_i e^{-2.022T_i} \quad \dots(4.83)$$

The performance of the developed model (Eq. 4.83) for the estimation of sediment yield for a few other storms, which have not been contributed in modeling process was evaluated to be satisfactory. The average error of estimation was found to be 21.9 %.

b-3 Selection of best applicable sediment yield sub-model

Based on the results of application of different erosion and sediment models, it was found that the models with runoff as the input are preferable for the study area over the models with rainfall as the input. The MUSLE with a new exponent of runoff parameters (Eq. 4.55) was validated for the prediction of total sediment yield in the Amameh watershed and found working quit satisfactory. The developed sediment routing sub-model (Eq. 4.83) was also found applicable well for the study area for prediction of sediment yield determined through the partial contribution of sub-watersheds in generation of total sediment yield. Thus, any of these two models viz. revised MUSLE (Eq. 4.55) and sediment routing sub-model (Eq. 4.83) can satisfactorily be applied for the determination of total excess sediment on storm basis in the Amameh watershed. As can be seen from earlier description, the revised MUSLE and sediment routing sub-model respectively gave 19.4 and 21.9 % error for prediction of total sediment yield in the study area. As far

Table 4.16 Determination of sediment routing parameter for Annameth watershed

Sub-area (No.)	Storm, April 23, 70		Storm, April 14, 71		Storm, Aug. 12, 71		Storm, Nov. 3, 72		Storm, July 18, 74		Storm, April 23, 75		Storm, July 22, 76		Storm, April 29, 80	
	Volume (m ³)	Peak (m ³ s ⁻¹)	Volume (m ³)	Peak (m ³ s ⁻¹)	Volume (m ³)	Peak (m ³ s ⁻¹)	Volume (m ³)	Peak (m ³ s ⁻¹)	Volume (m ³)	Peak (m ³ s ⁻¹)	Volume (m ³)	Peak (m ³ s ⁻¹)	Volume (m ³)	Peak (m ³ s ⁻¹)	Volume (m ³)	Peak (m ³ s ⁻¹)
1	940.4	0.169	6330.2	1.098	814.8	0.160	4276.4	0.283	2009.9	0.541	4529.5	0.805	4840.4	1.184	6201.2	0.393
2	1469.6	0.264	9827.6	1.705	1271.1	0.250	6676.0	0.442	3137.1	0.844	7082.0	1.259	7568.2	1.851	9626.0	0.610
3	242.4	0.044	1620.6	0.281	209.6	0.041	1100.9	0.073	517.3	0.139	1167.9	0.208	1248.0	0.305	1587.4	0.101
4	2207.5	0.365	14884.6	2.372	1839.2	0.340	10099.3	0.657	4471.6	1.155	10581.6	1.777	11241.9	2.701	14688.2	0.846
5	1733.8	0.279	11384.9	1.839	1444.1	0.267	7931.0	0.516	3511.3	0.907	8313.3	1.396	8832.1	2.122	11504.6	0.664
6	133.5	0.018	1251.8	0.181	117.2	0.019	661.9	0.041	287.5	0.066	643.7	0.097	662.6	0.153	1276.3	0.064
7	671.5	0.090	5739.6	0.829	569.4	0.095	3250.1	0.204	1406.4	0.323	3209.8	0.486	3303.8	0.764	5843.8	0.293
8	720.2	0.097	6156.3	0.889	610.7	0.102	3486.1	0.218	1508.5	0.346	3442.8	0.521	3543.7	0.819	6268.1	0.314
9	1876.2	0.197	13414.5	1.654	1579.1	0.199	8830.4	0.521	3781.5	0.717	9083.7	1.203	8860.4	1.923	13611.0	0.611
10	780.6	0.082	5210.9	0.643	645.0	0.081	3633.5	0.214	1551.8	0.294	3802.0	0.503	3708.6	0.805	5280.4	0.237
11	2988.9	0.254	20020.8	2.176	2476.6	0.257	13658.6	0.779	5959.2	0.970	14595.1	1.737	14109.0	2.772	20295.8	0.885
12	117.7	0.007	884.7	0.079	100.7	0.008	560.7	0.030	240.7	0.031	569.8	0.058	551.4	0.089	899.7	0.038
Watershed	13690.0	0.857	95590.0	8.552	11464.0	0.886	64350.0	3.400	27540.0	3.600	66600.0	6.800	64440.0	10.440	97065.0	4.148
	Z=2.040		Z=2.040		Z=1.998		Z=1.998		Z=2.064		Z=2.041		Z=2.066		Z=1.971	
	Max. error=5.23*10 ⁻¹²		Max. error=5.07*10 ⁻¹¹		Max. error=1.96*10 ⁻¹²		Max. error=1.15*10 ⁻¹²		Max. error=4.55*10 ⁻¹²		Max. error=1.12*10 ⁻¹³					

Continued Table 4.16

Sub-area (No.)	Storm, April 25, 83		Storm, May 5, 84		Storm, Aug. 5, 87		Storm, July 25, 88		Storm, Nov. 18, 88		Storm, March 13, 89		Storm, Oct. 28, 90		Storm, April 6, 97	
	Volume (m ³)	Peak (m ³ s ⁻¹)	Volume (m ³)	Peak (m ³ s ⁻¹)	Volume (m ³)	Peak (m ³ s ⁻¹)	Volume (m ³)	Peak (m ³ s ⁻¹)	Volume (m ³)	Peak (m ³ s ⁻¹)	Volume (m ³)	Peak (m ³ s ⁻¹)	Volume (m ³)	Peak (m ³ s ⁻¹)	Volume (m ³)	Peak (m ³ s ⁻¹)
1	4337.7	0.228	610.7	0.220	17396.9	1.735	2151.2	0.170	1083.5	0.089	5163.1	0.146	510.6	0.086	2388.0	0.221
2	6719.3	0.354	954.2	0.343	27180.4	2.711	3363.5	0.265	1699.1	0.139	8025.2	0.228	793.2	0.134	3733.7	0.346
3	1108.1	0.058	157.3	0.057	4482.2	0.447	554.7	0.044	278.5	0.023	1323.4	0.036	130.8	0.022	615.7	0.057
4	10258.6	0.537	1436.8	0.473	41063.2	3.676	5076.6	0.397	2558.8	0.191	12206.9	0.335	1166.2	0.188	5637.7	0.492
5	8043.7	0.421	1128.6	0.371	32253.0	2.888	3988.3	0.312	2008.9	0.150	9577.0	0.263	914.9	0.147	4429.2	0.387
6	987.4	0.051	87.1	0.025	2502.2	0.189	308.8	0.024	180.7	0.012	996.5	0.026	96.6	0.015	343.2	0.027
7	4358.8	0.227	443.2	0.127	12736.4	0.963	1540.0	0.118	869.3	0.056	4631.9	0.122	446.0	0.069	1711.2	0.136
8	4675.2	0.243	475.4	0.136	13661.1	1.033	1651.8	0.127	932.4	0.060	4968.1	0.130	478.4	0.075	1835.4	0.146
9	9698.6	0.501	1227.5	0.291	35545.8	2.156	4369.5	0.323	2261.7	0.134	11169.3	0.278	1080.9	0.154	4848.4	0.345
10	3690.0	0.191	509.8	0.121	14762.7	0.896	1824.7	0.135	917.2	0.054	4994.5	0.109	415.3	0.060	2029.3	0.144
11	14190.2	0.727	1940.3	0.394	56702.5	2.861	7009.7	0.502	3523.0	0.199	16887.1	0.403	1594.7	0.215	7798.8	0.505
12	648.7	0.032	75.2	0.012	2244.9	0.069	274.1	0.018	144.7	0.007	731.6	0.016	69.6	0.008	305.1	0.017
Watershed	68634.0	3.432	8712.0	1.381	260190.0	10.350	32040.0	2.149	16353.0	0.816	8064.0	1.802	7578.0	0.908	35656.0	2.005
	Z=1.964		Z=2.076		Z=2.076		Z=1.986				Z=1.986					
	Max. error=8.80*10 ⁻¹⁴		Max. error=8.30*10 ⁻¹⁴		Max. error=4.7*10 ⁻¹²		Max. error=4.7*10 ⁻¹²									

as total sediment yield prediction is concerned the revised MUSLE has little edge over the sediment routing sub-model. As already explained earlier the developed sediment routing sub-model has been found more efficient and accurate than the revised MUSLE in determining the partial contribution of sediment from various sub-watersheds for the study area.

4.1.1.3 Sediment mobilized sub-model

As explained at the beginning of this chapter (Article 4.1.1), the estimation of excess runoff (runoff excess) and excess sediment (sediment mobilized) are two necessary components for the development of the sediment mobilized sub-model, that is, the excess sediment-excess runoff relationship. The excess runoff and excess sediment were determined as per procedures described in Articles 4.1.1.1 and 4.1.1.2, respectively. Having the determined values of these above two parameters, the following power regression equation is developed for the study area by using 15 storm events with excess sediment yield as dependent variable:

$$ES = 8.486ER^{1.628} \quad (r=0.949) \quad \dots(4.83)$$

where ER is excess runoff in mm and ES is excess sediment in tonnes. The associated plot for Eq. (4.83) is depicted in Fig. 4.18.

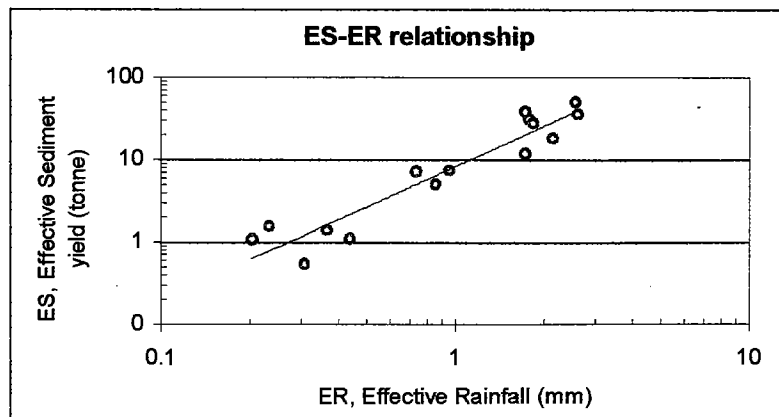


Fig. 4.18 Log transformed ES-ER relationship

4.1.2 Development of unit sediment graph

Development of a design *unit sediment graph* (USG) is the next step to obtain the direct sediment graph through its convolution with the estimated sediment mobilized. The general concepts and assumptions of the unit hydrograph are used for the simulation of unit sediment graph (**Rendon-Herrero, 1978**). The assumption of equality for effective duration of mobilized sediment and the excess rainfall over the entire watershed, as suggested by **Rendon-Herrero (1978)** and **Singh (1992)**, is taken to be applicable on the present study also. The base sediment flow was estimated by using the method of SRC as explained in estimation of excess sediment (Article 4.1.1.2), and subtracted from the total sediment graphs to obtain the direct sediment graphs. The excess sediment or sediment mobilized was expressed in t.ha^{-1} by dividing the sediment yield in tonnes by the area of respective watershed. The ordinates of direct sediment graph were then divided by the amount of excess sediment to obtain unit sediment graph with the same effective duration of excess runoff. The same storm events, which were used for the development of sediment routing sub-model, have also been considered for obtaining the unit sediment graph (USG) for more uniformity. The derived T-h USGs and the details of their characteristics are summarized in Table 4.17.

4.1.3 Development of average unit sediment graph

Due to the high degree of affinity in the process of generation of runoff and sediment yield during the effective period of precipitation, the effective duration of 0.5 h, considered as an appropriate duration for average unit hydrograph (Article 4.1.1.1) in this study, was also proposed for the derivation of average USG for the Amameh watershed. Thus, the USG with original 0.5 h effective duration and larger were selected. The USGs with a longer effective duration were converted into 0.5-h USG by using the *S-Curve*

Table 4.17 Ordinates of USGs for selected storms in Amameh watershed

Time (h)	0.5-h USG April 14,71	1-h USG Nov. 3,72	0.25-h USG July 18,74	2-h USG April 23,75	0.5-h USG July 22,76	1-h USG April 29,80	1.25-h USG April 25,83	0.25-h USG Mar. 13,89	1-h USG April 6,97
0.0	0.000	0.000	0.000	0.000	0.000	0.000	0.000	0.000	0.000
0.5	0.050	0.021	0.454	0.174	0.021	0.040	0.003	0.129	0.087
1.0	0.105	0.049	4.259	0.618	9.283	0.082	0.152	0.159	0.249
1.5	0.241	0.125	7.521	1.887	31.607	0.126	0.310	0.244	0.308
2.0	1.492	0.226	28.028	4.856	5.265	0.171	0.685	0.427	0.327
2.5	2.191	0.498	3.594	9.686	0.834	0.218	1.272	0.794	0.349
3.0	3.909	1.073	1.874	21.349	0.298	0.287	2.208	1.059	0.371
3.5	8.982	2.445	0.822	3.484	0.142	0.317	5.160	1.245	0.470
4.0	20.583	6.632	0.499	2.183	0.070	0.429	7.908	1.414	0.533
4.5	5.063	11.940	0.184	1.330	0.103	0.679	9.763	1.486	0.597
5.0	1.890	13.309	0.126	0.797	0.121	1.262	10.632	1.663	0.745
5.5	1.187	2.829	0.076	0.531	0.162	5.090	2.519	1.712	0.898
6.0	0.820	1.898	0.071	0.354	0.068	8.003	2.400	1.925	1.329
6.5	0.637	1.504	0.065	0.243	0.021	8.645	2.171	1.976	2.045
7.0	0.513	1.157	0.060	0.149	0.006	9.309	1.848	2.113	4.330
7.5	0.436	0.951	0.055	0.122	0.000	2.157	1.549	2.262	7.489
8.0	0.363	0.766	0.050	0.097		1.810	1.273	2.575	13.598
8.5	0.328	0.601	0.045	0.074		1.204	1.020	3.436	2.464
9.0	0.293	0.456	0.041	0.052		0.884	0.789	4.127	1.672
9.5	0.231	0.392	0.036	0.033		0.712	0.647	5.058	1.408
10.0	0.200	0.277	0.032	0.000		0.606	0.455	0.994	1.210
10.5	0.145	0.228	0.027			0.555	0.338	0.823	0.936
11.0	0.116	0.183	0.023			0.506	0.231	0.743	0.795
11.5	0.092	0.143	0.019			0.458	0.134	0.651	0.681
12.0	0.067	0.108	0.015			0.412	0.088	0.557	0.538
12.5	0.044	0.079	0.011			0.368	0.044	0.522	0.475
13.0	0.021	0.053	0.007			0.328	0.022	0.507	0.438
13.5	0.000	0.033	0.004			0.305	0.000	0.487	0.380
14.0		0.017	0.000			0.284		0.466	0.355
14.5		0.006				0.283		0.452	0.321
15.0		0.000				0.243		0.439	0.301
15.5						0.224		0.419	0.282
16.0						0.204		0.399	0.263
16.5						0.189		0.386	0.244
17.0						0.151		0.373	0.225
17.5						0.134		0.354	0.207
18.0						0.117		0.348	0.189
18.5						0.100		0.341	0.170
19.0						0.096		0.334	0.152
19.5						0.082		0.328	0.135
20.0						0.088		0.321	0.117
20.5						0.084		0.309	0.100
21.0						0.079		0.274	0.082
21.5						0.075		0.238	0.065
22.0						0.071		0.184	0.049
22.5						0.067		0.135	0.032
23.0						0.063		0.112	0.015
23.5						0.059		0.102	0.000
24.0						0.055		0.110	
24.5						0.051		0.132	
25.0						0.047		0.154	
25.5						0.043		0.158	
26.0						0.038		0.162	
26.5						0.034		0.166	
27.0						0.030		0.151	
27.5						0.026		0.150	
28.0						0.022		0.140	
28.5						0.018		0.134	
29.0						0.014		0.128	
29.5						0.010		0.123	
30.0						0.006		0.108	
30.5						0.002		0.099	
31.0						0.000		0.089	
31.5								0.075	
32.0								0.070	
32.5								0.065	
33.0								0.060	
33.5								0.056	
34.0								0.051	
34.5								0.046	
35.0								0.041	
35.5								0.037	
36.0								0.032	
36.5								0.027	
37.0								0.023	
37.5								0.018	
38.0								0.014	
38.5								0.009	
39.0								0.004	
39.5								0.000	

Note: The ordinates of USGs have been presented in unit of sediment mass (tonnes) per day.

method and were then averaged with the same manner used for derivation of average unit hydrograph (Article 4.1.1.1). The 0.25-h USG was also developed by conversion of 0.5-h USG. The USGs for various duration were also derived from 0.5-h USG and it was noticed that there was no difference in ordinates of T-h USGs, however, difference in time coordinates proportional to their effective duration was obtained. This may be perhaps due to the fact that the continuous sediment graphs of selected storms were obtained through the conversion of discrete sediment data with the help of sediment rating coefficient (Eqs. 4.28 and 4.29). With this in view, only 0.5h and 0.25-h USGs, shown in Fig. 4.19, have been used for simulation of sediment graphs in this study.

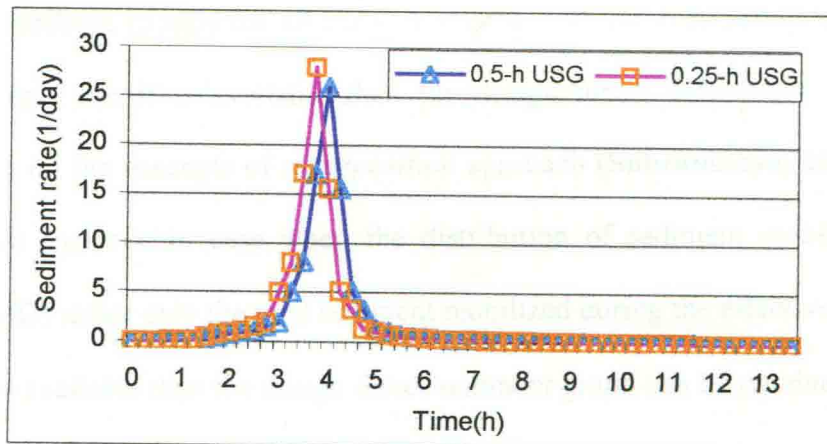


Fig. 4.19 Derived 0.5-h and 0.25-h unit sediment graph for Amameh watershed

Instead of developing average unit sediment graph, it would have been better to develop a *Dimensionless Unit Sediment Graph* (DUSG) using USGs obtained for various other watershed based on the concepts recommended for the development of dimensionless unit hydrograph (SCS, 1957). The DUSG is essentially a USG in which the ordinates and abscissa are represented respectively by the ratio of sediment flow rate to peak sediment flow rate and the ratio of time to time to peak. Thus if only peak rate of sediment flow and time to peak for any storm are known, the USG can easily be obtained

by multiplying the ordinates and abscissa values of the DUSG respectively by sediment peak rate and time to peak. Since the USGs from different other locations are not available, the average USG described above was used for development of sediment graph.

4.1.4 Design sediment graph

Based on the fundamental principle of the unit hydrograph, the ordinates of a direct sediment graph (SG) can be calculated if the appropriate unit sediment graph for the watershed is available. The derived USGs can be converted into direct sediment graph by multiplying the ordinates of USG with the sediment mobilized, estimated by the developed relationship between excess runoff and excess sediment (Eq. 4.83). If the distribution of the sediment mobilized (SMD) for all the incremental time interval during the effective duration of excess runoff is available then the design direct sediment graph can be simulated based on the concepts of *superposition* approach (Subramanya, 2000) used in unit hydrograph analysis. In case when the distribution of sediment mobilized is not available (NSMD) rather only the total sediment mobilized during the effective duration of excess runoff is available then the design direct sediment graph can be obtained as per the procedure described under Article 4.2.5.

4.2 Development of SG Model Based on Watershed Characteristics

Another technique of development of sediment graph model based on watershed characteristics is described in this section. For this purpose, an appropriate Instantaneous Unit Sediment Graph (IUSG) obtained from physical properties of the watershed is required. The instantaneous unit sediment graph (IUSG) is defined as the time distribution of suspended sediment flux associated with an instantaneous burst of rainfall producing one unit of sediment (Banasik, 1995). The definition is similar to that employed by

Williams (1978), except that in his definition the IUSG is the response to an instantaneous burst of rainfall producing one unit of runoff.

Thus, the sediment rate of the IUSG is the product of the instantaneous unit hydrograph (IUH) and the sediment concentration distribution for one unit of runoff, which can be expressed in the following form as,

$$s_i = u_i \cdot c_i \quad \dots (4.84)$$

where s_i is the ordinate of IUSG, u_i is the ordinate of IUH, c_i is the sediment concentration and t is the time.

4.2.1 Development of instantaneous unit hydrograph

Conceptual modeling for development of IUH has undergone rapid progress since the first work by Zoch (1937). In the present study the instantaneous unit hydrograph (IUH) is based on Clark's method (Clark, 1945) with the concept of *channel routing* instead of linear reservoir routing.

Clark's method also known as *Time-Area Histogram Method* aims at developing an IUH due to an instantaneous rainfall excess over a watershed. It is assumed that the rainfall first undergoes pure *translation* and then *attenuation*. The translation is achieved by time-area histogram (TAH) and the attenuation by routing the results of the above through a linear reservoir at the watershed outlet.

The basis for the derivation of IUH is the distribution of the arrival time of the rainfall excess (excess runoff) at the watershed outlet. The time of concentration is the maximum translation time of the surface runoff in the watershed. The rainfall excess is the inflow to the watershed system, and the outflow discharge in the present case is a unit hydrograph. To obtain the outflow discharge of a unit hydrograph, it is assumed that there is a uniform distribution of unit rainfall excess over the entire watershed.

4.2.1.1 Time area histogram

The time distribution of the rainfall excess gives the *time area histogram* (TAH), which could be viewed as the inflow hydrograph to the hypothetical storage reservoir at the outlet. The storage characteristics of the reservoir are assumed to be similar to those of the watershed (Das, 2000).

A line joining the points located on the map of the study area having equal time of travel, t_i ($t_i < t_c$), is called an *Isochrone* or *runoff Isochrone*. To assist in drawing isochrones, the longest watercourse for which the time of concentration had been estimated was chosen, and its longitudinal profile was plotted as shown Fig. 3.3 in chapter 3. Since the most appropriate period for UH analysis was found to be equal to 0.5 h, this particular time interval was used to develop TAH for the study watershed having time of concentration as almost 3 h. The distance scale of the abscissa was divided into 6 parts (3 divided by 0.5) and the elevation of subparts is measured on the profile transferred to the contour map of the watershed. The details of process and associated altitude with each isochrone are shown in Fig. 4.20.

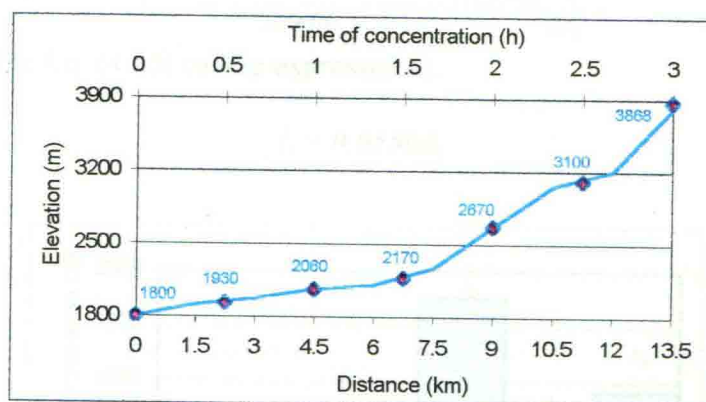


Fig. 4.20 Magnitude of Isochrones in Amameh watershed

The layout of isochrone has already been shown in Fig. 4.12. In further explanation the notations I to VI in Fig. 4.13 are replaced by A_1 to A_6 , respectively. The inter-isochrone areas were measured by the strip method with the equidistant lines of 0.5 cm on the

original map with a scale of 1:50,000. The specifications of inter-areas created by Isochrone are summarized in Table 4.18.

Table 4.18 *Time area histogram characteristics of Amameh watershed*

Inter-Isochrone	Travel time (h)	Elevation range (m)	Area (ha)	Area (%)
A ₁	0-0.5	Below 1930	66.26	1.79
A ₂	0.5-1.0	1930-2060	151.28	4.08
A ₃	1.0-1.5	2060-2170	237.55	6.40
A ₄	1.5-2.0	2170-2670	1767.86	47.63
A ₅	2.0-2.5	2670-3100	575.12	15.49
A ₆	2.5-3.0	Above 3100	913.93	24.62

Based on the information in Table 4.19, a *Time Area Histogram* (TAH) was obtained for the Amameh watershed as shown in Fig. 4.21. The figure shows that almost a half of the area is located at the center of the watershed having 1.5 to 2h of time of concentration.

The inflow rate I_i in $\text{m}^3 \text{s}^{-1}$ from an inter-Isochrone area A_i in ha at a time interval of Δt_c in h, which receives a unit of excess runoff ER in cm, is estimated by using the following equations (Clark, 1945):

$$I_i = \frac{(A_i \cdot 10^4)(ER \cdot 10^{-2})}{3600 \Delta t_c} = 0.0278 \frac{A_i}{\Delta t_c} \quad \dots(4.85)$$

Since $\Delta t_c = 0.5 \text{ h}$, the Eq. (4.85) can be expressed as,

$$I_i = 0.0556 A_i \quad \dots(4.86)$$

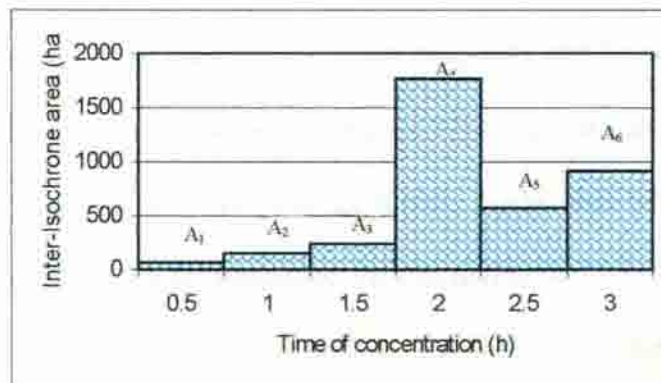


Fig. 4.21 *Time Area Histogram for Amameh watershed*

4.1.2 Flow routing

The inflow rate generated in each of the inter-Isochrone areas was routed to the outlet of the watershed through the channel routing procedure by applying the Muskingum routing equation (Eq. 4.76), explained earlier in the Reverse Routing Technique (Article 4.1.2).

The value of storage coefficient k was estimated by determining the total travel time of the watershed with the help of *average velocity technique* developed (Wilson *et al.*, 1981), and was found to be 1.543 h. The value of weighting factor, x was found to be equal to 0.395, by using the estimation technique given by *Kentucky University* Eq. (4.82). Since the value of t_c was considered to be 0.5 h, the values of C_0 , C_1 and C_2 were found to be -0.304, 0.726 and 0.578, respectively. The value of C_0 was obtained as negative due to selection of short interval period. If longer duration were chosen, then the whole watershed had to be divided into less numbers of sub-areas, and that would not have been appropriate to apply the concepts of TAH. Also the following inequality has been suggested by researchers (Singh, 1992 and Subramanya, 2000) by taking into account the effects of input and output on the storage,

$$k > \Delta t > 2kx \quad \dots(4.87)$$

For the obtained values of k and Δt the above inequality can be satisfied only if the x values is less than 0.16202. Now solving the Eq. (4.77) for given values of k , x and Δt , the values of C_0 , C_1 and C_2 are obtained as 0.000, 0.324 and 0.676, respectively. Accordingly, the value of 0.162 was considered for x to derive the IUH for the study area. The ordinates of the IUH were then estimated by the following equation obtained by substituting the values of C_0 , C_1 and C_2 in Eq. (4.76):

$$Q_n = 0.324I_{n-1} + 0.676Q_{n-1} \quad \dots(4.88)$$

The results of the calculation of IUH and corresponding 0.5-h UH derived by using the developed IUH and with the help of convolution integral (Subramanya, 2000) are summarized in Table 4.19.

Table 4.19 Derivation of IUH by using the concept of TAH and channel routing

Time (h)	Area (ha)	I (m ³ .s ⁻¹)	C0*I2	C1*I1	C2*Q1	IUH (m ³ .s ⁻¹)	0.5-h UH (m ³ .s ⁻¹)
0.0	0.00	0.000	0.000	0.000	0.000	0.000	0.000
0.5	66.26	3.684	0.000	0.000	0.000	0.000	0.000
1.0	151.28	8.411	0.000	1.194	0.000	1.194	0.597
1.5	237.55	13.208	0.000	2.725	0.807	3.532	2.363
2.0	1767.86	98.293	0.000	4.279	2.388	6.667	5.100
2.5	575.12	31.977	0.000	31.847	4.507	36.354	21.510
3.0	913.93	50.815	0.000	10.360	24.575	34.936	35.645
3.5	0.00	0.000	0.000	16.464	23.616	40.080	37.508
				0.000	27.094	27.094	33.587
					18.316	18.316	22.705
					12.381	12.381	15.349
					8.370	8.370	10.376
					5.658	5.658	7.014
					3.825	3.825	4.741
					2.586	2.586	3.205
					1.748	1.748	2.167
					1.182	1.182	1.465
					0.799	0.799	0.990
					0.540	0.540	0.669
					0.365	0.365	0.452
					0.247	0.247	0.306
					0.167	0.167	0.207
					0.113	0.113	0.140
					0.076	0.076	0.094
					0.052	0.052	0.064
					0.035	0.035	0.043
					0.024	0.024	0.029
					0.016	0.016	0.020
					0.011	0.011	0.013
					0.007	0.007	0.009
					0.005	0.005	0.006
					0.003	0.003	0.004
					0.002	0.002	0.003
					0.002	0.002	0.002
					0.001	0.001	0.001
					0.001	0.001	0.001
					0.000	0.000	0.001
					0.000	0.000	0.000

Note: $x=0.162$, $k=1.543h$, $\Delta t=0.5h$, $C_0=0.000$, $C_1=0.324$ and $C_2=0.676$.

The other possible combinations of weighting factor x and time interval Δt were also tried and associated IUHs were obtained. The developed IUHs were then convoluted into 0.5-h UHs for which the corresponding plots are shown in Fig. 4.22. The peak flow, the time to peak and the base time of the derived 0.5-h UHs were compared with those of

average 0.5-h UH of the watershed. It is seen from the figure that the 0.5-h UH obtained from IUH with x equal to 0.162 and 0.5h time interval is having a much better affinity with average 0.5-h UH of the watershed rather than the 0.5-h UHs derived from IUHs with other values of x and Δt . It is also observed that the initial ordinates of the UH obtained from the IUH with the actual value of x equal to 0.395 and the time interval 0.5h are negatives, which may be attributed to the negative value of C_0 . The value of C_0 was negative due to incompatibility of weighting factor x and time interval Δt .

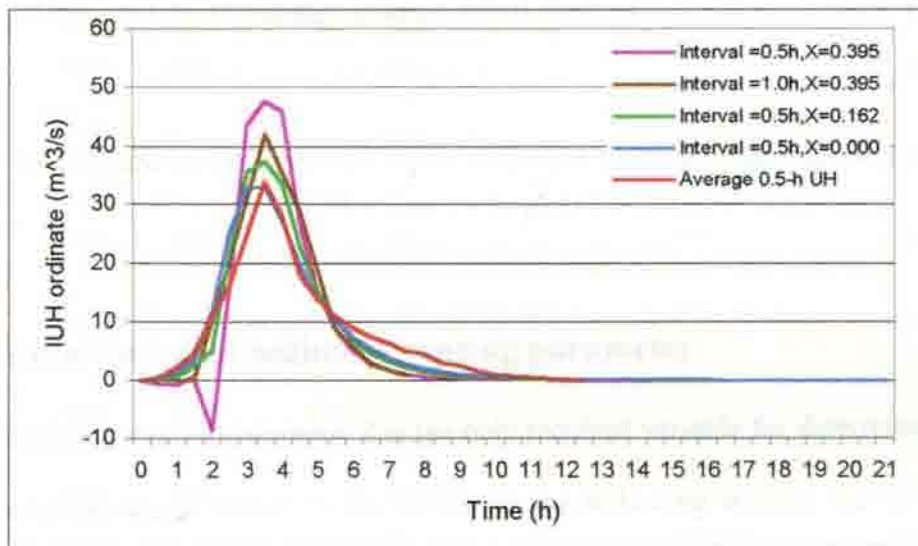


Fig. 4.22 Comparison of 0.5-h UHs obtained by using different IUH with average 0.5-h UH

4.2.2 Determination of sediment concentration

The distribution of suspended sediment concentration (SCD) is required to apply Eq. (4.84) to get the IUSG for the watershed. The sediment concentration at time t can be calculated by using the concept of the *first order kinetic equation* (Williams, 1975 and Banasik and Walling, 1996) shown as follows,

$$c_t = c_0 \exp(-\beta t d^{0.5}) \quad \dots (4.89)$$

where c_t is sediment concentration at time t , c_0 is initial (source) sediment concentration, β is a routing parameter and d is the particle diameter of the soil carried out by the flow. As

As explained in the section of sediment routing modeling under Article 4.1.1.2, the sediment routing coefficient and the particle diameter can be combined together and represented as Z shown in Eq. (4.58). By the substitution of Eq. (4.58) into Eq. (4.89), the following equation is produced:

$$c_t = c_0 \exp(-Zt) \quad \dots(4.90)$$

The given exponential equation can be expressed in a dimensionless form, and termed as *Dimensionless Sediment Concentration Distribution* (DSCD) model of the following form (Banasik and Walling, 1996):

$$c_t' = \exp(-Zt) \quad \dots(4.91)$$

where c_t' is the ordinate of the DSCD, Z is the sediment routing parameter (h^{-1}) and t is time (h).

4.2.2.1 Determination of sediment routing parameter

The sediment routing parameter Z is the only required variable for determination of sediment concentration, as shown in Eq. (4.91). In the following section, the Williams' and Banasik's methods of determination of Z are detailed. A modified model by incorporating the appropriate substitution in previous two methods has also been tried to get more applicable model for the study area.

a. Williams' method

Williams (1978) suggested the following equation for the determination of sediment routing coefficient (β) for each storm:

$$\beta = \frac{-\ln(q_p / Q_p)^{0.56}}{T_p(d)^{0.5}} \quad \dots(4.92)$$

where q_p is peak of direct runoff ($\text{m}^3 \text{s}^{-1}$), Q_p is the peak source runoff rate ($\text{m}^3 \text{s}^{-1}$), T_p is the watershed time to peak (h), and d is median sediment particle diameter (mm). If both sides are multiplied by $(d)^{0.5}$ then the left hand side of the equation will be equal to parameter Z as already shown in Eq. (4.58). Therefore, the following equation is obtained for determination of parameter Z in the Amameh watershed after substituting the value of 0.081, obtained for the study area, in place of 0.56 in original MUSLE:

$$Z = \frac{-\ln(q_p / Q_p)^{0.081}}{T_p} \quad \dots(4.93)$$

Equation (4.93) was applied for the storms for which hyetograph as well as hydrograph were available and the results are presented in Table 4.21. The average value of parameter Z by Williams' method was found to be 0.0187.

b. Banasik's method

Banasik (1990) suggested the following equation similar to the Williams' equation (Eq. 4.92),

$$Z = \frac{-\ln(q_p / \Delta Hm)^b}{T_p} \quad \dots(4.94)$$

where ΔHm is maximum intensity of effective rainfall ($\text{m}^3 \text{s}^{-1}$), b is dimensionless exponential parameter of the MUSLE, and the rest variables have been defined earlier. Calculations were made for the same storms used in the Williams' method and the estimated values of parameter Z with an average equal to 0.0885 are presented in Table 4.21.

c. Modified method

To avoid the necessity of availability of hyetograph and hydrograph for the determination of peak source runoff (Q_p), maximum intensity of effective rainfall (ΔHm)

and time to peak (T_p) to apply in Williams' and Banasik's methods, an attempt was made to find more reliable and easily applicable method for estimating parameter Z for the study area. With this in view, the factors of peak source runoff (Q_p) in Eq. (4.93) or maximum intensity of effective rainfall (ΔHm) in Eq. (4.94) were replaced by maximum 30-minute intensity ($Max I_{30}$) and the time to peak (T_p) in both the equations was substituted by time of concentration (T_c). As a result of these substitutions, the following equation was then obtained for the Amameh Watershed.

$$Z = \frac{-\ln(q_p / Max I_{30})^{0.081}}{T_c} \quad \dots(4.95)$$

where $Max I_{30}$ is in $m^3 s^{-1}$ and T_c is in h. The factors q_p and b are the same as defined in Williams' and Banasik's methods. The estimated values of parameter Z for selected storm events with the average value of 0.1100 are also reported in Table 4.20.

In all the above methods, both the runoff rates and the maximum intensity in $mm.h^{-1}$ have been converted into $m^3 s^{-1}$ by multiplying the values with the conversion factor 10.3111, equal to area (m^2)/(1000×3600). The values of $Max I_{30}$, the time of concentration and the peak flow of direct runoff in modified method (Eq. 4.95) can easily be found by using the *Intensity-Depth-Frequency* relationships and the empirical equations.

Table 4.20 Sediment routing parameter by various methods for selected storms in Amameh watershed

Methods	April 14, 71	Nov. 3, 72	July 18, 74	April 23, 75	July 22, 76	April 29, 80	April 25, 83	Mar. 13, 89	April 6, 97	Average
Williams	0.0229	0.0224	0.0305	0.0020	0.0292	0.0150	0.0126	0.0214	0.0192	0.0187
Banasik	0.0930	0.0729	0.2019	0.0723	0.1812	0.0408	0.0729	0.0522	0.0395	0.0885
Modified	0.0840	0.1214	0.1346	0.0723	0.0906	0.0953	0.1215	0.1654	0.1053	0.1100

4.2.2.2 Dimensionless sediment concentration distribution

Once the parameter Z in Eq. (4.91) is found, the values of sediment concentration with respect to time (DSCD) can be determined. In addition to the three methods of

determination of parameter Z described above, an attempt has also been made to estimate sediment concentration by considering the same value of Z obtained for the sediment routing sub-model in Eq. (4.83) under Article 4.1.12. The DSCDs' ordinates through all the above cases for the study area are presented in a graphical format as shown in Fig. 4.23. The ordinates of plot have been determined by using Eq. (4.91). The parameter t was simply taken as the elapsed time from the beginning of incident occurrence in IUH with a 0.5h time interval.

This can be concluded that if Z is equal to zero the characteristic values of the IUH and the IUSG would be the same i.e. s_t will be equal to u_t . It can also be shown that for $Z > 0$ the time to peak of the IUSG is shorter than that of the IUH, and the peak value of the IUSG is higher than the peak of the IUH (Banasik, 1996).

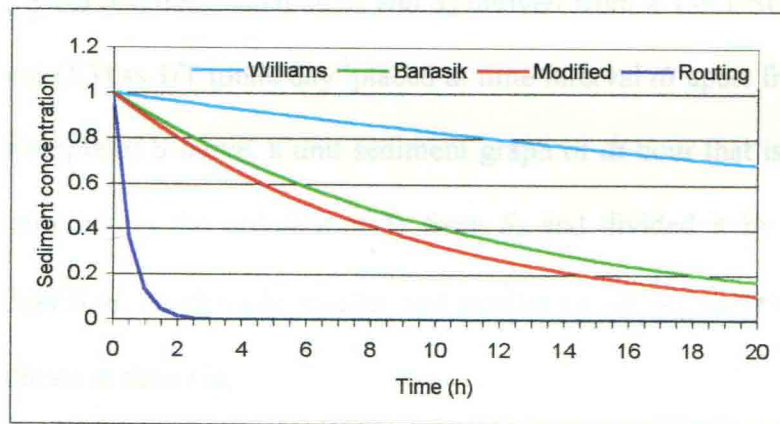


Fig. 4.23 Dimensionless Sediment Concentration Distribution curve by different methods for Amameh watershed

4.2.3 Development of instantaneous unit sediment graph

The Williams' model (1978) is used to develop the IUSG for which the ordinates of the IUH and the sediment concentration are required (Eq. 4.84). Insertion of equations of sediment concentration c_t (Eq. 4.91) and IUH ordinate u_t (Eq. 4.88) in equation Eq. (4.84) produced the following formula applied for calculation of IUSG ordinates s_t , (Banasik, 1995):

$$s_t = \frac{u_t c_t'}{\int_0^\infty u_t c_t' dt} \quad \dots(4.96)$$

where s_t , u_t and c_t are respectively the ordinates of IUSG, IUH and DSCD curve. The time interval dt is taken to be 0.5h. The components required for the determination of IUH and sediment concentration are calculated by using a few techniques already described in earlier sections.

4.2.4 Development of unit sediment graph

The *convolution integral* or *Duhamel integral*, which is essentially the same as the arithmetical computation of *superposition concept* in unit hydrograph (Subramanya, 2000), is used to derive the T-h USG from the simple geometric form of IUSG. Considering two S-curves, designated as S_1 and S_2 derived from a T-h USG with intensity of excess sediment (ES) as $1/T$ tonne.day⁻¹ placed at time interval dt apart from each other. Following the principle of S-curve, a unit sediment graph of dt hour that is dt -h USG can be obtained by subtracting the ordinate of S_1 from S_2 and divided it by intensity×time interval i.e. $(S_2-S_1)/ES.dt$. As dt made smaller and smaller i.e. $dt \rightarrow 0$, an IUSG results. For an IUSG, the ordinate at time t is,

$$s_t = \lim_{dt \rightarrow 0} \left(\frac{S_2 - S_1}{ES.dt} \right) = \frac{1}{ES} \frac{dS}{dt} \quad \dots(4.97)$$

If excess sediment (ES) is one tonne.day⁻¹, then $s_t = dS'/dt$ where S' represents a S-curve of intensity one tonne.day⁻¹ (i.e. S-curve derived from a unit sediment graph of T hour duration), that is,

$$dS' = s_t dt \quad \dots(4.98)$$

Integrating Eq. (4.98) within time interval t_1 and t_2 results:

$$S'_2 - S'_1 = \int_{t_1}^{t_2} s_t dt \quad \dots(4.99)$$

If s_t is essentially linear within the range of time interval, then for small values of time interval Δt ,

$$s_t = \bar{s}_t = 1/2[s_{t1} + s_{t2}] \quad \dots (4.100)$$

Substituting the equivalent value of s_t from Eq. (4.100) into Eq. (4.99) and solving the integration produces,

$$S'_2 - S'_1 = 1/2(s_{t1} + s_{t2})(t_2 - t_1) \quad \dots (4.101)$$

But $(S'_2 - S'_1)/(t_2 - t_1)$ represents the ordinates of a USG of duration $T = (t_2 - t_1)$ by considering that the effective duration of IUSG is negligible. Thus, for small values of time interval, the ordinates of T-h unit sediment graph can be obtained by the following equation,

$$(T\text{-h USG})_t = 1/2[(IUSG)_t + (IUSG)_{t+T}] \quad \dots (4.102)$$

Therefore, as per procedure proposed by **Schulz (1973)** for conversion of IUH into UH, a unit sediment graph (USG) for some finite time interval T , can be found from instantaneous unit sediment graph (IUSG) by lagging the IUSG with the time interval T and computing the average of ordinates of the IUSG at interval of T units.

4.2.5 Design sediment graph

As per the procedure explained under Article 4.1.4 the T-h USGs are convoluted into direct sediment graph by multiplying the ordinates of respective USG with the sediment mobilized. Since various USGs of different effective duration could be derived from T-h USG obtained by using an IUSG, this very concept can be used for derivation of direct sediment graphs for both the cases of sediment data availability viz. sediment mobilized distribution (SMD) and without sediment mobilized distribution (NSMD). In the first case i.e. SMD, as explained under Article 4.1.4 of sediment graph by using hydrological data, the sediment mobilized is estimated for each segment (incremental time interval) of excess runoff by using Eq. (4.84) and then the superposition approach is used

for derivation of direct sediment graph. Whereas in the second case i.e. NSMD, the direct sediment graph of a particular effective duration is derived by multiplying the ordinates of the USG of the same effective duration with the value of total sediment mobilized estimated by Eq. (4.84), for the entire excess runoff.

4.3 Evaluation of Models

Since the models are simplified systems and express formalized concepts of the real-life conditions, the qualitative and quantitative evaluation of the models is an essential task to assess their capability or potential of developed models in simulation of actual circumstances. There are many criteria for the selection of preferred model. Dawdy and Lichty (1968) suggested four criteria viz. *accuracy of prediction*, *simplicity of the model*, *consistency of parameter estimates* and *sensitivity of models*, which can be used to choose suitable model among many alternatives (Rahnama, 1994). Besides those, the methods of comparison may vary depending on the expected accuracy, the aims of study and the suitability of the method. Two concepts of qualitative and quantitative comparisons are generally being used in the hydrological studies.

4.3.1 Qualitative evaluation

The qualitative comparison is based on visual observation and is one of the simplest methods for the evaluation of models. The goodness of fit of a predicted sediment graph to an observed one is tentatively checked by qualitative comparison. This procedure is based on graphical comparison of the important shape parameters of a sediment graph. The compatibility of peak, time to peak and base time and overall shape of the sediment graph, are the important parameters, which are considered in a qualitative evaluation.

The trends of increment and reduction in sediment discharge on the rising and the falling limbs of sediment graph, respectively, are also other factors that may be used for better comparison.

4.3.2 Quantitative evaluation

Since the qualitative comparison may not lead to an accurate decision owing to varying the visual judgment from expert to expert, a certain statistical measures are used for the quantitative comparison of the observed and the predicted direct sediment graphs. Since contemporaneous occurrence of hydrograph and sediment graph is to be considered for quantitative evaluation besides many other factors such as volume, peak, time to peak and base time, the methods which emphasize on point wise assessment are likely to be not necessarily sufficient. With this in view, the *Absolute Relative Error (ARE)*, *Coefficient of Efficiency (CE)*, *Integral Square Error (ISE)*, *Relative Square Error (RSE)*, *Root Mean Square Error (RMSE)*, *Ratio of Error (REO)*, *Bias (B_s)* and *Coefficient of Determination (R^2)* are the techniques have been used for quantitative comparison.

4.3.2.1 Absolute relative error (ARE)

Flemming (1971) initiated the application of relative error in hydrology by comparing the recorded and the simulated flow. The simple assessment, using the measure of deviation of volume and peak was also found to be sufficient for comparison of runoff models (**Green and Stephenson, 1986** and **ASCE, 1993**). The absolute relative error method is therefore used as a criterion for the comparison of volume, peak discharge, time to peak and base time of observed and predicted sediment graphs. The *ARE* is estimated by the following equation in percentage:

$$ARE = \left| \frac{S_o - S_p}{S_o} \right| \times 100 \quad \dots(4.103)$$

where S_o and S_p are the considered parameters in the observed and the predicted sediment graphs, respectively. The lesser values of ARE are likely to give a better fit.

4.3.2.2 Coefficient of efficiency (CE)

The criterion for model efficiency suggested by Nash and Sutcliffe (1970) is reportedly the most appropriate standard for evaluation of a model. The coefficient of efficiency (CE) is similar to the coefficient of determination (R^2), but unlike R^2 which measures the degree of association between the simulated and recorded flows, the CE directly measures the ability of the model to reproduce the recorded flow (Chiew *et al.*, 1993). The magnitude of CE represents the proportion of variance of the observation accounted for by the model (Thirumalaiah and Deo, 2000). As proposed by Kitanidis and Bras (1980) the coefficient of efficiency is estimated by the following equation:

$$CE = \frac{S_{obs} - S}{S_{obs}} \times 100 \quad \dots(4.104)$$

where S_{obs} is the measure of variability of the observed values from their means i.e. $\sum(S_o - \bar{S}_o)^2$, and S is the measure of association between predicted and observed flows i.e. $\sum(S_o - S_p)^2$. Computationally, CE can have a negative value, but such a value is rather meaningless, as far as interpretation of the results is concerned (ASCE, 1993).

4.3.2.3 Integral square error (ISE)

The method of integral square error (ISE), originally suggested for evaluation of simulated hydrographs (Diskin *et al.*, 1978), can also be used for quantitative comparison of the observed and the predicted sediment graphs. The ISE is generally less than one and calculated by using the following equation:

$$ISE = \frac{\sqrt{\sum_{i=1}^m (S_{pi} - S_{oi})^2}}{\sum_{i=1}^m S_{oi}} \times 100 \quad \dots(4.105)$$

in which m is the number of sediment flow ordinates, and S_e and S_o are the predicted and the observed sediment flow ordinates at i , respectively.

4.3.2.4 Relative square error (RSE)

The goodness of fit of a predicted sediment graph to an observed one can also be determined by means of another parameter, known as relative square error, suggested by Wang *et al.* (1992) for the assessment of overall shape of the hydrograph. It is expressed as following with the same variables used in Eq. (4.105):

$$RSE = \frac{\sum_{i=1}^m (S_{pi} - S_{oi})^2}{\sum_{i=1}^m S_{oi}^2} \quad \dots(4.106)$$

4.3.2.5 Root mean square error (RMSE)

Root mean square error is another method for comparative evaluation between simulated and observed watershed response. The *RMSE* of the model is determined by using the following equation.

$$RMSE = \frac{\sqrt{\sum_{i=1}^m (S_p - S_o)^2}}{m} \quad \dots(4.107)$$

The variables have been defined in the previous methods.

4.3.2.6 Ratio of error (REO)

The ratio of mean error to the mean observed output of the models (*REO*), which has been suggested by Papamichal and Papagafiriou (1992) for evaluation of generation and prediction performance of multiple input-output models, is also used for the determination of ability of developed models for simulation of sediment graphs in the

present study. The *REO* is estimated by the same variables defined earlier using the following equation,

$$REO = \frac{\frac{1}{m} \sum_{i=1}^m (S_{pi} - S_{oi})}{\frac{1}{m} \sum_{i=1}^m S_{oi}} \quad \dots(4.108)$$

Besides the methods discussed above for the quantitative comparison of the developed models, many other techniques, such as *sum of squares of the residuals (G)*, *total sum of squared residual (TSSR)*, and *total sum of absolute residuals (TSAR)* were recommended by **Green and Stephenson (1986)** for an overall goodness of fit or measure of hydrograph shape for a number of events, which could also be applied for the analysis of sediment graph. Since the equations for estimation of *G* as well as *TSSR*, and *TSAR* are respectively similar to the numerator of the relative square error (*RSE*) and the ratio of error (*REO*) and they are then divided by constant values, similar results are likely to occur. With this in mind, these techniques of quantitative comparison have not been used in this study.

4.3.2.7 Bias (B_s)

The bias (B_s) used for the evaluation of goodness of fit of predicted runoff and sediment yield (**Wu et al. 1993**) is expressed as the ratio of predicted and observed values.

That is,

$$B_s = \frac{S_p}{S_o} \quad \dots(4.109)$$

in which B_s is bias in sediment estimation, and S_p and S_o are the predicted and the observed sediment yield, respectively.

4.3.2.8 Coefficient of determination (R^2)

A comparative assessment can also be conducted for point-wise evaluation of sediment graphs by using the coefficient of determination (R^2) besides the total sediment yield and peak flow rate. The coefficient of determination may be used only to evaluate the trend of prediction, since it does not consider the parameter of time and the magnitude of differences between observed and predicted data. The R^2 is calculated by using the proportion of explained variance by the model to unexplained variance. The residual square error (RSE) and the output standard error of estimate (S_y) are required to determine R^2 by using the following formula (Wang *et al.* 1991):

$$R^2 = 1 - \left(\frac{RSE}{S_y}\right)^2 \quad \dots(4.110)$$

Chapter Five

RESULTS AND DISCUSSION

5. RESULTS AND DISCUSSION

In this chapter, the applicability of developed models for fulfillment of the research objectives envisaged in the present study is investigated. The recorded hydrometeorological data in the Amameh watershed, an important gauged watershed in the Jajroud basin of Iran and comprising an area of 3712ha, were collected for development of models and evaluation of their workability. Since the accurate measurement of sediment data particularly in mountainous watershed is difficult, time-consuming, uneconomical and tedious, an attempt has been made to conceptualize the sediment yield prediction based on its temporal and spatial distribution.

The plausibility of various sub-models required for developing the main model of sediment yield prediction for the watershed has been ascertained at the time of their development in chapter 4. Therefore, the results and respective discussions regarding these sub-models such as *excess runoff*, *excess sediment*, *sediment routing* and *sediment mobilized* have already been presented in chapter 4. In this chapter the distribution of total runoff in the watershed is evaluated by the results obtained through the reverse routing technique (RRT). The developed sediment routing sub-model is used for determination of partial contribution of sub-watersheds in total sediment yield from the watershed. The details of applicability of both types of *sediment graph* models developed based on the hydrological data and the watershed characteristics are also discussed.

The validity of models has been ascertained by using eight selected storm events during 1970-1997 and the best performing sediment graph model for the Amameh watershed based on qualitative and quantitative evaluation parameters is selected.

5.1 Spatial Distribution of Total Runoff and Sediment Yield

A spatially distributed approach for the prediction of sediment yield is required, since the factors that influence the sediment yield of the watershed vary considerably with space and are not usually distributed uniformly throughout the watershed. As explained in Estimation of runoff parameters under Article 4.1.1.2, the reverse flood routing technique (RRT) was found to be fairly accurate in estimating partial contribution of each sub-watershed in generation of total runoff. The average contributions of each sub-watershed, shown in Fig. 4.17, to the total runoff that reaches to the main outlet are summarized in Table 5.1.

Table 5.1 *Average partial contributions of individual sub-watershed in total runoff from Amameh watershed*

Sub-watershed	Sub-watershed wise runoff contribution		
	(m ³)	(%)	(m ³ .ha ⁻¹)
1	3977.89	6.70	18.41
2	6204.33	10.45	18.61
3	1021.19	1.72	18.57
4	9244.16	15.57	17.88
5	7278.96	12.26	18.16
6	653.09	1.10	8.30
7	3093.26	5.21	9.99
8	3336.66	5.62	10.04
9	8104.23	13.65	15.30
10	3295.12	5.55	17.70
11	12646.16	21.30	17.67
12	516.53	0.87	13.77

A Critical observation of Table 5.1 shows that sub-watershed 11 with 21.30% partial contribution in total runoff is the most important sub-watershed. Probably it may be due to its larger area and proximity to the main outlet. Sub-watersheds 4,9,5 and 2 with contributory more than 10% with their respective contribution of 15.57%, 13.65%, 12.26% and 10.45% stand in the second priority as far as total runoff generation is concerned due to having larger areas and comparatively higher *CN* values. The rest of the sub-watersheds have partial contribution less than 7%. The least effect on the watershed

runoff is made by the sub-watershed 12, which probably may be due to its smallest size and low *CN* value. The potential of runoff production in an individual sub-watershed was assessed by relative contribution in terms of volume of runoff (m^3) per unit of area (ha) as shown in Table 5.1. The sub-watersheds with higher values of relative contributions have more readiness to produce runoff than those with lower values of relative contribution, though they may have lesser percentage of contribution. That means sub-watersheds 1,2,3,4,5,10 and 11 with 17 to 19 $\text{m}^3.\text{ha}^{-1}$, sub-watersheds 12 and 9 with 13 to 15 $\text{m}^3.\text{ha}^{-1}$ and sub-watersheds 6, 7 and 8 with 8 to 10 $\text{m}^3.\text{ha}^{-1}$ relative contributions respectively stand in the first to the third priority for runoff generation. The classification of sub-watersheds based on their impacts on runoff generation that passes through the main outlet of the watershed is very important for designing water resources management projects.

The developed sediment routing sub-model (Eq. 4.83) was used for the determination of contribution from individual sub-watersheds to the total sediment yield in the Amameh watershed as per the procedure described under Article 4.1.1.2. The estimated values of average contribution of each sub-area to the sediment yield were obtained and are summarized in Table 5.2a. The revised MUSLE (Eq. 4.55), developed for the watershed, was also examined for the estimation of partial contribution and associated results are given in Table 5.2b.

It can be seen from Table 5.2.a that the sub-area number 11 with a contribution of 66 % contributes the maximum sediment yield. The sub-areas number 10, 9 and 12 with a contribution of 14, 9 and 7 %, respectively also have an important role to play in the delivery of sediment yield to the main outlet of the Amameh watershed. It is further observed that the contribution of other sub-areas declined below 1 % and even reached to the least value of 0.09 % for the sub-watershed 1. It may be noticed from Table 5.2 that

the partial contribution of sub-watersheds in sediment yield by using sediment routing model is much different as compared to that made by the MUSLE.

Table 5.2 Average partial contributions of individual sub-watershed in sediment yield from Amameh watershed

Sub-watershed	<i>a. Using sediment routing sub-model</i>			<i>b. Using revised MUSLE</i>		
	Contribution			Contribution		
	(tonne)	(%)	(tonne.ha ⁻¹)	(tonne)	(%)	(tonne.ha ⁻¹)
1	0.015	0.09	0.00007	0.163	9.45	0.00075
2	0.021	0.13	0.00006	2.125	13.00	0.00637
3	0.020	0.12	0.00036	1.985	12.14	0.03610
4	0.043	0.26	0.00008	2.354	14.40	0.00455
5	0.038	0.23	0.00009	2.066	12.64	0.00515
6	0.118	0.72	0.00150	0.420	2.57	0.00534
7	0.062	0.38	0.00020	0.219	1.34	0.00071
8	0.121	0.74	0.00036	0.425	2.60	0.00128
9	1.515	9.27	0.00286	0.875	5.35	0.00165
10	2.333	14.27	0.01253	1.345	8.23	0.00722
11	10.865	66.46	0.01518	2.709	16.57	0.00379
12	1.200	7.32	0.03200	0.276	1.69	0.00736

As can be seen from the Table 5.2b the sub-watershed 11 has the maximum contribution to the tune of 17 %, while sub-watersheds 2, 3, 4, and 5 by having almost 12 to 14 % stand in the second priority. It may also be mentioned that the contribution of sub-watersheds 1, 10 and 9 are respectively 9, 8 and 5 % and the least contribution is made by the sub-watershed 7, i.e. 1.34 %. By summing the storm-wise partial contribution of sediment yield estimated by revised MUSLE from different sub-watersheds, it was observed that the value thus obtained is far different than the actual measured value of the sediment yield at the outlet. Whereas, the total sediment yield estimated from different sub-watersheds by the sediment routing sub-model, applied in present study, compares well with observed values. Thus it is implied from the above explanation that although the MUSLE may give a reasonable prediction of total sediment yield from the watershed but it fails to provide acceptable results as far as estimation of partial contribution of sediment yield from various sub-watersheds is concerned. On critical investigation of Tables 5.1 and 5.2 it can further be observed that the contributions of sub-watersheds in generation of

total runoff and sediment individually are not in the same proportions. This may be due to various watershed characteristics influencing the generation of the runoff and the sediment differently. For example the sub-watershed 10 contributes the runoff to the tune of only 5.55 % where it stands in the second priority in generation of sediment. It is further be seen that the sub-watershed 11 contributes the maximum share in creation of both runoff and sediment output. The inherent susceptibility of sub-watersheds in sediment yield could also be determined with the help of relative contribution. The ratios were obtained in the case of sediment routing model in terms of tonne.ha^{-1} and are also shown in Table 5.2a. On scrutinizing the table, it is found that the higher values of relative contributions belonging to sub-watersheds 12, 11, 10 and 9 are almost corresponding the higher percentage of partial contributions associated with the same watersheds. Such types of assessment shall prove to be very useful in soil and water conservation projects.

The summary of above discussion regarding partial contribution of each particular sub-watershed in generation of total runoff and sediment yield in the Amameh watershed is shown in Table 5.3. The graphical presentation of sub-watershed contributory on storm-wise basis in the output generation of the watershed and their inter-relationships is illustrated in Figs. 5.1a and 5.1b.

Table 5.3 *Partial contribution of individual sub-watershed in total outputs from Amameh watershed*

Sub-watershed	Area		Average contribution			
			Runoff		Sediment yield	
	(ha)	(%)	(%)	($\text{m}^3.\text{ha}^{-1}$)	(%)	(tonne.ha^{-1})
1	216.1	5.82	6.70	18.41	0.09	0.00007
2	333.5	8.98	10.45	18.61	0.13	0.00006
3	55.0	1.48	1.72	18.57	0.12	0.00036
4	517.1	13.93	15.57	17.88	0.26	0.00008
5	400.9	10.80	12.26	18.16	0.23	0.00009
6	78.7	2.12	1.10	8.30	0.72	0.00150
7	309.8	8.35	5.21	9.99	0.38	0.00020
8	332.3	8.95	5.62	10.04	0.74	0.00036
9	529.6	14.27	13.65	15.30	9.27	0.00286
10	186.2	5.02	5.55	17.70	14.27	0.01253
11	715.7	19.28	21.30	17.67	66.46	0.01518
12	37.5	1.01	0.87	13.77	7.32	0.03200
Total	3712.0	100.00	100.00	----	100.00	----

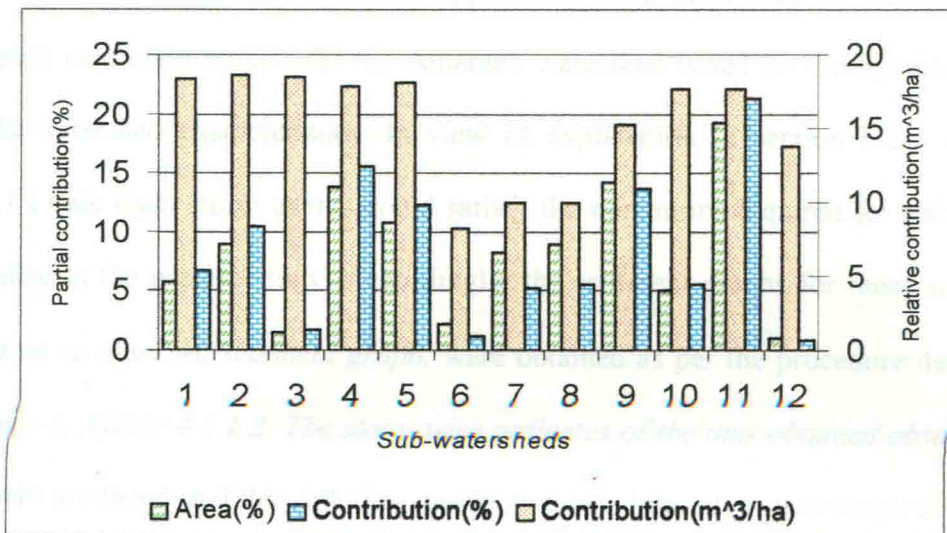


Fig. 5.1a Average partial contribution of different sub-watersheds in generation of total runoff from Amameh watershed

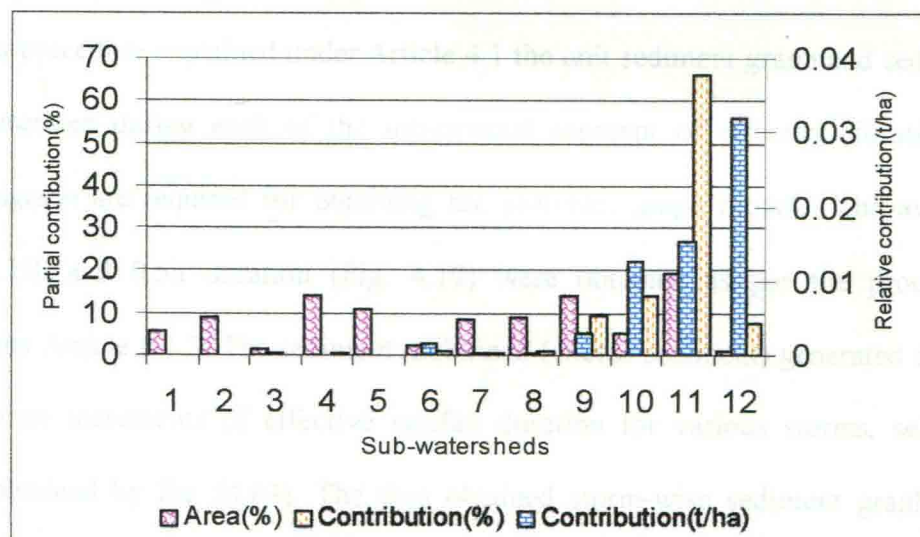


Fig. 5.1b Average partial contribution of different sub-watersheds in total sediment yield from Amameh watershed

5.2 Temporal Distribution of Sediment Yield (Sediment Graph)

As explained under chapter 4, two approaches have been used to develop the sediment graph prediction models for the Amameh watershed based on the hydrological data and the watershed characteristics. In view of explanation in section b-2-3 under Article 4.1.1.2 only eight storm events could satisfy the conditions required for sediment graph modeling in the present study. Accordingly, the sediment graphs for these storms, called hereafter as *observed sediment graph*, were obtained as per the procedure detailed under section a-3, Article 4.1.1.2. The storm-wise ordinates of the thus obtained observed sediment graphs are listed in Table 5.4. The model developed based on hydrological data hereafter referred as *Model 'A'* and the sediment graph derived based on watershed characteristics is called as *Model 'B'*.

5.2.1 SGs derived based on hydrological data (Model A)

As per procedure explained under Article 4.1 the unit sediment graph and sediment mobilized generated during each of the incremental segment of effective duration of rainfall hyetograph are required for obtaining the sediment graph models. The average USGs for 0.25h and 0.5h duration (Fig. 4.19) were obtained as per the procedure explained under Article 4.1.3. The sediment mobilized (excess sediment) generated during each of the time increments of effective rainfall duration for various storms, selected above, was obtained by Eq. (4.83). The thus obtained storm-wise sediment graphs are presented in Table 5.5.

Table 5.4 Observed sediment graphs (SGs) for selected storms in Amameh watershed

Time(h)	Sediment Graph ordinates for storm events (tonne.day ⁻¹)							
	April 14,71	Nov. 3,72	July 18,74	April 23,75	July 22,76	April 29,80	April 25,83	April 6,97
0.00	0.000	0.000	0.000	0.000	0.000	0.000	0.000	0.000
0.25	1.293	0.131	1.685	2.766	0.417	0.742	0.045	0.330
0.50	2.586	0.262	3.369	5.532	0.834	1.484	0.089	0.659
0.75	4.000	0.436	17.486	12.578	183.813	2.256	2.000	1.274
1.00	5.414	0.610	31.603	19.624	366.791	3.029	3.911	1.889
1.25	8.894	1.080	43.709	39.445	572.051	3.831	5.941	2.108
1.50	12.374	1.550	55.814	59.265	777.310	4.634	7.970	2.327
1.75	44.539	2.174	84.112	106.696	693.539	5.466	12.540	2.408
2.00	76.704	2.798	112.411	154.128	609.768	6.298	17.109	2.488
2.25	94.666	4.482	99.748	230.795	356.268	7.160	24.910	2.570
2.50	112.627	6.167	87.085	307.481	102.768	8.022	32.710	2.651
2.75	156.777	9.723	68.085	355.512	57.264	8.914	44.745	2.734
3.00	200.926	13.279	49.084	403.563	11.760	9.806	56.781	2.817
3.25	279.917	21.773	27.594	329.775	8.692	10.726	64.448	3.196
3.50	358.907	30.267	6.103	255.987	5.624	11.647	72.115	3.574
3.75	528.962	56.185	4.902	226.993	4.201	13.706	92.595	3.812
4.00	699.016	82.104	3.702	198.000	2.779	15.764	113.076	4.049
4.25	659.206	114.961	2.534	120.140	3.415	20.362	127.228	4.292
4.50	619.394	147.818	1.366	42.228	4.051	24.960	141.380	4.534
4.75	358.265	156.294	1.150	33.767	4.410	35.670	148.081	5.097
5.00	97.137	164.770	0.934	25.307	4.769	46.380	154.782	5.659
5.25	79.068	99.894	0.749	21.077	5.589	116.693	151.274	6.242
5.50	60.998	35.018	0.563	16.847	6.410	187.006	147.767	6.824
5.75	51.571	29.261	0.543	14.043	4.551	240.530	144.329	8.461
6.00	42.144	23.503	0.524	11.239	2.693	294.054	140.891	10.098
6.25	37.453	21.062	0.504	9.471	1.755	305.850	134.308	12.817
6.50	32.762	18.621	0.485	7.703	0.818	317.646	127.724	15.536
6.75	29.571	16.470	0.466	6.220	0.522	329.834	116.537	24.216
7.00	26.379	14.319	0.447	4.737	0.225	342.022	105.349	32.896
7.25	24.391	13.045	0.428	4.306	0.113	210.629	96.673	44.897
7.50	22.402	11.771	0.409	3.874	0.000	79.235	87.997	56.898
7.75	20.542	10.624	0.391	3.474		72.862	75.452	80.107
8.00	18.683	9.478	0.373	3.074		66.489	62.908	103.315
8.25	17.765	8.458	0.355	2.705		55.366	49.066	61.020
8.50	16.848	7.438	0.337	2.336		44.243	35.224	18.725
8.75	15.962	6.543	0.320	1.998		38.354	27.761	15.716
9.00	15.076	5.649	0.303	1.660		32.465	20.298	12.707
9.25	13.471	5.249	0.286	1.352		29.314	18.474	11.704
9.50	11.867	4.849	0.269	1.045		26.163	16.649	10.700
9.75	11.076	4.141	0.252	0.523		24.217	14.172	9.946
10.00	10.284	3.434	0.236	0.000		22.270	11.696	9.192
10.25	8.870	3.127	0.219			21.331	10.193	8.154
10.50	7.456	2.820	0.203			20.392	8.691	7.115
10.75	6.758	2.543	0.188			19.486	7.317	6.577
11.00	6.060	2.267	0.172			18.580	5.943	6.038
11.25	5.393	2.021	0.156			17.706	4.697	5.531
11.50	4.726	1.775	0.141			16.831	3.450	5.024
11.75	4.090	1.559	0.126			15.990	2.856	4.549
12.00	3.453	1.343	0.111			15.148	2.262	4.073
12.25	2.847	1.158	0.097			14.338	1.699	3.841
12.50	2.241	0.972	0.082			13.528	1.137	3.608
12.75	1.666	0.816	0.068			12.750	0.849	3.468
13.00	1.090	0.661	0.054			11.972	0.561	3.327
13.25	0.545	0.535	0.040			11.581	0.280	3.107
13.50	0.000	0.409	0.027			11.189	0.000	2.887
13.75		0.312	0.013			10.806		2.794
14.00		0.215	0.000			10.422		2.700
14.25		0.147				10.047		2.568
14.50		0.079				9.671		2.436
14.75		0.040				9.303		2.363
15.00		0.000				8.935		2.289
15.25						8.575		2.216
15.50						8.215		2.143
15.75						7.863		2.071
16.00						7.511		1.998

Continued Table 5.4

Time(h)	Sediment Graph ordinates for storm events (tonne.day ⁻¹)							
	April 14,71	Nov. 3,72	July 18,74	April 23,75	July 22,76	April 29,80	April 25,83	April 6,97
16.25						6.860		1.927
16.50						6.209		1.855
16.75						5.880		1.784
17.00						5.552		1.713
17.25						5.231		1.643
17.50						4.910		1.572
17.75						4.597		1.503
18.00						4.284		1.433
18.25						3.979		1.364
18.50						3.673		1.295
18.75						3.598		1.227
19.00						3.522		1.159
19.25						3.446		1.092
19.50						3.371		1.024
19.75						3.295		0.957
20.00						3.220		0.890
20.25						3.144		0.824
20.50						3.068		0.757
20.75						2.993		0.692
21.00						2.917		0.627
21.25						2.842		0.562
21.50						2.767		0.497
21.75						2.691		0.433
22.00						2.616		0.369
22.25						2.540		0.306
22.50						2.465		0.242
22.75						2.390		0.179
23.00						2.315		0.116
23.25						2.239		0.058
23.50						2.164		0.000
23.75						2.089		
24.00						2.014		
24.25						1.939		
24.50						1.864		
24.75						1.789		
25.00						1.713		
25.25						1.638		
25.50						1.563		
25.75						1.489		
26.00						1.414		
26.25						1.339		
26.50						1.264		
26.75						1.189		
27.00						1.114		
27.25						1.039		
27.50						0.965		
27.75						0.890		
28.00						0.815		
28.25						0.740		
28.50						0.666		
28.75						0.591		
29.00						0.516		
29.25						0.442		
29.50						0.367		
29.75						0.293		
30.00						0.218		
30.25						0.144		
30.50						0.069		
30.75						0.035		
31.00						0.000		

Table 5.5 Predicted sediment graphs for Amameh watershed using Model 'A'

Time(h)	Sediment Graph ordinates for storm events (tonne.day ⁻¹)							
	April 14,71	Nov. 3,72	July 18,74	April 23,75	July 22,76	April 29,80	April 25,83	April 6,97
0.00	0.000	0.000	0.000	0.000	0.000	0.000	0.000	0.000
0.25	0.493	0.331	0.130	0.061	0.261	0.200	0.126	0.030
0.50	0.987	0.522	0.204	0.121	0.523	0.400	0.322	0.047
0.75	1.540	0.710	0.277	0.207	0.816	0.759	0.462	0.094
1.00	2.092	1.163	0.454	0.294	1.109	1.119	0.704	0.153
1.25	3.434	1.621	0.632	0.535	1.820	1.815	1.050	0.241
1.50	4.777	5.800	2.265	0.776	2.531	2.510	2.816	0.678
1.75	17.113	10.020	3.894	2.404	9.067	7.874	5.970	1.114
2.00	29.450	12.428	4.807	4.036	15.603	13.238	8.440	1.747
2.25	36.358	14.828	5.720	5.474	19.263	19.435	10.234	2.379
2.50	43.268	20.668	7.991	6.959	22.923	25.633	13.391	3.497
2.75	60.419	26.915	10.256	10.714	32.011	34.481	18.061	4.614
3.00	77.572	68.198	26.352	14.446	41.099	43.329	36.017	9.088
3.25	199.318	109.951	42.448	30.817	105.602	97.341	67.245	13.580
3.50	321.064	229.676	89.323	47.232	170.105	151.354	128.163	28.732
3.75	675.604	351.170	136.197	97.107	357.945	328.436	218.885	43.873
4.00	1030.144	215.565	81.577	147.427	545.786	505.518	212.401	45.822
4.25	617.001	78.603	26.952	122.935	326.896	436.003	110.211	47.788
4.50	203.858	54.931	17.030	99.433	108.007	366.489	52.239	43.721
4.75	128.812	40.890	7.109	115.846	68.247	222.224	42.250	39.838
5.00	53.767	47.758	5.496	128.991	28.487	77.960	36.383	24.711
5.25	41.549	30.118	3.878	77.941	22.013	52.327	25.154	9.994
5.50	29.331	14.904	3.194	28.329	15.540	26.695	16.527	7.788
5.75	24.160	10.694	2.510	18.743	12.800	21.233	11.322	4.222
6.00	18.988	7.394	2.182	9.424	10.060	15.772	6.777	2.882
6.25	16.482	6.135	1.848	7.546	8.732	13.332	5.466	2.138
6.50	13.975	5.418	1.728	5.698	7.404	10.891	4.392	1.743
6.75	13.067	4.940	1.608	4.911	6.923	9.833	3.975	1.457
7.00	12.159	4.581	1.534	4.135	6.442	8.774	3.617	1.314
7.25	11.586	4.298	1.456	3.748	6.139	8.292	3.385	1.182
7.50	11.014	4.106	1.414	3.367	5.835	7.810	3.191	1.118
7.75	10.698	3.969	1.373	3.205	5.668	7.525	3.076	1.058
8.00	10.382	3.515	1.206	3.044	5.501	7.239	2.842	0.988
8.25	9.099	3.052	1.033	2.810	4.821	6.633	2.498	0.919
8.50	7.816	2.761	0.929	2.577	4.141	6.026	2.214	0.845
8.75	7.007	2.468	0.819	2.397	3.712	5.345	1.997	0.769
9.00	6.198	2.201	0.720	2.212	3.284	4.664	1.781	0.682
9.25	5.448	1.904	0.621	1.945	2.886	4.137	1.558	0.593
9.50	4.698	1.738	0.574	1.681	2.489	3.610	1.387	0.534
9.75	4.323	1.578	0.522	1.516	2.290	3.252	1.266	0.471
10.00	3.948	1.377	0.454	1.352	2.092	2.893	1.124	0.419
10.25	3.415	1.164	0.381	1.188	1.809	2.574	0.967	0.366
10.50	2.882	1.043	0.344	1.026	1.527	2.255	0.841	0.329
10.75	2.605	0.938	0.308	0.930	1.380	1.996	0.758	0.290
11.00	2.329	0.830	0.271	0.834	1.234	1.737	0.674	0.256
11.25	2.073	0.733	0.240	0.732	1.098	1.557	0.594	0.223
11.50	1.816	0.634	0.209	0.632	0.962	1.377	0.520	0.198
11.75	1.579	0.544	0.177	0.562	0.837	1.211	0.450	0.174
12.00	1.342	0.454	0.146	0.493	0.711	1.044	0.381	0.150
12.25	1.105	0.365	0.115	0.426	0.586	0.883	0.313	0.128
12.50	0.868	0.276	0.084	0.359	0.460	0.722	0.245	0.106
12.75	0.651	0.201	0.057	0.297	0.345	0.568	0.183	0.085
13.00	0.434	0.112	0.026	0.235	0.230	0.415	0.121	0.063
13.25	0.217	0.037	0.000	0.174	0.115	0.267	0.058	0.043
13.50	0.000	0.028		0.113	0.000	0.120	0.026	0.028
13.75		0.020		0.081		0.060	0.020	0.015
14.00		0.014		0.048		0.000	0.014	0.008
14.25		0.006		0.024			0.007	0.001
14.50		0.000		0.000			0.002	0.001
14.75							0.001	0.000
15.00							0.000	

5.2.2 SGs derived based on watershed characteristics (Model B)

The instantaneous unit sediment graph is needed to develop a sediment graph model by taking physiographical characteristics of the watershed into consideration. The concept of IUSG has already been discussed under Article 4.2, for which the ordinates of instantaneous unit hydrograph (IUH) and sediment concentration were required. For the development of the IUH, different values of weighting factor (x) and time interval (Δt), with the same value of storage coefficient (k) were assumed and explained under Article 4.2.1 in chapter 4. The reliability and reasonability of the developed IUH were checked by comparing the ordinates of the derived 0.5-h UH with the measured master 0.5-h UH. As shown in Fig. 4.22, the 0.5-h UH developed through the conversion of IUH with a weighting factor of 0.162, which happens to be close to the typical value of $x=0.2$ for natural streams (**Bedient, 1988**), and a time interval of 0.5h gave the best fit for the measured master 0.5-h UH. The respective sediment concentration was calculated by using the dimensionless sediment concentration distribution (DSCD) depicted in Fig. 4.23. To find the most appropriate value of parameter Z for the study area the different values of Z viz. 0.0187, 0.0885 and 0.1100 as calculated respectively by using Williams', Banasik's and modified methods (Eqs. 4.93 to 4.95) were tried to determine IUSGs. The sediment graphs were then developed by using the determined IUSGs. It was found that values of 0.0187 and 0.0885 underestimated the peak of sediment graphs for all the selected storms, since smaller is the value of parameter Z lower is the value of peak of IUSG, whereas the value 0.110 gave a balanced estimation of the peak. Therefore, the value of Z as equal to 0.110 was found to be appropriate for the estimation of sediment concentration for the study area. In addition, the value of parameter Z equal to 2.020 obtained for developing

sediment routing sub-model (Section b-2, Article 4.1.1.2), was also considered in search of the most efficient sediment graph model.

The time interval and the storage coefficient for all of the IUSG models were considered to be equal to 0.5hr and 1.543hr, respectively. The corresponding values of C_0 , C_1 and C_2 were respectively found to be 0.139, 0.139 and 0.721 for $x=0.000$ and 0.000, 0.324 and 0.767 for $x=0.162$. The ordinates of IUSGs derived from the two above alternatives are presented in Table 5.6. It may be seen from the table that for $Z=2.020$ the entire sediment load is distributed within a very short duration in the early period of the storm event while the base time of the instantaneous unit sediment graphs for $Z=0.110$ is almost double. The unit of the ordinates of the IUSG is the same as that of the IUH, which is s^{-1} for a unit volume of excess sediment or sediment mobilized (m^3). The graphical presentations of the developed IUSG for the studied cases are shown in Fig. 5.2.

The ordinates of USGs required to be convoluted for prediction of sediment graph were obtained as per the procedure of conversion of IUH into UH, explained under Article 4.2.4 and are shown in Fig. 5.3. The dimension of USG ordinates is also the same as that of IUSG. The ordinates of USG have been converted to day^{-1} for a unit volume of sediment mobilized (one tonne) by the conversion factor of 106963.2 equal to (86400×1.238) , since the popular unit of sediment flow rate in Iran is $t.day^{-1}$. The specific gravity of sediment has been found to be equal to 1.238 $t.m^3$ by conducting the gravimetry of sediment samples.

Since two values of x (0.162 and 0.000) and two values of parameter Z (0.110 and 2.020) were found to be applicable for the derivation of IUSG, and two methods of USG convolution (SMD and NSMD) were used, the following models for various combinations have been tried for arriving at the most applicable sediment graph for the watershed.

- B-1)** Parameter $Z=0.110$, $x=0.162$ and SMD,
- B-2)** Parameter $Z=0.110$, $x=0.162$ and NSMD,
- B-3)** Parameter $Z=0.110$, $x=0.000$ and SMD,
- B-4)** Parameter $Z=0.110$, $x=0.000$ and NSMD,
- B-5)** Parameter $Z=2.020$, $x=0.162$ and SMD,
- B-6)** Parameter $Z=2.020$, $x=0.162$ and NSMD,
- B-7)** Parameter $Z=2.020$, $x=0.000$ and SMD and
- B-8)** Parameter $Z=2.020$, $x=0.000$ and NSMD.

The results of trial of above eight models for prediction of direct sediment graphs for the Amameh watershed were investigated and their comparative assessment with the observed sediment graphs are presented respectively through Tables 5.7 to 5.14.

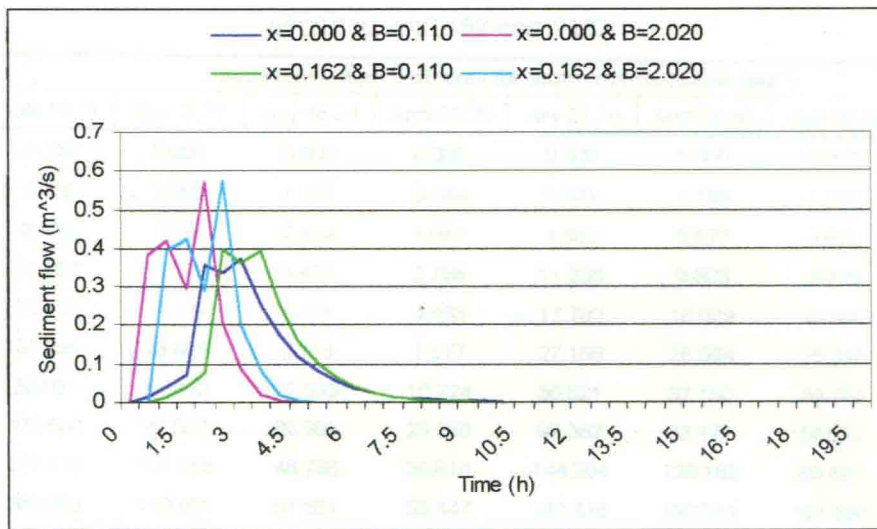


Fig. 5.2 Derived IUSGs using different alternatives for Amameh watershed

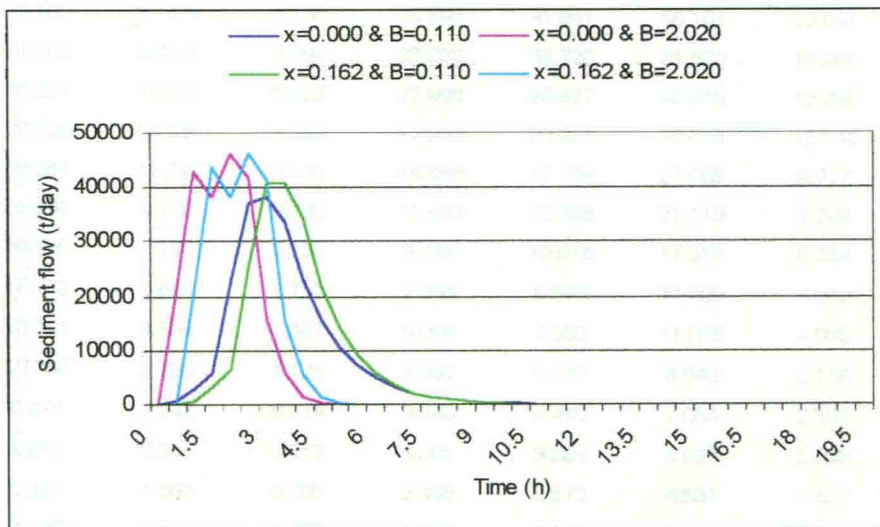


Fig. 5.3 Derived USGs using different alternatives for Amameh watershed

Table 5.7 Predicted sediment graphs for Amameh watershed using Model 'B-1'
($Z=0.110$, $x=0.162$ and SMD)

Time(h)	Sediment Graph ordinates for storm events (tonne.day ⁻¹)							
	April 14,71	Nov. 3,72	July 18,74	April 23,75	July 22,76	April 29,80	April 25,83	April 6,97
0.00	0.000	0.000	0.000	0.000	0.000	0.000	0.000	0.000
0.25	4.418	2.960	1.168	0.544	2.341	1.789	1.125	0.271
0.50	8.837	7.158	2.804	1.087	4.682	3.577	3.825	0.650
0.75	21.207	11.377	4.439	2.766	11.236	9.803	6.975	1.301
1.00	33.578	17.374	6.776	4.463	17.790	16.029	10.800	2.222
1.25	51.255	23.405	9.113	7.577	27.155	26.594	15.346	3.414
1.50	68.931	57.840	22.549	10.724	36.521	37.160	30.764	7.451
1.75	170.554	92.907	35.985	25.258	90.362	83.171	56.937	11.489
2.00	272.178	121.255	46.768	39.814	144.204	129.182	80.627	17.663
2.25	353.738	149.651	57.551	55.447	187.416	190.211	101.881	23.844
2.50	435.297	150.252	57.356	71.437	230.627	251.241	112.987	29.437
2.75	433.823	153.062	57.162	85.672	229.846	273.127	115.139	35.040
3.00	432.350	145.751	52.973	99.822	229.065	295.012	113.344	36.555
3.25	400.667	137.602	48.784	105.130	212.280	281.781	107.747	38.219
3.50	368.985	117.782	39.994	110.083	195.494	268.549	97.299	35.344
3.75	302.500	95.056	31.204	100.616	160.269	232.902	80.747	32.433
4.00	236.015	80.349	25.581	91.019	125.044	197.255	67.093	28.263
4.25	193.489	64.810	19.959	79.841	102.513	161.712	55.497	23.947
4.50	150.963	54.398	16.363	68.515	79.982	126.170	45.676	19.768
4.75	123.762	42.953	12.766	56.119	65.571	103.436	36.995	15.535
5.00	96.561	34.795	10.466	43.824	51.159	80.703	29.683	12.808
5.25	79.162	27.474	8.166	35.895	41.941	66.161	23.897	10.019
5.50	61.763	22.256	6.694	28.032	32.723	51.620	18.986	8.192
5.75	50.634	17.573	5.223	22.960	26.827	42.319	15.285	6.408
6.00	39.506	14.236	4.282	17.930	20.931	33.018	12.144	5.240
6.25	32.387	11.240	3.341	14.686	17.159	27.069	9.777	4.099
6.50	25.269	9.106	2.739	11.469	13.388	21.119	7.768	3.352
6.75	20.716	7.190	2.137	9.394	10.976	17.314	6.254	2.622
7.00	16.163	5.824	1.752	7.336	8.563	13.509	4.969	2.144
7.25	13.251	4.599	1.367	6.008	7.020	11.075	4.000	1.677
7.50	10.338	3.725	1.121	4.692	5.477	8.640	3.178	1.371
7.75	8.476	2.942	0.874	3.843	4.490	7.084	2.559	1.073
8.00	6.613	2.383	0.717	3.001	3.504	5.527	2.033	0.877
8.25	5.421	1.882	0.559	2.458	2.872	4.531	1.637	0.686
8.50	4.230	1.524	0.458	1.920	2.241	3.535	1.300	0.561
8.75	3.468	1.204	0.358	1.572	1.837	2.898	1.047	0.439
9.00	2.705	0.975	0.293	1.228	1.433	2.261	0.832	0.359
9.25	2.218	0.770	0.229	1.006	1.175	1.854	0.670	0.281
9.50	1.730	0.624	0.188	0.785	0.917	1.446	0.532	0.230
9.75	1.419	0.492	0.146	0.643	0.752	1.186	0.428	0.180
10.00	1.107	0.399	0.120	0.502	0.586	0.925	0.340	0.147

Table 5.8 Predicted sediment graphs for Amameh watershed using Model 'B-2'
($Z=0.110$, $x=0.162$ and NSMD)

Time(h)	Sediment Graph ordinates for storm events (tonne.day ⁻¹)							
	April 14,71	Nov. 3,72	July 18,74	April 23,75	July 22,76	April 29,80	April 25,83	April 6,97
0.00	0.000	0.000	0.000	0.000	0.000	0.000	0.000	0.000
0.25	4.252	1.160	1.168	0.613	2.341	2.265	1.035	0.444
0.50	8.503	2.319	2.804	1.226	4.682	4.531	2.069	0.889
0.75	20.407	6.725	4.439	3.555	11.236	13.139	6.001	2.577
1.00	32.311	11.131	6.776	5.883	17.790	21.748	9.933	4.265
1.25	49.320	19.016	9.113	10.664	27.155	37.154	18.004	7.287
1.50	66.329	26.902	22.549	15.445	36.521	52.560	25.040	10.309
1.75	164.117	58.210	35.985	34.321	90.362	113.730	55.874	22.306
2.00	261.905	89.518	46.768	53.198	144.204	174.899	83.811	34.303
2.25	340.386	137.591	57.551	82.775	187.416	268.824	130.848	52.724
2.50	418.867	185.664	57.356	112.352	230.627	362.748	173.745	71.146
2.75	417.449	206.682	57.162	140.008	229.846	403.811	216.298	79.199
3.00	416.031	227.699	52.973	167.665	229.065	444.874	235.052	87.253
3.25	385.545	218.997	48.784	188.475	212.280	427.874	246.387	83.919
3.50	355.058	210.296	39.994	209.285	195.494	410.874	238.623	80.584
3.75	291.082	184.534	31.204	206.777	160.269	360.540	215.289	70.712
4.00	227.107	158.772	25.581	204.269	125.044	310.206	192.300	60.840
4.25	186.186	130.164	19.959	184.549	102.513	254.312	159.353	49.878
4.50	145.265	101.555	16.363	164.829	79.982	198.418	133.825	38.916
4.75	119.090	83.257	12.766	141.541	65.571	162.666	101.927	31.904
5.00	92.916	64.958	10.466	118.252	51.159	126.914	85.599	24.892
5.25	76.174	53.254	8.166	96.945	41.941	104.046	65.196	20.407
5.50	59.432	41.549	6.694	75.638	32.723	81.178	54.752	15.921
5.75	48.723	34.063	5.223	62.009	26.827	66.551	41.701	13.053
6.00	38.015	26.576	4.282	48.381	20.931	51.924	35.021	10.184
6.25	31.165	21.788	3.341	39.663	17.159	42.568	26.674	8.349
6.50	24.315	16.999	2.739	30.946	13.388	33.212	22.401	6.514
6.75	19.934	13.936	2.137	25.370	10.976	27.228	17.061	5.340
7.00	15.553	10.873	1.752	19.794	8.563	21.244	14.328	4.167
7.25	12.751	8.914	1.367	16.227	7.020	17.416	10.913	3.416
7.50	9.948	6.955	1.121	12.661	5.477	13.588	9.165	2.665
7.75	8.156	5.702	0.874	10.380	4.490	11.140	6.980	2.185
8.00	6.363	4.449	0.717	8.098	3.504	8.691	5.862	1.705
8.25	5.217	3.647	0.559	6.639	2.872	7.125	4.465	1.397
8.50	4.070	2.845	0.458	5.180	2.241	5.559	3.750	1.090
8.75	3.337	2.333	0.358	4.247	1.837	4.558	2.856	0.894
9.00	2.603	1.820	0.293	3.313	1.433	3.556	2.398	0.697
9.25	2.134	1.492	0.229	2.716	1.175	2.915	1.827	0.572
9.50	1.665	1.164	0.188	2.119	0.917	2.274	1.534	0.446
9.75	1.365	0.954	0.146	1.737	0.752	1.865	1.168	0.366
10.00	1.065	0.745	0.120	1.356	0.586	1.455	0.981	0.285

Table 5.9 Predicted sediment graphs for Amameh watershed using Model 'B-3'

(Z=0.110, x=0.000 and SMD)

Time(h)	Sediment Graph ordinates for storm events (tonne.day ⁻¹)							
	April 14,71	Nov. 3,72	July 18,74	April 23,75	July 22,76	April 29,80	April 25,83	April 6,97
0.00	0.000	0.000	0.000	0.000	0.000	0.000	0.000	0.000
0.25	3.896	2.610	1.030	0.479	2.064	1.577	0.992	0.239
0.50	7.793	6.367	2.495	0.959	4.129	3.155	3.394	0.579
0.75	18.868	10.145	3.959	2.459	9.996	8.712	6.214	1.157
1.00	29.943	15.628	6.096	3.976	15.864	14.269	9.682	1.992
1.25	46.108	21.143	8.233	6.799	24.429	23.866	13.838	3.066
1.50	62.274	51.868	20.221	9.652	32.993	33.463	27.643	6.682
1.75	152.948	83.158	32.210	22.638	81.034	74.625	50.997	10.297
2.00	243.622	109.688	42.319	35.646	129.075	115.787	72.607	15.932
2.25	320.083	136.296	52.428	50.093	169.585	171.734	92.519	21.571
2.50	396.543	138.935	53.070	64.857	210.095	227.681	103.692	26.865
2.75	401.402	143.548	53.712	78.449	212.669	250.725	107.186	32.167
3.00	406.260	138.562	50.566	91.980	215.243	273.768	106.961	33.959
3.25	382.467	132.938	47.421	97.903	202.637	265.476	103.195	35.884
3.50	358.674	116.183	39.886	103.521	190.031	257.183	94.840	33.716
3.75	301.682	96.901	32.351	96.219	159.836	227.554	80.832	31.523
4.00	244.691	83.680	27.211	88.795	129.641	197.924	68.984	27.990
4.25	205.811	69.643	22.070	79.296	109.042	166.475	58.538	24.329
4.50	166.931	59.738	18.563	69.657	88.443	135.026	49.497	20.585
4.75	140.407	48.832	15.057	58.550	74.390	113.571	41.256	16.790
5.00	113.882	40.754	12.664	47.520	60.337	92.116	34.180	14.187
5.25	95.787	33.314	10.272	39.943	50.749	77.480	28.351	11.526
5.50	77.692	27.803	8.640	32.419	41.162	62.843	23.318	9.679
5.75	65.347	22.727	7.007	27.250	34.622	52.857	19.342	7.863
6.00	53.002	18.967	5.894	22.117	28.081	42.872	15.908	6.603
6.25	44.580	15.505	4.781	18.590	23.619	36.060	13.195	5.364
6.50	36.159	12.940	4.021	15.088	19.157	29.248	10.852	4.505
6.75	30.413	10.577	3.261	12.682	16.113	24.600	9.002	3.660
7.00	24.668	8.828	2.743	10.293	13.069	19.953	7.404	3.073
7.25	20.748	7.216	2.225	8.652	10.993	16.783	6.141	2.497
7.50	16.829	6.022	1.871	7.022	8.916	13.612	5.051	2.097
7.75	14.155	4.923	1.518	5.903	7.499	11.449	4.190	1.703
8.00	11.481	4.108	1.277	4.791	6.083	9.286	3.446	1.430
8.25	9.656	3.358	1.036	4.027	5.116	7.811	2.858	1.162
8.50	7.832	2.803	0.871	3.268	4.150	6.335	2.351	0.976
8.75	6.588	2.291	0.706	2.747	3.490	5.329	1.950	0.793
9.00	5.343	1.912	0.594	2.230	2.831	4.322	1.604	0.666
9.25	4.494	1.563	0.482	1.874	2.381	3.635	1.330	0.541
9.50	3.645	1.304	0.405	1.521	1.931	2.949	1.094	0.454
9.75	3.066	1.066	0.329	1.279	1.624	2.480	0.907	0.369
10.00	2.487	0.890	0.277	1.038	1.318	2.012	0.746	0.310

Table 5.10 Predicted sediment graphs for Amameh watershed using Model 'B-4'
($Z=0.110$, $x=0.000$ and NSMD)

Time(h)	Sediment Graph ordinates for storm events (tonne.day ⁻¹)							
	April 14,71	Nov. 3,72	July 18,74	April 23,75	July 22,76	April 29,80	April 25,83	April 6,97
0.00	0.000	0.000	0.000	0.000	0.000	0.000	0.000	0.000
0.25	3.749	1.023	1.030	0.540	2.064	1.998	0.912	0.392
0.50	7.498	2.045	2.495	1.081	4.129	3.996	1.825	0.784
0.75	18.156	5.974	3.959	3.158	9.996	11.672	5.331	2.289
1.00	28.813	9.903	6.096	5.234	15.864	19.348	8.837	3.795
1.25	44.368	17.052	8.233	9.553	24.429	33.316	16.128	6.534
1.50	59.923	24.201	20.221	13.872	32.993	47.283	22.507	9.274
1.75	147.175	52.239	32.210	30.768	81.034	102.063	50.120	20.018
2.00	234.427	80.277	42.319	47.665	129.075	156.844	75.140	30.762
2.25	308.001	124.139	52.428	74.626	169.585	242.540	118.065	47.569
2.50	381.576	168.000	53.070	101.588	210.095	328.236	157.204	64.377
2.75	386.251	189.341	53.712	127.687	212.669	369.932	197.481	72.554
3.00	390.926	210.682	50.566	153.786	215.243	411.627	216.524	80.732
3.25	368.031	205.713	47.421	174.343	202.637	401.918	229.995	78.828
3.50	345.136	200.743	39.886	194.900	190.031	392.210	225.561	76.924
3.75	290.296	179.543	32.351	194.974	159.836	350.788	207.781	68.800
4.00	235.455	158.343	27.211	195.048	129.641	309.367	188.863	60.676
4.25	198.043	133.183	22.070	179.123	109.042	260.211	160.840	51.035
4.50	160.630	108.023	18.563	163.199	88.443	211.054	138.389	41.394
4.75	135.107	90.859	15.057	142.921	74.390	177.519	109.727	34.817
5.00	109.584	73.695	12.664	122.643	60.337	143.983	94.411	28.239
5.25	92.172	61.985	10.272	103.156	50.749	121.105	74.857	23.752
5.50	74.759	50.275	8.640	83.669	41.162	98.227	64.408	19.265
5.75	62.880	42.287	7.007	70.374	34.622	82.619	51.068	16.204
6.00	51.002	34.298	5.894	57.080	28.081	67.012	43.940	13.143
6.25	42.898	28.849	4.781	48.010	23.619	56.364	34.839	11.055
6.50	34.794	23.399	4.021	38.940	19.157	45.716	29.976	8.966
6.75	29.265	19.681	3.261	32.753	16.113	38.452	23.768	7.542
7.00	23.737	15.963	2.743	26.566	13.069	31.188	20.450	6.117
7.25	19.965	13.426	2.225	22.344	10.993	26.232	16.215	5.145
7.50	16.193	10.890	1.871	18.123	8.916	21.277	13.951	4.173
7.75	13.620	9.160	1.518	15.244	7.499	17.896	11.062	3.510
8.00	11.047	7.429	1.277	12.364	6.083	14.515	9.518	2.847
8.25	7.537	6.249	1.036	10.399	5.116	12.209	7.546	2.395
8.50	7.537	5.068	0.871	8.435	4.150	9.902	6.493	1.942
8.75	6.339	4.263	0.706	7.095	3.490	8.329	5.148	1.634
9.00	5.142	3.458	0.594	5.754	2.831	6.756	4.430	1.325
9.25	4.325	2.908	0.482	4.840	2.381	5.682	3.512	1.114
9.50	3.508	2.359	0.405	3.926	1.931	4.609	3.022	0.904
9.75	2.950	1.984	0.329	3.302	1.624	3.876	2.396	0.760
10.00	2.393	1.609	0.277	2.678	1.318	3.144	2.062	0.617
10.25	2.013	1.354	0.224	2.253	1.108	2.645	1.635	0.519
10.50	1.632	1.098	0.189	1.827	0.899	2.145	1.406	0.421

Continued Table 5.10

[illegible]

Table 5.11 Predicted sediment graphs for Amameh watershed using Model 'B-5'
($Z=2.020$, $x=0.162$ and SMD)

[illegible]

Table 5.12 Predicted sediment graphs for Amameh watershed using Model 'B-6'
($Z=2.020$, $x=0.162$ and NSMD)

[illegible]

Table 5.13 Predicted sediment graphs for Amameh watershed using Model 'B-7'
($Z=2.020$, $x=0.000$ and SMD)

[illegible]

5.3 Performance Evaluation of Developed Models

The efficiency of developed sediment graphs models for their prediction performance has been evaluated by using graphical and statistical methods as explained under Article 4.3. The *Absolute Relative Error (ARE)*, *Coefficient of Efficiency (CE)*, *Integral Square Error (ISE)*, *Relative Square Error (RSE)*, *Root Mean Square Error (RMSE)*, *Relative Square Error (RSE)*, *Ratio of Error (REO)*, *Bias (B_s)* and *Coefficient of Determination (R^2)* are some of the statistical parameters, which have been used for the comparative evaluation. Since measured and simulated sediment graphs are necessary for any type of comparison, viz. qualitative and quantitative, the ordinates of observed sediment graphs (Table 5.4) and the predicted ones (Tables 5.5 to 5.14) are plotted on the same coordinates as shown in Figs. 5.4 to 5.11. The outputs of all the nine models developed based on hydrological data and watershed characteristics and the observed sediment graphs were discretized into 15-minutes time steps for consistent comparisons for a particular storm event.

5.3.1 Qualitative evaluation

The goodness of fit of a predicted sediment graph to an observed one was tentatively compared by qualitative evaluation. As it was mentioned earlier, this procedure is based on visual comparison of the important shape parameters of a sediment graph. The compatibility of peak, time to peak and base time, and in one word general shape of the sediment graph, are the important parameters, which have been considered in the qualitative evaluation. The trends of increment and reduction in sediment rate respectively on the rising and the falling limbs of sediment graph were also other factors that have been used for better comparison.

In order to compare the results of model simulation on sediment graphs, it was observed that the graphs (Figs. 5.4 to 5.11) predicted by using average USG obtained based on hydrological data (Model A) for different storm events have a sharp peak, and a steep rising as well as falling limbs. It, therefore, predicts higher peak, lesser volume and shorter time to peak as well as base time in comparison with the respective observed sediment graphs. The general shape of sediment graphs in all of the cases is almost the same, which implies that Model A is not able to simulate well.

In case of models based on watershed characteristics (Model B) a visual comparison of the performance of all the models appears to be difficult to evaluate, as can be seen from Figs. 5.4 to 5.11. The results revealed that the models with parameter Z as 2.020 have a shorter time to peak and also a shorter base time in comparison to the models with Z equal to 0.110. The developed sediment graph models with Z equal to 2.020 have an oscillation at the crest segment of the graph, which is not found in the observed ones. The results showed that the sediment graphs predicted by using Models B-1, B-2, B-3 and B-4, that is, the models developed with Z as 0.110 have a better affinity with the observed sediment graphs. The Models B-2 and B-4 appear to have an edge over other in predicting sediment graph peak.

5.3.2 Quantitative evaluation

The quantitative evaluation of performance of developed models was done based on a number of statistical parameters as explained earlier under Article 4.3.2. The details of performance evaluated based on each of the parameter are describe below.

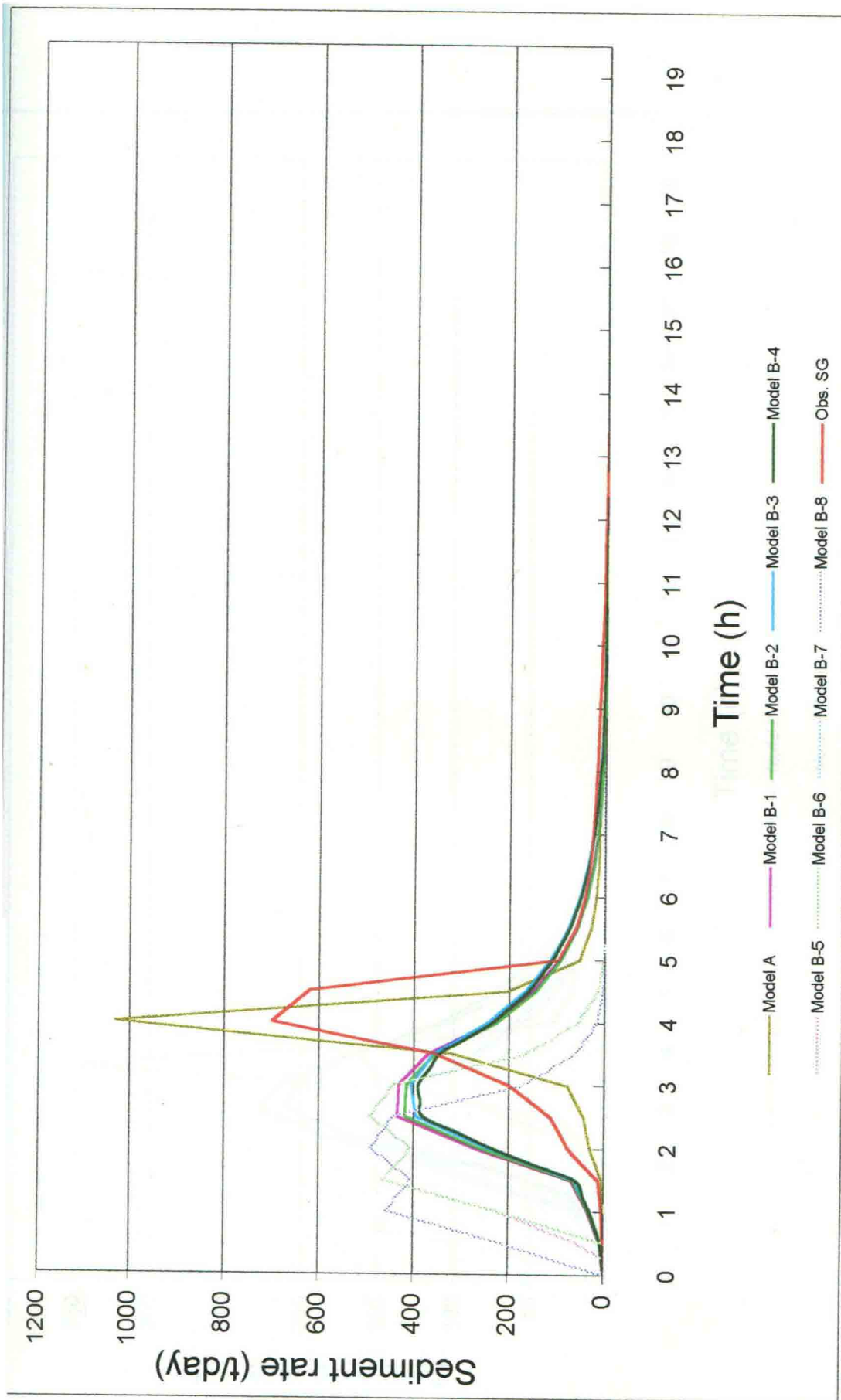


Fig. 5.4 Observed and predicted sediment graphs for the storm event of April 14, 1971

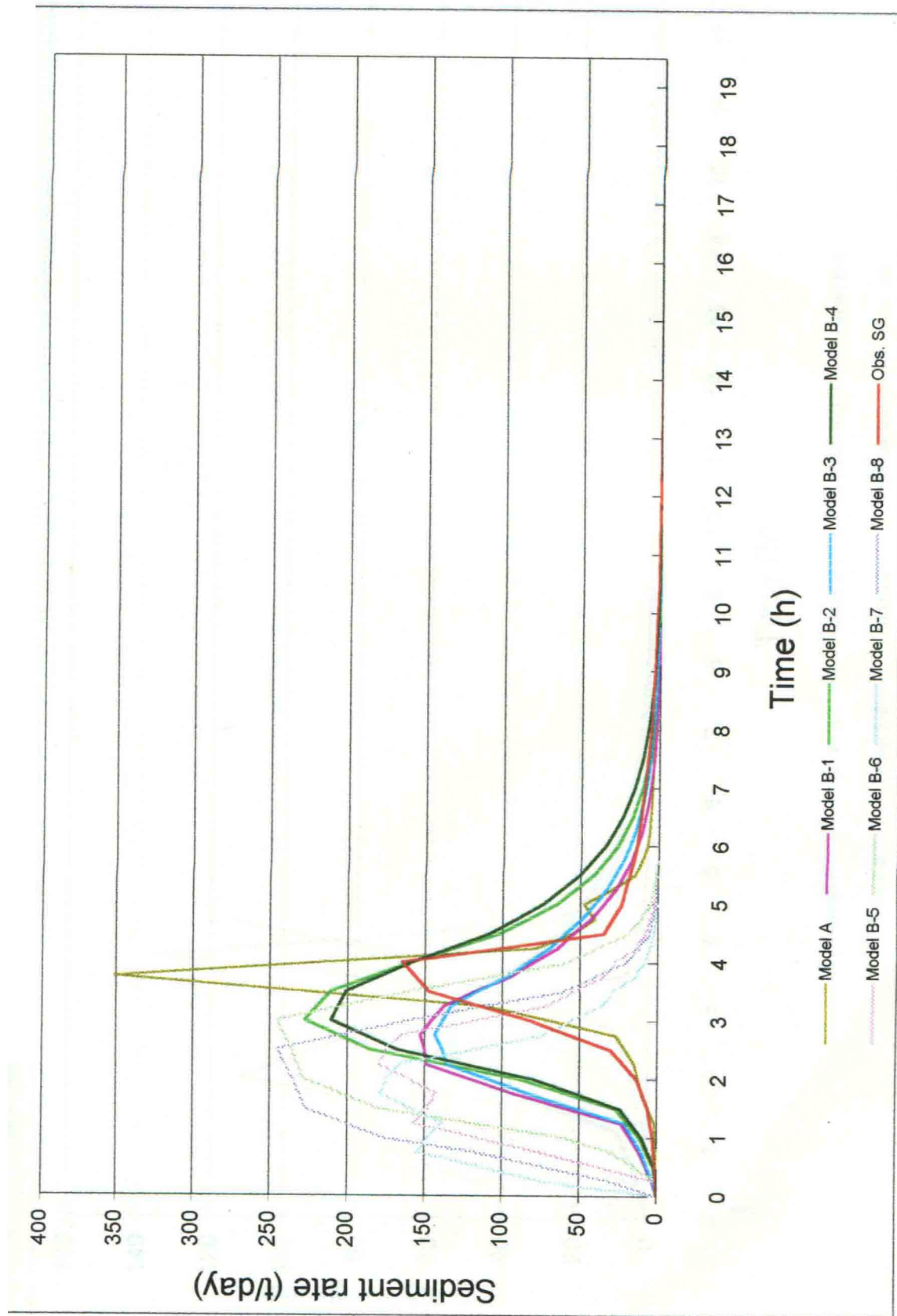


Fig. 5.5 Observed and predicted sediment graphs for the storm event of Nov. 3, 1972

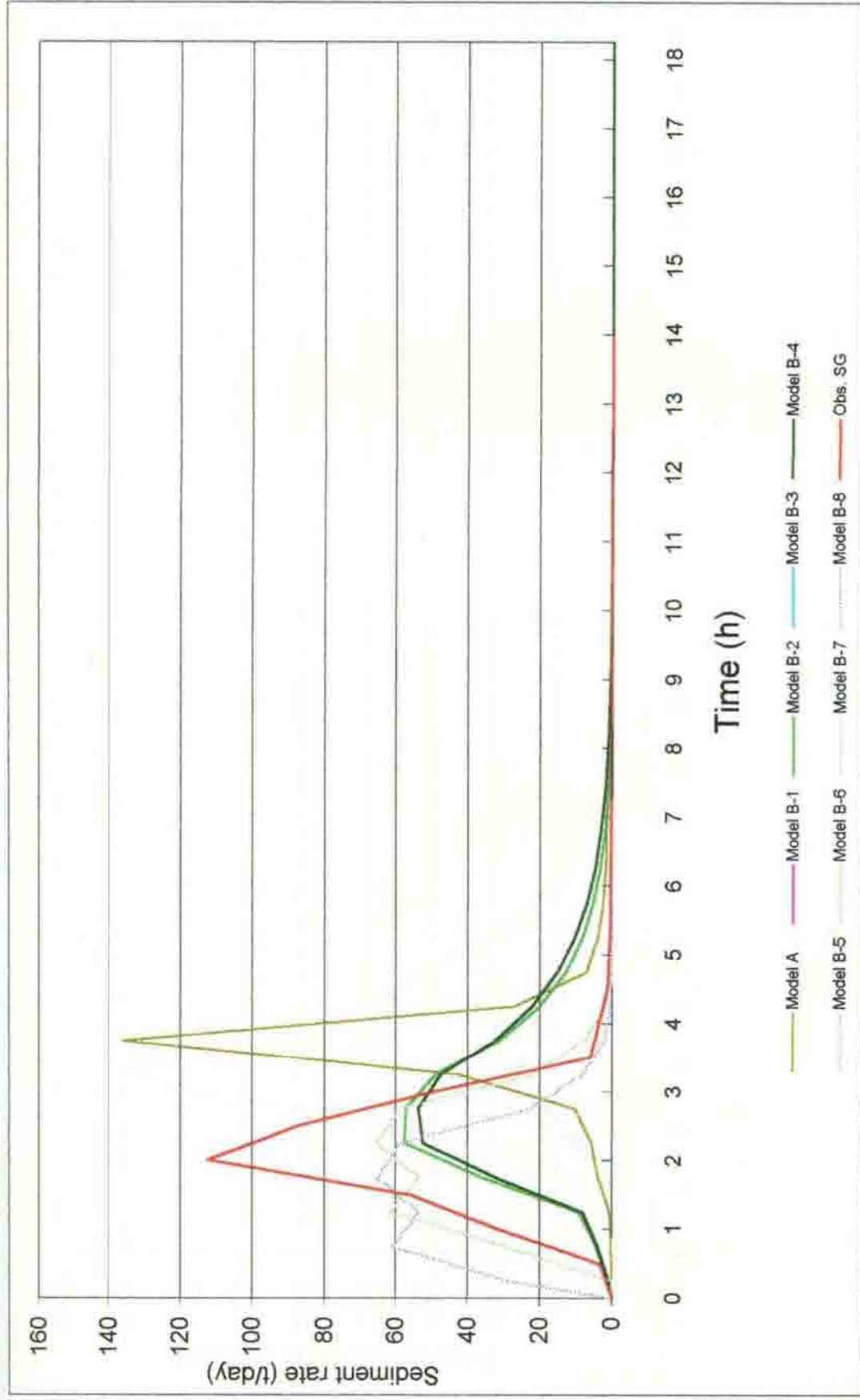


Fig. 5.6 Observed and predicted sediment graphs for the storm event of July 18, 1974

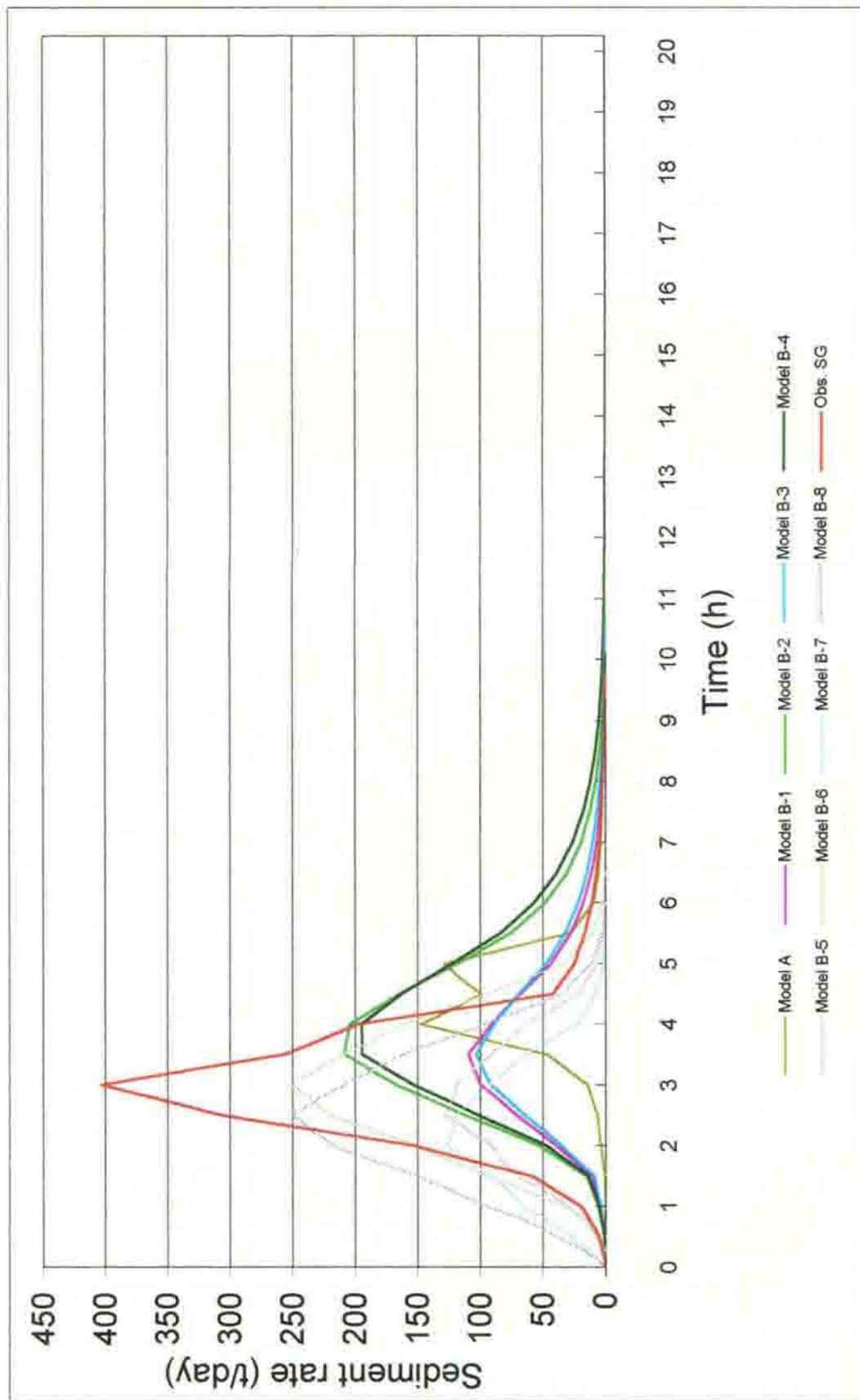


Fig. 5.7 Observed and predicted sediment graphs for the storm event of April 23, 1975

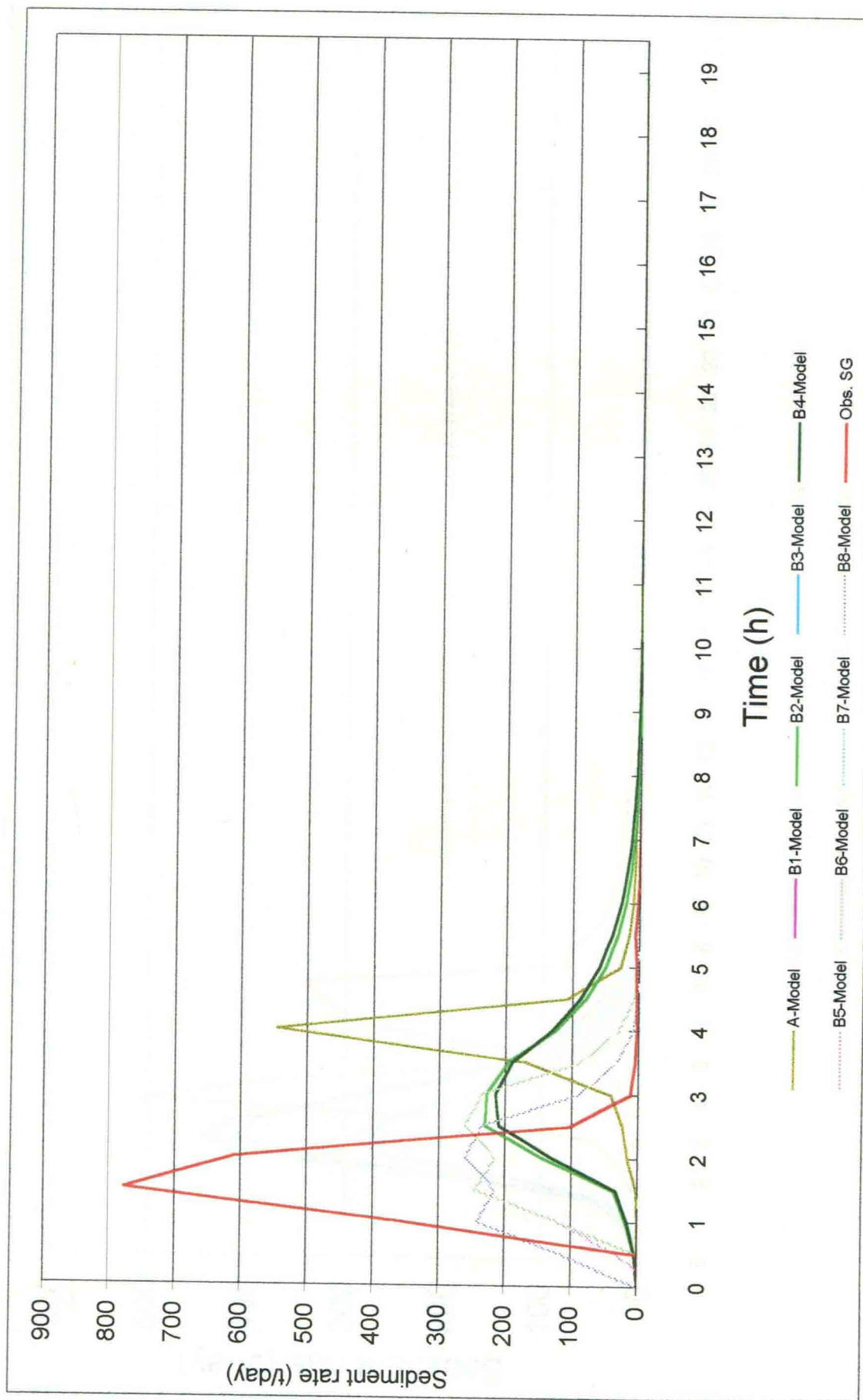


Fig. 5.8 Observed and predicted sediment graphs for the storm event of July 22, 1976

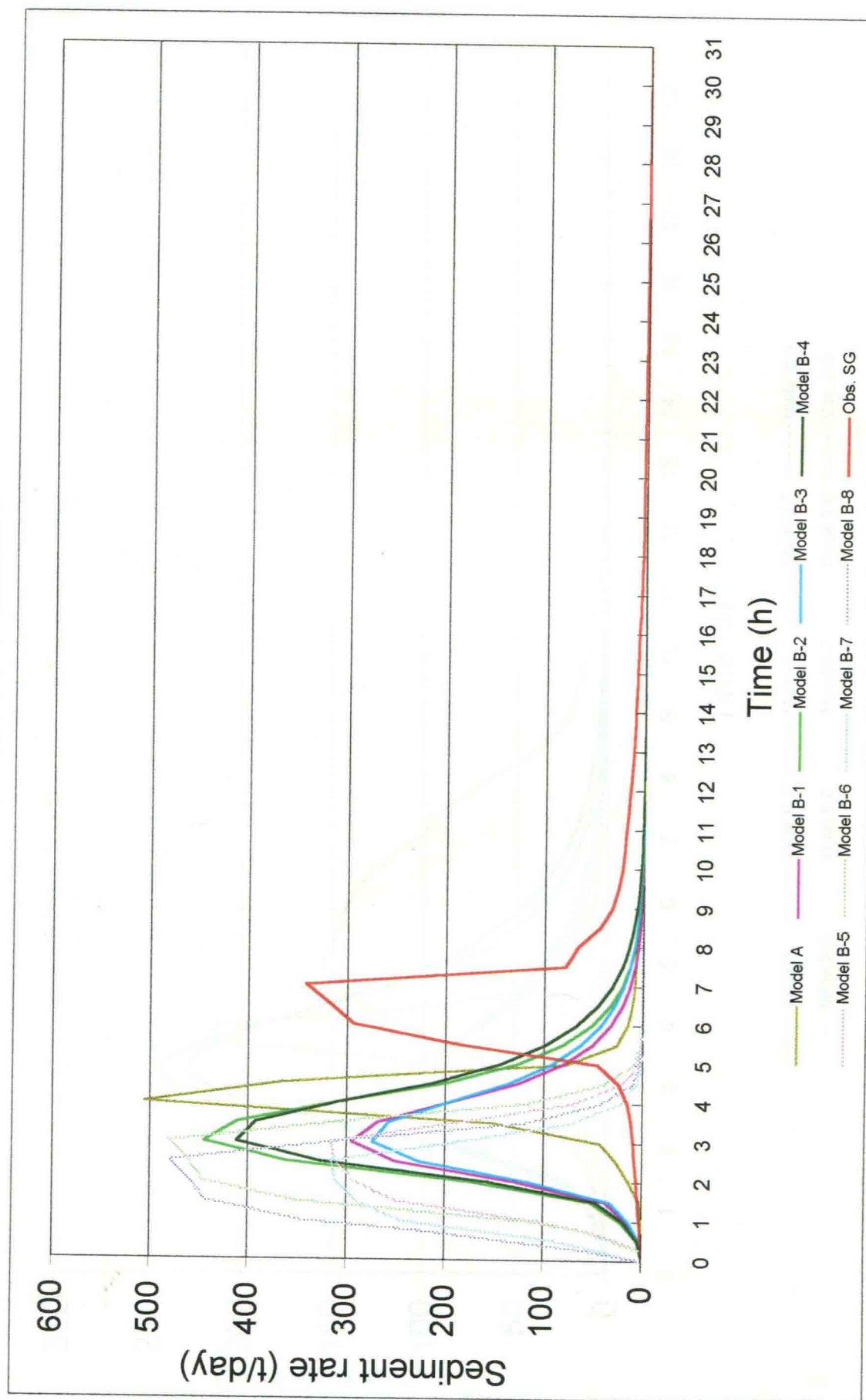


Fig. 5.9 Observed and predicted sediment graphs for the storm event of April 29, 1980

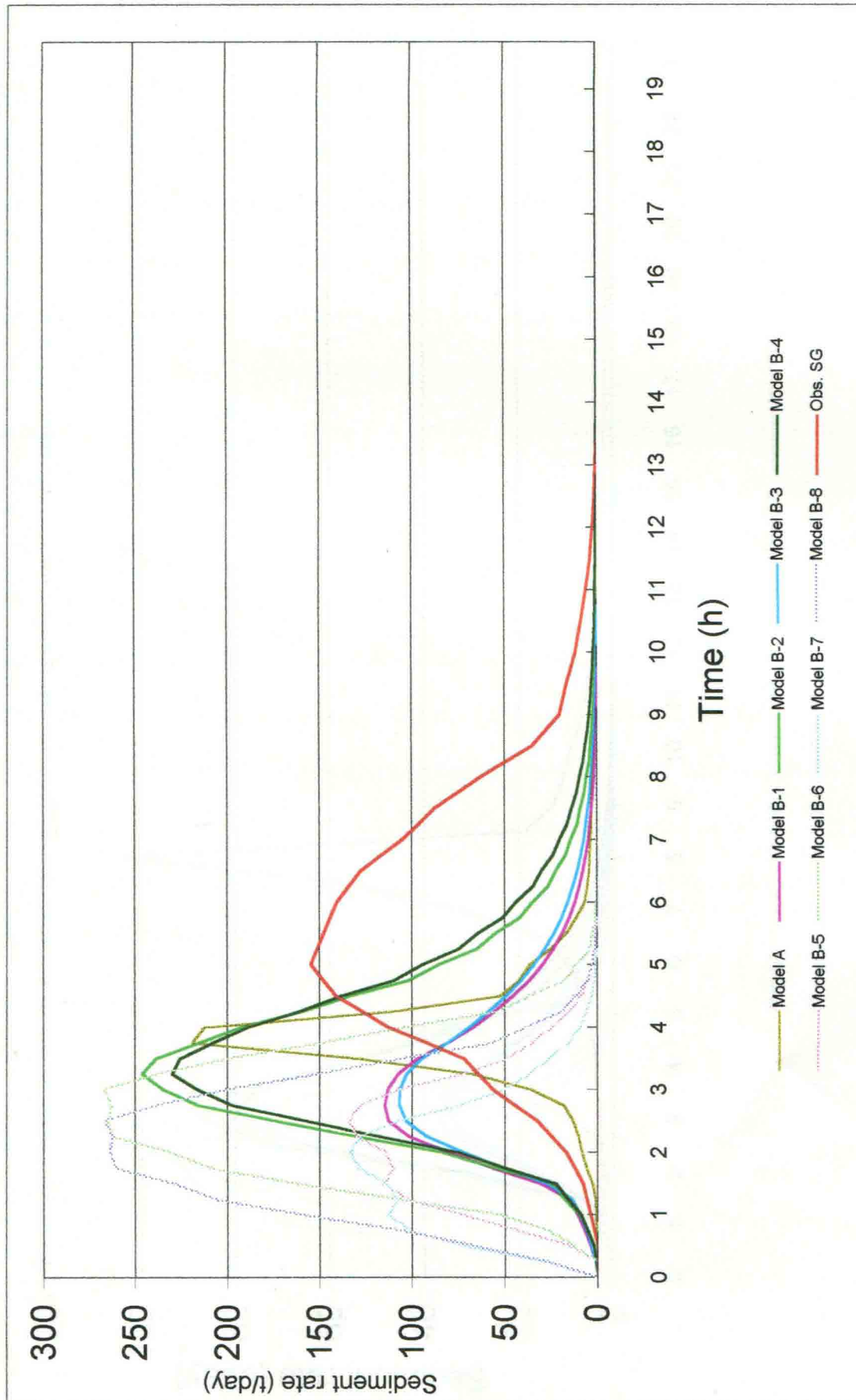


Fig. 5.10 Observed and predicted sediment graphs for the storm event of April 25, 1983

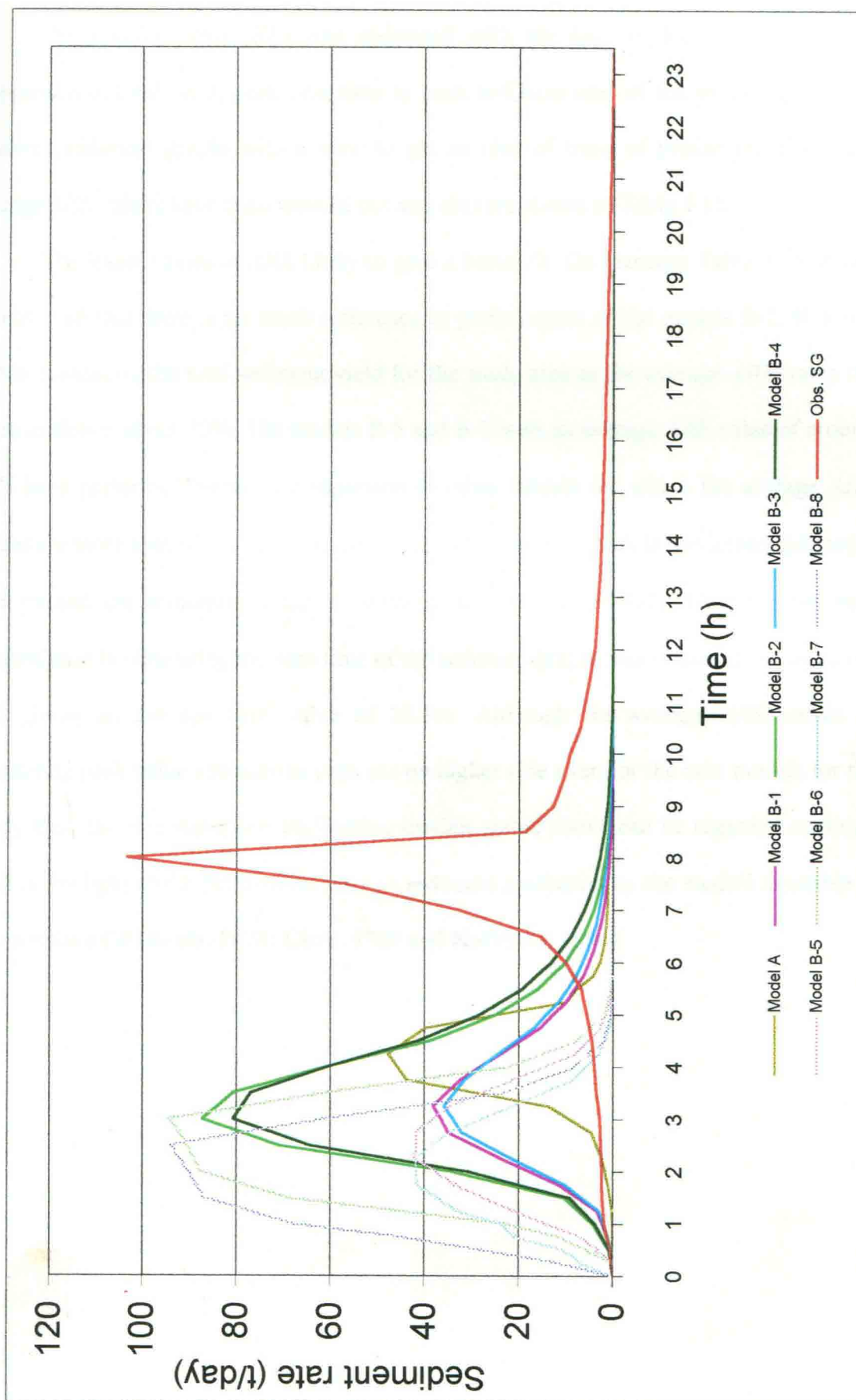


Fig. 5.11 Observed and predicted sediment graphs for the storm event of April 6, 1997

5.3.2.1 Absolute relative error (ARE)

The relative error (*RE*) was estimated with the help of Eq. (4.103) for the comparison of total yield, peak rate, time to peak and base time of the simulated and the observed sediment graphs with a view to get an idea of trend of prediction. However, average *ARE* values have been worked out and also are shown in Table 5.15.

The lesser values of *ARE* likely to give a better fit. On glancing Table 5.15, it can be observed that there is no much difference in performance of the models B-2, B-4 and B-6 in evaluating the total sediment yield for the study area as the average *ARE* value for these models is about 30%. The models B-5 and B-7 with an average *ARE* value of around 37% have performed better in comparison to other models for which the average *ARE* values are more than 42%. As far as the simulation of time to peak is concerned the model B-6 yielded the minimum value of average *ARE* that is 39.93%. However the best performance in simulating the base time of the sediment graphs was obtained by the model B-2 giving an average *ARE* value of 28.3%. Although the average *ARE* values in simulating peak value and time to peak are on higher side even for the best models for the study area, the respective best performing models stated above can be regarded as fitting well in the light of the permissible error in sediment prediction by the models available in the literature (Williams, 1978; Chen, 1986 and Kothyari, 1996).

Table 5.15 Storm-wise estimated values of Absolute Relative Error for developed models

Model A. Sediment graphs based on hydrological data												
Storm	Sediment yield (tonne)			Peak value (tonne/day)			Time to peak (h)			Base time (h)		
	Observed	Predicted	RE (%)	Observed	Predicted	RE (%)	Observed	Predicted	RE (%)	Observed	Predicted	RE (%)
April 14,71	51.417	39.482	23.20	699.017	1030.144	-47.37	4.0	4.00	0.00	13.5	13.50	0.00
Nov. 3,72	12.380	14.753	-19.17	164.770	351.170	-113.09	5.0	3.75	25.00	15.0	14.50	3.33
July 18,74	7.421	5.220	29.66	112.411	136.197	-21.16	2.0	3.75	-87.50	14.0	13.25	5.36
April 23,75	31.742	10.735	66.18	403.563	147.427	63.47	3.0	4.00	-33.33	10.0	14.50	-45.00
July 22,76	39.513	20.918	47.06	777.310	545.786	29.79	1.5	4.00	-166.67	7.5	13.50	-80.00
April 29,80	36.742	26.866	26.88	342.022	505.518	-47.81	7.0	4.00	42.86	31.0	14.00	54.84
April 25,83	28.718	11.198	61.01	154.782	218.885	-41.42	5.0	2.75	45.00	13.5	15.00	-11.11
April 6,97	7.598	3.701	51.29	103.315	47.788	53.75	8.0	4.25	46.88	23.5	14.75	37.23
Average			35.76			-15.48			-15.97			-4.42
Av. ARE			40.56			52.23			55.90			29.61
Model B. Sediment graphs based on watershed characteristics												
Model B-1(Z=0.110, x=0.162, SMD)												
Storm	Sediment yield (tonne)			Peak value (tonne/day)			Time to peak (h)			Base time (h)		
	Observed	Predicted	RE (%)	Observed	Predicted	RE (%)	Observed	Predicted	RE (%)	Observed	Predicted	RE (%)
April 14,71	51.407	47.398	7.80	699.02	435.297	37.73	4.0	2.50	37.50	13.5	18.50	-37.04
Nov. 3,72	12.38	17.695	-42.93	164.80	153.062	7.12	5.0	2.25	55.00	15.0	17.75	-18.33
July 18,74	7.421	6.260	15.64	112.41	57.551	48.80	2.0	2.25	-12.50	14.0	16.25	-16.07
April 23,75	31.742	12.887	59.40	403.56	110.083	72.72	3.0	3.50	-16.67	10.0	18.00	-80.00
July 22,76	39.512	25.112	36.44	777.31	230.627	70.33	1.5	2.50	-66.67	7.5	18.00	-140.00
April 29,80	36.742	32.252	12.22	342.00	295.012	13.74	7.0	3.00	57.14	31.0	18.50	-40.32
April 25,83	28.718	13.432	53.23	154.78	115.139	25.61	5.0	2.75	45.00	13.5	17.50	-29.63
April 6,97	7.598	4.439	41.58	103.32	38.219	63.01	8.0	3.25	59.38	23.5	16.50	29.79
Average			22.92			42.38			19.77			-41.46
Av. ARE			33.66			42.38			43.73			48.90
Model B-2 (Z=0.110, x=0.162, NSMD)												
Storm	Sediment yield (tonne)			Peak value (tonne/day)			Time to peak (h)			Base time (h)		
	Observed	Predicted	RE (%)	Observed	Predicted	RE (%)	Observed	Predicted	RE (%)	Observed	Predicted	RE (%)
April 14,71	51.407	45.609	11.28	699.02	418.867	40.08	4.0	2.50	37.50	13.5	13.50	0.00
Nov. 3,72	12.38	24.877	-100.95	164.80	227.699	-38.17	5.0	3.00	40.00	15.0	13.25	11.67
July 18,74	7.421	6.260	15.64	112.41	57.551	48.80	2.0	2.25	-12.50	14.0	11.00	21.43
April 23,75	31.742	26.298	17.15	403.56	209.285	48.14	3.0	3.50	-16.67	10.0	13.75	-37.50
July 22,76	39.512	25.112	36.44	777.31	230.627	70.33	1.5	2.50	-66.67	7.5	13.00	-73.33
April 29,80	36.742	48.605	-32.29	342.00	444.874	-30.08	7.0	3.00	57.14	31.0	14.00	54.84
April 25,83	28.718	27.749	3.38	154.78	246.387	-59.18	5.0	3.25	35.00	13.5	13.50	0.00
April 6,97	7.598	9.533	-25.47	103.32	87.253	15.55	8.0	2.75	65.63	23.5	17.00	27.66
Average			-9.35			11.93			17.43			0.60
Av. ARE			30.32			43.79			41.39			28.30
Model B-3 (Z=0.110, x=0.000, SMD)												
Storm	Sediment yield (tonne)			Peak value (tonne/day)			Time to peak (h)			Base time (h)		
	Observed	Predicted	RE (%)	Observed	Predicted	RE (%)	Observed	Predicted	RE (%)	Observed	Predicted	RE (%)
April 14,71	51.407	47.398	7.80	699.02	406.260	41.88	4.0	3.00	25.00	13.5	19.50	-44.44
Nov. 3,72	12.38	17.697	-42.95	164.80	143.548	12.90	5.0	2.75	45.00	15.0	19.00	-26.67
July 18,74	7.421	6.261	15.63	112.41	53.712	52.22	2.0	2.75	-37.50	14.0	18.25	-30.36
April 23,75	31.742	12.887	59.40	403.56	103.521	74.35	3.0	3.50	-16.67	10.0	19.50	-95.00
July 22,76	39.512	25.112	36.44	777.31	215.243	72.31	1.5	3.00	-100.00	7.5	19.25	-156.67
April 29,80	36.742	32.252	12.22	342.00	273.768	19.95	7.0	3.00	57.14	31.0	19.50	37.10
April 25,83	28.718	13.434	53.22	154.78	107.186	30.75	5.0	2.75	45.00	13.5	19.00	-40.74
April 6,97	7.598	4.440	41.56	103.32	35.884	65.27	8.0	3.25	59.38	23.5	18.50	21.28
Average			22.92			46.20			9.67			-41.94
Av. ARE			33.65			46.20			48.21			56.53
Model B-4 (Z=0.110, x=0.000, NSMD)												
Storm	Sediment yield (tonne)			Peak value (tonne/day)			Time to peak (h)			Base time (h)		
	Observed	Predicted	RE (%)	Observed	Predicted	RE (%)	Observed	Predicted	RE (%)	Observed	Predicted	RE (%)
April 14,71	51.407	45.590	11.32	699.02	390.926	44.07	4.0	3.00	25.00	13.5	19.50	-44.44
Nov. 3,72	12.38	24.877	-100.95	164.80	210.682	-27.84	5.0	3.00	40.00	15.0	19.50	-30.00
July 18,74	7.421	6.261	15.63	112.41	53.712	52.22	2.0	2.75	-37.50	14.0	18.25	-30.36
April 23,75	31.742	26.298	17.15	403.56	195.048	51.67	3.0	4.00	-33.33	10.0	20.25	-102.50
July 22,76	39.512	25.112	36.44	777.31	215.243	72.31	1.5	3.00	-100.00	7.5	19.25	-156.67
April 29,80	36.742	48.605	-32.29	342.00	411.627	-20.36	7.0	3.00	57.14	31.0	19.75	36.29
April 25,83	28.718	27.749	3.38	154.78	229.995	-48.59	5.0	3.25	35.00	13.5	19.75	-46.30
April 6,97	7.598	9.533	-25.47	103.32	80.732	21.86	8.0	3.00	62.50	23.5	19.00	19.15
Average			-9.35			18.17			6.10			-44.35
Av. ARE			30.33			42.37			48.81			49.14

Continued Table 5.15

Model B-5 (Z=2.020, x=0.162, SMD)												
Storm	Sediment yield (tonne)			Peak value (tonne/day)			Time to peak (h)			Base time (h)		
	Observed	Predicted	RE (%)	Observed	Predicted	RE (%)	Observed	Predicted	RE (%)	Observed	Predicted	RE (%)
April 14,71	51.407	48.270	6.10	699.02	494.101	29.31	4.0	2.50	37.50	13.5	8.25	38.89
Nov. 3,72	12.38	17.712	-43.07	164.80	179.516	-8.93	5.0	2.25	55.00	15.0	8.25	45.00
July 18,74	7.421	6.266	15.56	112.41	65.326	41.89	2.0	2.25	-12.50	14.0	7.25	48.21
April 23,75	31.742	13.124	58.65	403.56	127.813	68.33	3.0	2.50	16.67	10.0	8.50	15.00
July 22,76	39.512	25.574	35.28	777.31	261.782	66.32	1.5	2.50	-66.67	7.5	8.00	-6.67
April 29,80	36.742	32.847	10.60	342.00	315.703	7.69	7.0	3.00	57.14	31.0	8.50	72.58
April 25,83	28.718	13.445	53.18	154.78	134.721	12.96	5.0	2.50	50.00	13.5	8.25	38.89
April 6,97	7.598	4.444	41.51	103.32	42.071	59.28	8.0	2.25	71.88	23.5	8.00	65.96
Average			22.23			34.61			26.13			39.73
Av. ARE			32.99			36.84			45.92			41.40

Model B-6 (Z=2.020, x=0.162, NSMD)												
Storm	Sediment yield (tonne)			Peak value (tonne/day)			Time to peak (h)			Base time (h)		
	Observed	Predicted	RE (%)	Observed	Predicted	RE (%)	Observed	Predicted	RE (%)	Observed	Predicted	RE (%)
April 14,71	51.407	47.396	7.80	699.02	494.101	29.31	4.0	2.50	37.50	13.5	8.25	38.89
Nov. 3,72	12.38	25.030	-102.18	164.80	246.036	-49.29	5.0	3.00	40.00	15.0	8.50	43.33
July 18,74	7.421	6.266	15.56	112.41	65.326	41.89	2.0	2.25	-12.50	14.0	7.25	48.21
April 23,75	31.742	26.378	16.90	403.56	250.930	37.82	3.0	3.00	0.00	10.0	9.25	7.50
July 22,76	39.512	25.111	36.45	777.31	261.782	66.32	1.5	2.50	-66.67	7.5	8.00	-6.67
April 29,80	36.742	48.902	-33.10	342.00	480.700	-40.56	7.0	3.00	57.14	31.0	8.75	71.77
April 25,83	28.718	27.884	2.90	154.78	267.155	-72.60	5.0	3.00	40.00	13.5	8.75	35.19
April 6,97	7.598	9.591	-26.23	103.32	94.279	8.75	8.0	2.75	65.63	23.5	7.75	67.02
Average			-10.24			2.71			20.14			38.16
Av. ARE			30.14			43.32			39.93			39.82

Model B-7 (Z=2.020, x=0.000, SMD)												
Storm	Sediment yield (tonne)			Peak value (tonne/day)			Time to peak (h)			Base time (h)		
	Observed	Predicted	RE (%)	Observed	Predicted	RE (%)	Observed	Predicted	RE (%)	Observed	Predicted	RE (%)
April 14,71	51.407	47.402	7.79	699.02	492.114	29.60	4.0	2.00	50.00	13.5	8.00	40.74
Nov. 3,72	12.38	17.288	-39.64	164.80	178.661	-8.41	5.0	1.75	65.00	15.0	8.00	46.67
July 18,74	7.421	6.116	17.59	112.41	65.063	42.12	2.0	1.75	12.50	14.0	7.00	50.00
April 23,75	31.742	12.888	59.40	403.56	126.845	68.57	3.0	2.00	33.33	10.0	8.25	17.50
July 22,76	39.512	25.114	36.44	777.31	260.729	66.46	1.5	2.00	-33.33	7.5	7.75	-3.33
April 29,80	36.742	32.255	12.21	342.00	315.385	7.78	7.0	2.50	64.29	31.0	8.25	73.39
April 25,83	28.718	13.123	54.30	154.78	134.216	13.29	5.0	2.00	60.00	13.5	8.00	40.74
April 6,97	7.598	4.337	42.92	103.32	41.770	59.57	8.0	2.00	75.00	23.5	7.75	67.02
Average			23.88			34.87			40.85			41.59
Av. ARE			33.79			36.91			49.18			42.42

Model B-8 (Z=2.020, x=0.000, NSMD)												
Storm	Sediment yield (tonne)			Peak value (tonne/day)			Time to peak (h)			Base time (h)		
	Observed	Predicted	RE (%)	Observed	Predicted	RE (%)	Observed	Predicted	RE (%)	Observed	Predicted	RE (%)
April 14,71	51.407	47.402	7.79	699.02	492.114	29.60	4.0	2.00	50.00	13.5	8.00	40.74
Nov. 3,72	12.38	25.043	-102.29	164.80	245.663	-49.07	5.0	2.50	50.00	15.0	8.00	46.67
July 18,74	7.421	6.116	17.58	112.41	65.063	42.12	2.0	1.75	12.50	14.0	7.00	50.00
April 23,75	31.742	26.387	16.87	403.56	249.799	38.10	3.0	2.50	16.67	10.0	9.00	10.00
July 22,76	39.512	25.114	36.44	777.31	260.729	66.46	1.5	2.00	-33.33	7.5	7.75	-3.33
April 29,80	36.742	48.929	-33.17	342.00	479.972	-40.34	7.0	2.50	64.29	31.0	8.50	72.58
April 25,83	28.718	27.897	2.86	154.78	266.781	-72.36	5.0	2.50	50.00	13.5	8.25	38.89
April 6,97	7.598	9.596	-26.30	103.32	94.137	8.88	8.0	2.50	68.75	23.5	8.00	65.96
Average			-10.03			2.92			34.86			40.19
Av. ARE			30.41			43.37			43.19			41.02

5.3.2.2 Coefficient of efficiency (CE)

The Eq. (4.104) was applied for assessing the efficiency of the present models during different storm events and the results are shown in Table 5.16. Since the prediction models with the parameter Z as 2.020 have yielded higher and more number of negative values of CE , it represents a lower ability of these models in the simulation of sediment

graphs as compared to the models with Z equal to 0.110. The average values of CE are low due to the effect of negatives values, whereas the average values of CE considering only positive values for models B-4, B-2, B-3 and B-1 (shown as per priority) are nearer to the level of acceptable simulation of 60 % (Chiew *et al.*, 1993).

Table 5.16 Coefficient of Efficiency (CE) values for different sediment graph models

Storm	Model A	Model B-1	Model B-2	Model B-3	Model B-4	Model B-5	Model B-6	Model B-7	Model B-8
April 14,71	74.47	35.35	36.17	50.45	50.72	-62.12	-61.52	-92.71	-92.71
Nov. 3,72	-122.59	-96.28	-89.77	-73.86	-132.24	-239.67	-446.13	-255.18	-489.69
July 18,74	-78.40	60.32	60.32	53.13	53.13	84.11	84.11	62.87	63.52
April 23,75	31.42	54.06	72.50	59.30	73.79	41.53	87.12	26.60	72.93
July 22,76	25.95	49.13	49.13	55.09	56.36	36.37	36.21	48.13	48.13
April 29,80	-127.51	-92.68	-207.08	-78.29	-178.98	-140.20	-299.22	-139.97	-301.32
April 25,83	-32.30	-39.92	-67.33	-9.14	-11.76	-112.72	-277.36	-131.67	-329.12
April 6,97	60.64	32.99	-100.71	43.44	-54.79	-30.86	-339.04	-63.95	-411.51
Average	-21.04	0.37	-30.85	12.52	-17.97	-52.95	-151.98	-68.24	-179.97

5.3.2.3 Integral square error (ISE)

The integral square error (ISE) criterion, Eq. (4.105), was also used for quantitative comparison of the observed and the predicted sediment graphs and obtained results are tabulated in Table 5.17.

A close scrutiny of Table 5.17 reveals that if 40% error is taken as the permissible limit for sediment yield predictions, then all the developed models can be said performing satisfactorily but models B-3 and B-1 with average values of ISE as 25.13 and 25.64 certainly have shown better performing ability to simulate the observed sediment graphs for the study area.

Table 5.17 Integral Square Error (ISE) values for different sediment graph models

Storm	Model A	Model B-1	Model B-2	Model B-3	Model B-4	Model B-5	Model B-6	Model B-7	Model B-8
April 14,71	12.97	21.59	21.45	20.33	20.27	32.69	32.63	35.65	35.65
Nov. 3,72	37.63	35.33	42.93	32.91	39.62	46.48	58.94	47.53	61.24
July 18,74	38.28	17.86	17.86	19.19	19.19	11.42	11.42	17.46	17.46
April 23,75	25.98	20.17	16.66	20.78	17.70	18.37	8.62	2.58	12.5
July 22,76	42.62	35.78	35.78	36.05	36.05	26.85	26.88	24.24	24.24
April 29,80	33.02	30.39	38.36	29.23	36.56	33.93	43.74	33.91	43.85
April 25,83	16.94	17.13	19.68	16.41	17.90	21.12	28.13	22.04	29.99
April 6,97	22.06	26.87	48.17	26.16	45.19	36.63	67.10	41.00	72.43
Average	28.69	25.64	30.11	25.13	29.06	28.44	34.68	28.05	37.17

5.3.2.4 Relative square error (RSE)

For further evaluation of models' performance, the goodness of fit of a predicted sediment graph to an observed one was determined by *RSE* (Eq. 4.106) and the results are presented in Table 5.18. If *RSE* is zero, the predicted graph will coincide with the observed one.

It is clear from the table that models B-3 and B-1 have better performing capability in predicting storm wise sediment yield for the study area in view of the lower *RSE* values. Based on this criterion the developed sediment yield prediction models can be performance wise prioritized in the order of B-3, B-1, A, B-4, B-5, B-2, B-7, B-6 and B-8.

Table 5.18 *Relative Square Error (RSE) values for different sediment graph models*

Storm	Model A	Model B-1	Model B-2	Model B-3	Model B-4	Model B-5	Model B-6	Model B-7	Model B-8
April 14,71	0.20	0.55	0.55	0.49	0.49	1.27	1.27	1.51	1.51
Nov. 3,72	1.77	1.56	2.30	1.35	1.96	2.70	4.34	2.82	4.69
July 18,74	1.44	0.31	0.31	0.36	0.36	0.13	0.13	0.30	0.30
April 23,75	0.82	0.50	0.34	0.53	0.38	0.41	0.09	0.52	0.19
July 22,76	1.25	0.88	0.88	0.89	0.89	0.50	0.50	0.40	0.40
April 29,80	1.95	1.65	2.64	1.53	2.40	2.06	3.43	2.06	3.45
April 25,83	0.73	0.75	0.99	0.69	0.82	1.14	2.02	1.24	2.30
April 6,97	0.39	0.59	1.88	0.55	1.65	1.09	3.65	1.36	4.25
Average	1.07	0.85	1.24	0.80	1.12	1.16	1.93	1.28	2.14

5.3.2.5 Root mean square error (RMSE)

The values of *RMSE*, determined by using Eq. (4.107) and listed in Table 5.19 verifies that the models B-1 to B-4 and the model A with average value within a range of 9.20 to 10.70 performing better in comparison to other models. However, based on this criterion, the model B-3 with the least value of *RMSE* is the most efficient model for the study area.

Table 5.19 *Root Mean Square Error (RMSE) values for different sediment graph models*

Storm	Model A	Model B-1	Model B-2	Model B-3	Model B-4	Model B-5	Model B-6	Model B-7	Model B-8
April 14,71	11.64	18.06	17.95	15.20	15.16	29.34	29.28	31.98	31.98
Nov. 3,72	7.33	6.88	8.36	6.52	7.36	9.06	11.48	9.26	11.93
July 18,74	4.87	2.31	2.31	2.53	2.53	1.45	1.45	2.22	2.22
April 23,75	13.42	11.18	8.46	10.21	8.05	13.65	6.41	15.29	9.29
July 22,76	29.39	24.23	24.23	21.71	21.71	32.85	32.89	29.66	29.66
April 29,80	9.17	9.17	10.65	8.12	10.16	9.42	12.15	9.42	12.18
April 25,83	8.34	8.56	9.36	7.54	7.59	10.59	14.10	11.05	15.03
April 6,97	1.44	1.96	3.32	1.73	2.79	2.78	5.10	3.12	5.50
Average	10.70	10.29	10.58	9.20	9.42	13.64	14.11	14.00	14.72

5.3.2.6 Ratio of error (REO)

The ratio of mean error to the mean observed output of the models (*REO*), was also used for quantitative comparison of developed models. The calculations for the determination of ratio of error (*REO*) were made by using Eq. (4.108) and the corresponding results are presented in Table 5.20.

A critical analysis of results shows that the models B-3 and B-1 have had the best performance with the smallest respective absolute values of *REO* as 0.20 and 0.21, while the other models except B-8 with little higher values stand in the next priority list.

Table 5.20 Ratio of Error (*REO*) values for different sediment graph models

Storm	Model A	Model B-1	Model B-2	Model B-3	Model B-4	Model B-5	Model B-6	Model B-7	Model B-8
April 14,71	-0.23	-0.06	-0.08	-0.05	-0.08	-0.06	-0.08	-0.08	-0.08
Nov. 3,72	0.19	0.35	0.83	0.34	0.78	0.43	1.02	0.40	1.02
July 18,74	-0.30	-0.14	-0.14	-0.12	-0.12	-0.16	-0.16	-0.18	-0.18
April 23,75	-0.46	-0.33	-0.09	-0.31	-0.09	-0.59	-0.17	-0.59	-0.17
July 22,76	-0.27	-0.15	-0.15	-0.14	-0.14	-0.33	-0.34	-0.35	-0.35
April 29,80	-0.27	-0.12	0.32	-0.12	0.32	-0.11	0.33	-0.12	0.33
April 25,83	-0.55	-0.41	-0.02	-0.38	-0.02	-0.53	-0.03	-0.54	-0.03
April 6,97	-0.02	0.12	1.03	0.11	0.93	0.17	1.52	0.14	1.53
Average	-0.24	-0.09	0.21	-0.08	0.20	-0.15	0.26	-0.17	0.26
Abs. Ave.	0.29	0.21	0.33	0.20	0.31	0.30	0.37	0.30	0.46

As can be observed from the table, simulation of sediment graph by all the developed models has yielded negative values of *REO* for all the storm events barring a few of them in the present study, which clearly confirms that all the developed models under predict the sediment yield in comparison to the respective observed sediment graph. This can be seen from the Figs. 5.4 to 5.11.

5.3.2.7 Bias in sediment yield (B_s)

Bias in prediction of sediment yield by various developed models was estimated as per the procedure already explained under Article 4.3.2.7. The frequently the biases are close to unity, the better the model estimates sediment yield. The results of application of the aforesaid equation are presented in Table 5.21.

Table 5.21 Bias (B_s) values for different sediment graph models

Storm	Model A	Model B-1	Model B-2	Model B-3	Model B-4	Model B-5	Model B-6	Model B-7	Model B-8
April 14,71	0.77	0.92	0.89	0.92	0.89	0.94	0.92	0.92	0.92
Nov. 3,72	1.19	1.43	2.01	1.43	2.01	1.43	2.02	1.40	2.02
July 18,74	0.70	0.84	0.84	0.84	0.84	0.84	0.84	0.82	0.82
April 23,75	0.34	0.41	0.83	0.41	0.83	0.41	0.83	0.41	0.83
July 22,76	0.53	0.64	0.64	0.64	0.64	0.65	0.64	0.64	0.64
April 29,80	0.73	0.88	1.32	0.88	1.32	0.89	1.33	0.88	1.33
April 25,83	0.39	0.47	0.97	0.47	0.97	0.47	0.97	0.46	0.97
April 6,97	0.49	0.58	1.25	0.58	1.25	0.58	1.26	0.57	1.26
Average	0.64	0.77	1.09	0.77	1.09	0.78	1.10	0.76	1.10

It is seen from the table that the models B-2 and B-4, due to having the closest value of 1.09 to the unity have the least bias from the observed sediment yield. Whereas, the maximum deviation in sediment yield prediction is evident in the case of model A with a bias of 0.64. The critical examination of the table further reveals that model B-1 and B-3 have yielded exactly the same B_s values for all the storms, which clearly conforms the same degree of accuracy of these two models in predicting sediment yield for the Anameh watershed. The overlapping of the predicted sediment graphs by these two models in Figs. 5.4 to 5.11 also confirm the above statement. The similar trend can also be observed in case of models B-2 and B-4 as well as B-6 and B-8.

5.4 Comparison of Models' Performance

As discussed earlier, nine models were developed for the prediction of sediment graphs for the Anameh watershed, among which the best performing model or models, based on the performance evaluation criteria employed in the study had to be distinguished. Since the performance of models was a little different from criterion to criterion, a method of *factorial scoring* has been employed to find out the best performing model for the study area. With this in view, the results of the models' performance by using each evaluation criterion for all the storm events are summarized in the Table 5.22. The variation of each of the evaluation parameters were determined by subtracting the least value from the highest one estimated for all of the developed models. The variation

was then divided by the total number of models (in this case nine) to classify the values of a particular parameter obtained by all models. Thereafter, each of the models was assigned a score depending upon the number of the class in which the corresponding value of the parameter falls. That means the scoring was started by allotting the least score to the best performing model based on the parameter under consideration. Since each class contained a range of values, in some cases more than one models lie in the same class and in some cases not even a single model falls in a particular class. The scores got by a particular model considering all the evaluation parameters were then summed up and the model with the least total score considered as the best performing model. For better understanding of the reader let's consider the first row of the Table 5.22, which shows that the *ARE* values for different models vary from 30.14 to 40.56. Thus the range of each class is approximately 1.158 resulting from $(40.56-30.14)/9$. Therefore nine classes viz. 30.14-31.30, 31.30-32.46, 32.46-33.61, 33.61-34.77, 34.77-35.93, 35.93-37.09, 37.09-38.24, 38.24-39.40, 39.40-40.56 are obtained. It can be seen that *ARE* values in respect of four models B-2, B-4, B-6 and B-8 fall in the first class and as such each of them has been assigned score of one. The details of procedure and necessary information are given in Table 5.22.

From the table, it can be seen that the models B-1 and B-2 are having almost the same score and thus any of them can be applied efficiently for the prediction of sediment graph in the Amameh watershed. However, model B-2 with least score of 28 can be regarded as the best performing model and is therefore recommended for sediment graph prediction for the study area.

A comparative assessment was also made for point-wise evaluation of sediment graphs by using the *Coefficient of Determination* (R^2) in respect of total sediment yield

Table 5.22 Summary of prediction performance of different sediment graph models using factorial scoring for Amameh watershed.

Models Parameters	Average USG Model A	Parameter Z=0.110						Parameter Z=2.020					
		x=0.162			x=0.000			x=0.162			x=0.000		
		S.M.D.	N.S.M.D.	S.M.D.	S.M.D.	N.S.M.D.	S.M.D.	S.M.D.	N.S.M.D.	S.M.D.	S.M.D.	N.S.M.D.	S.M.D.
		Model B-1	Model B-2	Model B-3	Model B-4	Model B-5	Model B-6	Model B-7	Model B-8	Model B-9	Model B-10	Model B-11	Model B-12
ARE (Total yield)	40.56 (9)	33.66 (4)	30.32 (1)	33.65 (4)	30.33 (1)	32.99 (3)	30.14 (1)	33.79 (4)	30.41 (1)				
ARE (Peak rate)	52.23 (9)	42.38 (4)	43.79 (5)	46.20 (6)	42.37 (4)	36.84 (1)	43.32 (4)	36.91 (1)	43.37 (4)				
ARE (Peak time)	55.90 (9)	43.73 (3)	41.39 (1)	48.21 (5)	48.81 (6)	45.92 (4)	39.93 (1)	49.18 (6)	43.19 (2)				
ARE (Base time)	29.61 (1)	48.90 (7)	28.30 (1)	56.53 (9)	49.14 (7)	41.40 (5)	39.82 (4)	42.42 (5)	41.02 (5)				
CE	-21.04 (2)	0.37 (1)	-30.85 (3)	12.52 (1)	-17.97 (2)	-52.95 (4)	-151.98 (8)	-68.24 (4)	-179.97 (9)				
ISE	28.69 (3)	25.64 (1)	30.11 (4)	25.13 (1)	29.06 (3)	28.44 (3)	34.68 (8)	28.05 (3)	37.17 (9)				
RSE	1.07 (2)	0.85 (1)	1.24 (3)	0.80 (1)	1.12 (3)	1.16 (3)	1.93 (8)	1.28 (4)	2.14 (9)				
RMSE	10.70 (3)	10.29 (2)	10.58 (3)	9.20 (1)	9.42 (1)	13.64 (8)	14.11 (9)	14.00 (8)	14.72 (9)				
REO	0.29 (4)	0.21 (1)	0.33 (5)	0.20 (1)	0.31 (4)	0.30 (4)	0.37 (6)	0.30 (4)	0.46 (9)				
B _s	0.64 (7)	0.77 (5)	1.09 (2)	0.77 (5)	1.09 (2)	0.78 (5)	1.10 (2)	0.76 (5)	1.10 (2)				
Sum of score	49	29	28	34	33	40	51	44	59				

Note: Figures shown in parentheses represent the score of model for a particular performance evaluation criterion.

and peak flow rate obtained by using various developed models. Different types of regression models such as linear, logarithmic, polynomial, power and exponential were tried to get the best fit between observed and predicted sediment yield and peak sediment flow rate by different developed models. Since the polynomial regression models with order more than two did not improve their performance, the model with order two has been considered in this study. The coefficients of determination (R^2) between observed and predicted sediment yield as well as peak sediment flow rate values obtained for all the nine models are presented respectively in Table 5.23a and 5.23b.

Table 5.23a *Coefficient of determination (R^2) values between observed and predicted total sediment yield by using various regression equations*

Regression Model	R^2 values for various sediment graph model								
	A	B-1	B-2	B-3	B-4	B-5	B-6	B-7	B-8
Linear	0.740	0.741	0.697	0.741	0.696	0.744	0.704	0.745	0.704
Logarithmic	0.612	0.612	0.712	0.612	0.712	0.614	0.710	0.614	0.710
Polynomial (2)	0.849	0.849	0.701	0.849	0.701	0.852	0.706	0.853	0.706
Power	0.749	0.749	0.787	0.749	0.787	0.753	0.787	0.754	0.785
Exponential	0.763	0.763	0.693	0.763	0.693	0.767	0.698	0.769	0.696
Max. R^2	0.849	0.849	0.787	0.849	0.787	0.852	0.787	0.853	0.785

Table 5.23b *Coefficient of determination (R^2) values between observed and predicted sediment peak by using various regression equations*

Regression model	R^2 values for various sediment graph model								
	A	B-1	B-2	B-3	B-4	B-5	B-6	B-7	B-8
Linear	0.596	0.564	0.288	0.565	0.293	0.577	0.341	0.576	0.339
Logarithmic	0.581	0.614	0.433	0.616	0.438	0.622	0.491	0.621	0.489
Polynomial (2)	0.598	0.613	0.566	0.614	0.568	0.618	0.615	0.618	0.614
Power	0.585	0.681	0.488	0.683	0.492	0.681	0.532	0.680	0.531
Exponential	0.523	0.563	0.323	0.565	0.327	0.563	0.360	0.561	0.358
Max. R^2	0.598	0.681	0.566	0.683	0.568	0.681	0.615	0.680	0.614

It is seen from the Tables 5.23a and 5.23b that for the sediment graphs predicted by using models based on considering sediment mobilized distribution (B-1, B-3, B-5 and B-7) the polynomial and power regression models have performed better than other types of models for the prediction of total sediment yield and peak sediment flow rate, respectively. Whereas the situation is just the reverse in the case of the sediment graphs predicted by using models, which are based on not considering sediment mobilized distribution (B-2, B-4, B-6 and B-8). However, the polynomial regression model has performed better than other models in regressing the observed total sediment yield as well as peak sediment flow

rate with respective predicted values obtained by model A. All the values of coefficients of determination for the polynomial and power regression for all the developed models are statistically significant at level of 5 %.

As already explained earlier the performance of the models B-1 and B-2 based on the factorial scoring for the prediction of sediment graphs in the Amameh watershed is almost identical. However, the model B-2 with lowest score of 28 has been regarded as the best performing model for the watershed. Now, since the coefficient of determination in case of model B-1 is more than model B-2 in both the cases of sediment yield and peak sediment flow rate prediction, the *student t* test (*t distribution*) has been performed to establish the most suitable one between these two models for the study watershed. The results of *t* distribution analysis showed that in spite of the difference in R^2 values for the models B-1 and B-2, the mean values of their prediction on sediment yield and sediment peak flow rate for all the storms under considerations are not statistically different (Null hypothesis was accepted), which also conforms with the earlier statements. Therefore, it can now be concluded that the model B-2, i.e. model developed based on watershed characteristics with $x=0.162$, $Z=0.110$ and not considering sediment mobilized distribution (NSMD) stands in the top most rank of priority list and is recommended to be applied for prediction of sediment graph in the Amameh watershed.

Since based on factorial scoring and also the coefficient of determination the model B-2 was established as the best performing model, the following power and polynomial equations were also obtained to define the relationship between observed and predicted sediment yield and peak rate of sediment flow estimated by model B-2 for the Amameh watershed, respectively.

$$S_p = 1.797S_o^{0.819} \quad (r = 0.887) \quad \dots (5.1)$$

$$P_{sp} = -0.0016P_{so}^2 + 1.697P_{so} - 46.851 \quad (r = 0.752) \quad \dots (5.2)$$

where S_p and S_o are the predicted and the observed sediment yield in tonnes, and P_{sp} and P_{so} are the predicted and the observed peak rate of sediment flow in $t.day^{-1}$, respectively.

The graphical presentation of the developed equations are shown in Figs. 5.12 and 5.13.

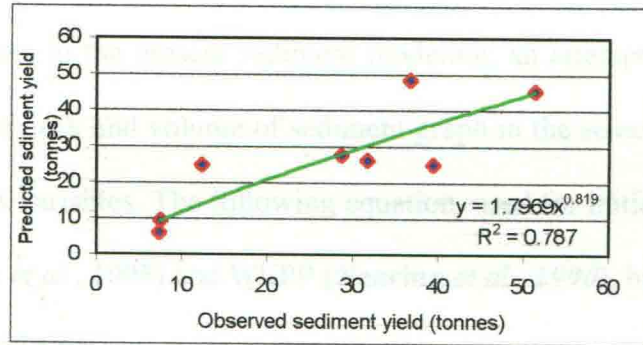


Fig. 5.12 Relationship between observed and predicted total sediment yield values

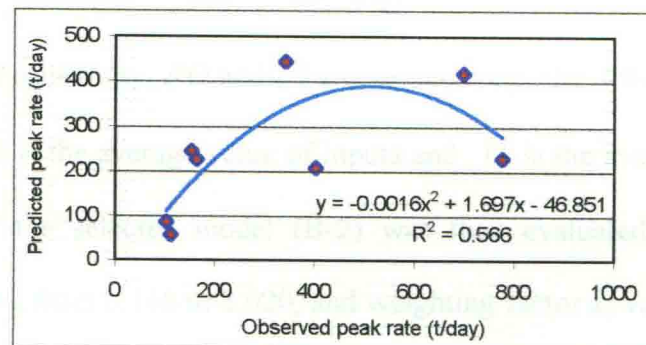


Fig. 5.13 Relationship between observed and predicted sediment peak values

To have a better understanding between the generated sediment and its peak rate, the following power equation with 91.7 % coefficient of determination and 0.210 standard error of estimate was developed between the sediment yield (Y_s) in tonnes and peak rate of sediment flow (Q_{sp}) in $tonnes.day^{-1}$ for the study area.

$$Q_{sp} = 20.238 Y_s^{0.8998} \quad (r=0.958) \quad \dots (5.3)$$

5.5 Sensitivity Analysis

Sensitivity is the rate of change in one factor with respect to change in another factor. Investigation of the sensitivity of model parameters to model performance is an

integral and a vital part of the modeling process (Overton and Meadows, 1976). Therefore, to assess the relative importance of the basic components and determine the level of accuracy in the estimation of parameters, the sensitivity analysis was conducted.

Since the parameter Z and weighting factor x were considered to be the two important parameters in the present sediment modeling, an attempt was made to analyze the susceptibility of peak and volume of sediment graph in the selected model (B-2) to the variations of these variables. The following equation, used for initial sensitivity testing of the WEPS (Hagen *et al.*, 1995) and WEPP (Nearing *et al.*, 1990), has been applied for the purpose in this study also:

$$R_S = \frac{\partial O}{\partial I} \frac{\bar{I}_i}{\bar{O}_i} \quad \dots(5.3)$$

where R_S is relative sensitivity, ∂O and ∂I are, respectively, the difference between output and input values, \bar{I}_i is the average value of inputs and \bar{O}_i is the average value of outputs. The sensitivity of the selected model (B-2) was then evaluated with respect to the parameter Z , varying from 0.110 to 2.020, and weighting factor x , varying from 0.000 and 0.162. The relative sensitivity values of the model to parameter Z for the estimation of volume and peak rate of sediment flow were found to be 0.00653 and 0.06493, respectively. Whereas the values of 0.00004 and 0.03627 were obtained, respectively, for volume and peak rate of sediment flow when sensitivity analysis on weighting factor (x) was performed. It, therefore, may be implied that the model B-2 is more sensitive to the parameter Z as compared to the weighting factor x . From the higher values of relative sensitivity, it can also be inferred that the susceptibility of peak rate of sediment flow is more than volume of sediment to the variation of both the parameters Z and weighting factor x .

Chapter Six

SUMMARY AND CONCLUSIONS

6. SUMMARY AND CONCLUSION

The knowledge of quality and quantity of the watershed outputs in terms of runoff and sediment is the basic requirement for comprehensive watershed management projects. The main objective for conducting the present study was to develop sediment yield models through which temporal and spatial distributions of the watershed sediment generated during a storm event could be estimated. The models were developed based on the easily accessible hydrological as well as physiographical data of the Amameh watershed in Iran comprising an area of 3712ha, as per the hypotheses detailed in chapter 4. The physiographical information of the watershed were explored by using the 1:50,000 scaled toposheet provided by the Geographical Organization of Iran. The watershed is located in an undulated mountainous area with elevations ranging from 1800 to 3868m above the mean sea level and having a very humid to humid climate. The annual precipitation of the watershed is 848.8mm which falls mostly during winter and early spring i.e. from November to May. The watershed is well equipped with hydrological instruments so as to be a representative watershed for the southern skirt of the Albourz mountain range since about the last 30 years. The available hydrological data viz. precipitation, runoff and sediment concentration from the beginning till 1997 were obtained from the archives of the authorized organizations and pre-requisite analyses were performed before subjecting to the modeling processes. The data were analyzed on personnel computer with the help of different computer packages viz. *Excel*, *Eureka*, *Curve Expert*, *STATISTICA* and *StatView* and other developed computer programs in *Fortran language*.

The spatial distribution of sediment yield within the watershed was estimated with the help of a sediment routing sub-model. The storm-wise temporal distribution of

sediment yield was predicted by using two different approaches, one based on the hydrological data and the other on watershed characteristics.

To accomplish the objectives explained above, first of all an appropriate discharge rating curve was developed by using the available discharge-stage data. The discharge-stage relationship was then used for the estimation of associated discharge values for the stages for which the values of flow discharge were not available. Different precipitation-runoff relationships were investigated for their capability to estimate excess runoff in the study watershed. Close relationships were established between maximum storage index coefficient (*MSIC*) and Curve Number (*CN*), as well as *MSIC* and depth of precipitation in mm (*P*) with a correlation coefficient of 82 % in each case. However, the following multiple regression equation was found as the most appropriate relationship for the estimation of *MSIC* amongst the many other equations developed for the watershed:

$$MSIC = -0.881 + 0.013CN + 0.015P \quad (r=0.952) \quad \dots(6.1)$$

The runoff volume Q in m^3 was then related to the *MSIC* by using a logarithmic regression and the following equation was selected with the highest value of correlation coefficient,

$$Q = 123988 + 49746.194 \ln(MSIC) \quad (r=0.821) \quad \dots(6.2)$$

subject to $0.014CN + 0.016P > 1$

Different types of relationship were also developed between peak runoff, q_p in s^{-1} versus runoff volume, Q in m^3 out of which the following equation was found to fit better than others in the Amameh watershed,

$$q_p = 0.0009Q^{0.7627} \quad (r=0.803) \quad \dots(6.3)$$

The verification of various precipitation-runoff models strongly showed that the modified SCS curve number method developed by introducing the concept of recessive

equations is more reliable and efficient than other precipitation-runoff relationships for the estimation of runoff in the Amameh watershed.

From the sediment rating curve (SRC) that is the plot of runoff discharge on the abscissa and sediment discharge on the ordinate (Fig. 4.9), it was observed that in most of the cases there were more than one value of sediment discharge for the same value of runoff discharge. On comparing with the respective storm hydrographs, it was found that the points falling above the fitted regression line of SRC belong to the rising limb of the hydrograph whereas the points below the line correspond to the falling limb of the hydrograph. With this in view, an attempt has been made to develop two separate regression equations for the sets of points falling respectively above and below the fitted regression line. The following two power equations corresponding to rising and falling limbs were obtained when the flow discharge (q) and the sediment discharge (S_d) are expressed in $\text{m}^3 \cdot \text{s}^{-1}$ and $\text{tonne} \cdot \text{day}^{-1}$, respectively. The equations were used to fill up the missed sediment data on the rising and falling limbs of the hydrograph and ultimately continuous observed sediment graphs were obtained.

$$\text{Rising limb:} \quad S_d = 16.41q^{1.8424} \quad (R^2=0.892) \quad \dots(6.4)$$

$$\text{Falling limb:} \quad S_d = 2.84q^{2.0519} \quad (R^2=0.880) \quad \dots(6.5)$$

Different annual and storm-wise models viz. USLE (Wischmeier and Smith, 1965), Hudson's method (Hudson, 1981), EUSLE (Nicks *et al.*, 1994), AOF (Onstead and Foster, 1975), Time Area Method (Kothyari *et al.*, 1994), MUSLE for sediment (Williams, 1975), MUSLE for erosion (Nicks *et al.* 1994) and MUSLT (Nicks, 1994) were evaluated for their workability to estimate excess sediment. It was found that the MUSLE for sediment with a new power quotient works reasonably well for the prediction of sediment yield on storm basis on the Amameh watershed. Since the MUSLE for

sediment is recommended to be applied preferably for large storms, the following multiple regression equation was developed to determine the appropriate value of power quotient m of the MUSLE to quantify the magnitude of storms (large or small) for the study area:

$$m = -1.005 + 0.089 \ln(Q) + 0.078 \ln(q_p) \quad (r=0.982) \quad \dots (6.6)$$

where Q and q_p are the volume and peak rate of flow discharge in m^3 and $\text{m}^3 \cdot \text{s}^{-1}$, respectively. The storm is categorized as large or small if the value of m is respectively positive or negative. Thus, the original MUSLE was modified as shown below for the sediment yield (Y) prediction in the Amameh watershed by substituting the average of all the positive values of the power quotient m .

$$Y = 11.8(Q \cdot q_p)^{0.081} K.L.S.C.P \quad \dots (6.7)$$

subject to $0.089 \ln(Q) + 0.078 \ln(q_p) \geq 1$

where K, L, S, C and P are soil erodibility, topography, crop management and land management factors, respectively, which have been determined for different sub-watersheds and their weighted values have been considered as the representative value for the entire watershed.

The performance of the developed model (Eq. 6.7) for the estimation of sediment yield for the watershed was found to be satisfactory with an error of estimation of 19.40 % and mean ratio of the observed sediment values to the estimated ones as 1.29.

In fulfillment of the second objective, a new and a very novel approach, called as Reverse Routing Technique (RRT), has been introduced in this study for determination of partial contribution of each sub-watershed in generation of total runoff. By using this approach the outflow hydrographs at the outlet of each of the sub-watersheds can be obtained by proceeding upwards from the outlet and thus the runoff volume and peak rate of runoff for each sub-area could be determined. The applicability of RRT was verified by comparing the simulated hydrographs with the respective observed hydrographs for some

of the solved examples. The plausibility of this concept was also tested by comparing the thus hydrograph obtained for all the sub-watersheds draining to the Baghtangeh station located at the center of the watershed (Fig. 3.4) with the available recorded outflow hydrograph for the same station.

Having known runoff parameters (Q and q_p) besides other required factors such as soil erodibility (K), topography (LS), crop management (C), land management (P) and travel time (T) for each sub-watershed, which have already been determined earlier, the contribution of sediment yield individually from all the sub-watersheds in generation of total sediment yield from the watershed is estimated by a sediment routing sub-model. By knowing all the required parameters and factors, the following sediment routing model has been developed, which is found to be applicable on the Anameh watershed with a reasonable error of estimation of 21.90%,

$$Y = \sum_{i=1}^n Y_i e^{-2.022T_i} \quad \dots(6.8)$$

where Y_i represents the sediment yield from i^{th} sub-watershed estimated by Eq. (6.7), T_i is the travel time of sediment flow for the i^{th} sub-watershed and n represents the number of sub-watersheds.

Two different approaches based mainly on the hydrological data (model A) and the watershed characteristics (model B) were developed to predict temporal distribution of sediment yield (sediment graph) generated during a storm. In the first approach, all the available data of flow discharge and sediment discharge were analyzed to obtain the complete continuous sediment graphs as per the procedure explained under Article 4.1.1.2. The direct sediment graphs were then obtained by separating the base sediment flow from the total sediment graphs. Consequently, the unit sediment graphs (USG) with effective duration equal to the period of excess runoff were determined by using the same procedure

applied in derivation of the unit hydrograph. Since the time intervals of effective duration of available hyetographs were either 0.25h or 0.5h, the developed unit sediment graphs for different storms were then converted to 0.25-h and 0.5-h USGs and average USGs for these duration were obtained for the watershed. The direct sediment graph of a storm was then predicted with the help of superposition technique after multiplying the ordinates of appropriate T-h USG by the respective sediment mobilized for each time increment. The following equation was established between excess sediment or sediment mobilized (*ES*) in tonne and excess runoff or rainfall excess (*ER*) in mm:

$$ES = 8.486ER^{1.628} \quad (r=0.949) \quad \dots(6.9)$$

In the second approach for the development of sediment graphs based on the watershed characteristics, the instantaneous unit sediment graph (IUSG) is needed. To obtain the IUSG, the instantaneous unit hydrograph (IUH) and the sediment concentration are required. The various IUHs were obtained for different values of weighting factor (*x*) and time interval (Δt) as per the procedure explained under Article 4.2.1 in chapter 4. Since the average (master) unit hydrograph for the study watershed was derived for the effective duration of 0.5h, the obtained IUHs were also converted to 0.5-h UH to be compared with the average 0.5-h UH for evaluation of their reliability and reasonability. The results of comparison showed that the 0.5-h UH developed through the conversion of IUH with a weighting factor of 0.162 and a time interval of 0.5h gave the best overall fit for the measured average (master) 0.5-h UH. The sediment concentration values, required to be multiplied with corresponding ordinates of IUH, were estimated by using the dimensionless sediment concentration distribution (DSCD) graph (Fig. 4.23). To find the most appropriate value of parameter *Z*, an essential variable for obtaining DSCD graph, the different values of *Z* viz. 0.0187, 0.0885 and 0.1100, respectively obtained by Williams', Banasik's and modified methods and also *Z*=2.020, obtained for development

of sediment routing sub-model were tried in search of the most efficient sediment graph model for the study area. Thus, four IUSGs were obtained by multiplying the ordinates of the above IUH with corresponding sediment concentration values. The derived IUSGs were then converted into USGs and the respective direct sediment graphs were obtained. It was found that values of 0.0187 and 0.0885 underestimated the peak of sediment graphs for all the selected storms while the value of Z equal to 0.110 and 2.020 gave a balanced prediction and therefore found to be appropriate for the estimation of sediment concentration for the study area.

The time interval and the storage coefficient for all of the IUSG models were considered to be equal to 0.5hr and 1.543hr, respectively. It has been seen that for the value of $Z=2.020$ the entire sediment load is distributed within a very short duration in the early period of the storm event while the base time of the instantaneous unit sediment graphs for $Z=0.110$ is comparatively almost double. The ordinates of the USGs, required for prediction of sediment graphs, were obtained as per the procedure of conversion of IUH into UH. The USGs obtained based on the watershed characteristics were then convoluted into direct sediment graphs by the sediment mobilized estimated with the help of the Eq. (6.9).

Since two values of weighting factor x (0.162 and 0.000) and two values of parameter Z (0.110 and 2.020) were found applicable for the derivation of IUSG, and two methods of the USG convolution viz. considering the sediment mobilized distribution (SMD) and not considering the sediment mobilized distribution (NSMD) were used, the following models for various combinations were tried for arriving at the most applicable sediment graph model for the Amameh watershed.

B-1) Parameter $Z=0.110$, $x=0.162$ and SMD,

B-2) Parameter $Z=0.110$, $x=0.162$ and NSMD.

B-3) Parameter $Z=0.110$, $x=0.000$ and SMD,

B-4) Parameter $Z=0.110$, $x=0.000$ and NSMD,

B-5) Parameter $Z=2.020$, $x=0.162$ and SMD,

B-6) Parameter $Z=2.020$, $x=0.162$ and NSMD,

B-7) Parameter $Z=2.020$, $x=0.000$ and SMD and

B-8) Parameter $Z=2.020$, $x=0.000$ and NSMD.

The applicability of the model developed based on hydrological data (model A) and the above eight models (model B) for prediction of direct sediment graphs was verified by considering eight storm events to arrive at the best performing model for the study area. The efficiency of developed sediment graph models for their prediction performance was evaluated by using graphical (qualitative) and statistical (quantitative) methods. The statistical criteria such as Relative Error (RE), Coefficient of Efficiency (CE), Integral Square Error (ISE), Relative Square Error (RSE), Root Mean Square Error (RMSE), Relative Square Error (RSE), Ratio of Error (REO), Bias (B_s) and Coefficient of Determination (R^2) were applied for the quantitative evaluation.

Based on graphical comparison, it was found that the model A predicts higher peak, lesser volume and shorter time to peak as well as base time in comparison to respective observed sediment graphs. The results of qualitative comparison also showed that the sediment graphs predicted by using models B-1, B-2, B-3 and B-4, that is, the models developed with Z as 0.110 have a better affinity with the observed sediment graphs.

Based on statistical comparison, it was found that the results of model evaluation were a little different from criterion to criterion. Therefore a method of factorial scoring was used to find out the quantitatively best performing model for the study area. From the factorial scoring (Table 5.22), it was observed that the models B-1 and B-2 were having

almost the same score and thus any of them can be applied efficiently for the prediction of sediment graph in the Amameh watershed. However model B-2 with least score of 28 can be regarded as the best performing model and was therefore recommended for sediment graph prediction for the study area.

A comparative assessment was also made for a point-wise evaluation of the sediment graphs by using the Coefficient of Determination (R^2) in respect of total sediment yield and peak flow rate obtained by using various developed models. Different types of regression models such as linear, logarithmic, polynomial, power and exponential were tried. It was observed (Tables 5.23a and 5.23b) that for the sediment graphs, predicted by using models B-1, B-3, B-5 and B-7, the 2nd order polynomial and power regression models fitted better than other types of models respectively for the prediction of total sediment yield and peak sediment flow rate, whereas the situation was found to be just the reverse in the case of sediment graphs predicted by using models B-2, B-4, B-6 and B-8. However, the polynomial regression model with order two has performed better than other models in regressing the observed total sediment yield as well as the peak sediment flow rate with respective predicted values obtained by model A.

Since based on factorial scoring and also the coefficient of determination the model B-2 ($x=0.162$, $Z=0.110$ and NSMD) was established as the best performing model, the following power and polynomial equations were obtained to define the relationship between observed and predicted sediment yield and peak rate of sediment flow estimated by model B-2 in the Amameh watershed, respectively.

$$S_p = 1.797S_o^{0.819} \quad (r=0.887) \quad \dots (6.10)$$

$$P_{sp} = -0.0016P_{so}^2 + 1.697P_{so} - 46.851 \quad (r=0.752) \quad \dots (6.11)$$

where S_p and S_o are the predicted and the observed sediment yield in tonnes, and P_{sp} and P_{so} are the predicted and the observed peak rate of sediment flow in $t.day^{-1}$, respectively.

To have a better understanding between the generated sediment and its peak rate, the following power equation with 91.7 % coefficient of determination and 0.210 standard error of estimate was developed between the sediment yield (Y_s) in tonnes and peak rate of sediment flow (Q_{sp}) in tonnes.day⁻¹ for the study area.

$$Q_{sp} = 20.238Y_s^{0.8998} \quad (r=0.958) \quad \dots (6.12)$$

To assess the relative importance of the basic components and determine the level of accuracy in the estimation of parameters, the sensitivity analysis was conducted. The results of the sensitivity analysis for the model B-2 revealed that the model is more sensitive to the parameter Z as compared to the weighting factor x . In view of the higher values of relative sensitivity, it can also be inferred that the peak rate of sediment flow, is more susceptible than the sediment yield to the variation of both the parameters Z and weighting factor x .

The following are the salient conclusions that can be drawn from the investigations attempted in the present study:

1. The performance of globally used SCS curve number in its initial form was found to be weak for the study watershed, however the concept of recessive equation for finding appropriate values of maximum storage index coefficient (MSIC) has performed satisfactorily.
2. The results of F-statistic for analysis of variance (ANOVA) showed a significant relationship between sediment discharge and flow discharge data of the study area. The power regression equation between sediment flow discharge and flow discharge, called as sediment rating curve (SRC), was found to be the most suitable relationship for the watershed.
3. All the recorded sediment discharge and flow discharge in a particular month as well as season during the entire period, i.e. 1970-1997, were considered and

interrelated. Similarly, the entire data were grouped in different periods and classes of flow discharge and corresponding relationships were developed. However, these classifications of aforesaid hydrological data could not improve the correlation coefficient beyond 72% for the established power regressions. Therefore, the entire data was considered at a stretch and the associated relationship with a correlation coefficient of 85.4% was found to be the most usable SRC equation for the study watershed.

4. Since the sediment discharge corresponding to the rising limb of the respective hydrograph was higher than the value corresponding to the falling limb for the same discharge, two different regression equations were developed separately for two groups of data belonging to respective rising and falling limbs of hydrographs.
5. The concepts of confidence area ellipse as an applicable approach to obtain the appropriate sediment rating curve equations for pre and post peak ordinates of hydrograph was found to be not applicable for the watershed, since the flow discharge data were not distributed normally.
6. Most of the soil erosion and sediment yield models developed for specific conditions elsewhere such as USLE, Hudson's method, EUSLE, AOF, Time Area Method, MUSLE for sediment, MUSLE for erosion and MUSLT were not found to be applicable in their original forms for the prediction of storm-wise sediment yield from the study area.
7. A new version of MUSLE, developed for the watershed, with an exponent of 0.081 and a proposed constraint for the determination of storm magnitude (Eq. 6.7), performed well with an error of estimation of 19.40% only.

8. A new approach called as reverse routing technique (RRT), developed for the determination of outflow hydrographs at the outlet of each sub-watershed and the partial contributions to the total runoff, proved to be very efficient for the watershed.
9. For the determination of spatial distribution of sediment yield within the watershed, a sediment routing model based on the Williams' model to predict total sediment yield from the watershed was developed and found to be satisfactory with an acceptable error of estimation of 21.9%.
10. Based on the results of factorial scoring employed in the study, it was inferred that out of the two main approaches proposed for the determination of temporal distribution of sediment yield during a storm, the models based on watershed characteristics, in overall, performed better than the model based on the hydrological data.
11. The sediment graph model with specifications of weighting factor $x=0.162$ (for derivation of IUH) and parameter $Z=0.110$ obtained by using modified equation for the study area (for determination of sediment concentration) and not considering the distribution of sediment mobilized (for convolution of USG into direct sediment graph) was found to be the best performing model for the prediction of the sediment graph in the study watershed.
12. Through the sensitivity analysis, it was found that the preferred model, quoted above, for the prediction of sediment graph is more sensitive to the parameter Z as compared to the weighting factor x . The sensitivity analysis further showed that the peak rate of sediment flow, is more susceptible than the sediment yield to the variation of both Z and x .

The following suggestions are being proposed for future studies by the researchers working in the field of sediment modeling:

1. Distributed modeling is suggested for simulation of runoff and sediment yield owing to the spatial variation of influencing parameters on their generation within a watershed.
2. Extension of the development of spatial and temporal distribution models for sediment yield prediction with respect to the natural variations like global warming and human's interferences in natural ecosystems such as urbanization, extensive agricultural activities and deforestation are invariably suggested.
3. The role of snow as a major type of precipitation in mountainous area in generation of soil erosion and sediment yield also needs to be investigated.
4. The performance of the developed model should be verified for a study area by employing as many appropriate statistical techniques as possible to overcome the bias affinity for one or a few selected criteria.

LITERATURE CITED

LITERATURE CITED

- Abbasi, A. 1992.** Development and calibration of computer model for runoff estimation in small watersheds. Thesis, M.Sc. Sharif University, Iran. (Translation of original Article in Persian).
- Abbott, M.B. and Refsgaard, J.C. 1996.** Distributed hydrological modelling, Water Sciences and Technology library: Vol.22, Kluwer Academic Publisher, Netherlands.
- Academy of sciences, USSR, Section for Scientific Study of Water Engineering Problems. 1961.** Problems of river runoff control. Translated by Y. Prushansky. Israel program for scientific translation Ltd. Jerusalem.
- Agarwal, A., Das, G., Mangalik, V.P. and Chaurasia, P.R. 1989.** Stochastic sediment yield model for upper catchment of Ramganga River. *Journal of Agriculture Engineering, ASAE*, 26(2): 85-96.
- Agricultural Research Service. 1973.** HYMO: problem-oriented computer language for hydrologic modeling, user manual. USDA, southern region.
- Alonso, C.U., De Coursey, D.G., Prasad, S.N. and Bowie, A.J. 1978.** Field test of a distributed sediment yield model. *In: Verification of Mathematical and Physical Models in Hydraulic Engineering: Proceedings, USA*, pp. 671-678.
- Arnold, G.J. 1989.** Simulation of Complex Hydrologic Basins. *In: 1989 summer computer simulation conference, Austin Tx July 24-27, 1989: proceedings*, pp. 682-687.
- Arnold, J.G., Williams, J.R., Nicks, A.D. and Sammons N.B. 1990.** SWRRB: A basin scale simulation model for soil and water resources management. Texas A&M Univ. Press, College Station, TX.
- Arnold, J.G., Williams, J.R. and Maidment, D.R. 1995.** Continuous-time water and sediment-routing model for large basins. *Journal of Hydraulic Engineering* 121(2):171-183.
- ASCE task committee on application of Artificial Neural Networks in Hydrology. 2000.** Artificial Neural Networks in Hydrology (I: Preliminary Concepts). *Journal of Hydrologic Engineering*. 5(2): 115-137.
- Ascough II, J. C., Baffaut, C., Nearing, M. A. and Liu, B. Y. 1997.** The WEPP watershed model: I. Hydrology and erosion. *Transactions of the ASAE*. 40(4): 921-933.
- Ashmore, P.E. and Day, T.J. 1988.** Effective discharge for suspended sediment transport in streams of the Saskatchewan River Basin. *Water resources research*, 24(6): 864-870
- Asokan , K. 1981.** Runoff and sediment yield from Bino subwatershed of Ramganga catchment. Thesis, M.Tech. G. B. Pant university of Agriculture and Technology, Pantnagar, India.

- Baffaut, C., Nearing, M. A., Ascough II, J. C. and Liu, B. 1997.** The WEPP watershed model: II. Sensitivity analysis and discretization on small watersheds. *Transactions of the ASAE*. **40(4)**: 935-943.
- Bagarello, V. and Asaro, F.D. 1994.** Estimating single storm erosion index. *Transactions of the ASAE*. **37(3)**: 785-791.
- Bajpai, A.k. 1986.** Development of sediment graph model for a catchment of Ramganga river. Thesis, M.Tech. G. B. Pant university of Agriculture and Technology, Pantnagar, India.
- Banasik, K. 1989.** Analysis of rainfall-runoff-sediment yield events from river Dart for the period 1962-84. Warsaw Agricultural University.
- Bansik, K. 1990.** Sedimentgraph model for a small watershed. Atelier international UNESCO- AISH- ENIT Convoque par le comite national Tunisien pour le PHI Tunis: 302-311.
- Banasik, K. 1995.** A conceptual model of the instantaneous unit sedimentgraph. Department of Hydraulic Structure, Warsaw Agricultura University, Poland.
- Banasik, K. and Walling, D.E. 1996.** Predicting sedimentgraphs for a small agricultural catchment. *Nordic hydrology*, **27 (4)**: 275-294.
- Banasik, K. and Woodward, D.E. 1992.** Prediction of sedimentgraph from a small watershed in poland in a changing environment. *In: Irrigation & Drainage session: proceedings. Water forum '92 EE, HY, IR, WR Div/ASCE*: 493-497.
- Barfield, B.J., Moore, I. D. and Williams R. G. 1979.** Prediction of sediment yield from surface mined watershed. *In: Symposium on Surface Mining Hydrology, and Reclamation. University of Kentucky, Lexington.*
- Barfield, B.J., Warner, R. C. and Haan C. T. 1981.** Applied hydrology and sedimentology for disturbed areas. Oklahoma Technical Press, Stillwater, OK.
- Basu, S.S. 1993.** System models of sediment yield for Mynally and Ebband subwatersheds of lower Bhawani catchment. Thesis, Ph.D. G.B.Pant University of Agriculture and Technology, India.
- Benson, V. W. 1989.** EPIC: A planning tool for soil and water conservation programs. *In: 1989 summer computer simulation conference, Austin Tx., July 24-27, 1989: proceedings*, pp. 718-721.
- Bingner, R.L. 1996.** Runoff simulated from Goodwin creek watershed using SWAT. *Transactions of the ASAE*, **39(1)**: 85-90.
- Bingner, R.L, Murphree, C.E. and Mutchler, C.K. 1989.** Comparison of sediment yield models on watersheds in Mississippi. *Transactions of the ASAE*. **32(2)**: 529-534.
- Blau, Jeff B., Woolhiser, D.A. and Lane, L.J. 1988.** Identification of erosion model parameters. *Transactions of the ASAE*, **31(3)**: 839-845.
- Bondelid, T.R., McCuren, R.H. and Jackson, T.J. 1982.** Sensitivity of SCS model to curve number variation. *Water Resources Bulletin*, **18(1)**: 111-116.

- Bonta, J.V. and Rao, A.R. 1988.** Comparison of four design-storm hyetographs. *Transactions of the ASAE*, **31** (1): 102-106.
- Borah, D.K. 1989.** Runoff simulation model for small watersheds. *Transactions of the ASAE*. **32**(3): 881-886.
- Borah, D.K. 1989.** Sediment discharge model for small watersheds. *Transactions of the ASAE*. **32**(3): 874-880.
- Borah, D.K. and Ashraf, M.S. 1990.** Modeling storm runoff and sediment with seasonal variations. *Transactions in Agriculture*, **33**(1): 105-110.
- Bradford, J. M. and Foster, G. R. 1996.** Interrill soil erosion and slope steepness factors. *Soil Science Society American Journal*. **60**: 909-915.
- Brown, L. C. and Foster, G.R. 1987.** Storm erosivity using idealized intensity distributions. *Transactions of the ASAE*. **30**(2): 379-386.
- Browning, F.M., Norton, R.A., McCall, A.G. and Bell, F.G. 1948.** Investigation in erosion control and the reclamation of land at the Missouri Valley Loess Conservation Experiment Station, Iowa, 1931-1942. United States Department Agricultural Technical Bulliten.
- Bruce, R.R., Harper, L.A. Leonard, R.A., Snyder, W.M. and Thomas, A.W. 1975.** A model for runoff of pesticides from small upland watersheds. *J. Environ. Qual.* **4**(4):541-548.
- Bundela, D.S., Singh, R. and Mishra, K. 1995.** Sediment yield modelling for small watersheds in Barakhar river valley. *Journal of the Institution of Engineers-AG*. **76**: 22-25.
- Burn, D.H. and Boorman, D.B. 1993.** Estimation of hydrological parameters at Ungauged catchments. *Journal of Hydrology*, **143**: 429-454.
- Chakrapani, G.j. and Subramanian, V. 1990.** Factors controlling sediment discharge in the Mahanadi River Basin, India. *Journal of Hydrology*, **117**: 169-185.
- Chang, H.H. and Stow, D.A. 1988.** Sediment delivery in a semi-arid coastal stream. *Journal of Hydrology*, **99**: 201-214.
- Chaurasia, P.R. 1985.** Stochastic modelling of sediment flow from a Ramganga catchment. Thesis, M.Tech. G.B.Pant University of Agriculture and Technology, India.
- Chen, V.J. and Kuo, C.Y. 1986.** A study on synthetic sedimentgraphs for Ungaged watersheds. *Journal of Hydrology*, **84**: 35-54.
- Chiew, F.H.S., Swteardson, M.J. and McMahon, T.A. 1993.** Comparison of six rainfall-runoff modelling approaches. *Journal of Hydrology*, **147**: 1-36.
- Chikita, K. A. 1996.** Suspended sediment discharge from snowmelt: Ikushunbetsu River, Hokkaido, Japan. *Journal of Hydrology* **186**: 295-313.
- Chow, Ven. Te. 1964.** Handbook of applied hydrology. McGraw-Hill book company, New York.

- Clark, C.O. 1945.** Storage and the unit hydrograph. Transactions of ASCE, **110**:1419-1446.
- Clark, R.T. 1973.** Mathematical models in hydrology. Food and Agriculture Organization of United Nations, Irrigation and Drainage paper No. 19, Rome.
- Cook, H.L. 1936.** The nature and controlling variables of the water erosion. *Soil Sciences Society Am. Proc.* **1**: 60-64.
- Cooper, A.B., Smith, C.M. and Bottcher, A.B. 1992.** Predicting runoff of water, sediment and nutrients from A New Zealand grazed pasture using CREAMS. *Transactions of the ASAE*, **35**(1): 105-112.
- Crawford, Ch. G. 1991.** Estimation of suspended-sediment rating curves and mean suspended-sediment loads. *Journal of Hydrology*. **129**:331-348.
- Das, G. 1982.** Runoff and sediment yield from Upper Ramganga catchment. Thesis, Ph.D. G.B.Pant University of Agriculture and Technology, India.
- Das, G. 2000.** Hydrology and soil conservation engineering. Printice-Hall of India Private Limited, New Delhi.
- Das, G. and Agarwal, A. 1990.** Development of conceptual sediment graph model. *Transactions in Agriculture*, **33** (1): 100-104.
- Das, G. and Chauhan, H.S. 1990.** Sediment routing for mountainous Himalayan regions. *Transactions in Agriculture*, **33** (1): 95-99.
- DeCoursey, D.G. and Snyder, W.M. 1969.** Computer-oriented method of optimizing hydrologic model parameters. *Journal of Hydrology*, **9**: 34-56.
- Dendy, F.E. and Bolton, G.C. 1976.** Sediment yield-runoff drainage area relationships in the United States, *Journal of Soil and Water Conservation*, **31**(6):264-266.
- Dharmasena, P.B. 1994.** An empirical formula to estimate runoff from small agricultural lands. *Journal of Agricultural Engineering*, ESAE, **XXXI** (1-4): 58-64.
- Dickens, P.S., Tschantz, B.A. and Minear, R.A. 1985.** Sediment yield and water quality from a steep- slope surface mine spoil. *Transactions of the ASAE*. **28**(6): 1838-1845.
- Diskin, M.H., Ince, S. and Nyarko, K.O. 1978.** Parallel cascades model for urban watersheds. *Journal of Hydraulic Division*, ASCE, **104**(HY2): 261-276.
- Dragoun, F.G. and Miller C.R. 1964.** Sediment characteristics of two small agricultural watersheds in central Nebraska, *In: Summer meeting of the American Society of Agricultural Engineers: proceedings*, Fort Collins, USA.
- Dube, S. 1987.** Development of HYMO sediment model. Thesis, M.Tech. G.B. Pant University of Agriculture and Technology, India.
- Ebisemiju, F.S. 1990.** Sediment delivery ratio prediction equations for short catchment slopes in a humid tropical environment. *Journal of Hydrology*, **114**: 191-208.

- Eijsackers, Herman. J.P. and Hamers, Timo. 1992.** Integrated soil and sediment research: A basis for proper protection. *In: the first European conference on integrated research for soil and sediment protection and remediation (EUROSOL) proceedings*, pp. 320-340.
- Einstein, H.A. 1950.** The bedload function for sediment transportation in Open Channel Flows. *USDA Technical Bulliten*.1026.
- Einstein, H.A. 1964.** Hand book of applied hydrology. Section 17-II, Sedimentation, Part II, River Sedimentation, Ven Te Chow(Editor-in-Chief), McGraw Hill.
- Elliot, W.J. and Laflen, J.M. 1993.** A Process-based rill erosion model. *Transactions of the ASAE*, **36(1)**: 65-72.
- Elwell, H.A. 1978.** Modelling soil losses in southern Africa. *Journal of Agricultural Engineering Research*, **23(2)**:117-127.
- F.A.O. 1979.** Deterministic models in hydrology. Food and Agriculture Organization of the United Nations, Rome.
- Fellow, H.Wu., Hall, J.A. and Bonta, J.V. 1993.** Evaluation of runoff and erosion models. *Journal of Irrigation and Drainage Engineering*, **119(4)**: 364-382.
- Ferro, V. and Porto, P. 2000.** Sediment delivery distributed (SEDD) model. *Journal of Hydrologic Engineering*, **5(4)**: 411-422.
- Ferro, V., Porto, P. and Tusa, G. 1998.** Testing a distributed approach for modelling sediment delivery. *Hydrological Sciences-Journal-des Sciences Hydrologiques*, **43(3)**: 425-442.
- Finkner, S.C., Nearing, M.A., Foster, G.R. and Gilley, J.E. 1989.** A simplified equation for modeling sediment transport capacity. *Transactions of the ASAE*, **32 (5)**: 1545-1550.
- Finney, V.L., Banasik, K., Needham, S. and Young, R.A. 1993.** Comparison of DR-USLE, SEGMO and AGNPS with two rainfall events. *In: International Symposium on Runoff and Sediment yield Modelling: proceeding. SGGW-Warsaw*, pp. 195-200.
- Flemming, G., 1971.** A Comment on River Flow Forecasting through Conceptual Models I, II, III., *Journal of Hydrology*, **13**:251.
- Foster, G.R. 1981.** Estimating erosion and sediment yield on field-sized areas. *Transactions of the ASAE*, pp. 1253-1262.
- Foster, G. R. 1991.** Advances in wind and water erosion prediction. *Journal of Soil and Water Conservation*, pp. 27-29.
- Foster, G.R. and Lane, L.J. 1987.** Beyond the USLE: advancements in soil erosion prediction. A collection of SSSA golden anniversary contributions presented at the annual meeting in New Orleans, LA, 30Nov.-5Dec. 1986 (Future developments in soil science research), pp. 315-326.
- Foster, G.R., Lane, L.G., Newlin, J.D., Laflen, J.M. and Young, R.A. 1980.** A model to estimate sediment yield from field-sized area, development of the model in

- CREAMS. Conservation Research Report No. 26, US Dept. of Agriculture, Washington, pp. 36-64.
- Franchini, M. and Pacciani, M. 1991.** Comparative analysis of several conceptual rainfall-runoff models. *Journal of Hydrology*, **122**: 161-219.
- Ghidey, F. and Alberts, E.E. 1994.** Interrill erodibility affected by cropping systems and initial soil water content. *Transactions of the ASAE*, **37(6)**: 1809-1815.
- Gholami, S.A. 2000.** A distributed watershed modeling of the mountainous catchment. Thesis, Ph.D. Indian Institute of Technology, Delhi.
- Gilley, J.E., Kincaid, D.C., Elliot, W.J. and Laflen, J.M. 1992.** Sediment delivery on rill and interrill areas. *Journal of Hydrology*, **140**: 313-341.
- Gracia, S.J. 1994.** Generacion sintetica de sedimentogramas. Coordinacion de investigacion area de riesgos hidrometeorologicos, pp. 1-63.
- Gracia, S.J. 1996.** Generation of synthetic sedimentgraphs. *Hydrological processes*, **10**: 1181-1191.
- Graf, W.H. 1971.** Hydraulics of sediment transport. McGraw-Hill Book Co., Inc. New York.
- Grawford, C.G. 1991.** Estimation of suspended-sediment rating curves and mean suspended-sediment loads. *Journal of Hydrology*, **129**: 331-348.
- Green, L.R.A. and Stephenson, D. 1986.** Criteria for comparison of single event models. *Hydrological Sciences Journal*, **31(3)**: 395-411.
- Guang-Te, W., Singh, V.P., Changling, G. and Kexin, H. 1991.** Discrete linear models for runoff and sediment discharge from the Loess Plateau of China. *Journal of Hydrology*, **127**: 153-171.
- Gunawardena, E.R.N. 1989.** Identification of land cover and physiographic parameters in computer simulations of soil erosion, land and water use. In: Eleventh International Congress on Agricultural Engineering, Dublin, September-4th-8th 1989: Proceedings, 757-765.
- Gupta, B.L. 1991.** Engineering hydrology. Delhi, Standard Publishers Distributors.
- Guy, B.T., Dickinson, W.T. and Rudra, R.P. 1992.** Evaluation of fluvial sediment transport equations for overland flow. *Transactions of the ASAE*. **35(2)**:545-555.
- Gyasi-Agyei, Y., De Troch, F.P. and Torch, P.A. 1996.** A dynamic hillslope response model in a geomorphology based rainfall- runoff model. *Journal of Hydrology* **178**: 1-18.
- Hadely, R.F., Lal, R., Onstad, C. A., Walling, D.E. and Yair, A. 1985.** Recent Developments in Erosion and Sediment Yield Studies. Rep. UNESCO, (IHP) Publ. Paris, France.
- Hagen, L.J., Wagner, L.E. and Skidmore, E.L. 1999.** Analytical Solutions and Sensitivity Analyses for Sediment Transport in WEPS. *Transactions of the ASAE*, **42(6)**: 1715-1721.

- Hagen, L.J., Wagner, L.E., Tatarko, J., Skidmore, E.L., Durar, A.A., Steiner, J.L., Shomberg, H.H., Retta, A., Armbrust, D.V., Zobek, T.M., Unger, P.W., Ding, D. and Elminawi, I. 1995. USDA Wind Erosion Prediction System: Technical Description. *In: WEPP/WEPS Symposium: Proceeding, Ankey, USA.*
- Hamlett, J.M., Baker, J.L., Kimes, S.C. and Johnson, H.P. 1984. Runoff and sediment transport within and from small agricultural watersheds. *Transactions of the ASAE*, pp. 1355-1363.
- Hartley, D. M. 1987. Simplified process model for water sediment yield from single storms part I-model formulation. *Transactions of the ASAE*. **30(3)**: 710-717.
- Hartley, D.M. 1987. Simplified process model for water and sediment yield from single storms part II-performance. *Transactions of the ASAE*. **30(3)**: 718-723.
- Hawkins, R.H. 1975. The importance of accurate curve numbers in estimation of storm runoff. *Water Resources Bulletin*. **11(5)**:887-891.
- Heidel, S.G. 1956. The progressive lag of sediment concentration with flood waves. *Trans. Am. Geophys. Union*. **37(1)**:56-66.
- Heydarian, S.A. 1994. Evaluation of erosion and its prediction in a mountainous area. Thesis, M.Ag., Tehran University, Iran.
- Hibbert, A.R. and Cunningham, G.B. 1967. Stream flow data processing opportunities and application. *In: International symposium on forest hydrology: Proceedings, Oxford*, pp. 725-736.
- Horton, R.E. 1932. Drainage basin characteristics. *Transactions of American Geography Union*, **13**:350-361.
- Hromadka, T.V. 1997. Stochastic evaluation of rainfall-runoff prediction performance. *Journal of Hydrologic Engineering*, **2(4)**: 188-196.
- Hudson, N.W. 1981. *Geografisca Ann.* **54-A**: 203-220.
- Hussein, M.H. 1996. An analysis of rainfall, runoff and erosion in the low rainfall zone of northern Iraq. *Journal of Hydrology*, **181**: 105-126.
- Jaiswal, S.K. 1982. Runoff and sediment yield from Gagas watershed of Ramganga catchment. Thesis, M.Tech. G.B. Pant University of Agriculture and Technology, India.
- Jansen, J.M.L. and Painter, R.B. 1974. Predicting sediment yield from climate and topography. *Journal of Hydrology*, **21**: 371-380.
- Jansson, M.B. 1996. Estimating a sediment rating curve of the Reventazon river at Palomo using logged mean loads within discharge classes. *Journal of Hydrology* **183**: 227-241.
- Jha, R. 1988. Conceptual models of suspended sediment flow from Chaukhutia watershed of Ramganga river. Thesis, M.Tech. G.B. Pant University of Agriculture and Technology, India.
- Johnson, J. W. 1943. Distribution graphs of suspended-matter concentration. *Transactions of the ASCE*, **108**: 941-964.

- Julien, P.Y. and Simons, D.B. 1985.** Sediment transport capacity of overland flow. *Transaction of the ASAE*. **28(3)**: 755-762.
- Kitanidis, P.K. and Bras, R.L. 1980.** Real time forecasting with a conceptual hydrological model. 2. Applications and results. *Water Resources Research*, **16(6)**:1034-1044.
- Kothyari, U.C. and Jain, S.K. 1997.** Sediment yield estimation using GIS. *Hydrological Sciences- Journal-Sciences des Hydrologiques*, **42(6)**: 833-843.
- Kothyari, U.C., Tiwari, A.K. and Singh, R. 1994.** Prediction of sediment yield. *Journal of Irrigation and Drainage Engineering*, **120(6)**: 1122-1131.
- Kothyari, U.C., Tiwari, A.K. and Singh, R. 1996.** Temporal variation of sediment yield. *Journal of Hydrologic Engineering*, **1(4)**: 169-176.
- Kothyari, U.C., Tiwari, A.K. and Singh, R. 1997.** Estimation of temporal variation of sediment yield from small catchments through the kinematic method. *Journal of Hydrology*, **203**: 39-57.
- Kumar, A. and Das, G. 2000.** Dynamic model of daily rainfall, runoff and sediment yield for a Himalayan watershed. *Journal of Agricultural Engineering Research* (**75**): 189-193.
- Kumar, D. 1994.** Input-output models of sediment discharge from Chaukhutia watershed of Ramganga river. Thesis, Ph.D. G.B.Pant University of Agriculture and Technology, India.
- Kumar, S. and Rastogi, R.A. 1987.** A conceptual catchment model for estimating suspended sediment flow. *Journal of Hydrology*, **95**: 155-163.
- Kumar, S., Rastogi, R.A. and Raghuwanshi, N.S. 1990.** Application of conceptual model to determine sediment flow. *Australian Civil Engineering Transactions, CE*, **32(4)**: 199-2.4.
- Kumar, V. 1988.** Modelling of sediment yield from a mountainous watershed. Thesis, Ph.D. G.B.Pant University of Agriculture and Technology, India.
- Kumbhrae, P.S. and Rastogi, R.A. 1985.** Determination of temporal distribution of sediment mobilized from a Kumaon Himalayan watershed. *Journal of Agricultural Engineering, ISAE*. **22(4)**:73-81..
- Laflen, J. M., Lane, L. J. and Foster, G. R. 1991.** WEPP A new generation of erosion prediction technology. *Journal of Soil and Water Conservation*: 34-38.
- Liu, B.Y., Nearing, M.A., Baffaut, C. and Ascough II, J.C. 1997.** The WEPP watershed model: III. Comparisons to measured data from small watersheds. *Transactions of the ASAE*. **40(4)**: 945-952.
- Loughran, R.G., Cambell, B.L. and Elliot, G.L. 1986.** Sediment dynamics in partially cultivated catchment in New South Wales, Australia. *Journal of Hydrology*, **83**:285-297.
- Madeyski, M. and Banasik, K. 1989.** Applicability of the Modified Universal Soil Loss Equation in small Capathian watersheds. *Catena Supplement*, **14**: 75-80.

- Mahdavi, M. 1992.** Applied hydrology. Tehran University Publication, Tehran, Iran. (Translation of original book in Persian).
- Mal, B. C. 1994.** Introduction to soil and water conservation engineering. Kalyani Publishers, Ludhiana, India.
- Mall, R.K. 1990.** Simulation of sediment yield from stochastically predicted rainfall. Thesis, M.Tech. G.B. Pant University of Agriculture and Technology, India.
- Maner, S.B. 1958.** Factors affecting sediment delivery ratios in the Red Hills physiographic area. *Transactions American Geophysical union*, **39(4)**:669-675.
- McConkey, B.G., Nicholaichuk, W., Steppuhn, H. and Reimer, C.D. 1997.** Sediment yield and seasonal soil erodibility for semiarid cropland in western Canada. *Canadian Journal of Soil Science* **77**: 33-40.
- McCuen, R.H. and Snyder, W.M. 1983.** Hydrologic modeling: Statistical methods and applications. Prentice-Hall, New Jersey, USA.
- McPherson, H.J. 1975.** Sediment yields from intermediate- sized stream basins in Southern Alberta. *Journal of Hydrology*, **25**: 243-257.
- Meyer, L.D. 1981.** How rain intensity affects inter-rill erosion. *Transactions of the ASAE*, **24**:1472-1475.
- Meyer, L.D. and Harmon, W.C. 1992.** Soil erosion varies during the crop year. *Transactions of the ASAE*. **35(2)**: 459-464.
- Meyer, L.D. and Wischmeier, W.H. 1969.** Mathematical simulation of the process of soil erosion by water. *Transactions of the ASAE*, pp. 754-758.
- Moore, R.J. 1984.** A dynamic model of basin sediment yield. *Water Resources Research*. **20(1)**: 89-103.
- Moore, R.J. and Clarke, R.T. 1983.** A distribution function approach to modelling basin sediment yield. *Journal of Hydrology*, **65**: 239-257.
- Morgan, R.P.C. 1986.** Soil erosion and its control. Van nostrand reinhold, U.K.
- Muphree, C.E., and Mutchler, C.K. 1981.** Sediment yield from a flatland watershed. *Transactions of the ASAE*: 966-969.
- Murty, V.V.N. 1985.** Land and water management engineering. Kalyani Publishers, Ludhiana, India.
- Musgrave, G.W. 1947.** The quantitative evaluation of factors in water erosion, a first approximation. *Journal of Soil and Water Conservation*.
- Nash, J.E. 1957.** The form of the instantaneous unit hydrograph. International Association of Scientific Hydrology, Publication No. 45, Vol. 3-4, pp. 114-121.
- Nash, J.E. and Sutcliffe, J.V. 1970.** River flow forecasting through conceptual models. Part I-A discussion of principles, *Journal of Hydrology*, **10(3)**: 282-290.

- Nearing, M.A., Deer-Ascough, L. and Laflen, J.M. 1990.** Sensitivity analysis of the WEPP hillslope profile erosion model. *Transactions of the ASAE*, **33 (3)**: 839-849.
- Negev, M. 1967.** A sediment model on a digital computer. Report No. 39, Department of Civil Engineering, Stanford University, Stanford, USA.
- Nema, A.K. 1998.** Laboratory studies on interrill soil erosion and sediment transport capacity of rainfall induced flow. Thesis, M.Tech. G.B. Pant University of Agriculture and Technology, India.
- Nicks, A. D., Williams, R.D. Williams, J. R., and Gander, G. A. 1994.** Estimating erosion with models having different technologies. *In: 25th Annual Conference International Erosion Control Association*, February 15-18, 1994: proceedings, Reno, Nevada, pp. 51-61.
- Novotny, V. 1980.** Delivery of suspended sediment and pollutants from nonpoint sources during overland flow. *Water Resources Bulletin*, **16**: 1057-1065.
- Ojasvi, P.R., Panda, R.K. and Satyanarayana, T. 1994.** Hydrological and morphological investigation in a hilly catchment. *Agricultural Engineering Journal*, **3(3)**:77-89.
- Onstad, C.A. and Bowie, A.J. 1977.** Basin sediment yield modeling using hydrological variables. *In: Erosion and Solid Matter Transport in Inland Waters: Proceedings*, Paris, pp. 191-202.
- Onstad, C.A. and Foster, G.R. 1975.** Erosion modeling on a watershed. *Transactions of the ASAE*, pp. 288-292.
- Overton, D.E. and Meadows, M.E. 1976.** Stormwater Modeling. Academic Press, INC, New York, USA.
- Papamichal, D.M. and Papagafiriou, Z.G. 1992.** Multiple input-single output linear functional models for river flow routing. *Journal of Hydrology*, **133**:365-377.
- Pathak, K.C. 1990.** Sediment prediction through Walsh Auto-Regressive (WAR) model. Thesis, M.Tech. G.B. Pant University of Agriculture and Technology, India.
- Perrone, J. and Madramootoo, C.A. 1999.** Sediment yield prediction using AGNPS. *Journal of Soil and Water Conservation*, pp. 415-418.
- Piest, R.F., Bradford, J.M. and Spomer, R.G. 1975.** Mechanism of erosion and sediment movement from gullies. *In: Present and Perspective Technology for Predicting Sediment Yields and Sources*, ARS-S-40, pp.162-176.
- Ponce, V.M., and Hawkins, R.H. 1996.** Runoff curve number: has it reached maturity?, *Journal of Hydrologic Engineering*, **1(1)**: 11-19.
- Prasad, K.R. 1983.** Runoff and sediment yield from Himalayan watershed of Ramganga catchment. Thesis, M.Tech. G.B. Pant University of Agriculture and Technology, India.
- Purveen, H., Lzaurralde, R.C., Chanasyk, D.S., Williams, J. R. and Grant, R.F. 1997.** Evaluation of EPIC's snowmelt and water erosion submodels using data from the Peace River region of Alberta. *Canadian Journal of Soil Sciences*, **77**: 41-50.

- Pyasi, S.K.** 1997. Memory based input-output runoff and sediment yield models for the upper Ramganga Himalayan catchment. Thesis, Ph.D. G.B.Pant University of Agriculture and Technology, India.
- Qiangguo, CAI.** 1997. Rainfall erosion influenced by slope length in the hilly loess region, CHINA. In: 8th international conference on rainwater catchment system, 21-25 April 1997: Proceedings, Tehran. Iran.
- Raghuwanshi, N.S.** 1986. mathematical watershed models for runoff and sediment flow from Chaukhtia catchment of Ramganga river. Thesis, M.Tech. G.B. Pant University of Agriculture and Technology, India.
- Raghuwanshi, N.S., Rastogi, R.A. and Kumar, S.** 1993. A conceptual model for washload estimation. *Agricultural Engineering Journal*. 2(3):91-104.
- Rahnama, F.** 1994. Erosion Models. Watershed Management Bureau, Jahad-e-Sazandegi Organization, Isfahan, Iran.
- Renard, K.G.** 1969. Sediment rating curves in ephemeral streams. *Transactions of the ASAE*, pp. 80-85.
- Renard, K.G. and Laursen, E.N.** 1975. Dynamic behavior model of ephemeral stream. *Journal of Hydraulic Division, ASCE*, 101(HY5): 511-528.
- Renard, K. G., Foster, G. R., Weesies, G. A. and Porter, J. P.** 1991. RUSLE, Revised Universal Soil Loss Equation. *Journal of Soil and Water Conservation*, pp. 30-33.
- Renard, K.G., Foster, G.R., Weesies, G.A., McCool, D.K. and Yoder, D.C.** 1997. Predicting soil erosion by water: A guide to conservation planning with the Revised Universal Soil Loss Equation (RUSLE). United States Department of Agriculture.
- Rendon-Herrero, O.** 1972. A method for the prediction of wash load in certain small watersheds. Thesis, Ph.D. Va. PolyTech. Inst. And State Univ., Blacksburg.
- Rendon-Herrero, O.** 1974. Estimation of washload produced on certain small watersheds. *Journal of the Hydraulics Division*, pp. 835-848.
- Rendon-Herrero, O.** 1976. Closure estimation of washload produced on certain small watersheds. *Journal of Hydraulic Division, ASCE* 101(HY7):1061-1064.
- Rendon-Herrero, O.** 1978. Unit sediment graph. *Water Resources Research*. 14(5): 889-901.
- Rodriguez-Iturbe, I. and Nordin, C.F.** 1968. Time series analysis of water and sediment discharge. *Hydrological Science Bulletin*, 13(2): 69-78.
- Roehl, J.R.** 1962. Sediment Source Areas, Delivery Ratios and influencing Morphological Factors. Publication No. 59, Wallingford, England: International Association of Scientific Hydrology, pp. 202-213.
- Rubey, W.W.** 1933. Equilibrium conditions in debris laden streams. *Transactions AGU*.
- Sabol, G.V.,** 1988. Clark unit hydrograph and k-parameter estimation. *Journal of Hydraulic Engineering*, 114(1): 103-111.

- Sadeghi, S.H.R. 1993.** Evaluation of accuracy and efficiency of computer model SEDIMOT II on flood and sediment yield prediction. Thesis, M.E. Tarbiat Modarres University, Iran. (Translation of original Article in Persian).
- Schulz, E.F. 1973.** Problems in applied Hydrology. Water Resources Publications, Fort Collins, Colorado, USA.
- Schumm, S.A. 1969.** A geomorphic approach to erosion control in semiarid regions. *Transactions of the ASAE*, pp. 60-68.
- SCS, 1957.** Engineering Handbook. USDA, Soil Conservation Service, Washington.
- Sepulveda, N. 1997.** Application of two direct runoff prediction methods. *Journal of Hydrologic Engineering*, 2(1): 10-17.
- Sharma, K.D. and Joshi, D.C. 1987.** Fluvial sedimentation in the Indian Arid zone. *Transactions of the ASAE*. 30(3): 724-728.
- Sharma, K.D. and Murthy, J.S.R. 1994.** Modelling sediment transport in stream channels in the Arid Zone of India. *Hydrological Processes*, 8: 567-572.
- Sharma, K.D., Murthy, J.S.R. and Dhir, R.P. 1996.** Modeling sediment delivery in arid upland basins. *Transactions of the ASAE*. 39(2): 517-524.
- Sharma, K.D., Vangani, N.S. and Kalla, A.K. 1993.** A linear time invariant dynamic model of sediment transport in arid region. *Indian Journal of Agricultural Engineering*, 3(1-2): 29-33.
- Sharma, K.N., Pandey, N.C. and Panigrahi, B. 1989.** Computation of silt production rate for small watersheds-A case study of Muchkund basin-land and water use, (Eds.) Dodd and Grace, 1:771-778.
- Sharma, R.K. and Sharma, T.K. 1997.** A text book of Hydrology and Water resources Engineering. Dhanpat Rai Publications (P), New Delhi, India.
- Sharma, T.C. and Dickinson, W.T. 1980.** System model of daily sediment yield. *Water Resources Research*, 16(3): 501-506.
- Sharma, T.C., Hines, W.G.S. and Dickinson, W.T. 1979.** Input-output model for runoff-sediment yield processes. *Journal of Hydrology*, 40:299-322.
- Shen, H.W. 1971.** River mechanics. Vol. I, Colorado State University, Fort Collin.
- Singh, J.K. 1979.** Some aspects of rainfall analysis, forecasting and its application. Thesis, Ph.D. Indian Institute of Technology, Kharagpur, India.
- Singh, S.K. 1990.** Development of Fourier-Autoregressive (FAR) model and its application for rainfall and sediment yield prediction. Thesis, M.Tech. G.B. Pant University of Agriculture and Technology, India.
- Singh, V.P. 1992.** Elementary hydrology. Eastern Economy Edition, New Delhi, India.
- Singh, V.P. and Chen, V.J. 1981.** On relation between sediment yield and runoff volume. In: International Symposium on Rainfall-runoff modeling components of

hydrologic cycle: Proceedings, Mississippi State University, Mississippi, pp.555-570.

- Singh, V. P. and Krstanovic, P.F. 1987.** A stochastic model for sediment yield using the principle of maximum entropy. *Water resources research*, **23(5)**: 781-793.
- Singh, V.P., Baniukiewics, A. and Chen, V.J. 1981.** An instantaneous unit sediment graph study for upland watersheds. *In: International Symposium on Rainfall-runoff modeling components of hydrologic cycle: Proceedings, Mississippi State University, Mississippi*, pp.539-554.
- Smith, D.D. 1941.** Interpretation of soil conservation data for field use. *Agricultural Engineering*, **22**:173-175.
- Smith, D.D. and Whitt, D.M. 1948.** Evaluating soil losses from field areas. *Agricultural Engineering*, **29**:394-398.
- Smith, D.D. and Wischmeir, W.H. 1962.** Rainfall erosion. *Adv. Agron.* **14**: 109-148.
- Snedecor, G.W., and Cochran, W.G. 1989.** Statistical methods. The Iowa State University Press, 8th edition, USA.
- Spomer, R.G., Mahurin, R.L. and Piest, R.F. 1986.** Erosion, deposition and sediment yield from dry creek basin, Nebraska. *Transactions of the ASAE*. **29(2)**: 489-493.
- Springer, E.P., Johnson, C.W., Colley, K.R. and Robertson, D.C. 1983.** Modeling of runoff and sediment yield from rangeland watersheds in southwest Idaho. *American Society of Agricultural Engineers*. Paper No. 83-2055.
- Srivastava, P.K., Rastogi, R.A. and Chauhan, H.S. 1984.** Prediction of storm sediment yield from a small watershed. *Journal of Agricultural Engineering, ISAE*, **21(1-2)**:121-126.
- Stehlik, O. 1975.** Potencialni eroze pudy proudici vodou na uzemi CSR, Studio, Geographica, Brnsi.
- Storm, D.E., Barfield, B.J. and Altendorf, C.T. 1994.** CREAMS/WEPP Sediment deposition equation: A semitheoretical evaluation. *Transactions of the ASAE*. **37(4)**: 1105-1108.
- Subramanya, K. 2000.** Engineering Hydrology. 2nd edition, Tata McGraw Hill Publishing Company Limited, Eighth reprint, New Delhi, India.
- Tabrizi, M.H.N., Jameluddin H, Billing S.A. and Skaggs, R.W. 1990.** Use of identification techniques to develop a water table prediction model. *Journal of the ASAE*, **33(6)**: 487-494.
- The ASCE task committee on definition of criteria for evaluation of watershed models of the watershed management committee, irrigation and drainage division. 1993.** Criteria for evaluation of watershed models. *Journal of Irrigation and Drainage Engineering*, **119(3)**: 429-442.
- Thirumalaiah, K. and Deo, K.C., 2000.** Hydrological forecasting using neural networks. *Journal of Hydrologic Engineering*, **5(2)**:180-189.

- Tiscareno-Lopez, M., Lopes, V.L. Stone, J. J. and Lane, L.J. 1993.** Sensitivity analysis of the WEPP watershed model for rangeland applications I: hillslope processes. *Transactions of the ASAE*. **36(6)**: 1659-1672.
- Tiwari, Y.K. 1986.** Development of sediment routing model for a catchment of Ramganga river. Thesis, M.Tech. G.B. Pant University of Agriculture and Technology, India.
- Todini, E. 1988.** Rainfall- runoff modeling- Past, present and future. *Journal of Hydrology*, **100**: 341-352.
- Tripathi, R.P. and Singh, H.P. 1990.** Soil erosion and conservation. Wiley Eastern Limited, New Delhi, India.
- Tulu, T. 1991.** Simulation of streamflows for ungauged catchments. *Journal of Hydrology*, **129**: 3-17.
- U.S. Soil Conservation Service. 1969.** National engineering handbook, Section 4, hydrology. U.S. Department of Agriculture, Washington, D.C., pp. 10.1-10.24.
- Vansickle, J. 1982.** Stochastic prediction of sediment yield from small watershed in Oregon, U.S.A. *Journal of Hydrology*, **56**: 309-323.
- Walling, D.E. 1988.** Erosion and sediment yield research- some recent perspectives. *Journal of Hydrology*, **100**: 113-141.
- Walling, D.E. and Webb, B.W. 1982.** Sediment availability and the prediction of storm-period sediment yields. *In: The Exeter Symposium: proceeding*, **137**: 327-337.
- Wang, G.T., Singh, V.P. and Yu, F.X. 1992.** A rainfall- runoff model for small watersheds. *Journal of Hydrology*, **138**: 97-117.
- Wang, G.T., Singh, V.P., Guo, C. and Haung, K.X. 1991.** Discrete linear models for runoff and sediment discharge from the Loess plateau of China. *Journal of Hydrology*, **127**: 153-171.
- Ward, A.D., Haan, C.T. and Tapp, J.S. 1979.** The DEPOSITS sedimentation pond design manual. University of Kentucky, Lexington, USA.
- Warner, R.C., Wilson, B.N., Barfield, B.J., Lostdon, D.S. and Nebgen, P.J. 1982.** A hydrology and sedimentology watershed model. Part II: Users' manual, University of Kentucky, Department of Agricultural Engineering, Special publication, Lexington, USA.
- Water Resources Research Center (WRRC),** Water Year Reports, 1969-1970 to 1994-1995. Water Resources Management organization, Ministry of Energy, Iran. (Translation of original reports in Persian).
- Williams, G. P. 1989.** Sediment concentration versus water discharge during single hydrologic events in rivers. *Journal of Hydrology*. **111**: 89-106.
- Williams, J. R. 1972.** Concept of A technique for an analysis of watershed runoff events. *In: Second international hydrology symposium (decisions with inadequate hydrologic data): Proceeding*, water resources publication: 111-120.

- Williams, J.R., 1974.** Predicting sediment yield frequency for rural basins to determine man's effect on long-term sedimentation. *In: Paris symposium on Effects of man on the interface of the hydrological cycle with the physical environment: Proceedings, IAHS-AISH Publication, 113: 105-108.*
- Williams, J. R. 1975.** Sediment routing for agricultural watersheds. *Water resources research bulletin.* American Water Resources Association, **11(5): 965-974.**
- Williams, J. R. 1975.** Sediment-yield prediction with universal equation using runoff energy factor. *In: Sediment-Yield Workshop: Proceeding, USDA Sedimentation Laboratory, Oxford, Mississippi, USA.*
- Williams, J.R. 1977.** Sediment Delivery Ratios Determined with Sediment and Runoff Models. Publication No. 122, Wallingford, England: International Association of Scientific Hydrology, pp. 168-178.
- Williams, J.R. 1978.** A sediment graph model based on an instantaneous unit sediment graph. *Water Resources Research, 14(4): 659-664.*
- Williams, J.R. 1981.** Hydrology and sediment transport in small watersheds. *In: the national conference on Agricultural Management and Water Quality: Proceedings, Ames, IA.*
- Williams, J.R. and Arnold, J. G. 1993.** A system of Hydrologic models. *In: Federal Interagency Workshop on Hydrologic Modeling Demands for the 90's: proceedings. USA.*
- Williams, J.R. and Berndt, H.D. 1972.** Concept of a technique for an analysis of watershed runoff events. *In: Decisions with an inadequate hydrologic data: Proceedings of the second international symposium in hydrology, pp. 111-120.*
- Williams, J.R. and Berndt, H.D. 1972.** Sediment yield computed with universal equation. *Journal of Hydraulic Division, ASCE, 98(HY12): 2087-2098.*
- Williams, J.R. and Berndt, H.D. 1976.** Determining the universal soil loss equation's length-slope factor for watersheds. *Soil Conservation Society of America, Ankeny, Iowa, pp. 217-225.*
- Williams, J.R. and Berndt, H.D. 1977.** Sediment yield prediction based on watershed hydrology. *Transactions of the ASAE, 20(6):1100-1104.*
- Williams, J. R., Hiler, E.A. and Baird, R.W. 1971.** Prediction of sediment yields from small watersheds. *Transactions of the ASAE, 14(6): 1158-1162.*
- Williams, J.R. and LaSeur, W.E. 1976.** Water yield model using SCS Curve Number. *Journal of Hydraulics Division, ASCE, 102(HY9): 1241-1253.*
- Williams, J.R., Nearing, M., Nicks, A., Skidmore, E., Valentin, C., King, K. and Savabi, R. 1996.** Using soil erosion models for global change studies. *Journal of Soil and Water Conservation, pp. 381-385.*
- Wilson, B.N., Barfield, B.J., Ward, A.D. and Moore, I.D. 1984.** A hydrology and sedimentology watershed model. Part I: Operational format and hydrologic component. *Transactions of the ASAE, pp.1378-1384.*

- Wilson, B.N., Barfield, B.J., Ward, A.D. and Moore, I.D. 1984.** A hydrology and sedimentology watershed model. Part II: Sedimentology component. *Transactions of the ASAE*, pp.1370-1377.
- Wilson, B.N., Barfield, B.J., Warner, A.D. and Moore, I.D. 1981.** SEDIMOT II: A design hydrology and sedimentology model for surface mine lands. In: Surface Mining Hydrology, Sedimentology and Reclamation: proceeding, Univ. of Kentucky, Lexington, USA.
- Wischmeier, W.H. 1975.** Estimating of soil loss equations cover and management factor for undisturbed lands. In Present and Perspective Technology for Predicting Sediment Yields and Sources, pp.118-125. USDA, ARS-S-40.
- Wischmeier, W.H. and Smith, D.D. 1958.** Rainfall energy and its relationship to soil loss. *Transactions AGU*, 39:285-291.
- Wischmeier, W.H. and Smith, D.D. 1965.** Predicting rainfall-erosion losses from cropland east of the Rocky Mountains. Agriculture Handbook 282. USDA-ARS.
- Wong, T.S.W. and Chen, C.N. 1997.** Time of concentration formula for sheet flow of varying flow regime. *Journal of Hydrologic Engineering*, 2(3): 136-139.
- Wood, M.K. and Blackburn, W.H. 1984.** An evaluation of the hydrological soil groups as used in SCS runoff method on range lands. *Water Resources Bulletin*, 20(3):379-389.
- Woolhiser, D. A. and Todorovic, P. 1971.** A stochastic model for sediment yield for ephemeral streams. In: International Association for Statistics in Physical Science Symposium: Proceeding, Tuscon, Arizona.
- Wu, T.H. Hall, J.A. and Bonta, J.V. 1993.** Evaluation of runoff and erosion models. *Journal of Irrigation and Drainage Engineering*, 119(4): 364-382.
- Yoo, K.H., Yoon, K.S. and Soileau, J.M. 1993.** Runoff curve numbers determined by three methods under conventional and conservation tillage's. *Transactions of the ASAE*. 36(1): 57-63.
- Zigg, A.W. 1940.** Degree and length of land slope as it affects soil loss in runoff. *Agrcultural Engineering*, 21: 59-64.
- Zoch, R.T. 1937.** On the relation between rainfall and stream flow. *Monthly Weather Rev.*, Vol. 65.
- Zollweg, J. A., Gburek, W.J. and Steenhuis, T.S. 1996.** Smormod-A GIS-integrated rainfall-runoff model. *Transactions of the ASAE*. 39(4): 1299-1307.

APPENDICES

Appendix A Discrete sediment data in Amameh watershed (Kamarkhani station)

Table A Discrete Sediment data in Amameh watershed (Kamarkhani station)

Date	Discharge (m ³ /s)	Sed. Con. (mg/litter)	Sed. dis. (t/day)	Date	Discharge (m ³ /s)	Sed. Con. (mg/litter)	Sed. dis. (t/day)
29/11/70	0.176	25.680	0.391	16/4/72	2.069	470.000	84.030
29/11/70	0.176	20.320	0.309	16/4/72	2.069	294.000	52.564
30/11/70	0.177	19.512	0.298	27/4/72	2.237	134.000	25.896
30/11/70	0.177	6.250	0.096	28/4/72	1.662	148.000	21.252
15/12/70	0.127	6.349	0.070	28/4/72	1.662	55.000	7.898
15/12/70	0.127	1.753	0.019	3/5/72	1.556	91.500	12.303
16/12/70	0.127	15.745	0.173	3/5/72	1.556	75.000	10.085
16/12/70	0.127	1.459	0.016	4/5/72	1.240	64.000	6.857
29/12/70	0.135	36.070	0.421	4/5/72	1.240	30.000	3.214
29/12/70	0.135	15.143	0.177	7/5/72	0.876	31.500	2.384
30/12/70	0.125	14.667	0.158	7/5/72	0.876	22.000	1.665
30/12/70	0.125	5.051	0.055	11/5/72	0.679	70.000	4.104
12/1/71	0.410	80.476	2.851	11/5/72	0.797	84.000	5.786
12/1/71	0.410	3.453	0.122	11/5/72	0.828	19.000	1.360
13/1/71	0.224	8.350	0.162	17/5/72	0.957	111.400	9.215
13/1/71	0.224	5.260	0.102	17/5/72	0.957	107.400	8.884
14/1/71	0.250	4.715	0.102	18/5/72	1.171	99.400	10.060
14/1/71	0.250	2.220	0.048	18/5/72	1.171	90.290	9.138
30/1/71	0.250	33.865	0.731	27/5/72	0.860	38.000	2.823
30/1/71	0.250	12.860	0.278	30/5/72	0.679	59.000	3.459
31/1/71	0.262	131.610	2.979	6/6/72	0.770	72.000	4.789
31/1/71	0.262	64.500	1.460	18/6/72	0.290	116.000	2.906
1/2/71	0.238	22.330	0.459	19/6/72	0.199	113.000	1.939
1/2/71	0.238	5.130	0.105	24/6/72	0.151	55.000	0.718
13/1/71	0.286	127.320	3.146	2/7/72	0.151	53.000	0.692
13/1/71	0.286	5.240	0.129	9/7/72	0.396	35.000	1.198
14/1/71	0.274	7.730	0.183	14/7/72	0.123	31.000	0.328
14/1/71	0.274	2.560	0.061	26/7/72	0.109	71.000	0.671
16/3/71	1.073	200.000	18.541	10/8/72	0.097	63.410	0.530
16/3/71	1.073	106.000	9.827	3/11/72	0.097	62.710	0.524
28/3/71	1.303	106.000	11.933	3/11/72	0.443	28.000	1.070
29/3/71	1.150	147.000	14.606	3/11/72	0.452	27.930	1.091
14/4/71	1.136	18.000	1.767	3/11/72	0.452	17.000	0.664
14/4/71	1.400	253.000	30.603	5/12/72	0.290	2.710	0.068
14/4/71	1.550	266.000	35.623	6/12/72	0.362	3.000	0.094
4/5/71	1.040	36.000	3.235	31/12/72	0.271	4.000	0.093
5/5/71	2.200	1169.000	222.204	18/1/74	0.391	3.740	0.126
6/5/71	1.118	47.000	4.540	21/1/74	0.097	9.230	0.077
17/5/71	1.125	23.000	2.236	26/1/74	0.300	9.000	0.233
18/5/71	0.936	40.000	3.235	14/2/74	0.331	75.000	2.143
17/10/71	0.125	52.000	0.562	15/2/74	0.403	58.880	2.050
19/10/71	0.145	52.000	0.652	1/3/74	0.352	33.430	1.017
1/11/71	0.104	37.770	0.340	11/5/74	1.439	19.000	2.362
5/12/71	0.126	40.370	0.440	12/5/74	1.417	112.000	13.712
28/12/71	0.085	62.860	0.459	31/5/74	0.797	331.000	22.802
1/2/72	0.175	94.280	1.426	31/5/74	0.737	23.010	1.465
12/3/72	0.581	96.200	4.825	1/6/74	1.353	21.820	2.551
7/4/72	2.342	191.000	38.654	9/6/74	0.860	58.000	4.309
7/4/72	2.342	125.000	25.297	19/6/74	0.516	71.000	3.168

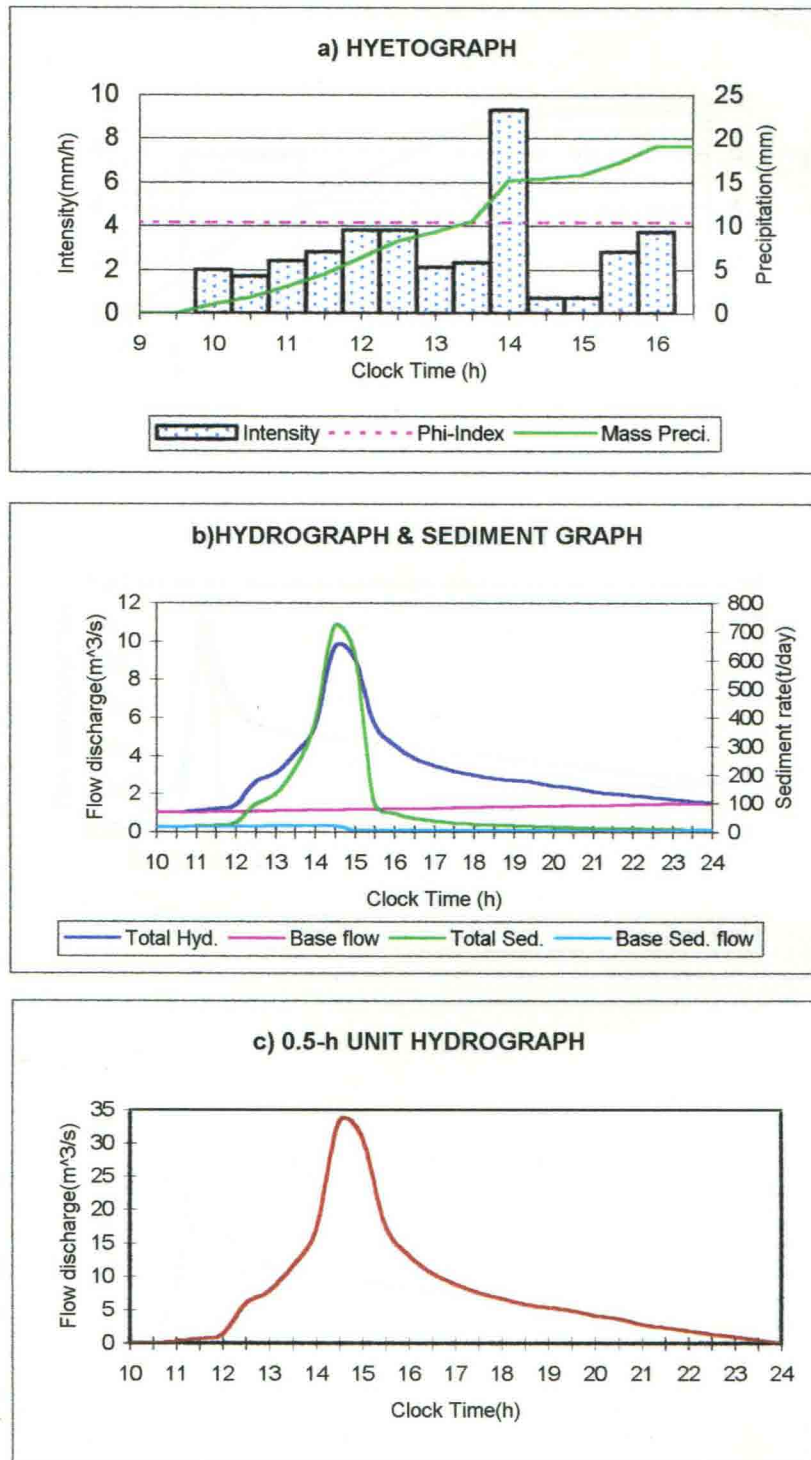
Continued Table A

Date	Discharge (m ³ /s)	Sed. Con. (mg/litter)	Sed. dis. (t/day)	Date	Discharge (m ³ /s)	Sed. Con. (mg/litter)	Sed. dis. (t/day)
18/6/74	0.123	15.410	0.163	13/1/76	0.287	49.000	1.215
18/6/74	0.123	5.000	0.053	30/3/76	0.851	176.000	12.941
22/2/75	0.212	9.000	0.165	4/4/76	1.278	526.000	58.080
18/3/75	0.450	45.000	1.750	4/4/76	1.278	374.000	41.297
26/3/75	0.957	110.000	9.099	9/4/76	2.835	438.000	107.285
27/3/75	0.828	42.000	3.006	11/4/76	2.730	188.000	44.344
23/4/75	1.079	10.000	0.932	12/4/76	2.011	219.000	38.051
23/4/75	1.107	7.000	0.670	2/5/76	5.712	4806.000	2371.842
23/4/75	0.874	41.000	3.096	3/5/76	5.625	1430.000	694.980
23/4/75	0.912	74.000	5.831	20/5/76	1.522	116.000	15.254
8/5/75	0.912	30.000	2.364	10/6/76	1.367	157.000	18.543
9/5/75	0.864	38.000	2.837	29/4/80	1.987	237.000	40.691
15/5/75	0.761	39.000	2.564	29/4/80	1.426	172.000	21.192
22/5/75	0.643	23.000	1.278	7/6/80	1.213	133.000	13.939
23/5/75	0.720	22.000	1.369	7/6/80	0.991	98.000	8.390
6/6/75	1.156	370.000	36.955	5/7/80	0.359	58.000	1.799
6/6/75	1.156	206.000	20.575	5/7/80	0.359	61.000	1.892
12/6/75	0.851	424.000	31.175	8/5/80	1.804	271.000	42.240
13/6/75	1.115	434.000	41.810	13/6/80	1.239	94.000	10.063
18/6/75	0.762	44.000	2.897	11/3/83	2.062	1624.000	289.327
19/6/75	0.762	6.000	0.395	17/3/83	1.219	196.000	20.643
20/6/75	0.729	48.000	3.023	3/4/83	1.063	160.000	14.695
20/6/75	0.819	30.000	2.123	4/4/83	1.316	192.000	21.831
26/6/75	0.506	7.000	0.306	25/4/83	1.471	225.000	28.596
4/7/75	0.176	8.000	0.122	25/4/83	2.080	38.000	6.828
27/7/75	0.109	5.000	0.047	25/4/83	1.589	389.000	53.406
4/11/75	0.191	6.000	0.099	25/4/83	2.033	923.000	162.134
18/11/75	0.230	9.000	0.179	25/4/83	2.033	521.000	91.519
19/11/75	0.291	34.000	0.855	1/5/83	1.942	109.000	18.286
28/1/76	0.698	56.000	3.377	2/5/84	1.852	38.000	6.080
18/1/76	0.407	7.000	0.246	22/5/84	0.902	604.000	47.071
29/3/76	1.460	329.000	41.501	28/5/84	0.890	923.000	70.975
30/3/76	1.291	31.000	3.458	1/6/84	1.852	25.000	4.000
31/3/76	1.025	485.000	42.947	23/8/84	1.897	653.000	107.005
4/4/76	1.130	28.000	2.734	1/12/84	1.060	24.000	2.197
4/4/76	0.991	163.000	13.955	3/3/90	1.852	38.000	6.080
5/4/76	0.991	60.000	5.137	4/3/90	1.852	100.000	16.001
9/4/76	1.203	48.000	4.989	25/3/90	2.174	215.000	40.381
9/4/76	1.203	16.000	1.663	4/4/90	1.987	51.000	8.756
15/4/76	1.168	21.000	2.119	29/4/90	2.417	205.000	42.815
22/4/76	0.860	24.000	1.783	15/4/90	2.080	70.000	12.577
23/4/76	1.310	67.000	7.583	22/5/90	1.897	619.000	101.433
30/4/76	0.917	21.000	1.664	30/5/90	2.417	205.000	42.815
14/5/76	1.018	137.000	12.050	27/3/91	2.174	71.000	13.335
22/6/76	0.936	25.000	2.022	24/4/91	0.310	130.000	3.483
22/6/76	0.601	39.000	2.025	24/4/91	0.310	31.000	0.831
22/6/76	0.720	13.000	0.809	24/4/91	1.987	63.000	10.817
22/6/76	0.720	10.000	0.622	4/7/91	0.568	54.000	2.651
13/11/76	0.175	58.000	0.877	4/7/91	0.568	31.000	1.522

Continued Table A

Date	Discharge (m ³ /s)	Sed. Con. (mg/litter)	Sed. dis. (t/day)	Date	Discharge (m ³ /s)	Sed. Con. (mg/litter)	Sed. dis. (t/day)
3/4/92	1.721	42.000	6.245	*	1.118	541.642	52.320
13/4/92	1.721	126.000	18.735	*	1.125	22.634	2.200
14/4/92	3.047	875.000	230.361	*	0.936	40.188	3.250
18/4/92	2.417	289.000	60.359	*	0.58	95.985	4.810
3/6/92	2.417	518.000	108.187	*	2.34	157.981	31.940
18/6/92	2.518	647.000	140.753	*	2.07	411.019	73.510
20/4/92	2.467	479.000	102.115	*	2.24	133.980	25.930
22/4/92	2.620	396.000	89.649	*	1.66	80.809	11.590
22/4/92	2.620	257.000	58.181	*	1.47	69.996	8.890
29/4/92	2.467	6740.000	1436.856	*	1.71	83.997	12.410
14/4/93	3.047	1666.000	438.607	*	1.78	18.987	2.920
*	0.173	23.416	0.350	*	2.04	110.975	19.560
*	0.177	13.078	0.200	*	2.04	107.003	18.860
*	0.127	3.645	0.040	*	1.17	99.023	10.010
*	0.127	6.379	0.070	*	1.17	90.021	9.100
*	0.135	22.291	0.260	*	1.47	58.973	7.490
*	0.125	8.333	0.090	*	1.85	37.975	6.070
*	0.41	29.076	1.030	*	0.77	72.000	4.790
*	0.224	7.234	0.140	*	0.62	115.927	6.210
*	0.25	3.704	0.080	*	0.43	113.049	4.200
*	0.25	26.852	0.580	*	0.73	48.040	3.030
*	0.262	224.855	5.090	*	1.46	328.989	41.500
*	0.238	154.645	3.180	*	1.29	31.044	3.460
*	0.286	45.325	1.120	*	1.52	484.969	63.690
*	0.274	4.224	0.100	*	1.71	7.987	1.180
*	0.15	51.698	0.670	*	1.46	162.988	20.560
*	0.1	38.194	0.330	*	1.46	60.011	7.570
*	0.13	40.064	0.450	*	1.08	15.968	1.490
*	0.09	63.014	0.490	*	1.08	48.011	4.480
*	0.18	93.879	1.460	*	0.85	176.062	12.930
*	0.19	6.092	0.100	*	1.28	373.987	41.360
*	0.23	9.058	0.180	*	2.84	439.000	107.720
*	0.29	33.924	0.850	*	2.73	187.983	44.340
*	0.7	56.052	3.390	*	2.04	219.000	38.600
*	0.18	57.870	0.900	*	5.71	480.598	237.100
*	0.29	49.090	1.230	*	1.37	156.968	18.580
*	1.22	196.000	20.660	*	1.43	171.992	21.250
*	1.06	159.962	14.650	*	1.21	132.958	13.900
*	1.32	192.024	21.900	*	1.8	271.026	42.150
*	1.47	225.025	28.580	*	1.24	93.993	10.070
*	1.59	389.005	53.440	*	0.32	54.977	1.520
*	1.076	156.938	14.590	*	0.32	53.168	1.470
*	1.303	105.615	11.890	6/4/97	0.86	34.991	2.600
*	1.15	147.142	14.620	6/4/97	0.25	31.019	0.670
*	1.136	17.524	1.720	6/4/97	0.05	71.759	0.310
*	1.4	252.894	30.590	6/4/97	0.05	62.500	0.270
*	1.55	266.353	35.670	6/4/97	0.51	7.035	0.310
*	1.04	36.392	3.270	*	0.36	57.870	1.800

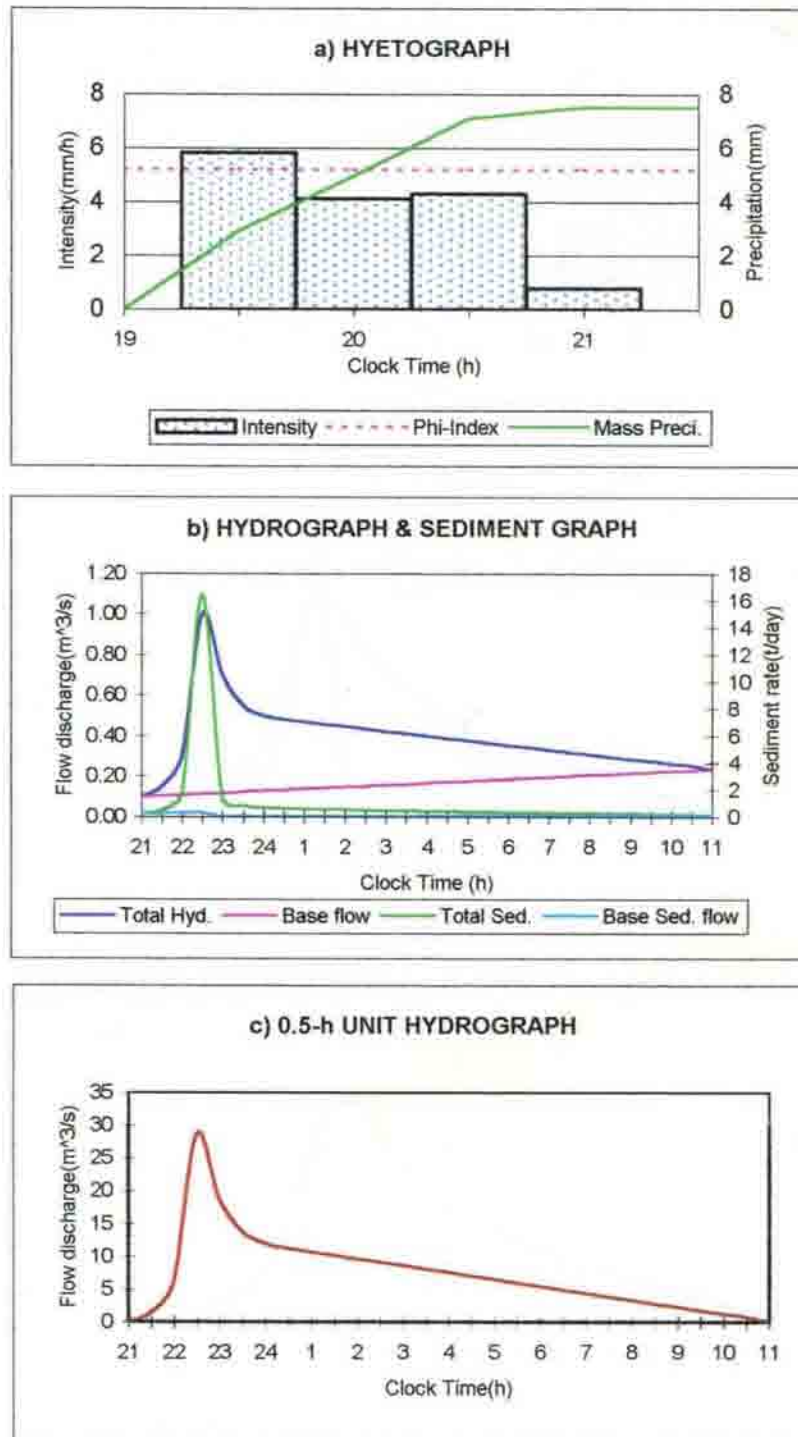
Appendix B Analysis of Hyetograph, Hydrograph and Sediment graph for the selected storms



Depth of the direct runoff=0.257cm
 Effective rainfall duration=0.5h
 Phi index=4.16mm/h

Runoff volume=96480m³
 Peak discharge=8.552m³/s
 Sediment yield=51.407tonnes

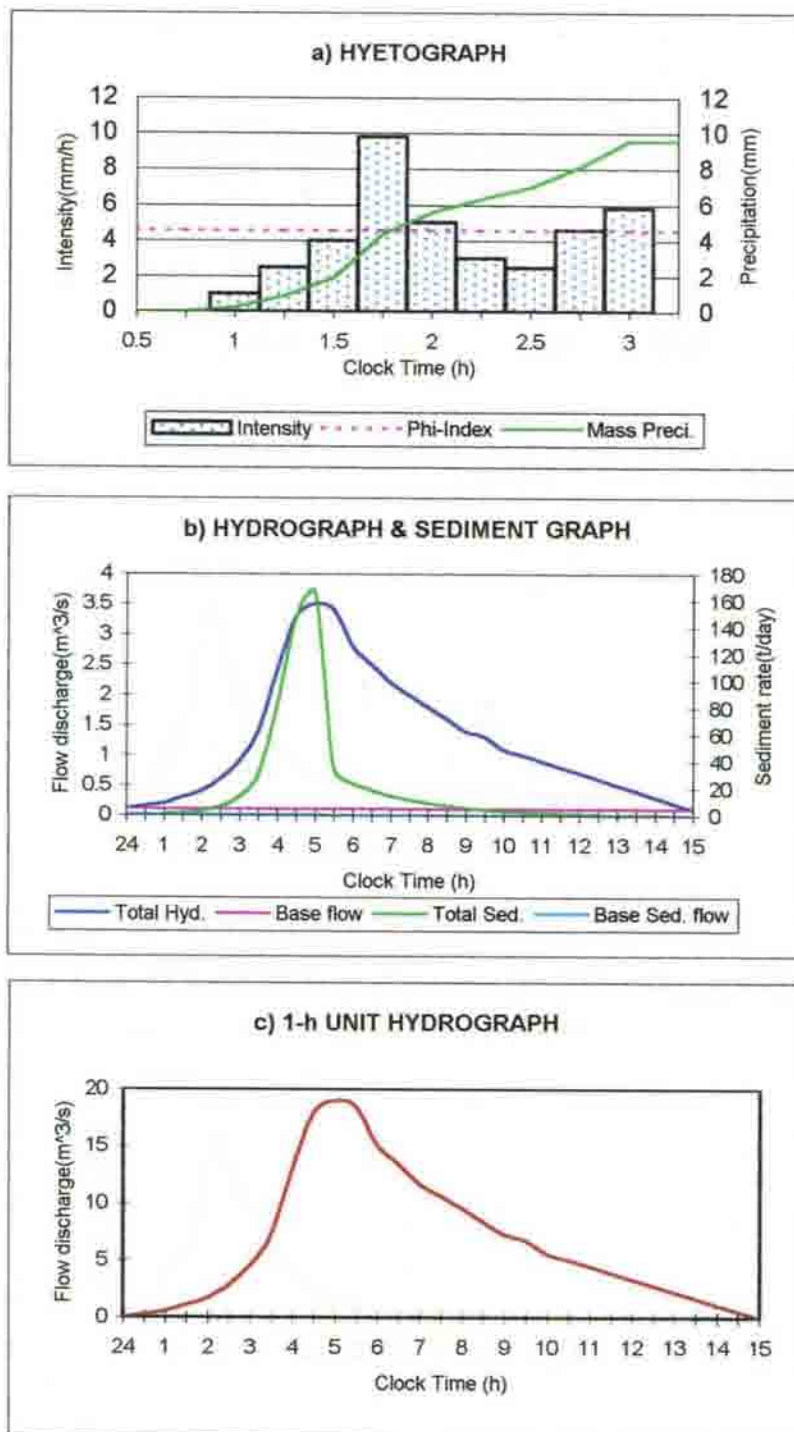
Fig. B-1 Analysis of observed hyetograph, hydrograph and sediment graph for the storm event of April 14,71



Depth of the direct runoff=0.031cm
 Effective rainfall duration=0.5h
 Phi index=5.18mm/h

Runoff volume=11466 m^3
 Peak discharge=0.890 m^3/s
 Sediment yield=0.555tonnes

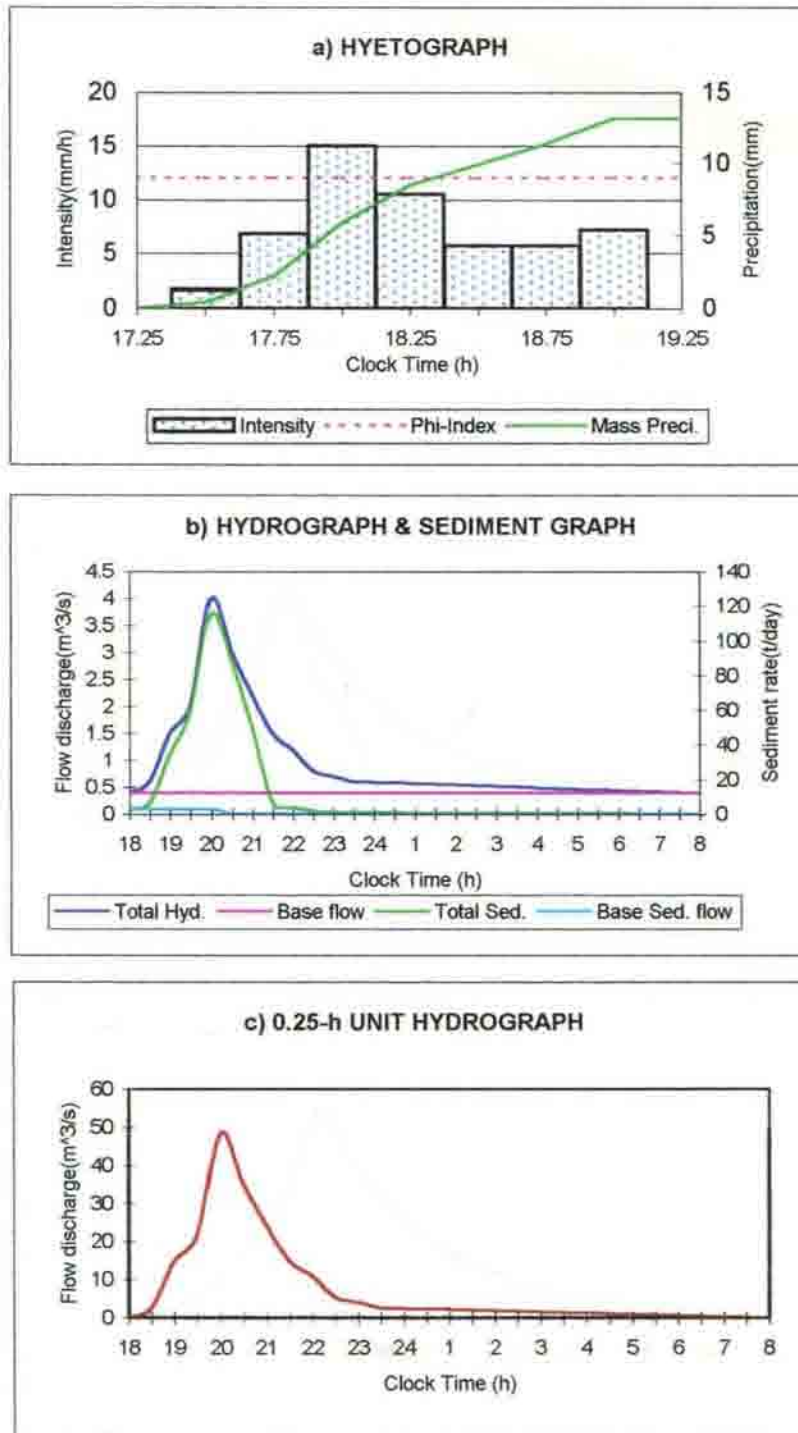
Fig. B-2 Analysis of observed hyetograph, hydrograph and sediment graph for the storm event of August 2, 72



Depth of the direct runoff=0.173cm
 Effective rainfall duration=1h
 Phi index=4.55mm/h

Runoff volume=64350m³
 Peak discharge=3.400m³/s
 Sediment yield=12.380tonnes

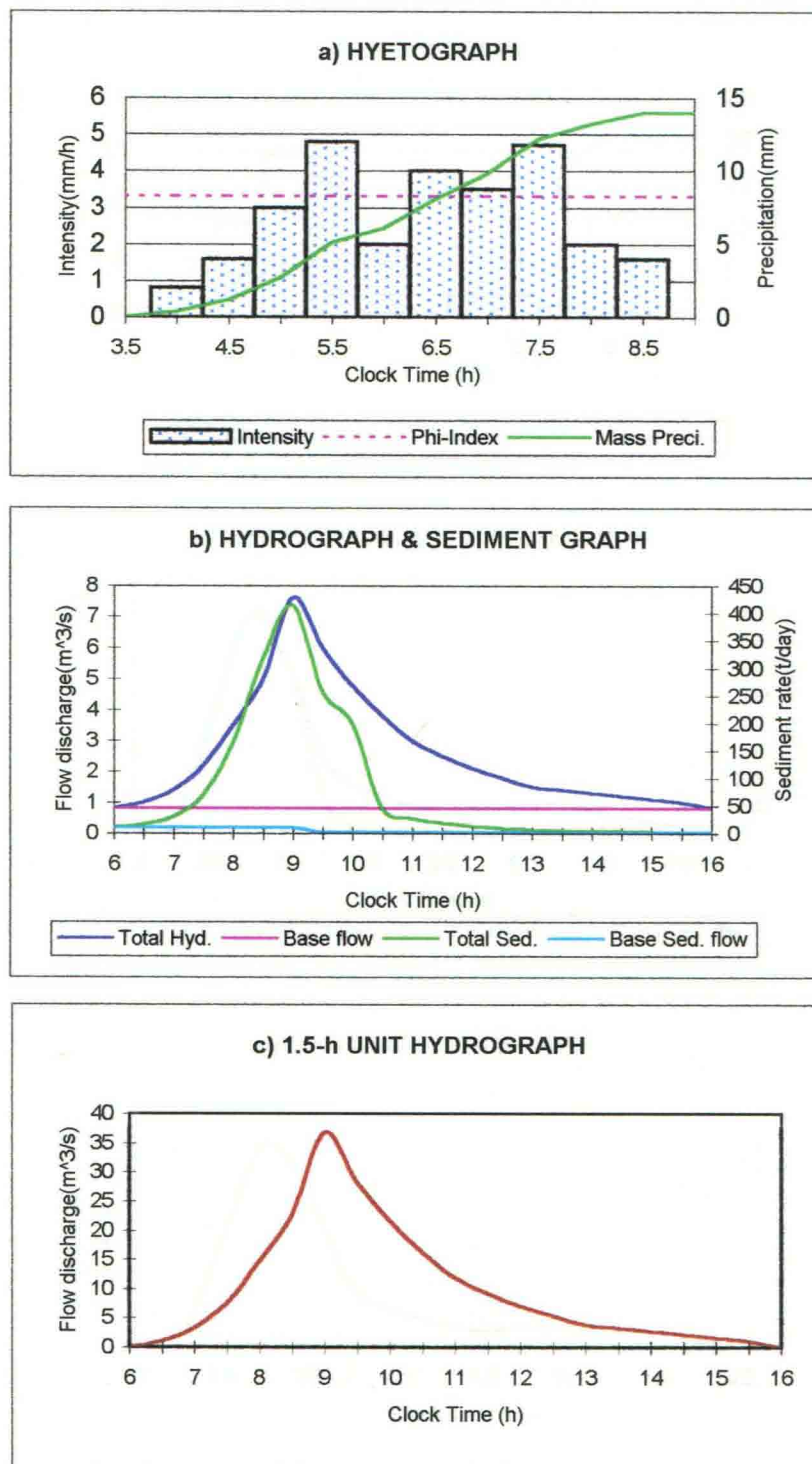
Fig. B-3 Analysis of observed hyetograph, hydrograph and sediment graph for the storm event of Nov. 3, 72



Depth of the direct runoff=0.074cm
 Effective rainfall duration=0.25h
 Phi index=12.03mm/h

Runoff volume=27540m³
 Peak discharge=3.600m³/s
 Sediment yield=7.421tonnes

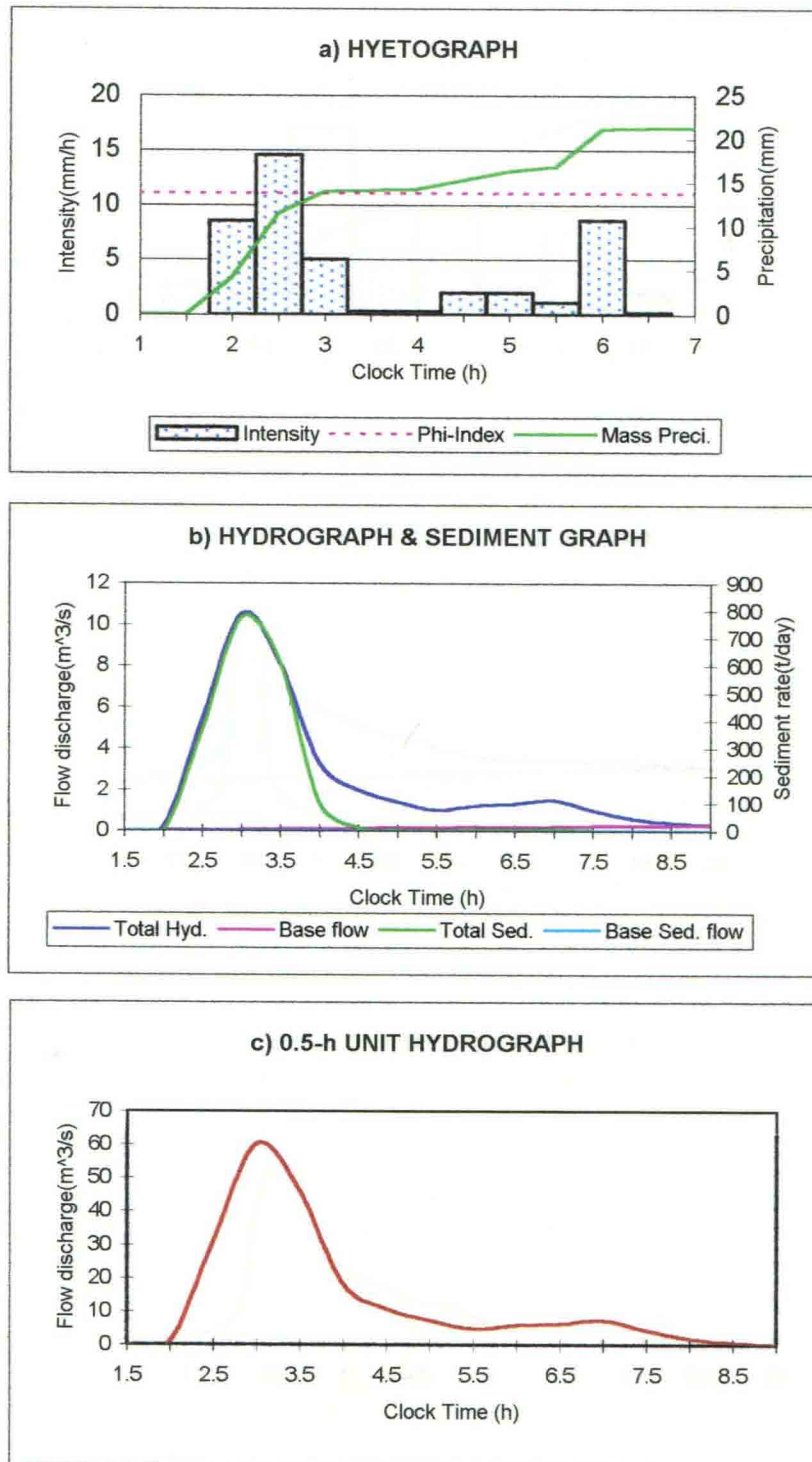
Fig. B-4 Analysis of observed hyetograph, hydrograph and sediment graph for the storm event of July 18,74



Depth of the direct runoff=0.179cm
 Effective rainfall duration=1.5h
 Phi index=3.30mm/h

Runoff volume=66600 m^3
 Peak discharge=6.800 m^3/s
 Sediment yield=31.742tonnes

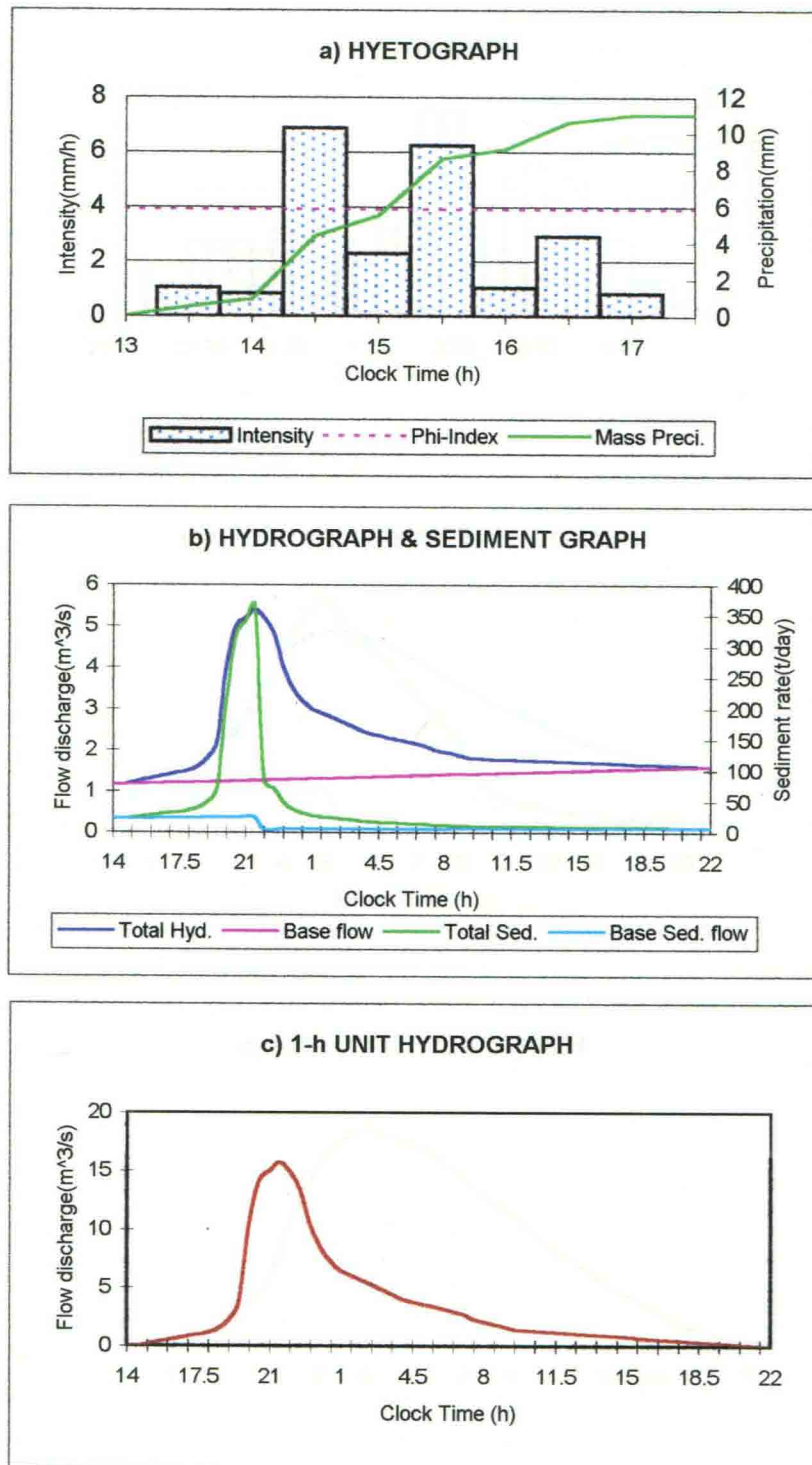
Fig. B-5 Analysis of observed hyetograph, hydrograph and sediment graph for the storm event of April 23, 75



Depth of the direct runoff=0.174cm
 Effective rainfall duration=0.5h
 Phi index=11.03mm/h

Runoff volume=64440m³
 Peak discharge=10.440m³/s
 Sediment yield=39.512tonnes

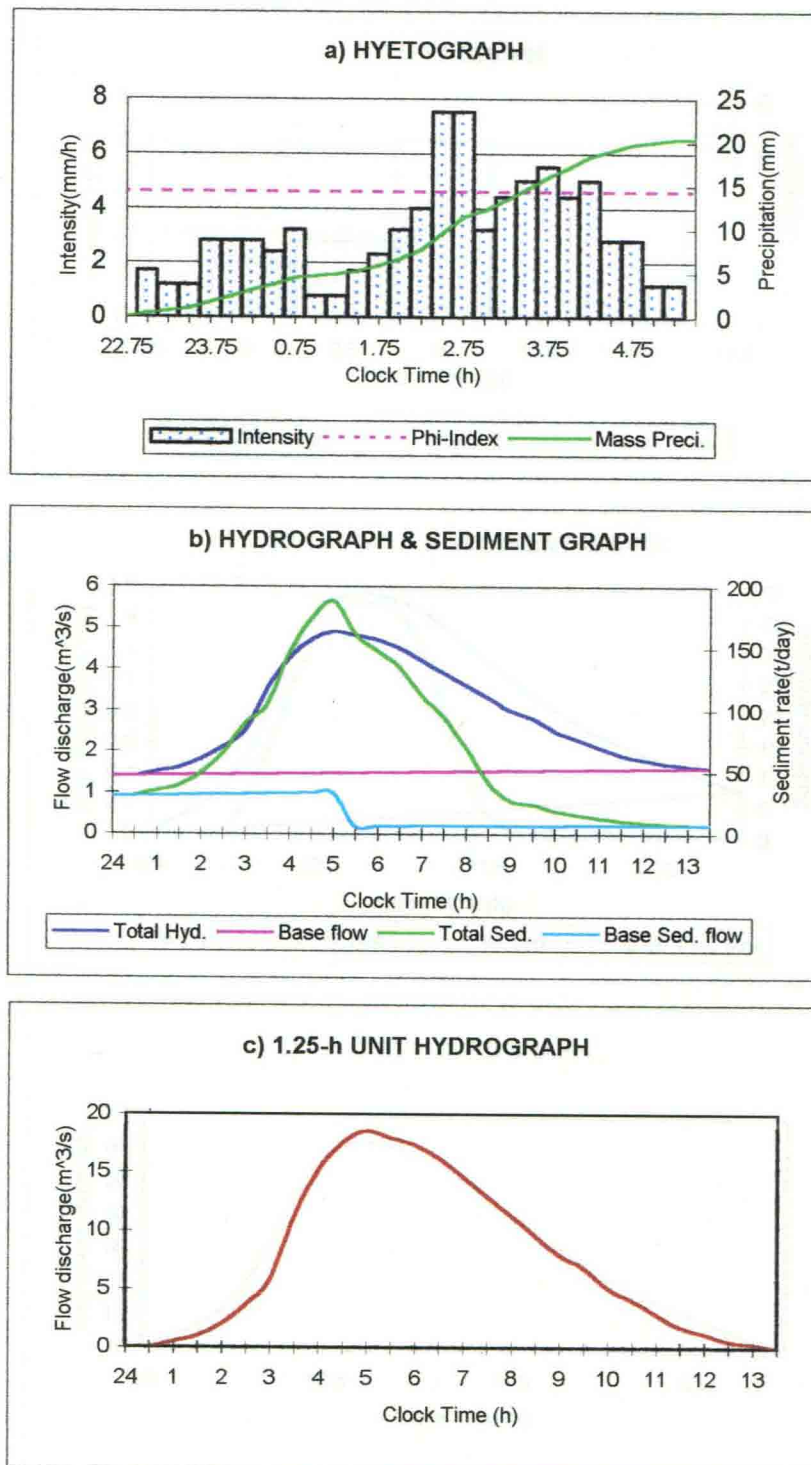
Fig. B-6 Analysis of observed hyetograph, hydrograph and sediment graph for the storm event of July 22, 76



Depth of the direct runoff=0.261cm
 Effective rainfall duration=1h
 Phi index=3.90mm/h

Runoff volume=97065 m^3
 Peak discharge=4.148 m^3/s
 Sediment yield=36.742tonnes

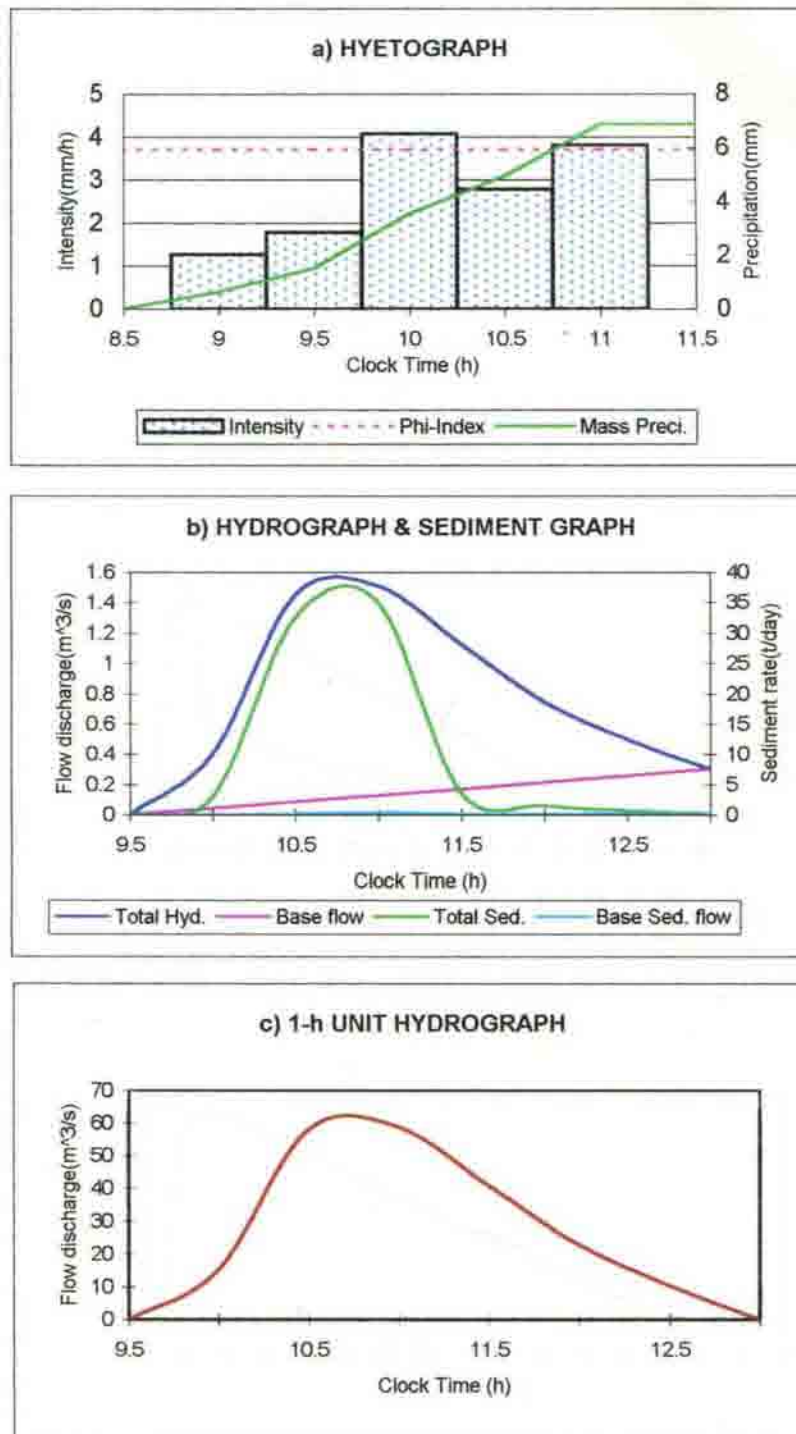
Fig. B-7 Analysis of observed hyetograph, hydrograph and sediment graph for the storm event of April 29,80



Depth of the direct runoff=0.185cm
 Effective rainfall duration=1.25h
 Phi index=4.60mm/h

Runoff volume=68634m³
 Peak discharge=3.432m³/s
 Sediment yield=28.718tonnes

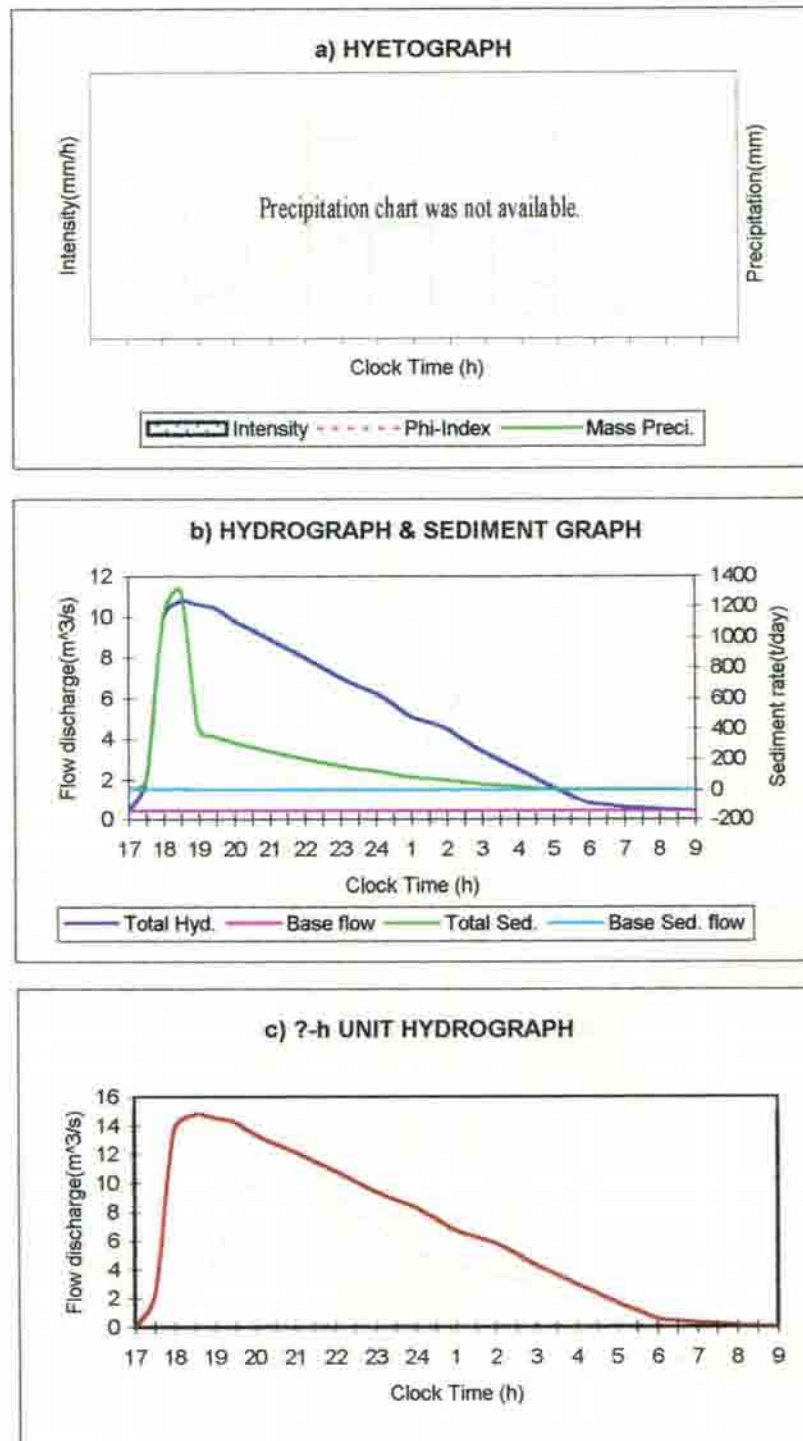
Fig. B-8 Analysis of observed hyetograph, hydrograph and sediment graph for the storm event of April 25, 83



Depth of the direct runoff=0.023cm
 Effective rainfall duration=1h
 Phi index=3.70mm/h

Runoff volume=8712m³
 Peak discharge=1.381m³/s
 Sediment yield=1.575tonnes

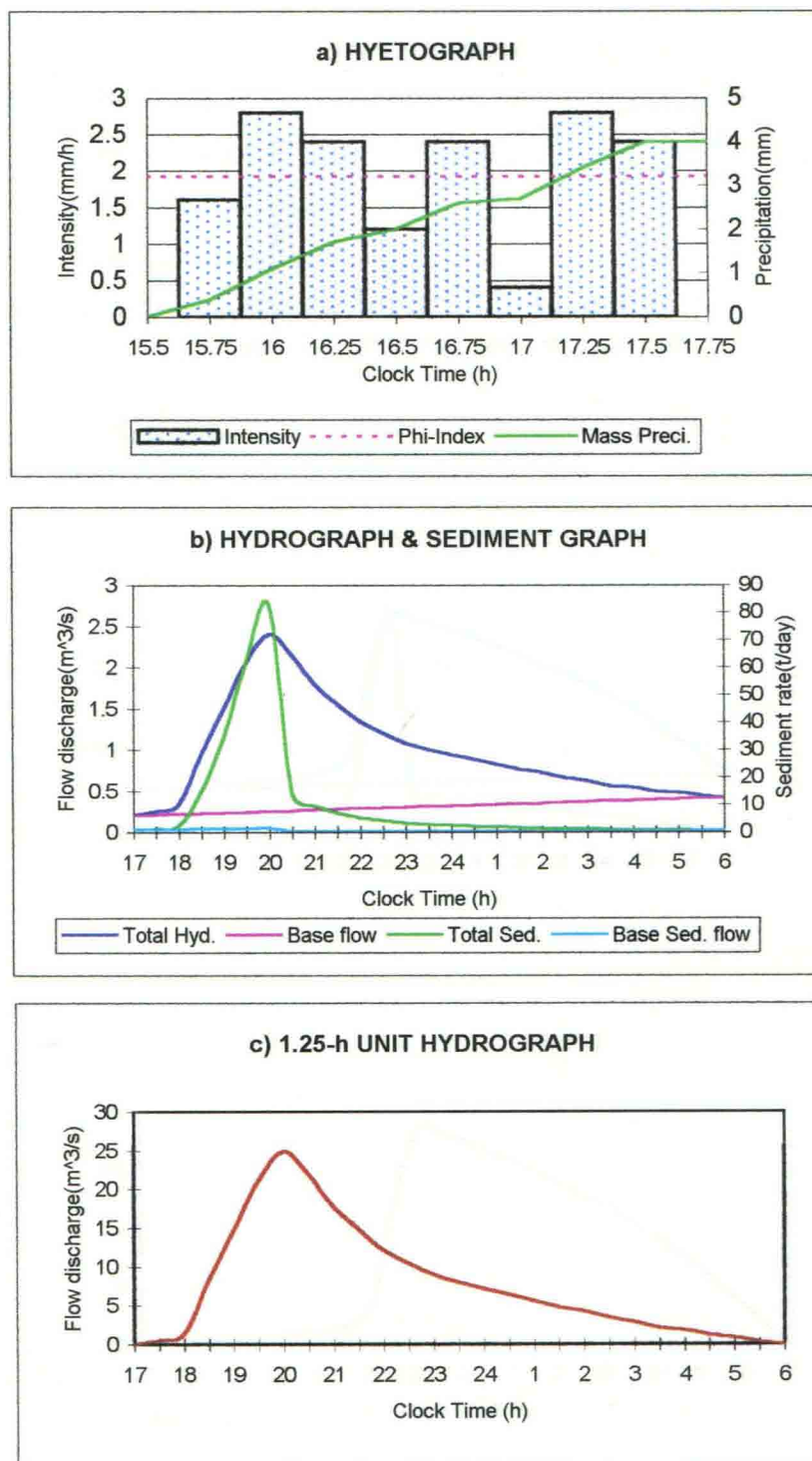
Fig. B-9 Analysis of observed hyetograph, hydrograph and sediment graph for the storm event of May 5, 84



Depth of the direct runoff=0.701cm
 Effective rainfall duration=?h
 Phi index=?mm/h

Runoff volume=260190 m^3
 Peak discharge=10.350 m^3/s
 Sediment yield=115.104tonnes

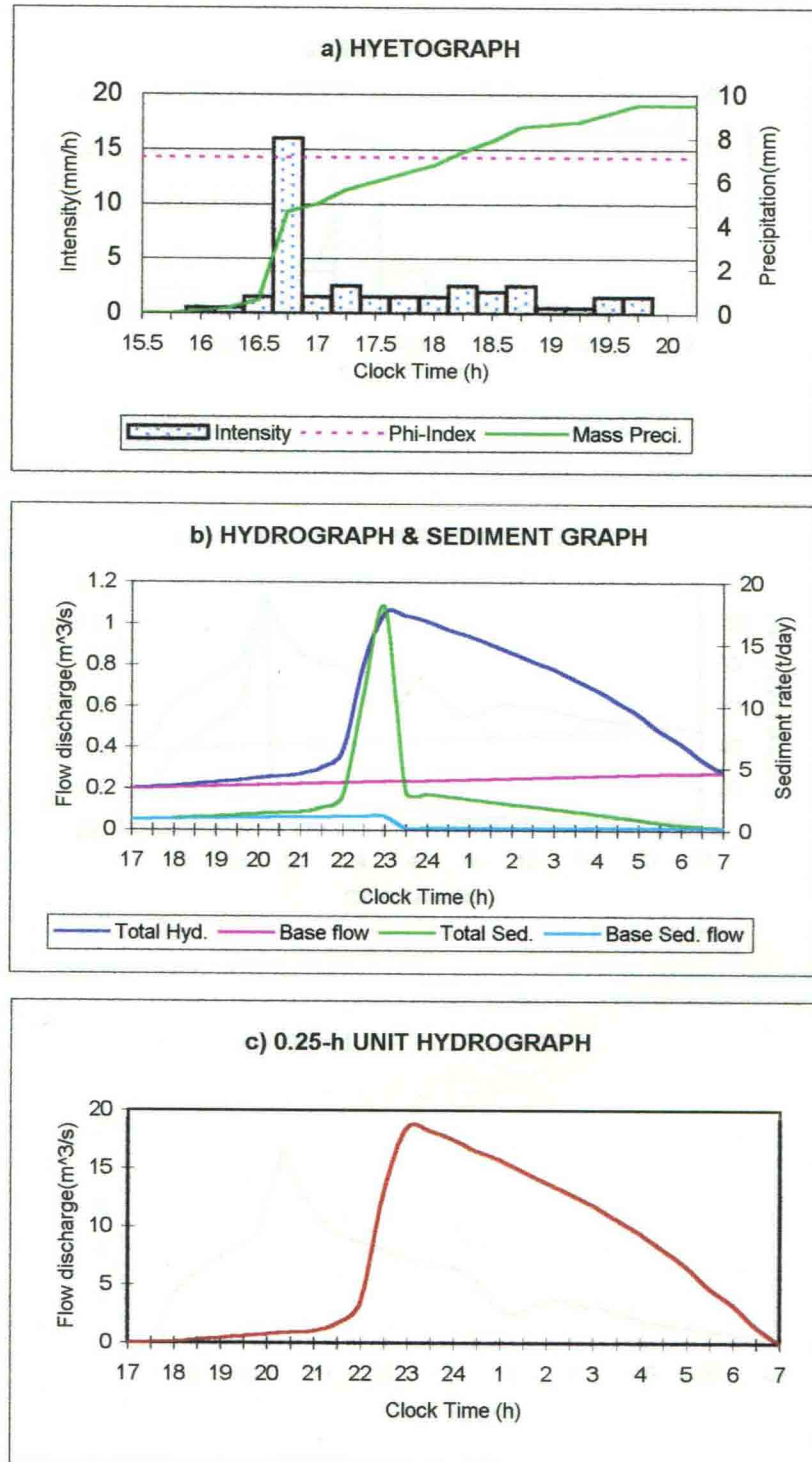
Fig. B-10 Analysis of observed hyetograph, hydrograph and sediment graph for the storm event of August 5,87



Depth of the direct runoff=0.109cm
 Effective rainfall duration=1.25h
 Phi index=1.92mm/h

Runoff volume=32040m³
 Peak discharge=2.149m³/s
 Sediment yield=5.133tonnes

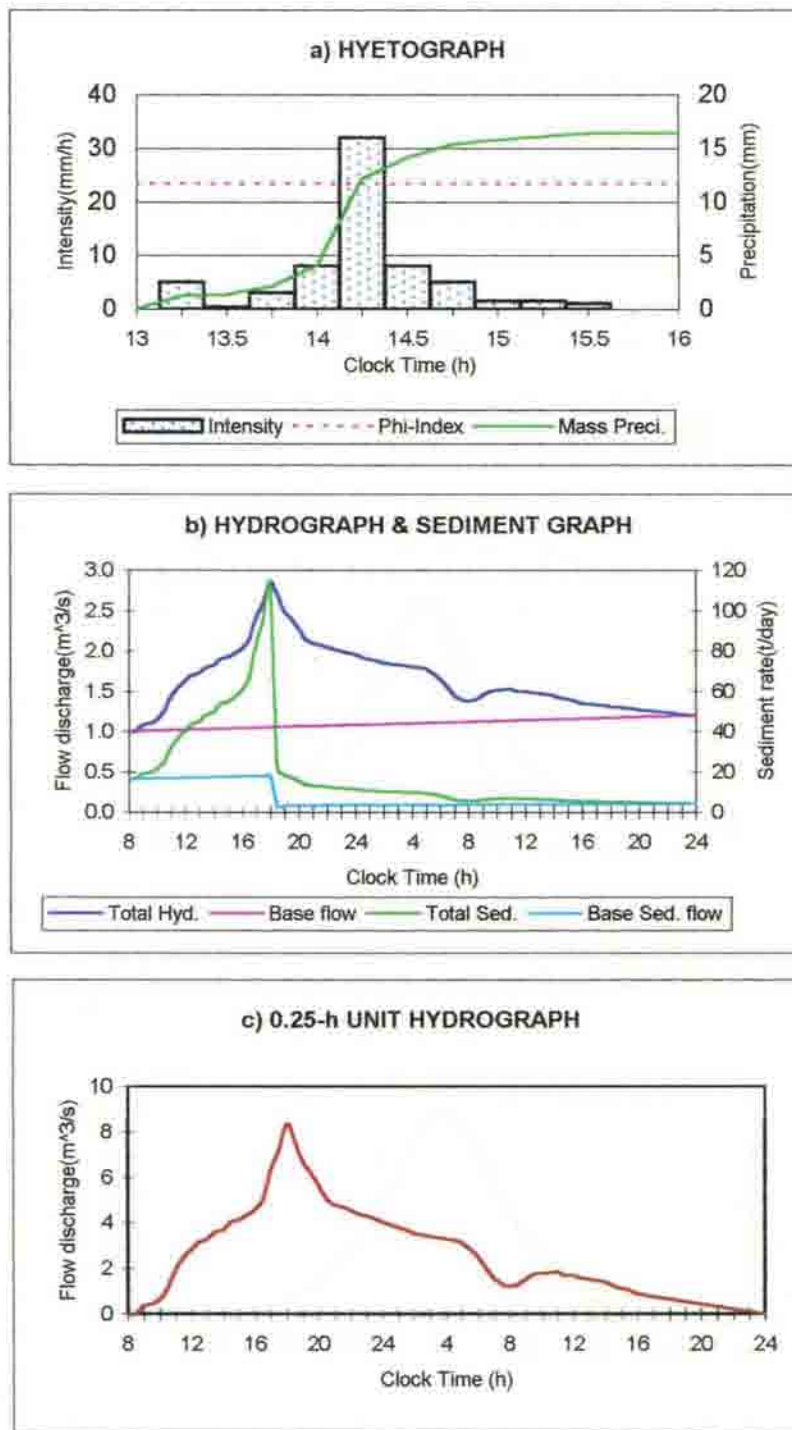
Fig. B-11 Analysis of observed hyetograph, hydrograph and sediment graph for the storm event of July 25,88



Depth of the direct runoff=0.050cm
 Effective rainfall duration=0.25h
 Phi index=14.24mm/h

Runoff volume=16353m³
 Peak discharge=0.816m³/s
 Sediment yield=1.110tonnes

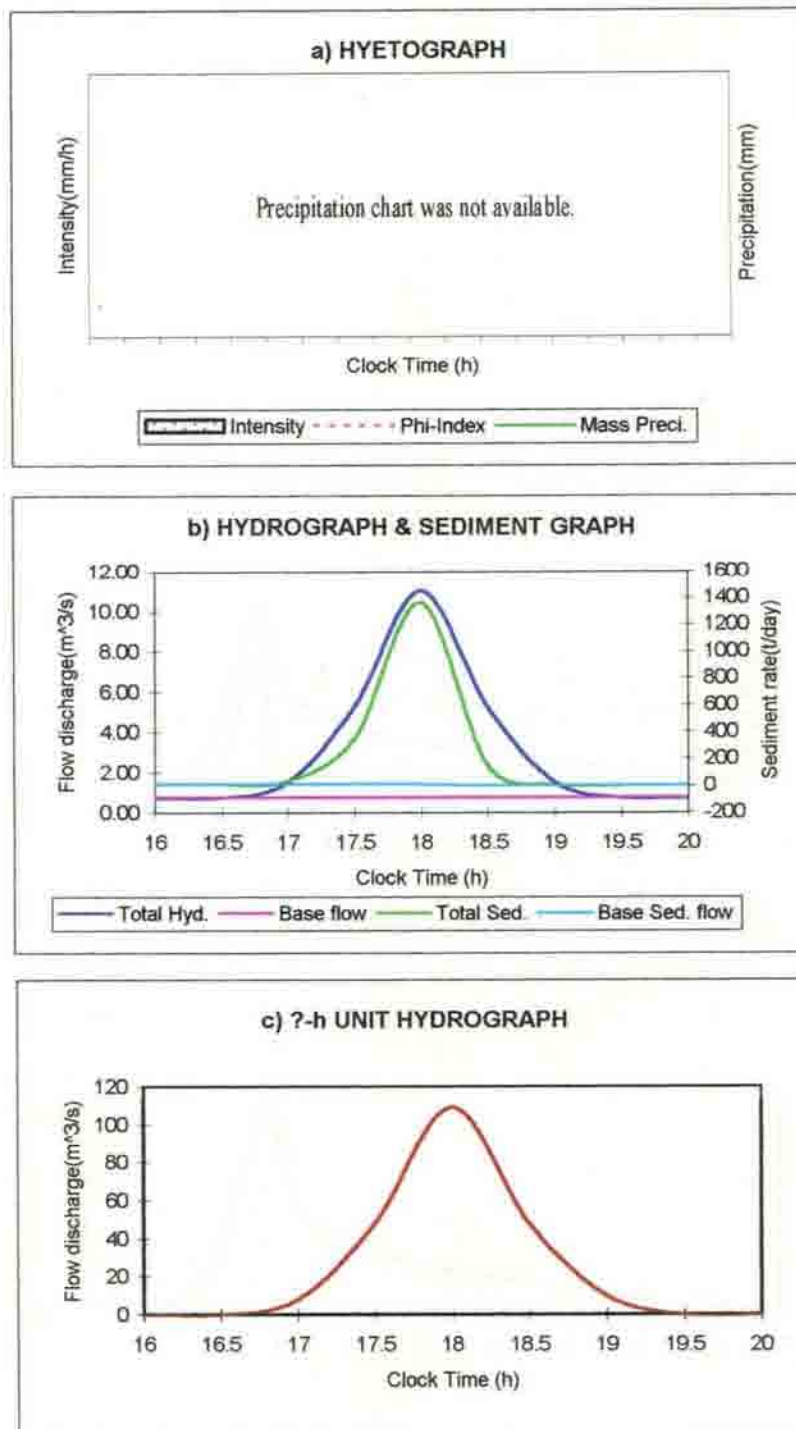
Fig. B-12 Analysis of observed hyetograph, hydrograph and sediment graph for the storm event of Nov. 18,88



Depth of the direct runoff=0.216cm
 Effective rainfall duration=0.25h
 Phi index=23.37mm/h

Runoff volume=80064m³
 Peak discharge=1.800m³/s
 Sediment yield=18.805tonnes

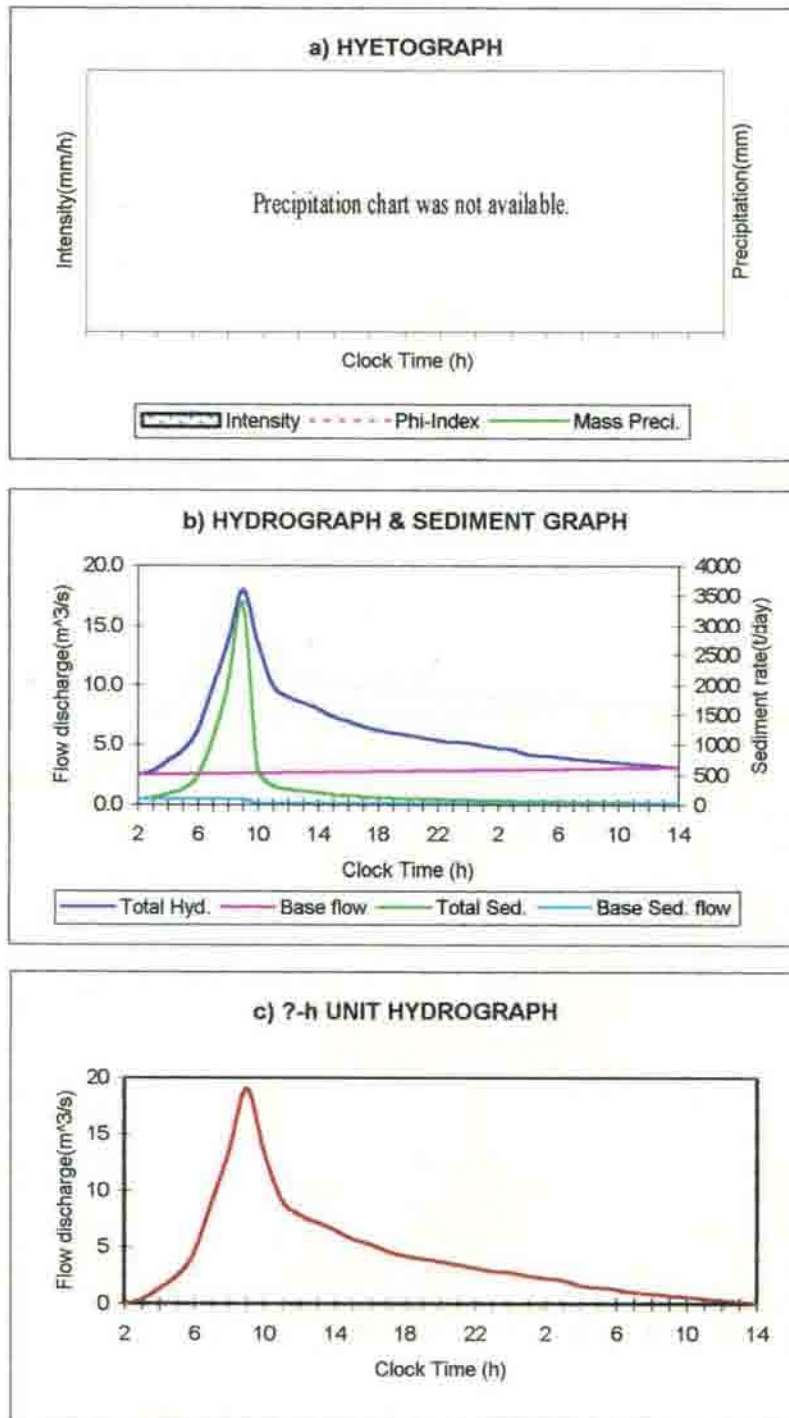
Fig. B-13 Analysis of observed hyetograph, hydrograph and sediment graph for the storm event of March 13, 89



Depth of the direct runoff=0.094cm
 Effective rainfall duration=?h
 Phi index=?mm/h

Runoff volume= 34920m^3
 Peak discharge= $10.250\text{m}^3/\text{s}$
 Sediment yield=36.964tonnes

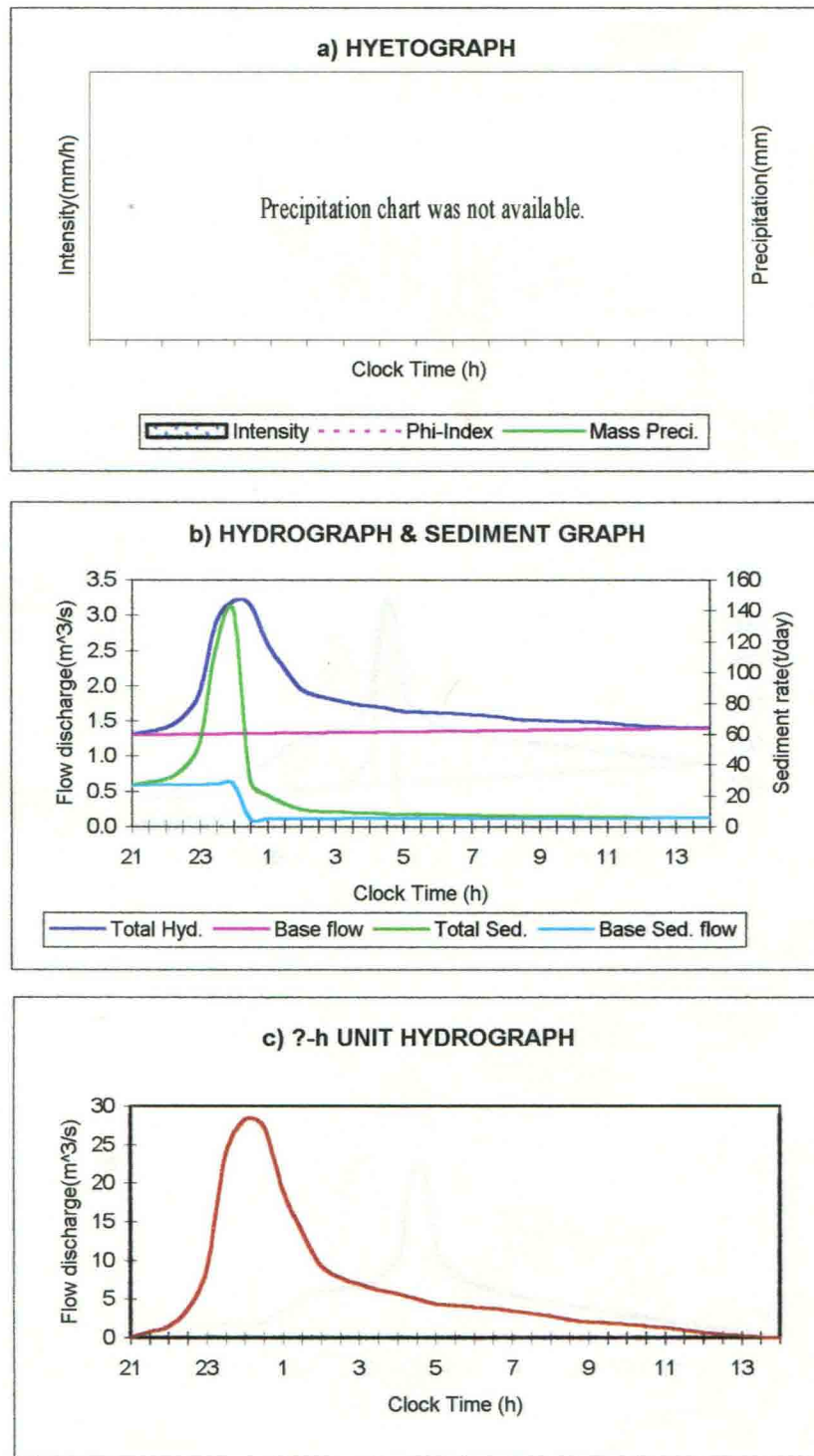
Fig. B-14. Analysis of observed hyetograph, hydrograph and sediment graph for the storm event of Feb. 24,91



Depth of the direct runoff=0.808cm
 Effective rainfall duration=?h
 Phi index=?mm/h

Runoff volume=299880m³
 Peak discharge=13.800m³/s
 Sediment yield=349.583tonnes

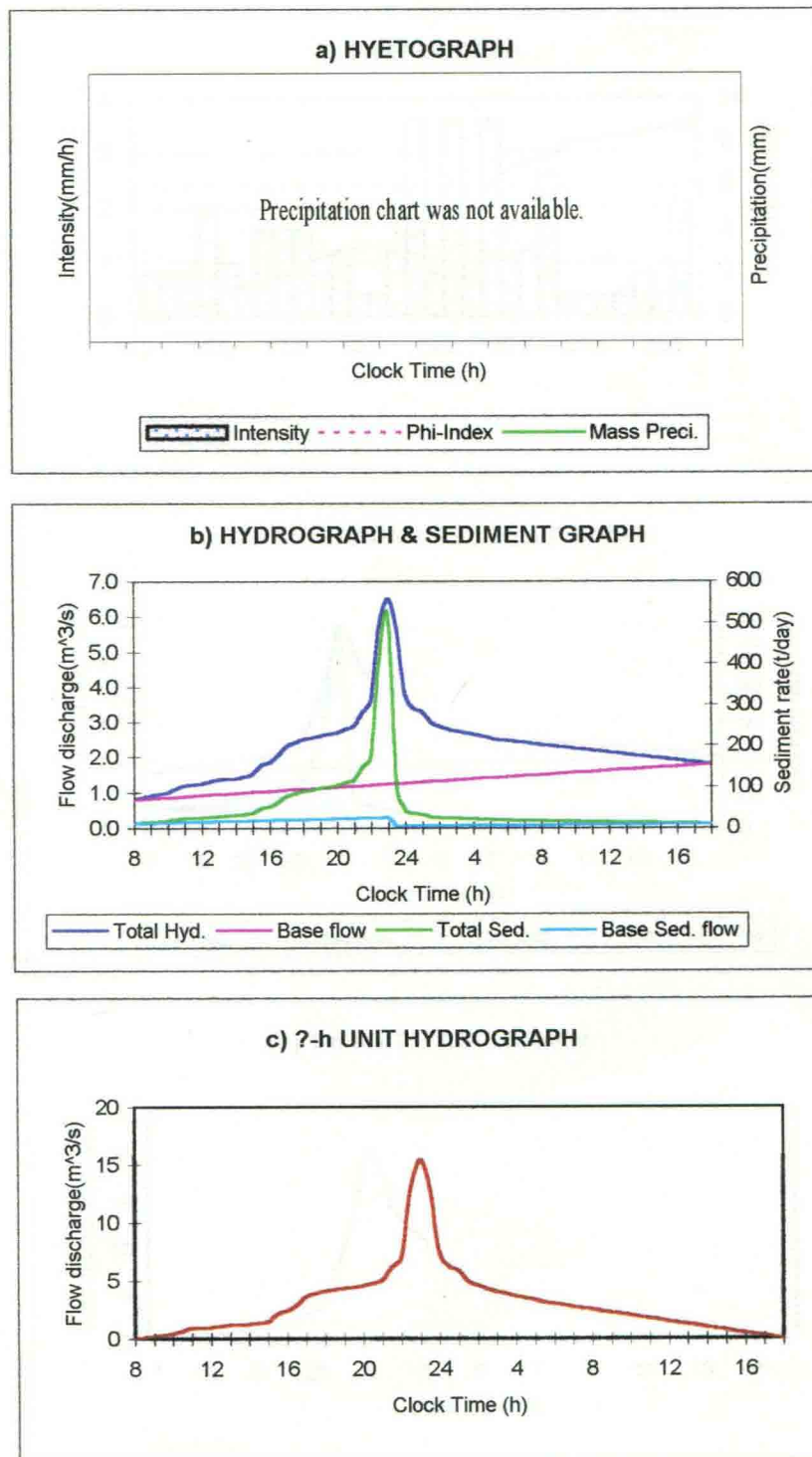
Fig. B-15 Analysis of observed hyetograph, hydrograph and sediment graph for the storm event of April 27, 92



Depth of the direct runoff = 0.067 cm
 Effective rainfall duration = ? h
 Phi index = ? mm/h

Runoff volume = 24822 m^3
 Peak discharge = 1.882 m^3/s
 Sediment yield = 7.130 tonnes

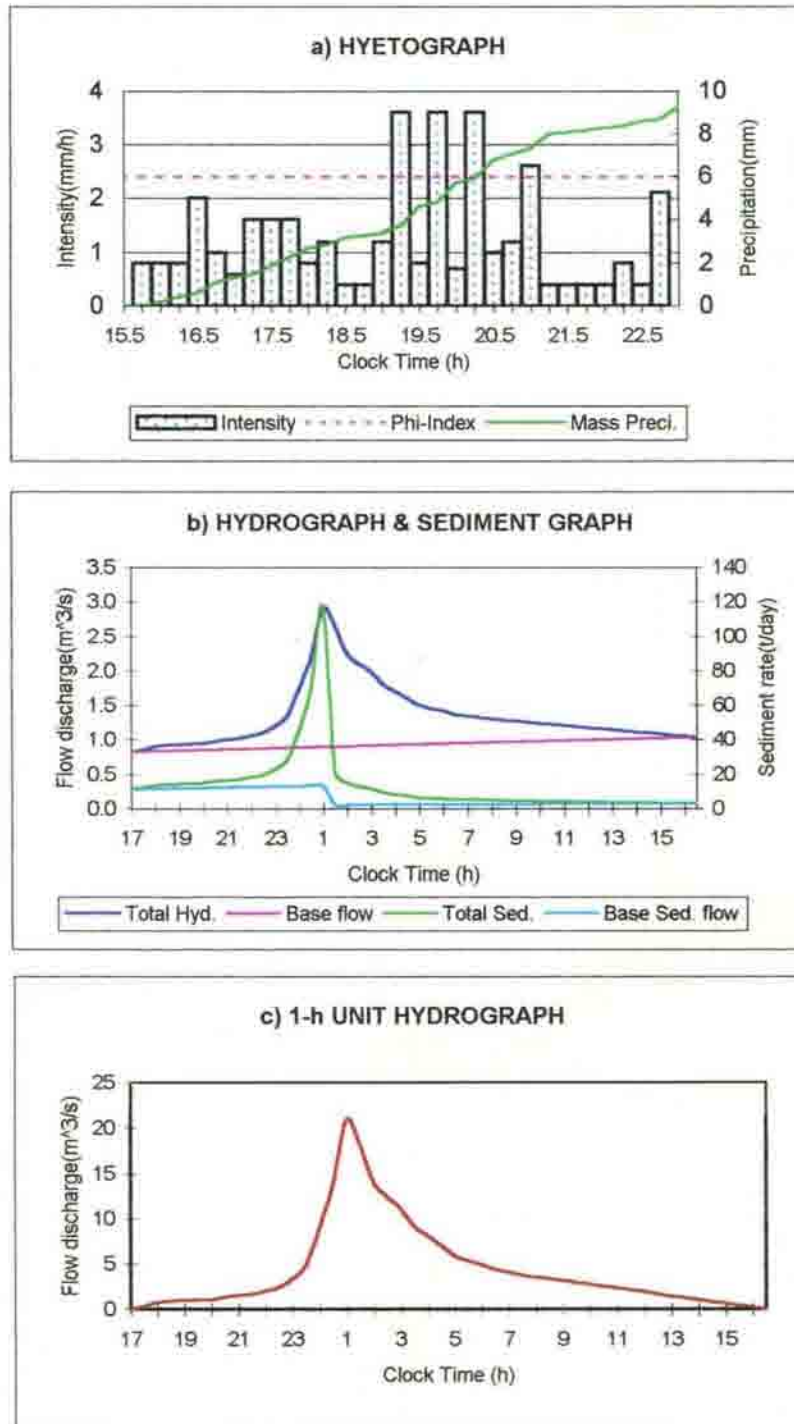
Fig. B-16 Analysis of observed hyetograph, hydrograph and sediment graph for the storm event of May 13, 93



Depth of the direct runoff=0.340cm
 Effective rainfall duration=?h
 Phi index=?mm/h

Runoff volume= 126306m^3
 Peak discharge= $5.259\text{m}^3/\text{s}$
 Sediment yield=53.410tonnes

Fig. B-17 Analysis of observed hyetograph, hydrograph and sediment graph for the storm event of April 30, 94



Depth of the direct runoff=0.096cm
 Effective rainfall duration=1h
 Phi index=2.39mm/h

Runoff volume=35656 m^3
 Peak discharge=2.005 m^3/s
 Sediment yield=7.598tonnes

Fig. B-18 Analysis of observed hyetograph, hydrograph and sediment graph for the storm event of April 6, 97

Appendix C Computer programs

Appendix C-1 Program to calculate sediment routing parameter using Newton technique

```

dimension A(12),Z(12)
open(7,file='parameter Z.dat',status='old')
open(8,file='parameter Z.out',status='new')
n=12
accuracy =0.0001
read(7,*)(A(I),I=1,n)
read(7,*)(Z(I),I=1,n)
101 write(*,*)'GIVE GUESS VALUE'
read(*,*)X0
102 df=0.0
do 10 I=1,n
10 df=df+A(I)*Z(I)*exp(-Z(I)*X0)
df=-df
write(*,*)'VALUE OF df X0 IS ', df
if(abs(df).le. accuracy) go to 110
F=-1.60
do 20 I=1,n
20 F=F+A(I)*exp(-Z(I)*X0)
write(*,*)'VALUE OF F IS' ,F
X=X0-F/DF
if(abs((X-X0)/X).le. accuracy) go to 100
X0=X
Go to 102
110 write(8,*)'df(X0) is 0, Please give another guess value'
go to 101
100 write(8,*)'value of X', X
close(7)
close(8)
stop
end

```

Appendix C-2 Program to predict outflow hydrographs of each sub-watershed

```

dimension DFLOW(33),CN(12),ACN(6),AREA(12),PAREA(6)
dimension run12(33), run11(33), run10(33), run9(33), run8(33)
dimension run7(33),run6(33), run5(33), run4(33), run3(33)
dimension run2(33), run1(33),rj5(33),rj4(33),rj3(33),rj2(33)
dimension rj1(33)
dimension rk(5),x(5),t(5),c0(5), c1(5), c2(5),ratio(12)
dimension rnetm(33),rnet5(33),rnet4(33),rnet3(33),rnet2(33)
dimension rnet1(33)

data DFLOW/0.0,0.0,0.0,0.0,0.0,0.0,0.0,0.011,0.013,0.024,0.816,
$0.857,0.549,0.490,0.462,0.443,0.425,0.406,0.398,0.369,0.351,
$0.322,0.294,0.255,0.227,0.198,0.180,0.151,0.123,0.104,0.076,
$0.037,0.019,0.0 /
data CN/77.47,78.45,78.45,76.47,77.47,30.60,39.11,39.11,64.62,
$76.47,76.47,57.53/
data ACN/67.53,67.63,65.49,64.79,77.38,78.10/
data AREA/216.08,333.46,54.99,517.04,400.86,78.69,309.77,
$332.26,529.54,186.18,715.62,37.50 /
data PAREA/3712.0,3674.5,2958.8,2243.1,1522.4,604.5/
data rk/0.072,0.355,0.486,0.234,0.222/
data x/0.347,0.388,0.378,0.411,0.433/
data t/0.05,0.3,0.4,0.2,0.2/
open(unit=20,file='rrrt',status='old')

do10 i=1,5
c0(i)=(-rk(i)*x(i)+0.5*t(i))/(rk(i)-rk(i)*x(i)+0.5*t(i))
c1(i)=(rk(i)*x(i)+0.5*t(i))/(rk(i)-rk(i)*x(i)+0.5*t(i))
c2(i)=(rk(i)-rk(i)*x(i)-0.5*t(i))/(rk(i)-rk(i)*x(i)+0.5*t(i))
10 continue
ratio(12)=(CN(12)/ACN(1))*(AREA(12)/PAREA(1))
ratio(11)=(CN(11)/ACN(2))*(AREA(11)/PAREA(2))
ratio(10)=(CN(10)/ACN(3))*(AREA(10)/PAREA(3))
ratio(9)=(CN(9)/ACN(3))*(AREA(9)/PAREA(3))
ratio(8)=(CN(8)/ACN(4))*(AREA(8)/PAREA(4))
ratio(7)=(CN(7)/ACN(4))*(AREA(7)/PAREA(4))
ratio(6)=(CN(6)/ACN(4))*(AREA(6)/PAREA(4))
ratio(5)=(CN(5)/ACN(5))*(AREA(5)/PAREA(5))
ratio(4)=(CN(4)/ACN(5))*(AREA(4)/PAREA(5))
ratio(3)=(CN(3)/ACN(6))*(AREA(3)/PAREA(6))
ratio(2)=(CN(2)/ACN(6))*(AREA(2)/PAREA(6))
ratio(1)=(CN(1)/ACN(6))*(AREA(1)/PAREA(6))
do20 i=1,33
run12(i)=DFLOW(i)*ratio(12)
rnetm(i)=DFLOW(i)-run12(i)
20 continue
do30 j=1,32
j1=33-j
rj5(j1)=(rnetm(j1+1)-c2(1)*rnetm(j1)-c0(1)*rj5(j1+1))/c1(1)
if(rj5(j1).lt.0.0) rj5(j1)=0.0
30 continue
do40 i=1,33

```

```

run11(i)=rj5(i)*ratio(11)
rnet5(i)=rj5(i)-run11(i)
40  continue
do50 j=1,32
j1=33-j
rj4(j1)=(rnet5(j1+1)-c2(2)*rnet5(j1)-c0(2)*rj5(j1+1))/c1(2)
if(rj4(j1).lt.0.0) rj4(j1)=0.0
50  continue
do60 i=1,33
run10(i)=rj4(i)*ratio(10)
run9(i)=rj4(i)*ratio(9)
rnet4(i)=rj4(i)-(run10(i)+run9(i))
60  continue
do70 j=1,32
j1=33-j
rj3(j1)=(rnet4(j1+1)-c2(3)*rnet4(j1)-c0(3)*rj4(j1+1))/c1(3)
if(rj3(j1).lt.0.0) rj3(j1)=0.0
70  continue
do80 i=1,33
run8(i)=rj3(i)*ratio(8)
run7(i)=rj3(i)*ratio(7)
run6(i)=rj3(i)*ratio(6)
rnet3(i)=rj3(i)-(run8(i)+run7(i)+run6(i))
80  continue
do90 j=1,32
j1=33-j
rj2(j1)=(rnet3(j1+1)-c2(2)*rnet3(j1)-c0(2)*rj3(j1+1))/c1(2)
if(rj2(j1).lt.0.0) rj2(j1)=0.0
90  continue
do100 i=1,33
run5(i)=rj2(i)*ratio(5)
run4(i)=rj2(i)*ratio(4)
rnet2(i)=rj2(i)-(run5(i)+run4(i))
100 continue
do110 j=1,32
j1=33-j
rj1(j1)=(rnet2(j1+1)-c2(1)*rnet2(j1)-c0(1)*rj2(j1+1))/c1(1)
if(rj1(j1).lt.0.0) rj1(j1)=0.0
110 continue
do120 i=1,33
run3(i)=rj1(i)*ratio(3)
run2(i)=rj1(i)*ratio(2)
run1(i)=rj1(i)*ratio(1)
120 continue
time=14.0
do220 i=1,33
time=time+0.5
write(20,200)time,run12(i),run11(i),run10(i),run9(i),run8(i),
$,run7(i),run6(i),run5(i),run4(i),run3(i),run2(i),run1(i)
200 format(4x,f4.1,4x,12f6.3)
220 continue
stop
end

```


Appendix C-3 Program to calculate ordinates of instantaneous unit sediment graph (IUSG)

```

dimension a(8),rit(8),c0it2(100),clit1(100),c2qt(100),ut(100)
dimension sct(100), riusg(100)

data a/0.0,66.26,151.28,237.55,1767.86,575.12,913.93,0.0/
rk=1.543
x=0.162
t=0.5
c0=(-rk*x+0.5*t)/(rk-rk*x+0.5*t)
c1=(rk*x+0.5*t)/(rk-rk*x+0.5*t)
c2=(rk-rk*x-0.5*t)/(rk-rk*x+0.5*t)
do30 i=1,8
rit(i)=0.0556*a(i)
c0it2(i)=c0*rit(i+1)
clit1(i)=c1*rit(i)
30 continue
ut(1)=c0it2(1)+clit1(1)+c2qt(1)
do50 i=2,100
c2qt(i)=ut(i-1)*c2
ut(i)=c0it2(i)+clit1(i)+c2qt(i)
if (ut(i).lt.0.0001) goto 70
50 continue
70 nr=i
time=0.0
do90 i=1,nr
time=time+0.5
sct(i)=exp(-0.11*time)
riusg(i)=sct(i)*ut(i)
write(*,80) time, ut(i), riusg(i)
80 format(f5.1,2f 8.4)
90 continue
stop
end

```

Notation: a=Area, rk=Storage coefficient, x=Weighting factor, t=Time, c0,c1 and c2=Routing coefficients, rit=Input ordinates at time t, ut=IUH ordinates, sct=Sediment concentration at time t, riusg= IUSG ordinates.



VITA

The author, Seyed Hamidreza Sadeghi, was born on 3rd September 1968 at Khonsar, a beautiful mountainous city of Isfahan province, Iran. He passed his higher secondary school examinations at Dr. Ali Shariati Higher Secondary School, Khonsar, with first division in 1985. He joined the Gilan University, Iran, for his Associate of Science program in the field of Natural Resources and was graduated in 1987. He completed his Bachelor degree in Rangeland and Watershed Management course of study with first division at University of Agricultural Sciences and Natural Resources Gorgan, Iran, in 1990. Then he joined the Tarbiat Modarress University, Iran, as a scholar of Ministry of Culture and Higher Education of Iran for his Master Degree in Watershed Management Engineering where he completed his program with first division in 1993. He was qualified through examination for pursuing higher studies leading to Ph.D. degree in abroad in 1993 and accordingly the Ministry of Culture and Higher Education of Iran awarded him a scholarship. Later, he got admission in Soil and Water Conservation Engineering, College of Technology at G.B. Pant University of Agriculture and Technology, India through which he joined to the varsity in the second semester 1997-1998.

He worked in the watershed management projects for more than three and half years in different parts of Iran and contributed in some of the national projects throughout the country. He has joined as an Assistant Professor in the Department of Watershed Management Engineering, College of Natural Resources and Marine Sciences, Tarbiat Modarress University, Noor, Iran since 1994.

ABSTRACT

Name: **Seyed Hamidreza Sadeghi** I.d. No. **24812**
Semester and Degree: **Ph.D.**
year of admission: **2nd semester, 1997-1998** Deptment: **SWCE**
Major: **Soil and Water Conservation Engineering**
Thesis Title: ***"Some Aspects of Spatial and Temporal distribution and Development of Prediction Models of Watershed Sediment Yield"***
Advisor: **Dr. J.K. Singh**

The main objective for conducting the present study was to develop sediment yield models through which temporal and spatial distributions of the watershed sediment generated during a storm event can be estimated. The models were developed based on the easily accessible hydrological as well as physiographical data of the Amameh watershed in Iran comprising an area of 3712ha.

Discharge rating curve, Precipitation-runoff relationships and sediment rating curves were developed for the watershed study for the completion and refining the collected hydrological data. Close relationships were established between maximum storage index coefficient (MSIC) and Curve Number (CN), as well as MSIC and depth of precipitation with a correlation coefficient of 82 % in each case and therefore a series of recessive equation was achieved to be applicable for estimation of runoff from the watershed. From the sediment rating curve (SRC), it was observed that in most of the cases there were more than one values of sediment discharge for the same value of runoff discharge located at the rising and the falling limbs of hydrograph. Therefore, the development of two separate regression equations for these sets of points were attempted by using regression and confidence area ellipse approaches.

Different annual and storm-wise erosion and sediment models were also evaluated for their efficacy in prediction of storm-wise excess sediment among which a new version of MUSLE, with a power of 0.081 and a proposed constraint, for the determination of storm magnitude, performed well with an error of estimation of 19.40%. A novel approach called as reverse routing technique (RRT), developed for the determination of outflow hydrographs at the outlet of each sub-watershed and the partial contributions to the total runoff, proved to be very efficient for the watershed. The direct runoff hydrographs obtained by RRT for different sub-watersheds were used for the determination of spatial distribution of sediment yield within the watershed, with the help of a sediment routing model based on the Williams' model.

Two different approaches, one based on the hydrological data and the other one on watershed characteristics (IUSG) were used for the development of storm-wise temporal distribution prediction model for sediment yield. Based on the results of factorial scoring, it was found that the models based on watershed characteristics, in general, performed better than the model based on the hydrological data. Accordingly, the sediment graph model with specifications of weighting factor $x=0.162$ (for derivation of IUH) and routing parameter $Z=0.110$, obtained by using modified equation for the study area (for determination of sediment concentration) and not considering the distribution of sediment mobilized (for convolution of USG into direct sediment graph) was found to be the best performing model for the prediction of the sediment graph in the study watershed.

Advisor
(Dr. J.K. Singh)

Author
(Seyed Hamidreza Sadeghi)